

**GROUNDWATER EXPLORATION, GROUNDWATER
QUALITY AND GROUNDWATER RECHARGE
STUDIES OF GURPUR WATERSHED USING
GEOINFORMATICS AND ELECTRICAL
RESISTIVITY METHODS**

Thesis

Submitted in partial fulfilment of the requirement for the degree of
DOCTOR OF PHILOSOPHY

By

VIRUPAKSHA H. S.



DEPARTMENT OF CIVIL ENGINEERING
NATIONAL INSTITUTE OF TECHNOLOGY KARNATAKA
SURATHKAL, MANGALORE – 575025

15th December 2021

DECLARATION

By

the Ph.D. Research Scholar

I hereby *declare* that the Thesis entitled "**Groundwater Exploration, Groundwater Quality and Groundwater Recharge Studies of Gurpur Watershed using Geoinformatics and Electrical Resistivity Methods**" is being submitted to the **National Institute of Technology Karnataka, Surathkal**, in partial fulfilment of the requirements for the award of the Degree of **Doctor of Philosophy in Civil Engineering** is a *bonafide report of the research work carried out by me*. The material contained in this Research Thesis has not been submitted to any University or Institution for the award of any degree.

Virupaksha H.S.
15/12/2021

VIRUPAKSHA H. S.

(Registration number: (155041 CV15F13))

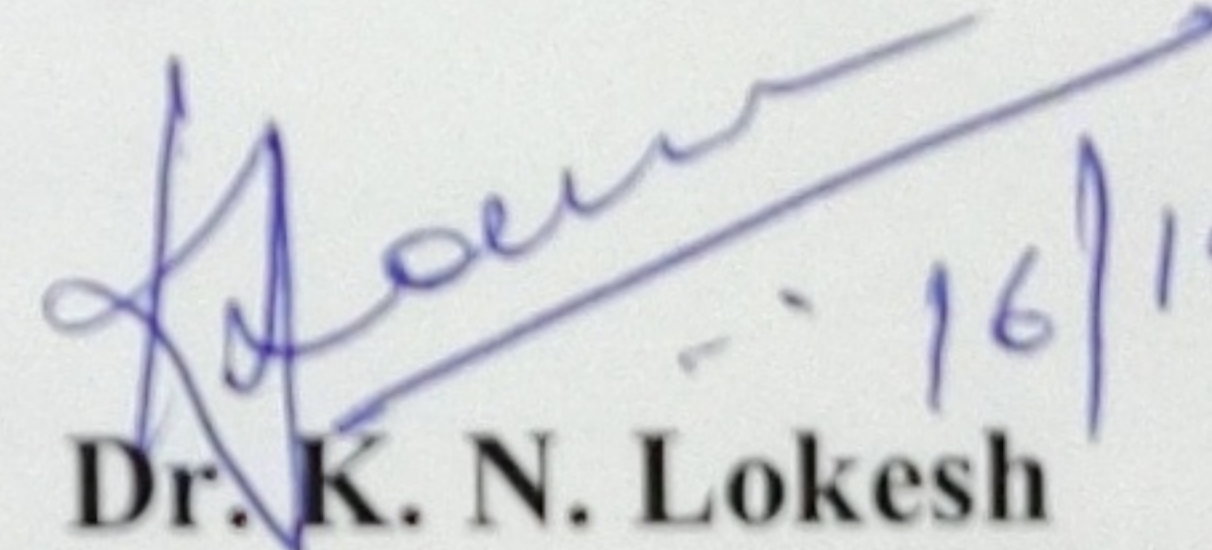
Department of Civil Engineering

Place: NITK, Surathkal

Date: 15th December 2021

CERTIFICATE

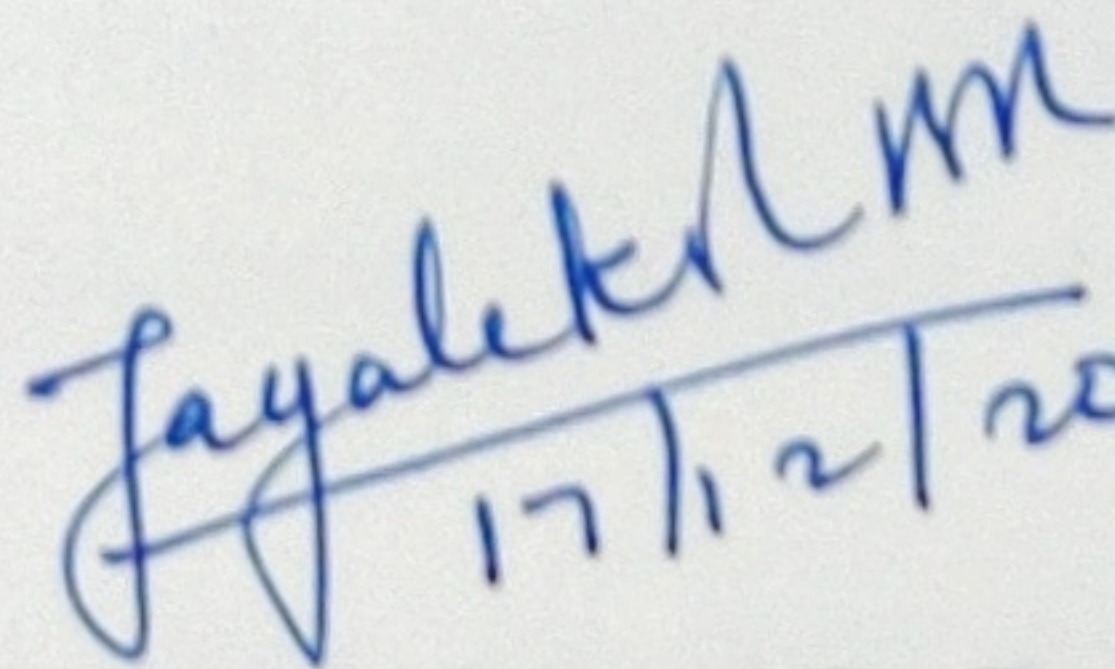
This is to *certify* that the Research Thesis entitled "**Groundwater Exploration, Groundwater Quality and Groundwater Recharge Studies of Gurpur Watershed using Geoinformatics and Electrical Resistivity Methods**" submitted by **Mr. VIRUPAKSHA H. S.**, (Registration number: 155041 CV15F13) as the record of the research work carried out by him, is *accepted as the Thesis submission* in Partial fulfillment of the requirements for the award of the degree of Doctor of Philosophy.


16/12/21

Dr. K. N. Lokesh

Research Supervisor

(Signature with Date and Seal)


17/12/2021.

Dr. Jayalekshmi B. R.

H.O.D. Civil and Chairman – DRPC

(Signature with Date and Seal)

Chairman (DRPC)
Department of Civil Engineering
National Institute of Technology Karnataka, Surathkal
Mysore - 575 025, Karnataka, INDIA



Dedicated

to my loving parents

Mr. Shivakumar H. R.

and

Nirmala H.K.

*To my siblings and family for their unconditional
support and inspiration!*

To my loving wife, Sowmya K. O.

This humble work is a sign of my love to you all..!

- Veeru

ACKNOWLEDGEMENT

With great pleasure, I express my sincere gratitude to the Director of NITK, **Prof. K. Umamaheshwar Rao**, and the former directors of NITK who extended the facilities in the institute as well as in the department. I would like to thank the National Institute of Technology Karnataka, Surathkal, for providing an Institute Fellowship and facilities. I sincerely thank **Prof. Nityananda Shetty, Dean (Academic)**, for his continuous support during my research.

I extend my heartfelt gratitude to my research supervisor, **Dr. K.N. Lokesh**, Professor, Civil Engineering Department, NITK Surathkal, for inspiration, relentless guidance, encouragement, and help in successfully completing the research program.

I am greatly indebted to Research Progress Assessment Committee members **Prof. K. Swaminathan** of the civil engineering department and **Prof. G. S. Dwarakisha** from the department of Water Resources and Ocean Engineering (formerly Applied Mechanics and Hydraulics) for their critical comments and invaluable suggestions during the progress of the research work.

I am thankful to **Dr. Jayalekshmi B. R.**, Head of the civil engineering department and chairman of DRPC. And I also thank **Dr. T. Palanisamy**, DRPC Secaratory of civil engineering department. I also thank DRPC and DTAC members.

I express my deep sense of gratitude to the research scholars **Vignesh Bhat, Venkanagouda B B Patil, Shannon M Pinto, Thejashree G.,** and **Krishnamurthy M. P.**, for their constant support, intensive discussions, and assistance in the field.

I also like to acknowledge the suggestions and efforts put forth by **Dr. G. Chandrakantha**, and **Dr. Vinoth Srinivasan**, which I believe have improved the research work.

I acknowledge my indebtedness to **Dr. Dinesh Kumar Y. K.**, Deputy Conservator of Forests, Mangalore & in charge Regional Director (Environment), Mangalore, and also **Mr. Mahesh Kumar U.**, Assistant Director (Fisheries), Mangalore for their keen

scientific insight, which helped me improve the practical relevance of the thesis.

I gratefully acknowledge the support rendered by my best friend, **Dr. Praveen G Deshbhandari**, for the timely suggestions and ideas of importance to improve the research. I sincerely thank the environmental engineering laboratory staff, especially **Mr. Manohara Shanubhoge**, for the help and knowledge during the laboratory analysis of the research.

I express my thanks to **Dr. Sharath B. S., Dr. Girish G. N., Dr. Prabhu Prasad, Mr. Akash Anand** and **Mr. Praveena T. M.** for their suggestions and support throughout this endeavour.

I would like to thank my wife and my best friend, **Ms. Sowmya K. O.**, who stood beside me unconditionally during our tough times and assisted in my research work. I thank all my friends at NITK, who were always supportive and friendly to me. I would also like to thank **Mr. Kiran K. O.**, for his timely assist and support during the field work.

I would like to remember The Almighty for providing such a splendid learning experience in my life through this journey.

"Om Shree Hampi Virupaksheshwaraaya Namah"

Lastly, I thank all my well-wishers who have directly or indirectly supported me in need of the hour.

Virupaksha H. S.

TABLE OF CONTENTS

TITLE PAGE	i
DECLARATION	ii
CERTIFICATE	iii
DEDICATION	iv
ACKNOWLEDGEMENTS	v
TABLE OF CONTENTS	vii
LIST OF FIGURES	xii
LIST OF TABLES	xiv
LIST OF ABBREVIATIONS	xvi
Chapter 1. INTRODUCTION	1
1.1 General	1
1.2 Study area description	5
1.2.1 Geology	5
1.2.2 Climate	6
1.2.3 Rainfall	7
1.2.4 Temperature	7
1.2.5 Humidity	7
1.2.6 Vegetation	7
1.3 Scope of the study	8
1.4 Objectives	8
1.5 Organization of thesis	9
Chapter 2. REVIEW OF LITERATURE	11
2.1 General	11
2.2 Electrical Resistivity technique for mapping sub-surface	13
2.3 Geology and geomorphology	18
2.4 Geoinformatics and groundwater exploration	23
2.5 Groundwater exploration studies	23
2.5.1 Integrated approach for GW exploration	24
2.6 Groundwater quality studies	26
2.6.1 Quality Assurance Practices (QAP) for water quality analysis	26
2.6.1.1 Anion – Cation Balance (ACB)	27
2.6.1.2 Total Dissolved Solids (TDS)	27
2.6.1.3 Measured EC and Ion sums	28
2.6.1.4 Calculated TDS to EC ratio	28
2.6.1.5 Total Hardness (TH)	28
2.6.1.6 Chloride’s relationship with Na and K	29
2.6.2 Drinking water quality parameters	29
2.6.3 Computation of Water Quality Index	29
2.7 Groundwater recharge studies	30

2.7.1	Groundwater recharge estimation studies.....	32
2.7.1.1	Runoff estimation.....	34
2.7.1.1.1	Hydrologic Soil Group classification.....	37
2.7.1.1.2	Antecedent Moisture/Runoff Condition.....	37
2.7.1.1.3	Development of Curve Numbers	38
2.7.1.2	Estimation of Actual Evapotranspiration	38
Chapter 3.	GEOLOGY AND GEOMORPHOLOGY	39
3.1	Introduction	39
3.2	Geology	39
3.2.1	Geology of West coast of India	39
3.2.2	Geology of Karnataka	40
3.2.3	Geology of Gurpur watershed.....	41
3.2.4	Lithology.....	41
3.3	Geomorphology.....	42
3.4	Digital Elevation Model data	44
3.4.1	Extraction of DEM Derivatives	45
3.4.2	Drainage network map	45
3.4.3	Slope map.....	46
3.4.4	Hill shade map	48
3.4.5	Contour map.....	48
3.5	Morphometric analysis	49
3.5.1	Materials and methodology.....	49
3.5.2	Results and discussions on linear, aerial & relief parameters.....	52
3.6	Land Use/Land Cover Map	57
3.7	Soil resource map	59
3.8	Summary	64
Chapter 4.	GROUNDWATER EXPLORATION	65
4.1	Introduction to groundwater exploration.....	65
4.2	Materials and methodology	65
4.2.1	Geophysical methods in groundwater exploration	65
4.2.2	Electrical resistivity method (ERM)	66
4.2.2.1	ER method and configurations.....	68
4.2.2.2	Interpretation methods	69
4.2.2.2.1	Dar-Zarrouk parameters.....	70
4.2.2.2.2	Hydraulic and geoelectric parameters.....	71
4.2.3	Geoinformatics and GW exploration	73
4.2.3.1	Thematic information database creation	74
4.2.4	Integrated approach for GW exploration	78
4.3	Results and discussion.....	79
4.3.1	Qualitative and Quantitative VES analysis – ISM.....	79
4.3.2	Qualitative and Quantitative VES analysis - CMT	82
4.3.2.1	A-type and AA-type curves	82

4.3.2.2	AK-type curves	83
4.3.2.3	H-type curves	83
4.3.2.4	HA-type curves	84
4.3.2.5	HK-type curves	84
4.3.2.6	HKA-type curves	84
4.3.2.7	K-type curve.....	85
4.3.2.8	KH-type curve.....	85
4.3.2.9	KHA-type curve.....	85
4.3.2.10	KQ-type curve.....	85
4.3.2.11	QH-type curves	87
4.3.2.12	QKA-type curve.....	88
4.3.2.13	QQ-type curves	88
4.3.3	Hydraulic and Geoelectric parameters.....	89
4.3.3.1	Transmissivity (T).....	90
4.3.3.2	Hydraulic Conductivity (K)	90
4.3.3.3	Porosity (Φ).....	91
4.3.3.4	Formation factor.....	91
4.3.4	Dar-Zarrouk parameters	91
4.3.5	Correlation studies	93
4.3.6	Thematic database creation.....	95
4.3.6.1	Geomorphology	96
4.3.6.2	Slope Map	97
4.3.6.3	Land Use/Land Cover Map.....	98
4.3.6.4	Soil Resources.....	98
4.3.6.5	Lithology.....	99
4.3.6.6	Lineament density	99
4.3.6.7	Drainage density	100
4.3.6.8	Depth to Bedrock	100
4.3.6.9	Rainfall distribution	102
4.3.6.10	Ground Water Contours	102
4.3.7	Groundwater potentiality studies	102
4.4	Summary and conclusion	105
Chapter 5. GROUNDWATER QUALITY	109
5.1	Introduction	109
5.2	Materials and methods	109
5.2.1	Groundwater quality analysis	109
5.2.2	Drinking water quality parameters.....	110
5.2.3	Phases of groundwater quality studies	110
5.2.4	Drinking water quality parameters.....	111
5.2.4.1	Ionic constituents	111
5.2.4.2	Non-ionic constituents	111
5.2.5	Water Quality Index method.....	112
5.2.6	QAP or CCA for water quality analysis	112

5.2.6.1	Anion – Cation Balance	113
5.2.6.2	Total Dissolved Solids (TDS)	113
5.2.6.3	Measured EC and Ion sums	114
5.2.6.4	Calculated TDS to EC ratio	114
5.2.6.5	Total Hardness (TH)	114
5.2.6.6	Chloride’s relationship with Na and K.....	115
5.2.7	Computation of Water Quality Index (WQI).....	115
5.3	Results and discussion.....	117
5.3.1	Groundwater quality analysis for drinking purposes	117
5.3.2	Drinking water quality parameters.....	118
5.3.2.1	Ionic constituents	118
5.3.2.1.1	Sodium.....	118
5.3.2.1.2	Potassium.....	119
5.3.2.1.3	Calcium.....	119
5.3.2.1.4	Magnesium.....	120
5.3.2.1.5	Iron.....	121
5.3.2.1.6	Chloride	121
5.3.2.1.7	Sulphate	123
5.3.2.1.8	Nitrate	124
5.3.2.1.9	Fluoride.....	124
5.3.2.2	Non-ionic constituents	125
5.3.2.2.1	The pH	125
5.3.2.2.2	Electrical conductivity	126
5.3.2.2.3	Total dissolved solids.....	126
5.3.2.2.4	Total Alkalinity.....	127
5.3.2.2.5	Total Hardness	127
5.3.3	Phases of groundwater quality studies	128
5.3.3.1	Phase-I (August – 2017)	128
5.3.3.2	Phase-II (December – 2017)	128
5.3.3.3	Phase-III (April – 2018).....	129
5.3.4	Computation of Groundwater Quality Index	129
5.3.5	Implementation of QAP	130
5.3.5.1	Correlation studies	130
5.4	Summary	137
Chapter 6. GROUNDWATER RECHARGE		139
6.1	Introduction	139
6.2	Objectives of the study.....	141
6.2.1	Geology.....	141
6.2.2	Groundwater Recharge Potential zones (GRPZ).....	142
6.2.2.1	Groundwater Potential Zones (GWPZ).....	143
6.2.2.2	Geomorphology	143
6.2.2.3	Land use/land cover	144
6.2.2.4	Depth to bedrock or weathered zone.....	144
6.2.2.5	Lineament density.....	145

6.2.2.6	Ground Water Fluctuation (GWF)	145
6.2.2.7	Slope	146
6.2.2.8	Drainage order and water bodies	146
6.2.2.9	Soil Depth Map	149
6.2.2.10	Groundwater recharge potential zones	149
6.2.3	Artificial recharge structures	152
6.2.3.1	Water conservation methods	153
6.2.4	Site specific approach for proposing ARS	154
6.2.4.1	Check dams	155
6.2.4.2	Nala bunds	156
6.2.4.3	Percolation tank	156
6.2.4.4	Farm pond	157
6.2.4.5	Contour trenching	157
6.2.4.6	Rainwater harvesting	157
6.2.4.7	Dug well / bore well recharge	160
6.2.4.8	Quarry reservoirs	160
6.2.4.9	Subsurface dams / dykes	160
6.2.4.10	Park recharge structures	160
6.2.4.11	Injection wells	161
6.2.4.12	Soil Aquifer Treatment (SAT)	161
6.2.5	Recharge estimation methods	162
6.2.5.1	Groundwater recharge ratio	162
6.2.5.2	Validation of the results	164
6.2.5.3	The empirical relationships	165
6.2.5.4	Rainfall Infiltration (RI) method	166
6.2.5.5	Hydrodynamic Method	167
6.2.5.6	Water table fluctuation method	168
6.2.5.7	Water balance method	168
6.3	Summary	173
Chapter 7. SUMMARY AND CONCLUSIONS		175
7.1	Limitations	180
7.2	Scope for future work	181
REFERENCES		183
APPENDIX-A		201
APPENDIX-B		225
APPENDIX-C		231
APPENDIX-D		235

LIST OF FIGURES

Figure 1.1 Base map of Gурpur watershed with False Colour Composite (FCC) of satellite imagery.....	6
Figure 3.1 Lithological map of Gурpur watershed.....	43
Figure 3.2 Spatial distribution of Geomorphology classes in Gурpur watershed.	44
Figure 3.3 The DEM thematic map of the study area.....	45
Figure 3.4 Drainage map of Gурpur watershed	46
Figure 3.5 Spatial distribution of slope classes in Gурpur watershed.....	47
Figure 3.6 The hill shade map of Gурpur watershed	48
Figure 3.7 The filled contour map of Gурpur watershed.	49
Figure 3.8 The spatial distribution of drainage density in Gурpur watershed.	56
Figure 3.9 Spatial distribution of lu/lc categories in Gурpur watershed	60
Figure 3.10 The lu/lc accuracy assessment using 300 random sampling	60
Figure 3.11 The classes of soil types in the study area.....	63
Figure 3.12 The classes of soil depth in the study area.	63
Figure 4.1 Schematic drawing of Electrical Resistivity principle (Clark & Page 2011)	67
Figure 4.2 Typical resistivity values for different rocks (geosci.xyz)	68
Figure 4.3 Wenner, Schlumberger and double di-pole arrays respectively.....	69
Figure 4.4 Flow chart for groundwater potential zones mapping.....	79
Figure 4.5 Selected graphs for ISM interpretation.....	80
Figure 4.6 Selected plots of each curve types obtained using CMT.....	87
Figure 4.7 Spatial distribution maps of the aquifer parameters	92
Figure 4.8 Correlative studies of CMT results with respect to the borehole lithology	94
Figure 4.9 Regression equations for hydraulic and geoelectric parameters	96
Figure 4.10 Thematic information used for preparation of GWPZ	97
Figure 4.11 Land use / land cover thematic layer of Gурpur watershed.....	99
Figure 4.12 The spatial distribution of depth to bedrock (weathered zone thickness)	101
Figure 4.13 Spatial distribution of GWC of all the Three Phases	103
Figure 4.14 Spatial distribution of Groundwater Potential Zones prepared using	

CMT.....	104
Figure 4.15 Spatial distribution of Groundwater Potential Zones prepared using WOI.....	104
Figure 5.1 Flow chart for spatial distribution of groundwater quality parameters.	117
Figure 5.2 Spatial distribution maps of groundwater quality parameters.....	122
Figure 5.3 Spatial distribution maps of Bicarbonates, Fluoride and Iron.....	124
Figure 5.4 Spatial distribution maps of GQI for three phases.	133
Figure 6.1 Flow chart for groundwater recharge potential zones mapping.	147
Figure 6.2 Thematic layers used in integration of GRPZ.....	148
Figure 6.3 Groundwater fluctuation map (average for 20 years 1998-2018)	149
Figure 6.4 Groundwater recharge potential zones of Gurgur watershed.....	152
Figure 6.5 Proposed artificial recharge structures using GRPZ and site specific approach.....	159

LIST OF TABLES

Table 2.1 Typical criteria for acceptance of percentage difference of ACB	27
Table 2.2 The rating and grading used in Weighted Arithmetic WQI method.....	30
Table 3.1 The general litho-stratigraphic sequence of Dakshina Kannada district.	41
Table 3.2 The categories of lithology and their corresponding area Statistics.	42
Table 3.3 Categories of Geomorphologic features and corresponding area statistics.	43
Table 3.4 Categories of slope and their corresponding slope percentage.....	47
Table 3.5 Formulae adopted for computation of Morphometric Parameters.....	50
Table 3.6 Basic morphometric parameters of Gurlur watershed.	52
Table 3.7 Morphometric analysis of basic and linear parameters of Gurlur watershed.	55
Table 3.8 Drainage density and corresponding area statistics.	56
Table 3.9 Morphometric analysis of areal parameters.	58
Table 3.10 Morphometric analysis of relief parameters.	58
Table 3.11 The lu/lc and corresponding area statistics.	59
Table 3.12 Categories of soil types and corresponding area statistics.....	61
Table 3.13 Theoretical error matrix of lu\lc classification.	62
Table 4.1 Quantitative analysis of VES data interpreted using Inverse Slope Method.....	81
Table 4.2 Curve types for qualitative interpretation of VES	83
Table 4.3 Resistivity and thickness of layers for quantitative interpretation of VES ..	86
Table 4.4 Resistivity and thickness of layers for quantitative interpretation of VES ..	89
Table 4.5 Aquifer hydraulic and geoelectric parameters of 35 VES locations.....	89
Table 4.6 The Dar-Zarrouk parameters for 35 VES locations.....	93
Table 4.7 Correlation matrix of hydraulic and geoelectric parameters for 35 VES locations	95
Table 4.8 Weightage assignment for thematic layers used in the preparation of GWPZ.....	104
Table 5.1 Drinking water quality parameters.	110
Table 5.2 Criteria for GQI	112
Table 5.3 Typical criteria for acceptance of percentage difference of ACB	113

Table 5.4 Statistics of groundwater quality parameters for 51 samples	119
Table 5.5 The GQI status for all the three phases of the study.....	131
Table 5.6 Correlation studies for QAP equations.	132
Table 5.7 Correlation matrix for Phase-I Groundwater quality data (August-2017).134	
Table 5.8 Correlation matrix for Phase-II Groundwater quality data (December-2017)	135
Table 5.9 Correlation matrix for Phase-III Groundwater quality data (April-2018).136	
Table 6.1 GRPZ weightage assignment and recharge ratio factors.	150
Table 6.2 Site specific approach for selection of artificial recharge structures.	158
Table 6.3 Rainfall statistics for 20 years from 1998 – 2018 for 12 rain gauging stations	163
Table 6.4 Calculation of recharge rate factors and statistics.	163
Table 6.5 The rainfall to recharge rate calculations with corresponding units.....	164
Table 6.6 Climatological data for 30 years from 1981 to 2010.....	171
Table 6.7 The groundwater recharge estimated for 12 rain gauging stations (20 years data from 2008 to 2018) using empirical equations.....	172

LIST OF ABBREVIATIONS

2 Dimensional (2-D)	14
3 Dimensional (3-D)	14
Actual evapotranspiration (AET).....	38
Advanced Spaceborne Thermal Emission and Reflection Radiometer (ASTER).....	20
Analytic Hierarchy Process (AHP)	24
Anion – Cation Balance (ACB)	27
Antecedent Moisture Condition (AMC)	37
Antecedent Runoff Condition (ARC)	37
Apparent resistivity (ρ_a)	14
Aquifer Anisotropy (λ)	17
Area Of Interest (AOI).....	59
Artificial Neural Network (ANN).....	34
Artificial Recharge Structures (ARS)	9
Basin Length (L_b)	52
Basin Relief (B_h)	52
Bicarbonate (HCO_3^-).....	29
Bifurcation ratio (R_b).....	21
Calcium (Ca^{2+}).....	29
Calculated Total Dissolved Solids (CTDS)	27
Central Groundwater Board (CGWB)	24
Central Water Commission (CWC)	7
Checking the Correctness of the Analysis (CCA)	4
Chloride(Cl^-)	29
Circularity ratio (R_c).....	22
Compactness Coefficient (C_c)	51
Conductance (C)	66
Constant of channel maintenance (C)	23, 51
Curve Matching Technique (CMT)	10

Dar-Zarrouk (D-Z)	16
Department of Mines and Geology (DMG)	24
Depth to bedrock (DBR)	9
Digital Elevation Model (DEM)	20
Drainage density (Dd)	21
Electric Current (I)	13
Electrical Conductivity (EC)	26
Electrical resistivity (ER)	3
Elongation Ratio (Re)	51
False Colour Composite (FCC)	6
Fluoride (F ⁻)	29
Form factor (Ff)	51
Formation factor (F)	18
Geographical Information System (GIS)	2
Geological Survey of India (GSI)	42
Geomorphological Instantaneous Unit Hydrograph (GIUH)	34
Global Navigation Satellite System (GNSS)	2
Government of India GOI)	7
Ground Water Fluctuation (GWF)	145
Groundwater (GW)	1
Groundwater contour (GWC)	24
Groundwater level (GWL)	145
Groundwater Potential Index (GWPI)	25
Groundwater Potential Zones (GWPZ)	9, 143
Groundwater Quality (GWQ)	28
Groundwater Quality Index (GQI)	112
Groundwater Recharge Potential Index (GRPI)	31
Groundwater Recharge Potential zones (GRPZ)	142
Groundwater Resource Estimation Methodology (GWREM)	33
Horizontal profiling (HP)	69

Hydraulic conductivity (K)	16
Hydrological Soil Group (HSG)	34
Image Processing (IP)	2
India Meteorological Department (IMD).....	24
Indian Remote Sensing (IRS)	42
Inverse Distance Weighted (IDW).....	18
Inverse Slope Method (ISM)	10
Iron (Fe ²⁺)	29
Karnataka State Natural Disaster Monitoring Centre (KSNDMC)	24
Karnataka State Remote Sensing Application Centre (KSRSAC)	42
Land Use & Land Cover (LULC).....	25
Layer thickness (<i>h</i>).....	17
Length of overland flow (Lg)	51
Light Detection and Ranging (LiDAR)	2
Linear Imaging Self scanning Sensor (LISS)	42
Longitudinal Unit Conductance (S).....	17
Magnesium (Mg ²⁺).....	29
Mean bifurcation ratio (Rbm)	51
Mean stream length (L).....	50
Measured Electrical Conductivity (MEC)	28
Measured Total Dissolved Solids (MTDS).....	27
Methyl Tertiary Butyl Ether (MTBE).....	1
Million Cubic Meters (MCM)	160
Multi Criteria Decision Making (MCDM)	3
Multi-Criteria Evaluation (MCE)	3
Multi-Influencing Factor (MIF).....	3
National Bureau of Soil Survey / Land Use Planning (NBSS/LUP).....	32
National Oceanic and Atmospheric Administration - Advanced Very High-Resolution Radiometer (NOAA-AVHRR)	181
National Remote Sensing Centre (NRSC).....	23

Natural Resources Conservation Service Curve Number method (NRCS-CN).....	34
Nitrate (NO ₃ ⁻).....	29
Normalized Difference Vegetation Index (NDVI)	181
Normalized Difference Water Index (NDWI)	181
Observatory (OB).....	3
Peninsular Gneiss Complex (PGC).....	5
Penman-Grindley (P-G)	33
Permanent Hardness (PeH)	28
Porosity (∅)	18
Potassium (K ⁺)	29
Potential evapotranspiration (PET).....	7
Potential of hydrogen (pH)	26
Quality Assurance Practices (QAP).....	26
Rainfall Infiltration (RI).....	166
Rainwater harvesting (RWH)	30
Relief Ratio (Rh).....	52
Remote Sensing (RS).....	2
Resistance (R)	13
Resistivity (ρ).....	16
Root Mean Square (RMS)	20
Sewage Treatment Plant (STP).....	162
Shape factor (Bs).....	51
Shuttle Radar Topographic Mission (SRTM).....	20
Signal Stacking Resistivity (SSR)	69
Sodium (Na ⁺)	29
Soil Aquifer Treatment (SAT).....	32
Soil Conservation Service Curve Number (SCS-CN)	34
Stream frequency (Fs).....	51
Stream Length (L _u)	50, 53
Stream length ratio (RI)	51

Stream Number (N_u)	52
Stream Order (N_u)	50
Sulfate (SO_4^{2-})	29
Survey Of India (SOI)	44
Temporary Hardness (TeH)	28
Texture ratio (T)	51
Total Alkalinity (TA)	29
Total Dissolved Solids (TDS)	26
Total Hardness (TH)	28
Transmissivity (T)	16
Transverse unit Resistance (TR)	16, 17
U.S. Department of Agriculture (USDA)	34
Universal Transverse Mercator (UTM)	50
University of British Columbia Watershed Model (UBCWM)	34
Vertical Electrical Sounding (VES)	14
Voltage (V)	13
Water Ecosystem Impact (WEI)	32
Water Harvesting (WH)	153
Water Quality Index (WQI)	4
Water storage (ΔS)	33
Weighted Overlay Analysis (WOA)	3
World Geodetic System (WGS)	50

Chapter 1

INTRODUCTION

1.1 General

Water is one of the most valuable natural resources which supports human health, economic development, and ecological diversity. A nation's growth relies on its renewable and non-renewable resources like water. Therefore, scientific research and effective management are essential for water resource analysis. Increasing agricultural and industrial activities coupled with recurrent monsoon vagaries make groundwater (GW) a scarce resource, unable to meet even the drinking water requirement. Thus, surface water and groundwater are of utmost importance both in quality and quantity. From the dawn of the Industrial and Green revolution, the surplus use of groundwater has led us to groundwater pollution and depletion. The leaching of noxious chemicals into the subsurface, polluting even the deeper aquifers, has become a point of precarious consideration. The Methyl Tertiary Butyl Ether (MTBE) contaminates the groundwater, even though it contributes oxygen to the atmosphere. Therefore, Fetter (2001) emphasized that "Even the best intentions can have unanticipated and extremely undesirable consequences on our limited water resources." Water resources in India are inconsistent in distribution, both spatially and temporally. In recent times, scientific and technological innovations have been persuaded. These innovations help us tap the water resources available on earth to meet the water needs of humans and many other living organisms. Hence, efficient scientific techniques for identifying potential aquifer zones for exploitation and recharge are highly essential.

In India, uneven distribution of water occurs because of diverse physiographic conditions and the peculiar mannerism of monsoons. In recent times, the urban lifestyle, population boom, unscientific agricultural practices have worsened the situation. Even today, most parts of the country are facing severe water scarcity. We should augment the planning, utilization, administration, and management of groundwater resources to better society and the nation. India has witnessed excess groundwater exploitation in the last two to three decades, especially for agricultural and industrial purposes, since

accessibility for surface water sources (rivers, lakes, and artificial basins) is less than the demand. According to 2015 statistics, India's total geographical area is 329 million hectares. Out of this, 195 million hectares is the gross cropped area, and 141 million hectares is the net sown area. On the other hand, the net irrigated area is only 65.3 million hectares. The rest of the land is rain-fed.

Geospatial technologies describe a set of tools primarily contributing to mapping and analysing any statistical data of any field with spatial information. These include Geospatial technologies, like Electronic surveying, Geographical Information System (GIS), Remote Sensing (RS), Photogrammetry, Light Detection and Ranging (LiDAR), Global Navigation Satellite System (GNSS), and Image Processing (IP). Geospatial technologies offer a radically different manner of collecting data to produce and analyse maps required for different applications. Several geospatial applications have emerged with the map as one of the most important end products. Electrical resistivity imaging is an indirect method of interpreting the subsurface geological conditions, especially the lineaments and weathered rock zone. The most significant advantage of using Remote Sensing data for hydrological modelling and monitoring is its ability to generate information in a spatial and temporal domain. RS and GIS techniques are efficient to minimize the time, labor, money to make quick decisions for sustainable water resources management (Tiwari & Shukla 2015).

The geologic features like lithology, thickness, structures, and permeability of aquifers play a prominent role in the occurrence, origin, and movement of groundwater. The aquifers are confined to fractured or weathered zones. Therefore, extensive hydrogeological investigations are often required to understand groundwater conditions systematically. A large volume of multidisciplinary data from various sources is required for groundwater management and development. The groundwater aquifers are a subsurface phenomenon. And there is a need to rely on indirect analysis of features like lithology, geology, geomorphology, drainage pattern, soil, land use/land cover (lu/lc), and hydrological characteristics, are observed directly. In the last few decades, geospatial techniques are extensively used to identify and demarcate groundwater resources.

In the recent past, Multi Criteria Decision Making (MCDM) has proved as an effective tool for resource mapping and management, especially for natural resources like water. (Chowdary et al. 2013; Okoli et al. 2017; Okoli et al. 2019) suggested that the MCDM technique plays a vital role in water resources quantification and management. Senanayake et al. (2016) emphasize that the Multi-Influencing Factor (MIF) is a subjective approach, where the accuracy of the final results depends significantly on the thematic information and their weightage factor. Several other suitability analysis types are available; one of them is the "Weighted Overlay Analysis" (WOA), which allows us to combine, weight, and rank several different types of thematic information. Integrating Multi-Criteria Evaluation (MCE) techniques with GIS allows users to evaluate various alternatives based on multiple and conflicting criteria and objectives. The potential use of a combined GIS-MCE approach in the development of spatial decision support systems plays an important role (Carver 1991).

Groundwater potential zonation means using the surface and sub-surface indicative parameters either by direct or indirect scientific methods for determining the potentiality of the groundwater zones in an area by quantitative and qualitative assessment. The surface features or parameters can be easily accessible through remote sensing and field verification. In contrast, the sub-surface parameters are possible through Observatory (OB) wells, Electrical resistivity (ER) methods, and direct observations in the possible exposures. Remotely sensed data is used for lu/lc and lineament mapping. Also, the geomorphological mapping and drainage basin analysis add up for it. The present work attempts to establish the relation between ER method and RS & GIS-based methodology in groundwater potential zone identification and mapping. Understanding geological, structural, geomorphological characteristics are necessary as it forms the basis for assigning Rank/Weightage.

Though the water table is almost to the ground level (in some cases overflowing) during the monsoon season, the study area suffers water scarcity during the summer season. Therefore, there is a need for proper water management studies. The construction of small water harvesting structures is gaining importance in recent years (Kumar et al. 2008) because they spread across spatially. Thus storage and recharge structures should be planned resourcefully so that that water can be utilized efficiently

during summer. There is a need for understanding the Runoff for realistic assessment and quantification of the surface and groundwater. The complexity of the aquifers and subsurface can mislead to propose improper recharge structure (Todd & Mays 2005). There are several variables to be considered for accurate results. Therefore, multi-criteria analysis is constructive in this regard.

The need for groundwater quality studies (especially for drinking water) is also one of the major concerns (Department of Mines and Geology 2011; Central Ground Water Board 2015). A close relationship between groundwater quality and industries is established by various resources (Asadi et al. 2011; Osibanjo & Majolagbe 2012; Basavaraddi et al. 2012; Rao et al. 2013; Nas & Berkay 2014). Also, the leaching of heavy metals (toxic metals) from landfills, industrial and biomedical wastes poses a severe threat to the groundwater quality (Patel & Devatha 2019). Even though saltwater intrusion is a natural phenomenon, it poses a threat to coastal aquifers. Several studies are conducted for mapping groundwater vulnerability with the DRASTIC model (Rahman 2008; Thapa et al. 2018) and Water Quality Index (WQI) (Shivanna & Nagendrappa 2015; Gidey 2018; Mukate et al. 2019; Adimalla & Qian 2019) approach using GIS. Checking the Correctness of the Analysis (CCA) with a systematic approach increases the confidence in the data generated. Also, several studies are conducted in this regard (Karanth 1987; APHA 1999; Rao et al. 2013). The correlation studies reduce uncertainty and understand the interrelationship between different variables (Joshi et al. 2009). A statistical tool like correlation studies widely used for analysing the concentrations, monitoring, and evaluating the water quality (Paudyal et al. 2016; Shrestha & Basnet 2018).

Several studies are conducted in the study area concerning different aspects of groundwater. The geology, geomorphology, morphometric analysis, and structural studies of the area have been carried out (Radhakrishna 1967; John & Cheriyan 1974; Balasubrahmanyam 1978; Subrahmanya & Jayappa 1987; Chandrasekharappa 1989; Radhakrishna 1989; Subrahmanya & Grangadhara Bhat 1995). Some have studied the groundwater quality, pollution, and hazard in and around the study area (Gajendragad & Ranganna 1989; Narayana & Suresh 1989; Ranganna et al. 1991). Ion chemistry and trace element studies have also been conducted (Gurumurthy et al. 2014). Pumping tests

and aquifer parameters were also studied in and around the study area (Reghunath 1999). The studies on infiltration characteristics of the river and soil types are also carried out (Ranganna et al. 1991).

1.2 Study area description

The Gurpur watershed covers mainly Dakshina Kannada district and part of the Udupi district (Karkala taluk). The study area traverses a short path. It has a dynamic change in topography and follows perpendicular flow with respect to the Western Ghats and west coast. The terrain features and altitude divides the catchment into three environs: high land, midland, and low land (ghats, hinterland, and coastal).

The study area (Figure 1.1) lies under longitude $74^{\circ} 47' 31''$ E to $75^{\circ} 17' 28''$ E and $12^{\circ} 50' 02''$ N to $13^{\circ} 11' 21''$ N latitudes, and the total area of the catchment is 878 km². This river, just like other west-flowing rivers, in its early stage, flows through a very steep slope (ghats), but in midland, it loses its effectiveness. When it reaches low land, the river traverses the south direction, perpendicular to its earlier flow and confluence with Nethravathi River to join the Arabian Sea finally.

1.2.1 Geology

The Deccan traps are the basement for the west coast, and most of it is capped by Lateritic terrain. The litho-units of the lower catchment belong to the tertiary or Quarternary era and of upper catchment belongs to the Archaean gneissic complex. The major litho unit is Peninsular Gneiss Complex (PGC). The greenstone-amphibolitic facies metamorphic rocks and granulites are in patches. The basin area is lithologically composed of about 83% migmatites and granodiorites, 5% of charnockites, about 6% metabasalts, and 2% laterites and amphibolites.

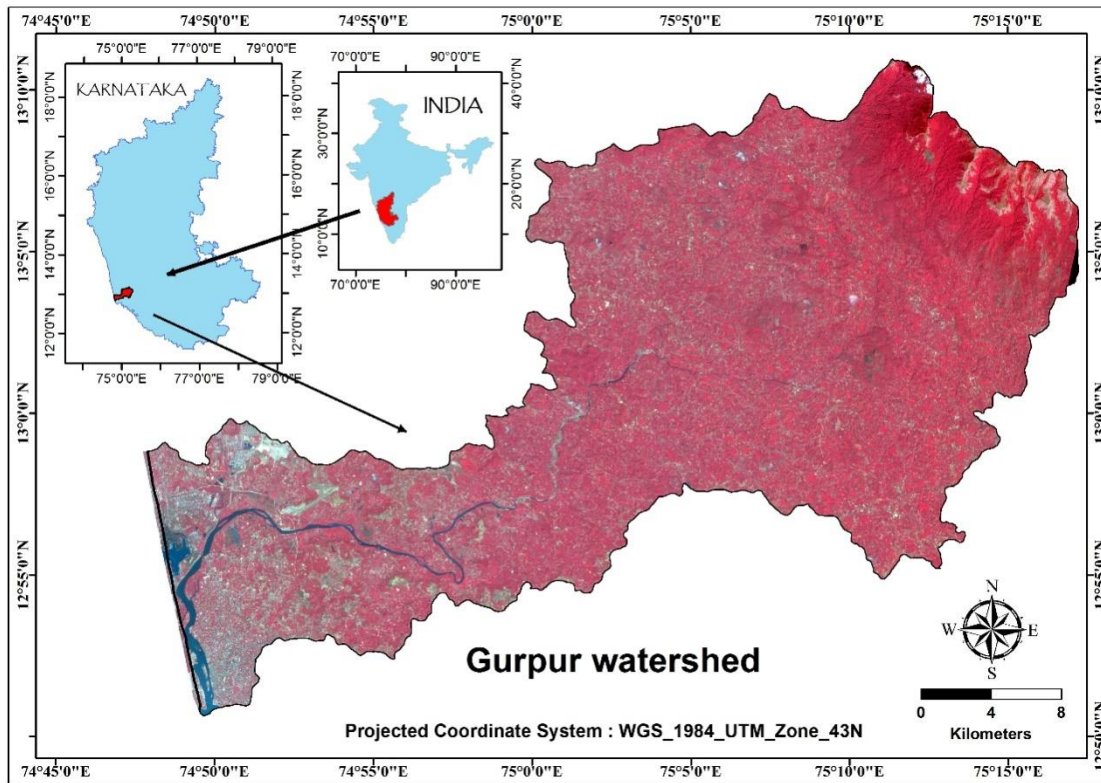


Figure 1.1 Base map of Gurpur watershed with False Colour Composite (FCC) of satellite imagery.

The weathered zone hosts groundwater in its fissures, fractures, and pore spaces of the weathered rocks. Most of the natural recharge occurs during the southwest monsoon season and infiltration due to irrigation. The present landscape along the coast is the reflectance of extensive Tertiary denudation, which leads to the formation of laterites. The Quarternary formations are along the coast, which includes the boulders, pebbles, and cobble beds in paleo-river channels (Gurumurthy 2013). The detailed geology of the study area is discussed in chapter 3 under the title "Geology and Geomorphology."

1.2.2 Climate

The climate of the Dakshina Kannada district is similar to other parts of the west coast of India. Here four seasons can be experienced. But in the broader picture, the overall climate remains the same throughout the year. The months of June, July, August, and September are associated with high humidity and rainfall with strong winds with a fall in temperature. Two warm and damp months during October and November of

southwest monsoon bring little or no rains. The months of December, January, and February having a dry and comparatively cool climate. Finally, in March, April and May, the humidity is relatively less with high temperatures. However, the climate is relatively uniform throughout the coastal stretch while the inland is relatively cooler.

1.2.3 Rainfall

The west coast experiences heavy rainfall of about 3000-5000 mm/yr, and most of the rainfall is due to Orographic and Convective precipitation. The tropical climate during the monsoon experiences convective winds from the southwest, which are usually local and results in high-intensity rainfall. The Western Ghats are the source for Orographic rainfall to the high lands making the east side of the rain shadow zone. The annual average rainfall over the basin is around 4000 mm. The depth of rainfall is more in the high land and hinterland near the Western Ghats. The rainfall in the Ghat section ranges from 4900mm to 5900mm and in the coastal belt from 3500mm to 4500mm.

1.2.4 Temperature

There are few meteorological observatories available with respect to temperature. The average temperature throughout the year is around $30^{\circ}\text{C}\pm 5$ (<http://www.imd.gov.in>).

1.2.5 Humidity

The relative humidity is high during the southwest monsoon. The Gurgur catchment is characterized by high humidity $>78\%$ (<http://www.imd.gov.in>). Over the last 16 years, the average runoff is 3500 mm for Gurgur River (Central Water Commission CWC, Government of India GOI). The Potential evapotranspiration (PET) estimates around 1400 mm along the coast.

1.2.6 Vegetation

The type of climate is reflected by the type of vegetation grown or vice versa. The high rainfall, humidity, and salinity associated with highly permeable lateritic soil support a wide variety of vegetation species, from evergreen forests to coastal mangroves, including the sparse vegetation in lateritic soils. The hinterland (midland) is associated

with densely cultivated Areca nut and Coconut trees along the river flow. Paddy and cashew are the other crops grown in the area.

1.3 Scope of the study

The earth is heterogeneous in composition and nature. Therefore the sub-surface is unknown, which means that the sub-surface shows spatial variation. Also, because of the dynamic geological activities of the earth, the nature of sub-surface structures may change. These geological structures are the main conduit for groundwater in hard rock terrains like the study area. Therefore, scientific understanding requires generating data of the sub-surface using cost-effective and reliable methods. The direct method (drilling) is too costly to carry out. Thus, there is a need for indirect methods (economically feasible) like geophysical methods, RS & GIS, modelling, and simulations. Even though water is a natural and renewable resource, much scarcity exists concerning groundwater quantity and quality. Thus with regard to water management, there is scope for groundwater potentiality, groundwater recharge potentiality, and groundwater quality studies. The groundwater quality is dynamically changing, and thus temporally, we cannot expect the same groundwater quality at the same place throughout the year. The GIS and mapping techniques are highly preferred nowadays because, with proper information, the maps provide maximum information graphically, spatially, temporally, and with legend information.

The artificial recharge structures can be suggested for targeted sites to improve groundwater quality and quantity (GW). This research work attempts to furnish first-hand information to local authorities and planners about suitable places for groundwater exploitation, type of the wells and bore wells required, depth of wells required, quality of the groundwater, site suitability for GW recharge structures, and type of recharge structures to be constructed. This type of work can be replicated in other river basins/catchments, especially in hard rock terrain.

1.4 Objectives

This study aims to use multi-disciplinary approaches like electrical resistivity, RS, GIS, groundwater quality parameters for identifying and mapping the groundwater

potentiality, groundwater recharge potentiality, and water quality index of Gurpur watershed Karnataka, India. The main objectives of the research work carried out are,

- a) To identify the Groundwater Potential Zones (GWPZ).
- b) To study the groundwater quality using the Water Quality Index of the study area.
- c) To identify suitable sites for Artificial Recharge Structures (ARS) based on groundwater recharge potentiality index.

1.5 Organization of thesis

Chapter 1 covers the general introduction to water resources, especially groundwater exploration. It also covers the study area description and location, scope, objectives of the study, and the thesis outlay.

Chapter 2 is the review of the literature regarding all the aspects of the research work carried out. It begins with a general introduction to water resources and multi-disciplinary applications in groundwater studies. This chapter links the geology, geomorphology, hydrogeology of the study area to the groundwater exploration studies.

Chapter 3 is the geology and geomorphology, which outlines a great deal of information about the surface and subsurface lithology, the geological structures, and their relationship with groundwater exploration in the study area. Geomorphology is an essential parameter for understanding groundwater exploration. The surface shape and deformation taking place give much information regarding its relationship with groundwater. Also, detailed morphometric analysis is carried out to understand the study area's geomorphology better.

Chapter 4 deals with groundwater exploration studies. In this chapter, the electrical resistivity method (a geophysical method) is used as an indirect means of collecting the sub-surface data. Later the resistivity data is interpreted using two of the most used interpretation techniques. The weathered zone or depth to bedrock (DBR) is identified using the resistivity data. This method is also used for finding the aquifer dimensions and aquifer parameters. The resultant thematic information is used for spatial distribution studies and their relationship with groundwater exploration studies. Also, multiple thematic information which is interrelated with respect to groundwater is used for multi-criteria analysis. And the resultant is the GWPZ thematic map.

Chapter 5 deals with the groundwater quality aspects, which is also an essential factor for the potential use of groundwater. In this chapter, a detailed study of drinking water quality is conducted for the study area. Also, the quality assurance practices or checking the correctness of analysis (APHA et al. 2012) is employed to improve the quality of the data used in water quality analysis. The correlation studies are conducted to understand the inter-relationship between the water quality parameters.

Chapter 6 discusses the groundwater recharge studies conducted in the study area. It includes the multi-criteria analysis methodology for identifying the groundwater recharge potentiality zones. Later the site suitability analysis for the selected artificial recharge structures is carried out. As a result, the best possible locations and ideal recharge methods can be employed for attaining the maximum recharge possible. The groundwater recharge estimation methods are employed for studying the amount of recharge possible.

The major conclusions of the investigations are summarised in **Chapter 7** of the thesis. Also, the scope for future work or the recommendations are given in this chapter.

After all the major chapters, the additional data, which is not much needed in the thesis but required for detailed studies, are **references**. All the cited literature is presented in the form of a bibliography. The references are ordered in research papers, books, reports, internet material, and websites. The sorting is carried out based on the author's names in alphabetical order.

An appendix follows references. **Appendix A** consists of the electrical resistivity raw data, data plots of Curve Matching Technique (CMT) and Inverse Slope Method (ISM) of all the 35 VES locations. **Appendix B** consists of the water quality data for all three phases of the study. **Appendix C** consists of plates of field and laboratory work photographs. **Appendix D** consists of a brief resume and the publication details.

Chapter 2

REVIEW OF LITERATURE

2.1 General

Writing the review of literature is an integral part of any thesis. The literature review is a "legitimate and publishable scholarly document." (LeCompte et al. 2003) with some modifications. It provides a solid basement or structure for conducting any research work, and it facilitates the valid reasons for the methodology adopted. Also, it gives an insight into the previous research before proposing the improved methodology or new findings (Randolph 2009). This chapter intends to provide an overview of the work done on groundwater. It provides an insight into the groundwater scenario, especially the groundwater exploration, quality, and recharge aspects. It discusses several types of methodologies adopted by the research community concerning those as mentioned above. It tries to emphasize the importance of electrical resistivity and geoinformatics in groundwater studies. Finally, this review chapter concludes with a discussion on suitable artificial recharge structures and recharge estimation methods for better groundwater resource management.

Jha et al. (2007) suggested that groundwater is one of the most valuable natural resources which supports human health, economic development, and ecological diversity. But, the understanding of the earth's sub-surface is a complex task because of the earth's heterogeneous composition and dynamic nature. Therefore, the economic exploration and exploitation of groundwater are challenging. Groundwater is contained in what is called 'aquifers.' An aquifer is a geological formation or part of it, consisting of permeable material capable of storing/yield a significant quantity of water. A fair understanding of the groundwater status must include scientific studies on groundwater exploration, recharge, water quality, and management aspects (Karanth 1987). The scientific studies of groundwater are essential in the present scenario, where the demand for groundwater is increasing day by day (Oseji 2010; Majumdar et al. 2016; Virupaksha & Lokesh 2019).

The dynamic geological activities of the earth may cause changes in the structures (folds, faults, joints, fissures & cracks). These geological structures are the main conduit for groundwater in hard rock terrains such as the Gurgur watershed (study area). Therefore, scientific understanding requires generating data of the sub-surface using cost-effective and reliable methods. The direct interpretation (drilling) is too costly to carry out. Thus, there is a need for indirect methods (economically feasible) like geophysical methods, Geographic Information System, Remote Sensing, modelling, etc. Water is a natural and renewable resource, but the qualitative and quantitative water scarcity is immense. The groundwater Quality is dynamically changing, and thus, temporally, we cannot expect the same groundwater quality at the same place throughout the year. Therefore, spatial and temporal mapping of GW is of great importance. And thus, the GIS mapping is highly desirable. The maps provide complete information graphically, spatially, temporally, and with proper legend information with accurate data. In this regard, there is much scope for groundwater potentiality, groundwater recharge potentiality, and groundwater quality studies.

Nowadays, groundwater exploration using multi-disciplinary fields like RS & GIS, geophysics, geology, geomorphology is getting wide recognition. Remote sensing and GIS techniques efficiently minimize the time, labour, and money and make quick, sustainable water resource management (Tiwari & Shukla 2015). In the recent past, the MCDM, WOA, MIF, and several other integration techniques prove effective for resource mapping and management, especially natural resources like water. The MCDM technique plays a vital role in water resource quantification and management. More emphasis is to be given initially, as the weightage is given for better and more accurate results (Chowdary et al. 2013; Okoli et al. 2017; Okoli et al. 2019). Senanayake et al. (2016) emphasize that a Multi-Influencing Factor is a subjective approach, where the accuracy of the final results depends significantly on the thematic information and their weightage factor. The potential use of a combined GIS-MCE approach for developing spatial decision support systems plays a vital role in GW resource mapping (Carver 1991; Carver 2017).

The quality of the groundwater is important for the existence of life. Most living organisms, including humans, use GW directly for drinking and domestic

purposes (Anwar & Aggarwal 2015). Therefore, the need for groundwater quality studies (especially for drinking water) is also one of the major concerns (Department of Mines and Geology 2011; Central Ground Water Board 2015).

Groundwater management is always considered to be the balance between withdrawing and recovering the aquifers. Kumar et al. (2008) emphasize that the construction of small water harvesting structures is gaining importance in recent years as they can be spatially distributed and cover maximum area. Todd & Mays (2005) noticed the complexity of the aquifers and subsurface, which may mislead to propose improper recharge structure. There are several variables to be considered for accurate results. Therefore, multi-criteria analysis is constructive in this regard. The ARS can be suggested for targeted sites for improvement of both quality and quantity of the groundwater.

2.2 Electrical Resistivity technique for mapping sub-surface

Electricity is the phenomenon associated with the flow of electrons (the negatively charged particles) and is best explained in "Electron Theory" (Partridge 1908). This phenomenon is always associated with the terms conductivity and resistivity. Electrical conductivity is the measure of a material's ability to allow the transfer of electricity through it. At the same time, electrical resistivity measures a material's ability to restrict the transfer of electricity through it. Therefore, their relationship is inversely proportional to each other. The electrical resistivity varies significantly for different materials of different compositions (Herman 2001). The electrical resistivity method is based on Ohm's law, coupled with equations for apparent resistivity calculation. The variables in Ohm's law are voltage (V) or the potential difference between electrodes, current (I), and resistance (R).

The electrical resistivity method is employed so that the only variable is R. That is, a known amount of current is used with a known amount of electrode spacing (because the potential difference is the factor of the length of the conductor). The potential difference (voltage) measurement at the potential electrodes is used to obtain the apparent resistivity.

This wide range of resistivities is greatly helpful in groundwater studies. The thickness of the material, composition, aquifer parameters (porosity, permeability), and associated structures play a significant role in electrical resistivity measurement. Water is a good conductor of electricity. So the presence of water gives less resistance relatively, which will give out the possibility of the water source.

The electrical resistivity method is one of the geophysical methods utilized to explore the sub-surface using physics laws indirectly. The working principle of the electrical resistivity method is to measure apparent resistivity at different depths. There are several geophysical methods available based on the physical law applied. The seismic prospecting involves recording the time intervals and intensity of the earth's elastic wave energy (seismic waves), reflected from a targeted depth (Dobrin & Savit 1988). On the contrary, gravity and magnetic method involve measurement of the natural force field of the earth. The electrical and electromagnetic methods involve reflection and refraction principles, and the source can be either natural or artificial. The gravity or magnetic methods measure the combined contribution of all the levels of depth.

In contrast, the seismic and electrical methods can give detailed and precise information of different depths. The seismic methods are beneficial in probing greater depths. Therefore, a seismic method is widely applicable in oil and natural gas exploration. Whereas the electrical resistivity method is widely applicable in groundwater exploration, and thus it is utilized in this study.

Our earth is heterogeneous in composition and thus shows a different range of electrical properties. Vertical Electrical Sounding (VES) is the method that is based on the electrical conductivity or resistivity of the sub-surface materials. This method is widely used for 1-dimensional depth probing. Other methods like electrical imaging for 2-D and electrical tomography for 3-D studies are gaining recognition nowadays. The four-electrode VES method with Schlumberger electrode configuration is still the favoured method for groundwater studies.

The formula for calculating apparent resistivity (ρ_a) of Schlumberger array can be seen in equation 2.1.

$$\rho_a = \left[\frac{\pi \left[\left(\frac{AB}{2} \right)^2 - \left(\frac{MN}{2} \right)^2 \right]}{2 \left(\frac{MN}{2} \right)} \right] * R \quad (\text{equation 2.1})$$

Where AB is the distance between current electrodes, MN is the distance between potential electrodes, and R is the resistance.

The ρ_a for each current electrode separation is calculated by multiplying the resistance value by Schlumberger configuration factor (Ramanuja 2012; Poongothai & Sridhar 2017). In 1934, the VES was first presented by Schlumberger for 1-dimensional work. Later on, a wide variety of VES systems was presented, but the Schlumberger method is still accepted as the best for depth probing (sounding) and depth profiling. Different electrical resistivity methods like Wenner array, Schlumberger, Pole-Pole, dipole-dipole, pole dipole, half Schlumberger method are available. These could be utilized based on the type of work be conducted. The Schlumberger method is suitable for depth probing, while the Wenner method is suitable for lateral variations at the same depths (Loke 2001).

There are different methods of analysing resistivity-sounding data, like qualitative and quantitative methods. Again, there are several methods in quantitative as well as qualitative interpretation methods. However, VES data can be interpreted by different techniques to get the subsurface profile, layer thickness, and true resistivity. The confusion occurs during the selection of suitable methods of interpretation, as the accuracy of the result largely depends on the interpretation technique (Asije & Igwe 2014; Prabhu & Sivakumar 2018). The CMT and ISM are widely utilized for interpretation.

The ISM is a direct method suggested by (Narayan & Ramanujachary 1967; Ramanuja 2012). The Quantitative analysis technique, which is popularly known as the "Curve matching technique" can interpret the results by comparing them to the standard curve types. Once the graph plots are ready, both qualitative and quantitative analysis can be done. There are standard curves like H-type, A-type, K-type, and Q-type, along with the combinations of those for the number of earth's layered subsurface. These standard curves and set of curves provides the basic understanding of the curve

matching technique. The ISM is simple to operate and gives good results (Narayan & Ramanujachary 1967).

The quantitative interpretation provides the details of the number of layers and their true resistivity, the thickness of the layer, and the depth encountered. In comparison, the qualitative interpretation is made using the curve matching technique (Barseem et al. 2015), which gives information about the curve type and several layered formations. Based on these curve types, the lithology and groundwater potential is interpreted. Generally, lineaments are associated with weathering and therefore increases porosity and permeability. Hence, lineament density and groundwater potential have a direct relationship (Hardcastle et al. 1995). The weathered zone hosts groundwater in its fissures, fractures, and pore spaces of the weathered rocks (Gurumurthy 2013).

The VES data can also be utilized to calculate the aquifer parameters, Dar-Zarrouk (D-Z) parameters like hydraulic conductivity, transmissivity, porosity, aquifer thickness (Singhal et al. 1998; Ekwe et al. 2006; Mahajan et al. 2015; Asfahani 2016). Niwas & Singhal (1981) found an analytical relationship associated with hydraulic parameters and D-Z parameters, i.e., an analytical relationship between aquifer transmissivity (T) and transverse unit resistance (TR) methodology for calculating aquifer parameters. The following methodology can achieve this well-established relationship.

The highly resistive subsurface medium shows an inverse relationship with the hydraulic conductivity (K) and resistivity (ρ) passing horizontally in a typical unit column of an aquifer. The electric current in the highly conductive medium exhibits vertical flow. However, hydraulic conductivity exhibits horizontal flow, indicating the direct relationship between ρ_0 and K. Consider the unit cross-section of an aquifer medium from top to bottom in the vertical prism form; the K obeys Darcy's law and ρ in the aquifer medium obeys Ohm's law. These two laws are combined using prism form (Niwas & Singhal 1981). Also, the Transmissivity is proportional to the transverse unit resistance (Niwas et al. 2011). The hydraulic and geoelectric parameters of an aquifer and their relationship are controlled by the composition and subsurface lithology of the aquifers (Niwas & Lima 2003). If the aquifers transmit the maximum

amount of water, it indicates the possibility for recharge potential, especially in humid regions. Lesser no transmissivity of the aquifers below the groundwater table indicates either the poor hydraulic conductivity or the lack of potential recharge zone.

Maillet (1947) suggested that the average geoelectrical properties of the subsurface formations can be outlined by parameters known as D-Z parameters. The surface resistivity and the thickness of different geoelectrical layers help obtain D-Z parameters. Several studies have been conducted on D-Z parameters and their relationship with aquifer parameters (Henriet 1976; Reghunath 1999; Utom et al. 2012; Batayneh 2013). The D-Z parameters coupled with pumping test results help establish empirical relationships and the hydraulic behaviour of the aquifers (Arétouyap et al. 2019). The layer resistivity and layer thickness (h) are the crucial components of geoelectric layers. The different types of D-Z parameters are Longitudinal Unit Conductance (S), Transverse unit Resistance (TR), and Aquifer Anisotropy (λ)

The variation of the S value of each layer can be utilized qualitatively to identify the low resistivity materials and their thickness (Zohdy, 1969). Large values interpret the high thickness of the layers. In contrast, the lesser thickness of shallow basement is interpreted by smaller values of S . Usually, λ will be near to unity and exceeds for the rocks having high resistivity, indicating that lesser the λ greater will be the Porosity and permeability (Keller & Frischknecht 1966).

Consider the unit cross-section of an aquifer medium from top to bottom in the vertical prism form; the K obeys Darcy's law, and ρ in the aquifer medium obeys Ohm's law. These two laws are combined using prism form (Niwas and Singhal, 1981). The aquifer medium with uniform resistivity and saturated with water will be constant for either TR or S .

For the highly resistive aquifer medium, the transmissivity will be proportional to longitudinal unit conductance. Also, for a highly conductive medium, the transmissivity is proportional to the transverse unit resistance (Niwas, et al., 2011).

All the minerals and rocks have high resistivity except a few. Therefore the electric current passing through water-saturated pore spaces will exhibit less resistivity. From Archie's law (Archie, 1942), the resistivity of the saturated clay-free material can be expressed.

Humble Oil Company first postulated the relationship between the Formation factor (F) and Porosity (\emptyset). The constants a and m are empirical with values 1 and 2, respectively, for a general average of typical reservoir rocks (Winsauer & Shearin 1952).

Once the hydraulic conductivity, transmissivity, and porosity are calculated, the thematic information is generated using Inverse Distance Weighted (IDW) method in the ArcGIS environment. This thematic information is integrated along with other thematic layers (Virupaksha & Lokesh 2019).

2.3 Geology and geomorphology

The geology and geomorphology of any basin are essential to understand the subsurface dynamics as the aquifers are composed of different rock types. The majority of the world's aquifer systems are made up of hard rocks. And therefore, groundwater is found only in rocks with secondary porosity like folds, faults, unconformity, fissures & cracks. In any hard rock terrain, the thickness of the soil and weathered zone together plays a vital role in groundwater availability. The weathered zone hosts groundwater in its fissures, fractures, and pore spaces of the weathered rocks. Geomorphology is the study of landforms (surface features) and their formation or evolution process. Geomorphology provides scientific evidence about the topographic and bathymetric features at or near the earth's surface. Therefore, by understanding the mechanisms and forces that happened in the past, the future could be extrapolated.

Morphometric studies of a river basin comprise discrete morphologic regions and have particular relevance to drainage patterns and geomorphology (Strahler 1957; Dornkamp & King 1971; Krishnamurthy et al. 1996). Drainage basins are the fundamental units to understand geometric characteristics of a fluvial landscape such as topology of stream networks, quantitative description of drainage texture, pattern, shape, and relief characteristics (Abrahams 1984). The coastal region possesses a specific set of geomorphological landforms. The west coast extends as a narrow stretch (about 10 km to 80 km) along the Arabian Sea in the west, to the Western Ghats in the east, and extends towards the north-south. The Karnataka state comes in the peninsular region of India in the Asian continent. Karnataka is classified into two geomorphic

zones - Coastal landform terrain and Karnataka Plateau terrain, the two zones being separated by Western Ghats scarp (Sreedhara Murthy & Raghavan 1994; Ranganathan & Jayaram 2006). The orientation of the peninsular west coast of India is towards the NNW-SSE direction (Raghavan 1988).

The Gurpur watershed is associated with the Nethravathi watershed in coastal Karnataka. Previously, many studies were carried out in and around this location. The geology, geomorphology, morphometric analysis, and structural studies have already been conducted (Radhakrishna 1967; John & Cheriyan 1974; Balasubrahmanyam 1978; Subrahmanya & Jayappa 1987; Chandrasekharappa 1989; Radhakrishna 1989; Subrahmanya & Grangadhara Bhat 1995). The groundwater quality, pollution, and hazard studies have also been carried out in the study area (Gajendragad & Ranganna 1989; Narayana & Suresh 1989; Ranganna et al. 1991). Ion chemistry and trace elements study have been conducted (Gurumurthy et al. 2014). Pumping tests and aquifer parameters were studied in and around the study area (Reghunath 1999). The studies on infiltration properties of the river and soil types are also conducted (Ranganna et al. 1991).

There are various hypotheses regarding the origin of western ghats and can be grouped as escarpment hypothesis; erosional origin; hypothesis of the dead cliff, etc., (Dikshit 1981). Based on the geological, geomorphological, and geophysical evidence, it is stated that the western ghats represent the edge of the disrupted continental block during the early Miocene (Radhakrishna 1967). Subramanya (1987) argued that the Western Ghats is the fault that receded due to marine erosion forming cliff.

The Indian peninsula dates back to the Precambrian era, and the oldest rocks are identified in this region. Geologically, Karnataka comprises the rock formations of diverse types from Archaean to Quarternary age. The plateau is the largest physiographical division of Karnataka. Radhakrishna and Vaidyanathan (1994) have opined that the ages of most landforms in Karnataka perhaps range from Eocene to Recent. However, they have formed rock formations ranging from Archaean to Quarternary. A large portion of the Darwar craton is made up of pre-cambrian rocks. The Karnataka coast is a linear belt traversing from Karwar, north to Mangaluru in the south (about 400 km). The coastline of Karnataka is associated with rocky coast and

barrier (Radhakrishna 1993). The present landscape along the coast is the reflectance of extensive Tertiary denudation, which leads to the formation of laterites. The Quarternary formations are found along the coast, which includes boulders, pebbles, and cobble beds in paleo-river channels (Gurumurthy 2013).

The morphological parameters can be extracted from the CartoSAT-1 or Shuttle Radar Topographic Mission (SRTM) or Advanced Spaceborne Thermal Emission and Reflection Radiometer (ASTER) Digital Elevation Model (DEM) data. Each data have its intrinsic errors due to data acquisition from satellite sensors. Das & Pardeshi (2018) suggested that CartoSAT DEM is most suitable for the Indian Territory than ASTER and SRTM. Mukherjee et al. (2012) found that the vertical accuracy of ASTER and SRTM data was having Root Mean Square (RMS) error of 12.62m and 1.6m, respectively. Rawat et al. (2013) revealed that relative RMS error of horizontal accuracy was about 2.17 for SRTM and 2.817 for ASTER DEM with respect to CartoSAT DEM.

Several researchers have accomplished this methodology over the years and provided a firm basement for this methodology (Agarwal 1998; Avinash et al. 2011; Joseph Markose et al. 2014; Sarkar et al. 2020; Oyedotun 2020). The contributing basin area can be extracted with the help of various geoprocessing techniques in ArcGIS 10.2. Flow direction data can be extracted from the subset DEM file, and it can also be used for delineating the basins. The various hydrological processing of spatial analyst tool helps in demarcating watershed boundary. For defining watershed boundary flow direction, raster data is being used as a base map. DEM derivatives that can be extracted are drainage, slope, hill shade, and contour. The output of this method is the basis for creating a stream/drainage network grid with stream order. As pointed out, Strahler's classification system designates a segment with no tributaries as a first-order stream. Whenever two same stream order joins, it will form a higher stream order and so on (Strahler 1964).

The contour interval of a contour map is the difference in elevation between successive contour lines. These lines help to deduce the slope direction and angle. Slope provides a basis so that by successive combination into layer units, general geomorphology could be constructed. A slope grid is identified as "the maximum rate of change in value from each cell to its neighbours" in DEM data (Burrough 1986). The

slope is a necessary terrain parameter for land utilization, land availability, and land capability assessment rather than aspect and altitude. The All India Soil and Land Use Survey guidelines on slope categories are followed for slope classification. The hill shade tool provides the hypothetical illumination values for each cell in raster data. It does this by setting a position for a hypothetical light source and calculating the illumination values of each cell in relation to neighbouring cells. It enhances the visualization effects by using transparency and overlaying on other thematic layers. It gives the 3D impression depending upon the angle of illumination.

Magesh et al. (2012) emphasized that the geomorphology of any drainage basin can be quantitatively explained using morphodynamic evaluation of drainage data. In the extraction of the drainage system, the flow direction and flow accumulation data are to be extracted first using various geoprocessing tools. It will be followed by stream ordering based on Horton's law. According to this law un-branched stream is termed a first-order stream. When two first-order streams join, it is designated as second-order, followed by two second-order streams joining to form third-order and so on (Horton 1932).

Morphometric parameters under linear, aerial, and relief features can be computed using standard methods and formulae. The fundamental parameter, namely, stream length, area, perimeter, number of streams, stream length, and basin length, are to be derived from the drainage layer. The values of morphometric parameters, namely; bifurcation ratio (Rb), drainage density (Dd), stream frequency, form factor, texture ratio, elongation ratio, circularity ratio (Rc), are prepared based on the formulae suggested (Horton 1945; Miller 1953; Schumm 1956).

The drainage density is the ratio of total stream length to the basin's total area (Horton 1932). The density factor is related to climate, type of rocks, relief, infiltration capacity, vegetation cover, surface roughness, and runoff intensity index. The lower drainage density of any watershed indicates that it has permeable subsurface material, good vegetation cover, and low relief, and vice versa. Drainage density is calculated as the "ratio of the total length of streams of all orders within the basin to the basin area" (Reddy 2004) and expressed as km/km². The orientation and style of the drainages have a relationship with lineaments as they are associated with structural complexity

(Shahzad et al. 2009). The total number of drainages of all orders per unit area is called stream frequency (Horton 1932). Stream frequency is inversely related to permeability, infiltration capacity and directly related to the relief of watersheds. The R_c is the ratio of the area of the basins to the area of the circle having the same circumference as the perimeter of the basin (Miller 1953). It is mainly concerned with the length and frequency of streams, geological structures, land use/land cover, climate, relief, and slope of the basin. Higher R_c indicates the circular shape of the watershed and the moderate to high relief and permeable surface.

The form factor is the ratio between basin area and the square of basin length (Horton 1932). The value of F_f should always be less than 0.78 in a perfectly circular basin. The higher values of form factors have high peak flows of shorter duration, and low values of form factors have lower peak flow for a shorter duration.

Elongation ratio is defined as the ratio of the diameter of a circle having the same area as the basin and maximum basin length. The watershed shows lower elongation ratio values that are highly susceptible to erosion, and the higher values indicate high infiltration capacity and low runoff.

The drainage texture is the total number of drainages of all orders per perimeter of that watershed (Horton 1945). The drainage texture depends on the climate, rainfall, vegetation, rock and soil type, infiltration capacity, relief, and stage of development of a basin (Smith 1950). The $d_t < 2$ indicates very coarse, between 2 and 4 is related to coarse, between 4 and 6 is moderate, between 6 and 8 is fine, and >8 is very fine drainage texture.

According to (Gravelius 1914), the compactness coefficient of a watershed is the ratio of the perimeter of a watershed to the circumference of the circular area, which equals the watershed area. The Compactness Coefficient of a watershed is directly related to the infiltration capacity of the watershed.

The shape factor provides a measurement of basin shape irregularity. The basin would be a perfect circle if the shape factor = 1, successively, lower factors represent a more convoluted flow, and close to 0 = approaching a line.

The constant of channel maintenance (C) is the inverse of drainage density (Schumm 1956), which depends on the rock type, permeability, climatic regime,

vegetation cover, relief, and the duration of erosion. It is also the area required to maintain one linear kilometre of the stream channel. Generally, the higher the C values of the basin, the higher the permeability of the rocks of that basin and vice-versa (Rao 2009).

2.4 Geoinformatics and groundwater exploration

The Multi-spectral and Hyper-spectral imageries provide data in many bands of the electromagnetic spectrum. These unique band data can be used to analyse the same features at a different wavelength, thus uniquely responding to it. As a result, the spatial-temporal information of large and even inaccessible locations can be utilized efficiently and thus forms the baseline information (Jha & Peiffer 2006; Jha et al. 2007; Kumar & Kumar 2010; Yousef et al. 2015). The GIS is a practical framework for easing and efficiently handling large and complex spatial data, integration, and analysis (Becker 2006; Thapa et al. 2017). The GWPZ studies integrate several surfaces and sub-surface indicative features (thematic information), either by direct or indirect scientific methods.

The land use/land cover analysis is essential to know the spatial distribution of land resources. In this study, Level-I classification of the National Remote Sensing Centre (NRSC) for lu/lc is used. The orientation and style of the drainages have a relationship with lineaments as they are associated with structural complexity (Shahzad et al. 2009). Generally, lineaments are associated with weathering and therefore increases porosity and permeability. Hence, lineament density and groundwater potential have a direct relationship (Hardcastle et al. 1995).

2.5 Groundwater exploration studies

Various works by researchers have established a close relationship between groundwater study, Remote Sensing, and GIS (Solomon & Quiel 2006; Babiker et al. 2007; Balakrishnan et al. 2011; Shekhar & Pandey 2015). The merit and demerit of the features and their influence over groundwater occurrence are precisely the points of consideration for assigning suitable weights (Jaiswal et al. 2003). Saaty (1980) developed the "Analytic Hierarchy Process (AHP)," which is a widely accepted and used MCDM technique in the field of Hydrogeology. In the MCDM technique, the

eigenvector of the square reciprocal matrix used to compare all possible pairs of criteria, which is possible, will be utilized for assigning Weights (Chowdary et al. 2013). Since then, the international scientific community has accepted AHP for the analysis of complex decision problems. Saaty emphasized that the AHP method has numerous applications in natural resources, environmental, hydrogeological planning & management.

There are several other suitability analysis types available. One of them is the "Weighted Overlay Analysis" which will allow us to combine, weight, and rank several different types of thematic information (Waikar & Nilawar 2014; Acharya et al. 2019; Das et al. 2019; Gyeltshen et al. 2020). The potential use of a combined GIS-MCE approach in the development of spatial decision support systems plays an important role (Carver 1991).

The rainfall data is collected from the India Meteorological Department (IMD) stations, Department of Mines and Geology (DMG), Central Groundwater Board (CGWB), , and Statistical Department, Mangaluru. Groundwater contour (GWC) map of the Gurple catchment is prepared using the observatory wells data of the groundwater level obtained from DMG and CGWB.

2.5.1 Integrated approach for GW exploration

The integration of several methodologies for obtaining better results is a trending development in recent studies. Several studies are carried out using the integrated approach (Khan & Moharana 2002; Anomohanran 2011; Bhattacharya et al. 2020; Warsi et al. 2020). The geospatial studies integrated with geophysical, geological, geomorphological, hydrological, socio-economical, geochemical can be used for integrated studies.

The weighted overlay index (or the weighted index overlay) is an important technique used in the integrated approach for modelling suitability (Gyeltshen et al. 2020). The WOA is used to solve multi-criteria problems such as site selection and suitability models (How Weighted Overlay works-ArcGIS Help). Venkateswara Rao & Briz-Kishore (1991) suggested that sum of the product of normalized weights (subscript w) of the thematic layers with their respective ranks (subscript r) of the classes

forms the Groundwater Potential Index (GWPI) as given in equation 2.2. The thematic information that needs to be integrated varies depending upon the data available for the researchers. Thematic information from 6 to 8 layers is most common (Venkateswara Rao & Briz-Kishore 1991; Kumar et al. 2009; Kumar & Kumar 2010; Srivastava et al. 2012; Shekhar & Pandey 2015; Bhattacharya et al. 2020). Therefore, it is suggested that more thematic information may yield more accurate results.

$$\begin{aligned}
 \text{GWPI} = & [(Lw) * (Lr)] + [(LULCw) * (LULCr)] + [(Gmw) \\
 & * (Gmr)] + [(STw) * (STr)] + [(Slw) * (Slr)] \\
 & + [(DDw) * (DDr)] + [(GWCw) * (GWCr)] \\
 & + [(RDw) * (RDr)] + [(LDw) * (LDr)] + [(DBRw) \\
 & * (DBRr)] + [(\Phi w) * (\Phi r)] + [(Kw) * (Kr)] \\
 & + [(Tw) * (Tr)]
 \end{aligned}
 \tag{equation 2.2}$$

Where, L-Lithology, LULC-Land Use & Land Cover, Gm-Geomorphology, ST-Soil types, Sl-Slope, DD-Drainage density, GWC-Groundwater contours, RD-Rainfall distribution, LD-Lineament density, DBR-Depth to bedrock, Φ – Porosity, K-Hydraulic Conductivity, and T-Transmissivity

A few of the primary thematic information used for integration of GWPZ are lithology, lu/lc, geomorphology, soil types, lineament density, slope, contours, and groundwater contours (groundwater level). Other than these thematic layers, few others can also be utilized. Thematic layers like hydraulic conductivity, porosity, transmissivity, rainfall distribution, drainage density, depth to bedrock, soil depth can also be utilized along with several others depending upon the necessity. This thematic information is either directly or indirectly related to groundwater potentiality. The relationship of each thematic layer with respect to groundwater potentiality is explained below.

The transmissivity can also be calculated using electrical resistivity data. Therefore, if the aquifers transmit the maximum amount of water, it indicates that recharge potential is high, especially in humid regions. Less or no transmissivity of the aquifers below the groundwater table indicates either the poor hydraulic conductivity or the lack of potential recharge zone.

Poor hydraulic conductivity indicates a lack of potential aquifer zones. Therefore ranking of 3 is given to the high K class. The porosity is having a direct

relationship with groundwater potentiality. An increase in porosity, especially effective porosity, increases the groundwater potentiality.

2.6 Groundwater quality studies

Several studies are conducted for mapping groundwater vulnerability with the DRASTIC model (Rahman 2008; Thapa et al. 2018) and WQI approach using Geoinformatics (Shivanna & Nagendrappa 2015; Gidey 2018; Mukate et al. 2019; Adimalla & Qian 2019). A close relationship between groundwater quality and industrial pollution (point source) is established as per various literature (Asadi et al. 2011; Osibanjo & Majolagbe 2012; Basavaraddi et al. 2012; Rao et al. 2013; Nas & Berktaş 2014). The leaching of heavy metals (toxic metals) from landfills, industrial and biomedical wastes from solid waste dump sites pose a serious threat to the groundwater quality (Patel & Devatha 2019). Even though saltwater intrusion is a natural phenomenon, it poses a threat to coastal aquifers in water quality. The leaching of noxious chemicals into the subsurface, which has been polluting the deeper aquifers, has become a point of precarious consideration. The reliable and accurate results depend on reliable and accurate initial data used in the research. Therefore, verifying the accuracy of the data is vital in any research work, and hence the systematic approach of CCA can be employed. The CCA method will boost the confidence in the data generated, and several studies are conducted in this regard (Friedman & Erdmann 1982; APHA 1999; Rao et al. 2013). Also, correlation studies can be conducted. A statistical tool like correlation studies is widely used for analysing the concentrations, monitoring and evaluating the water quality (Paudyal et al. 2016; Shrestha & Basnet 2018). The correlation studies reduce uncertainty and understand the interrelationship between different variables (Joshi et al. 2009).

The groundwater samples can be collected and analysed with respect to drinking water standards (Bureau of Indian Standards 2012). The groundwater samples are to be analysed for ionic and non-ionic constituents.

2.6.1 Quality Assurance Practices (QAP) for water quality analysis

The QAP or CCA constitutes the GW quality parameters like Potential of hydrogen (pH), electrical conductivity (EC), Total Dissolved Solids (TDS), Major cations, and

anions. The following procedures for CCA are considered for general and drinking water quality (APHA 1999).

2.6.1.1 Anion – Cation Balance (ACB)

ACB is one of the most utilized CCA methods (equation 2.3). The sums of anion and cation should be balanced and expressed in mill equivalents per litre (meq/l). The potable water is electrically neutral; thus, the anions and cations should be balanced.

$$\text{Percentage difference} = 100 * \left(\frac{\sum \text{cations} - \sum \text{anions}}{\sum \text{cations} + \sum \text{anions}} \right) \quad (\text{equation 2.3})$$

The criteria of acceptance (Table 2.1) considered for the present work is ± 0.2 meq/l as the Total Anions (TAn) or the Total cations (TCat) are well within the range of 0-3 meq/l.

Table 2.1 Typical criteria for acceptance of percentage difference of ACB

Anion sum	Acceptable difference
0 – 3.0	± 0.2 meq/l
3.0 – 10.0	± 2 meq/l
10.0 – 800	± 5 meq/l

2.6.1.2 Total Dissolved Solids (TDS)

The Calculated Total Dissolved Solids (CTDS) can be tabulated for all the groundwater samples. Later the results can be considered for correlation studies. The analysis for Measured Total Dissolved Solids (MTDS) was conducted in the laboratory. The MTDS must always be equal to CTDS, provided analysis is done without any error. The concentration of MTDS should always be higher than that of CTDS because a significant contribution may not have been considered for calculation. The acceptable ratio for TDS is considered for checking the correctness of the analysis.

$$1.0 < \frac{\text{measuredTDS}}{\text{calculatedTDS}} < 1.2 \quad (\text{equation 2.4})$$

2.6.1.3 Measured EC and Ion sums

The total anions or the total cations should be $1/100^{th}$ of the measured electrical conductivity (MEC) value. The acceptable criteria give the relationship of MEC with the TAn or TCat.

$$100 * TAn \text{ (or TCat)} = (0.9 - 1.1) * EC \quad \text{(equation 2.5)}$$

The equation 2.5 can be re-written in a simpler notation as,

$$(0.9 * EC) \leq 100 * TAn \leq (1.1 * EC) \quad \text{(equation 2.6)}$$

Where TAn (or TCat) is in meq/l

2.6.1.4 Calculated TDS to EC ratio

The ratio of CTDS to conductivity should always fall under the range of 0.55 to 0.7 (equation 2.7). The acceptable criteria are as follows,

$$0.5 < \frac{CTDS}{conductivity} < 0.7 \quad \text{(equation 2.7)}$$

2.6.1.5 Total Hardness (TH)

The hardness is one of the important Groundwater Quality (GWQ) parameters helpful in detecting pollution. The Sulphates and Chlorides together constitute Permanent Hardness (PeH), also known as non-carbonate hardness. The carbonates and bicarbonates together cause Temporary Hardness (TeH). The TH expresses a direct relationship with Ca and Mg. The equation for Calculated TH (Sawyer 1959; Karanth 2008) is as follows,

$$\text{Calculated TH} = (2.497 * Ca) + (4.115 * Mg) \quad \text{(equation 2.8)}$$

There must be a direct relationship between Bicarbonates (TeH) and (Ca+Mg) ions (Prasad & Saxena 1980). TH must also be equal to the sum of total alkalinity (TA), Sulphate, and Nitrate.

$$TH = (TA + SO_4 + NO_3) \quad (\text{equation 2.9})$$

The equation 2.9 gives the relationship between the TA, Sulphate, and Nitrate (values are in meq/l) which can be utilized to correlate the Ca and Mg values using equation 2.8.

2.6.1.6 Chloride's relationship with Na and K

The total chloride present in the water sample taken for analysis must be equal to the sum of total Sodium and Potassium.

$$Cl = Na + K \quad (\text{equation 2.10})$$

The equation 2.10 gives a direct relationship between Na and K. It is observed that these equations are interconnected somehow. Therefore these relationships can be sharply observed in the correlation.

2.6.2 Drinking water quality parameters

The parameters like pH, EC, and TDS are measured on the spot during sample collection. According to standard procedure, the laboratory analysis for the drinking water quality parameters is conducted (Bureau of Indian Standards 2012). The analysis for parameters like Sodium (Na^+), Potassium (K^+), Calcium (Ca^{2+}), Magnesium (Mg^{2+}), TH, Total Alkalinity (TA), Sulphate (SO_4^{2-}), Nitrate (NO_3^-), Bicarbonate (HCO_3^-), Chloride (Cl^-), Fluoride (F^-) and Iron (Fe^{2+}) are to be conducted in the laboratory.

2.6.3 Computation of Water Quality Index

There are several methods available from time to time for studying WQI. The Weighted Arithmetic Index method for evaluating WQI can be calculated using Brown's equation (Brown et al. 1972).

$$WQI = \frac{\sum_{i=1}^{i=n} (Q_i * W_i)}{\sum_{i=1}^{i=n} W_i} \quad (\text{equation 2.11})$$

The unit weight (W_i) of the i^{th} parameter depends on the standard value of the parameters and a proportionality constant. Whereas the Q_i is the water quality rating

dependent on the concentration of the parameters. The water quality rating and grading of the weighted arithmetic WQI method are used to index the water quality.

The WQI and grading are calculated parameter-wise by grouping all the groundwater samples. Therefore, the grading is given for parameters in the study area regardless of the number of samples. But, more samples with close spacing yield more promising results.

Table 2.2 The rating and grading used in Weighted Arithmetic WQI method.

WQI Value	Rating of Water Quality	Grading
0 – 25	Excellent water quality	A
26 – 50	Good water quality	B
51 – 75	Poor water quality	C
76 – 100	Very poor water quality	D
Above 100	Unsuitable for drinking purposes	E

2.7 Groundwater recharge studies

It is documented that ancient Romans and Greeks practiced rainwater harvesting (RWH) (Phoca & Valavanis 1999). And nowadays, the popularity and necessity of RWH have grown exponentially (Zhang et al. 2009). The need for water management and construction of small water harvesting structures is imminent and is gaining many scopes nowadays (Kumar & Rameshwar 2008). But the fact remains that the complexity of aquifers and misinterpretation of the subsurface can mislead to propose improper recharge structures (Todd & Mays 2005).

The relationship between GIS and artificial recharge structures can be found in various literature (Shankar & Mohan 2005; Patil & Mohite 2014; Selvam et al. 2017). Understanding geological, structural, geomorphological characteristics and their relationship with groundwater are necessary as it is the base for assigning ranks and weights.

The sum of the product of normalized weights (subscript w) of the thematic layers with their respective ranks (subscript r) of the classes forms the Groundwater Recharge Potential Index (GRPI) as given in the equation (Venkateswara Rao & Briz-Kishore 1991) below;

$$\begin{aligned}
 \text{GRPI} = & [(GWPZw) * (GWPZr)] + [(GWCw) * (GWCr)] \\
 & + [(LULCw) * (LULCr)] + [(DOw) * (DOr)] \\
 & + [(Slw) * (Slr)] + [(Gmw) * (Gmr)] \\
 & + [(SDw) * (SDr)] + [(DBRw) * (DBRr)] \\
 & + [(LDw) * (LDr)]
 \end{aligned}
 \tag{equation 2.12}$$

Where, GWPZ-Groundwater Potential Zones, GWC-Groundwater contours, LULC-Land Use & Land Cover, DO-Drainage Order, SI-Slope, Gm-Geomorphology, SD-Soil depth, DBR-Depth to bedrock, LD-Lineament density.

The merit and demerit of the features and their influence over groundwater occurrence are precisely the points of consideration for assigning suitable weights (Jaiswal et al. 2003). The high lineament density indicates the high intensity of weathering and, therefore, the possibility of maximum effective porosity and permeability of the aquifers. Hence, lineament density and groundwater potential have a direct relationship (Hardcastle et al. 1995).

A slope is a slanting surface at an angle of less than 90° to a flat surface. A significant portion of the earth's surface consists of the slope. Based on the All India Soil and Land Use Survey, also known as Soil and Land Use Survey of India (SLUSI) guidelines, the slope categories are prepared. The slope exhibits an inverse relationship with the recharge potential, i.e., the lesser the slope, the less is the intensity of runoff and, therefore, more time for infiltration. The soil depth map of the study area is collected from the National Bureau of Soil Survey / Land Use Planning (NBSS/LUP), an autonomous organization under the Ministry of Agriculture, GOI.

A few important recharge structures can be proposed based upon the GRPI and criteria for site suitability for ARS. A check dam is a small barrier constructed across the flow direction of streams to recharge the groundwater. The restoration of low footprint runoff harvesting vegetation on the hill slopes strengthens the source-sink relations and increases the streams' runoff (Stavi et al. 2020). The demand for freshwater is increasing rapidly due to population growth, contamination, little availability of groundwater. Therefore, harvesting the surface water, especially rainwater (superior quality), efficiently and adequately is highly suggested (Baby et al. 2019).

The water temperature used for recharge through injection wells is also a point of concern because the solubility of air increases with a decrease in temperature. The surface water at 10°C, when injected into an aquifer with 20°C of temperature, releases the saturated air into the aquifer. While some air escapes, most of it settles in the pore spaces, becoming tiny bubbles. This temperature change could seriously reduce the aquifer capacity. On the contrary, if the groundwater temperature is lower than the surface water, the saturated air in the groundwater is released. Therefore proper temperature is required for recharge through injection wells (USDA & NRCS 2010).

Wastewater reclamation is the most effective strategy in Water Ecosystem Impact (WEI) reduction (Xiong et al. 2020). The proof-of-concept experiments had shown that under normal recharge conditions, some of the pharmaceuticals, pathogens, and other organic wastewater compounds would prevail in the treated effluent after Soil Aquifer Treatment –SAT (Cordy et al. 2004). The soil adsorption capacity is finite, and considering the long-term SAT, the aquifers eventually get polluted (Vengosh & Keren 1996). The perched aquifers, evapotranspiration, water stored in unsaturated zones could make a considerable difference between recharge and transmission loss (Hughes & Sami 1992).

2.7.1 Groundwater recharge estimation studies

The recharge estimation methods are classified into five categories according to (Lerner et al. 1990), which are direct measurement, correlation methods, tracer techniques, Darcian approaches, and water balances. The groundwater response function yields similar results as the unit hydrograph and could be an excellent example of the correlation method (Besbes et al. 1978). The estimation of recharge from precipitation has broad applicability of the tracer techniques (Sukhija et al. 1996).

The Darcian methods include field data like hydraulic properties, flow net, infiltration equations, but it is not easy to gather enough data to model reality. The water balance methods use aquifer modelling, watershed modelling, and watertable fluctuation to estimate the recharge. The methods or approaches that can be used to estimate the groundwater recharge are discussed here. The groundwater recharge estimation also needs to estimate the recharge rate. The recharge rate in the watershed

is the product of average annual rainfall, with its corresponding area factor and the recharge factor (Selvam et al. 2014).

The groundwater recharge estimation can be classified as direct recharge (diffuse from recharge structures) and indirect recharge (from rivers and channels) depending upon the percolation of the surface water into groundwater. These methods are also used with different terminologies like localized or focused recharge (Lerner 1997) and also as direct (diffused) and localized (preferential flow) recharge estimation (Rushton 1997). The natural groundwater recharge can be estimated using the following empirical formulae and guidelines (Groundwater Resource Estimation Committee 2009). Therefore the empirical relationships proposed (Bhattacharya et al. 1954; Rao 1970; Chaturvedi 1973; Sehgal 1973; Kumar & Seethapathi 2002) are widely applicable for hard rock terrains to validate the results. Chaturvedi in 1936 derived a relationship based on groundwater level and rainfall to estimate recharge in Ganga-Yamuna doab (Kumar 1996). This formula helps understand the preliminary relationship between rainfall and recharge. Later this formula was updated in 1954 by the Uttar Pradesh Irrigation research Institute (U.P.I.R.I.).

The U.P.I.R.I formula was again updated as the Amritsar formula (Sehgal 1973). Also, the relationships between rainfall and recharge for a particular climate and homogenous area were proposed by Krishna Rao in the 1970s (Kumar 1996). Bhattacharya et al. (1954) also proposed the empirical relations for estimating recharge from rainfall alone. Later, Kumar & Seethapathi (2002) proposed a relationship for recharge estimation from rainfall in the upper Ganga canal command area (Kumar & Seethapathi 2002).

Based on the network of OB wells data, the quantitative changes in water level due to recharge or discharge could be measured (CBIP 1976; Adyalkar & Rao 1979). Also, the Groundwater Resource Estimation Methodology (GWREM) of the Ministry of water resources (MoWR), Government of India, recommends that about 5% to 10 % of the total recharge is lost as base flow discharge or evapotranspiration. The water table fluctuation method works under the assumption that the dynamic groundwater level is due to groundwater recharge alone, and then it moves to storage (Healy & Cook 2002).

The soil water balance can be estimated using the Penman-Grindley (P-G) method (Penman 1950; Grindley 1967), similar to the water balance equation. But the only difference is that the P-G method considers soil water storage (ΔS) instead of groundwater recharge.

2.7.1.1 Runoff estimation

Another important parameter for estimating recharge is the runoff. There are several approaches to estimate runoff in ungauged watersheds. Examples are the University of British Columbia Watershed Model (UBCWM), Artificial Neural Network (ANN), Soil Conservation Service Curve Number (SCS-CN) method, and Geomorphological Instantaneous Unit Hydrograph (GIUH) (Becker 2006). Among these methods, the SCS-CN method (now called as Natural Resources Conservation Service Curve Number method (NRCS-CN)) is widely used because of its flexibility and simplicity (Zhan & Huang 2004). Pandey & Sahu (2000) pointed out that land use is an essential input parameter of the SCS-CN method. Many researchers have worked on SCS-CN method for estimating runoff (Nandagiri 2007; Suresh Babu & Mishra 2011; Soulis & Valiantzas 2012; Gundalia & Dholakia 2014; Mishra & Kansal 2014). Nayak & Jaiswal (2003) found that there was a good correlation between the measured and estimated runoff depth using the GIS and NRCS-CN method

The SCS-CN method was developed in 1954 by the U.S. Department of Agriculture (USDA) SCS and is described in the Soil Conservation Service (National Engineering Handbook Section 4: Hydrology). The first version of the handbook containing the method was published in 1954. Subsequent revisions followed in 1956, 1964, 1965, 1971, 1972, 1985, and 1993 (Ponce & Hawkins 1996). In 1994, SCS became Natural Resources Conservation Service, and therefore, the name of Soil Conservation Service SCS-CN method changed as NRCS to widen its scope. The SCS-CN method results from exhaustive field investigations carried out during the late 1930s and early 1940s and the works of several early investigators, including (Andrews 1954; Ogrosky 1956).

Most of the works overlay the land use and Hydrological Soil Group (HSG) maps, label the CN's to each polygon, and take area-weighted CN's to describe the

behaviour of a hydrologic basin (Merzi & Aktas 2000; Chatterjee et al. 2001; Durbude et al. 2001; Chakraborty et al. 2005; Pradhan Ratika et al. 2010; Durbude et al. 2011; Suresh Babu & Mishra 2012). (Pandit & Heck 2009) added the slope information with the aid of GIS to modify the potential maximum retention (S) of water in the soil in the SCS-CN method. To the origin of the SCS-CN methodology, (Sherman 1949) was the first to propose the plotting of direct runoff against storm rainfall. Later, Mockus (1949) proposed that estimates of surface runoff for ungauged watersheds could be based on soil, land use, antecedent rainfall, storm duration, and average annual temperature.

Victor Mockus (1965) suggested that a more general relationship could be developed based on the following hypothesis

$$\frac{F}{S} = \frac{Q}{P} \quad (\text{equation 2.13})$$

Where F = actual rainfall retention during a storm. S = potential maximum retention at the start of the storm, Q = direct runoff, and P = total rainfall or maximum potential runoff. It should be noted that the ratios are accurate as limits when $P \rightarrow 0$, ($Q/P = F/S$) and as $P \rightarrow \infty$, ($Q/P \approx F/S$) $\rightarrow 1$. Also, it should be noted that the ratio carries a strong parallel to the constant in the rational equation.

Early versions of the runoff equation did not contain an initial abstraction term I_a , representing interception, surface storage, and infiltration before runoff began. This term was added later, changing equation 2.13 to the following equation.

$$\frac{F}{S} = \frac{Q}{P_a} \quad (\text{equation 2.14})$$

Where P_a is rainfall after runoff begins ($P - I_a$). equation 2.14 approaches the same limits as equation 2.13. In equation 2.13, substituting $P - Q$ for F and solving for Q yields,

$$Q = \left(\frac{P^2}{(P + S)} \right) \quad (\text{equation 2.15})$$

This is valid for $P > I_a$ after runoff begins, and $Q = 0$ otherwise. With initial abstraction in equation 2.14, the actual retention $P - Q$ asymptotically approaches a constant value $S + I_a$ as rainfall grows unbounded.

The equation 2.15 has two parameters: S and I_a ; The necessity for independent estimation of initial abstraction can be removed using a linear relationship between I_a and S was suggested.

$$I_a = \lambda S \quad (\text{equation 2.16})$$

Here the λ is the initial abstraction ratio. And, therefore substituting $P - I_a$ instead of P yields,

$$Q = \left(\frac{(P - I_a)^2}{(P - I_a)} \right) + S \quad (\text{equation 2.17})$$

The equation 2.17 was justified based on measurements in watersheds less than 10 acres in size. While there was considerable scatter in the data, NEH-4 reported that 50% of the data points lay within limits $0.095 \leq \lambda \leq 0.38$ (Soil Conservation Service 1985). This led SCS to adopt a standard value of the initial abstraction ratio $\lambda = 0.2$. However, values varying in the range of $0.0 \leq \lambda \leq 0.3$ have been documented in various studies encompassing various geographical locations in the United States and other countries (Cazier & Richard H. Hawkins 1984; Bosznay 1989).

Victor Mockus (1965) developed a relationship between I_a and S to reduce the number of variables in equation 2.16. The field data at that time indicated that

$$I_a = 0.2 * S \quad (\text{equation 2.18})$$

Which, when substituting for I_a into equation 2.17, results in the standard equation

$$Q = \left(\frac{(P - (0.2 * S))^2}{(P - (0.8 * S))} \right) \text{ when } P \geq (0.2 * S) \quad (\text{equation 2.19})$$

$$Q = 0 \quad P \leq (0.2 * S) \quad (\text{equation 2.20})$$

The equation 2.19 has an advantage over many others that have been proposed. It is easier to use because it requires only one parameter (S) related to watershed characteristics. S is related to Curve Number by the relationship where S is in inches.

$$CN = \left(\frac{1000}{10 + S} \right) \quad (\text{equation 2.21})$$

Victor Mockus (1965) described the significance and limitation of S using equation 2.18. Plotting of direct runoff (Q) versus storm rainfall (P) for watersheds showed that Q approaches P as P accumulated. S is constant and is the maximum difference of P and Q for the given storm and watershed conditions.

2.7.1.1.1 Hydrologic Soil Group classification

Musgrave (1955) described a hydrologic classification of soils depending on their infiltration rate. It grouped all soils into four primary groups depending on the minimum infiltration capacity, laboratory tests, and soil texture. The four groups were A, B, C, and D with sands in group A and clays in group D. The Hydrologic Soil Groups, as defined by ARS and NRCS engineers, are A, B, C, D, and dual groups A/D, B/D and C/D. Soils were initially assigned to Hydrologic Soil Groups within selected small watersheds, and assignments were based on rainfall-runoff data and infiltrometer plots in those watersheds.

2.7.1.1.2 Antecedent Moisture/Runoff Condition

Early development of the runoff curve number method confirmed that variability was real and that the same watershed could have more than one curve number, i.e., a set of curve numbers (Soil Conservation Service 1985; Suphunvorranop 1985; Hjelmfelt 1991). The latter was recognized very early as the primary or tractable source of the variability, and thus, the concept of antecedent moisture condition (AMC) originated. More recently, the same concept has been referred to as the antecedent runoff condition (ARC) to denote a shift of emphasis from soil moisture to runoff (USDA 1986).

2.7.1.1.3 Development of Curve Numbers

The standard curve number is given in the SCS and other applicable tables (Soil Conservation Service 1985). The low value is the dry curve number of AMC 1 (lowest runoff potential). The high value is the wet curve number of AMC 3 (highest runoff potential). The original values of this table, reported in the 1956 edition of NEH-4, were based on unsmoothed data. The present AMC conversion table values have been smoothed by fitting straight lines on a regular probability paper. While it is theoretically possible for its numbers to span the range 0-100, practical design values validated by experience are more likely to be in the range 40-98, with few exceptions (Van Mullem 1991).

2.7.1.2 Estimation of Actual Evapotranspiration

The evapotranspiration especially the actual evapotranspiration is also one of parameter which is important in recharge estimation. The actual evapotranspiration (AET) can be estimated using PET. The PET is estimated using one of the basic empirical equations given by Thornthwaite (1948). Chandrashekhar & Naganna (1979) established a relationship between AET and PET and proposed an equation to estimate the average AET.

$$AET = \left(\frac{PET_{monthly}}{N} \right) * 2 * r \quad \text{(equation 2.22)}$$

Where *AET* is actual ET, *N* is the number of days in the month, and *r* is the number of rainy days in the month.

Finally, the results obtained from methods like empirical formulae, groundwater recharge using groundwater recharge potential index integration method, and water balance equation are averaged to estimate the average groundwater recharge of the watershed.

Chapter 3

GEOLOGY AND GEOMORPHOLOGY

3.1 Introduction

Efficient management planning requires a detailed understanding of the factors which are influencing natural resources. Groundwater is one such natural resource influenced by climate, geology, geomorphology, and drainage characteristics. The climatic factors include hydrometeorological parameters like precipitation (rainfall), surface temperature, humidity, number of rainy days, and rainfall intensity. The geological factors include lithology, stratigraphy, and structures. These geological factors play an essential role in providing boundary conditions for the geological units (aquifers).

Morphometric studies of a river basin comprise discrete morphologic regions and have particular relevance to drainage patterns and geomorphology (Strahler 1957; Dornkamp & King 1971; Krishnamurthy et al. 1996). Morphometric analysis is an important technique to evaluate the behaviour of a hydrological system, which provides a quantitative specification of basin geometry to understand the initial slope. Drainage basins are the fundamental units to understand geometric characteristics of the fluvial landscape such as topology of stream networks, quantitative description of drainage texture, pattern, shape, and relief characteristics (Abrahams 1984). The present chapter describes the geology, geomorphology, and drainage characteristics of the Gurpur Watershed in Dakshina Kannada and Udupi districts using RS & GIS analysis. This study is helpful to understand the hydrological behaviour of the basin.

3.2 Geology

These geological factors play an important role in providing boundary conditions for the geological units (aquifers). The major litho-unit is the Gneiss which can be seen as Indian Peninsular Gneissic Complex or Achaean MGTG.

3.2.1 Geology of West coast of India

The west coast extends from Cape Comorin (Kanyakumari-Tamil Nadu) in the north to the Gulf of Cambay (Surat-Gujrat) in the south, which is about 1,500 km. It is a narrow stretch (about 10 km to 80 km) along the Arabian Sea in the west, to the Western Ghats

in the east, and extends north-south. The west coast of India is divided mainly into three parts – Konkan Coast (parts that include Goa and Maharashtra), Kanara (parts that include Karnataka), and Malabar Coast (parts include Kerala to Kanyakumari of Tamil Nadu). The west coast of India has many short and swift rivers. It is also associated with a few small estuaries, creeks, lagoons, lakes, backwaters, and bay. The elevation range varies from 150 m to 300 m above mean sea level.

3.2.2 Geology of Karnataka

The Karnataka state comes in the peninsular region of India in the Asian continent. Karnataka is classified into two geomorphic zones - Coastal landform terrain and Karnataka Plateau terrain, the two zones being separated by Western Ghats scarp (Sreedhara Murthy & Raghavan 1994; Ranganathan & Jayaram 2006). Whereas the Coastal landform terrain of Karnataka is considered as post-cretaceous landforms and the remaining parts like Deccan traps, Gneiss-Charnockite-Sargur schist belt is considered as pre-cretaceous landforms. The orientation of the peninsular west coast of India is towards the NNW-SSE direction (Raghavan 1988).

There are various hypotheses regarding the origin of western ghats and can be grouped as the Escarpment hypothesis; erosional origin; hypothesis of the dead cliff, etc., (Dikshit 1981). Based on the geological, geomorphological, and geophysical evidence, the western ghats represent the edge of the disrupted continental block during the early Miocene (Radhakrishna 1967). The western ghats are the fault that receded due to marine erosion forming cliff (Subramanya 1987). The rock formations of Karnataka can be broadly grouped into four principal divisions, namely;

- Archaean gneisses, granulites, and high-grade supra crustals.
- Palaeo-Proterozoic greenstone belts.
- Proterozoic sediments.
- Deccan Traps of Cretaceous - Eocene age.

This peninsula dates back to the Precambrian era, and the oldest rocks are identified in this peninsular region. Geologically, Karnataka comprises the rock formations of diverse types from Archaean to Quarternary age. The plateau is the largest physiographical division of Karnataka. Radhakrishna and Vaidyanathan (1994) have opined that the ages of most landforms in Karnataka perhaps range from Eocene

to Recent; although these are rock formations ranging from Archaean to Quarternary. A large portion of the Darwar craton is made up of pre-cambrian rocks. The Karnataka coast is a linear belt traversing from Karwar in the north to Mangaluru in the south (about 400 km). The coastline of Karnataka is associated with rocky coast and barrier (Radhakrishna 1993).

3.2.3 Geology of Gurpur watershed

The basin is lithologically composed of about 83% Migmatites and Granodiorites, 5% of charnockites, about 6% Metabasalts, and 2% laterites and Amphibolites. The greenstone-amphibolite facies and granulites could be seen in patches. Like any other hard rock terrains, the soil's thickness and weathered zone range from 20 m to 40 m, with the basement PGC. The weathered zone hosts groundwater in its fissures, fractures, and pore spaces of the weathered rocks.

The present landscape along the coast results from extensive Tertiary denudation, which leads to the formation of laterites. The Quarternary formations are found along the coast, which includes boulders, pebbles, and cobble beds in paleo-river channels (Gurumurthy 2013). The general litho-stratigraphic sequence of the Dakshina Kannada district (Table 3.1) is given by (Balasubrahmanyam 1978).

Table 3.1 The general litho-stratigraphic sequence of Dakshina Kannada district.

Recent	Gravel and sand deposits (marine and fluvial)
Tertiary	Laterites
Proterozoic	Dolerite dykes Younger green stones (meta-sediments and metavolcanics)
Archaean	Granitoids, Charnockites, and other metamorphic rocks

The Gurpur watershed is divided into high land, midland and low land (ghats, hinterland, and coastal area) depending on terrain features and altitude. The Gurpur River, just like other west-flowing rivers, in its early stage, flows through a very steep slope (ghats). Whereas when it reaches low land, the river traverses in the south direction, perpendicular to its earlier flow to the confluence with Nethravathi River, and flows into the Arabian Sea.

3.2.4 Lithology

Lithology map of the study area is prepared by using a published Geological Survey of India (GSI) quadrangle map, which is in the scale of 1:250,000. Also, the lithology maps obtained by the Karnataka State Remote Sensing Application Centre (KSRSAC) in a scale of 1:50,000 are collected, geo-referenced, and then digitized. The classification of lithological features present in the study area can be seen in Figure 3.1, and area statistics can be seen in Table 3.2.

Table 3.2 The categories of lithology and their corresponding area Statistics.

Sl. No.	Lithology Classes	Area (km²)
1	Alluvium / beach sand, alluvial soil	21.29
2	Charnockite	17.29
3	Laterite	82.93
4	Metabasalts including thin ironstone	94.27
5	Migmatites and Granodiorite - Tonalitic Gneiss	657.60
6	Pink hornblende granite	4.42
	Total	877

3.3 Geomorphology

The geomorphology maps and data are collected from GSI and KSRSAC. The available relief information in the topo-maps is correlated with the Indian Remote Sensing (IRS) P6 Linear Imaging Self scanning Sensor (LISS) -IV satellite imagery and SPOT imagery.

The Bird-eye-view of satellite imagery provides helpful information in mapping geomorphology, which along with the electrical resistivity data, helps verify and correlate the information on the depth of weathered zone, type of associated material, nature of the environment, agent of weathering. The final geomorphic map is prepared by incorporating these details in the pre-field interpretation map (Figure 3.2). The statistics of the geomorphology thematic layer indicate that the pediplain covers more than 50% of the study area (Table 3.3).

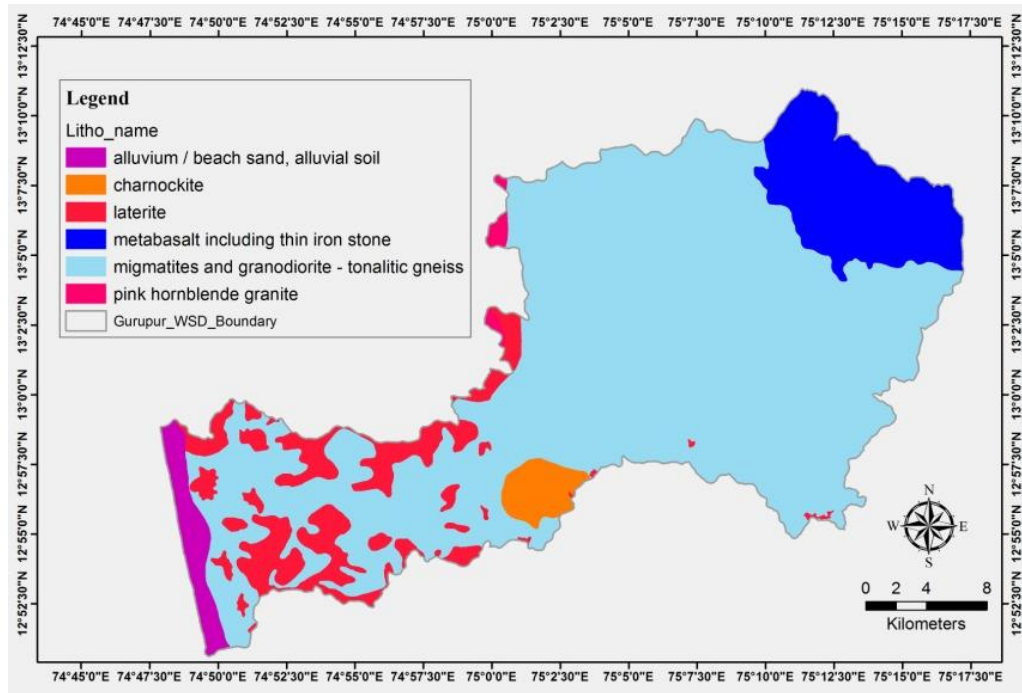


Figure 3.1 Lithological map of Gurpur watershed.

Table 3.3 Categories of Geomorphologic features and corresponding area statistics.

Sl. No.	Geomorphology Classes	Area (km ²)	Area (%)
1	Alluvial Plain	63.95	7.3
2	Coastal Plain	6.6	0.8
3	Denudational hills	43.13	4.9
4	Flood Plain	0.74	0.1
5	Pediplain	579.79	66.1
6	Plateau	45.65	5.2
7	Settlement	10.06	1.1
8	Structural hills	105.16	12.0
9	Waterbody	22.63	2.6
	Total	877	100

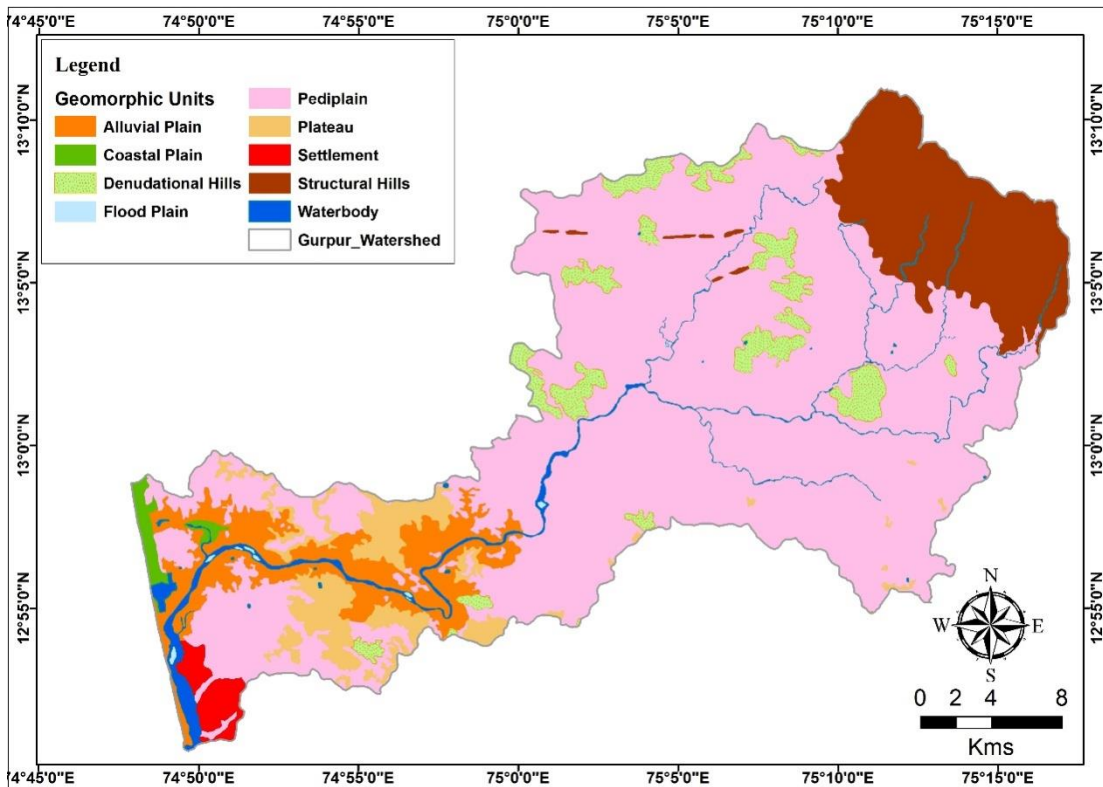


Figure 3.2 Spatial distribution of Geomorphology classes in Gurpur watershed.

3.4 Digital Elevation Model data

The DEM used for the study area is the computer graphic representation of its terrain surface (Figure 3.3). The DEM data is acquired from CartoSAT-1, and its spatial resolution is 30m. The DEM data is used for generating slope thematic layer. The DEM data is later verified using Survey of India (SOI) toposheets.

The DEM is used to deduce the morphometric parameters like drainage basin area, drainage density, drainage order, relief, and network diameter in the GIS environment. Combining remote sensing data, hydrological and spatial analysis tools in the GIS environment made it easier to identify and discriminate the drainage area. The geographic and geomorphic characteristics of a drainage basin are essential for hydrological investigations involving the assessment of groundwater potential and morphometric characters.

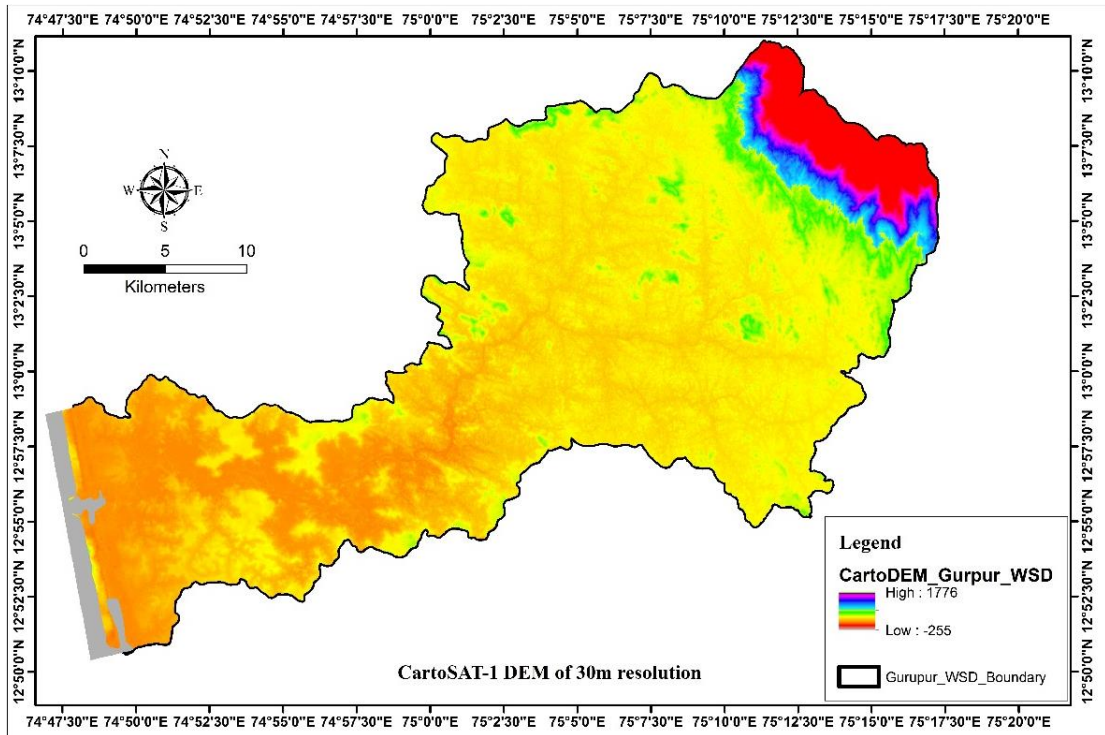


Figure 3.3 The DEM thematic map of the study area.

3.4.1 Extraction of DEM Derivatives

The watershed is extracted from the CartoSAT-1 DEM data. The contributing basin area was extracted with the help of various geoprocessing techniques in ArcGIS 10.2. Flow direction map was extracted from the subset DEM file, and it was used to delineate basins. The various hydrological processing of spatial analyst tool helps in demarcating watershed boundary. For defining watershed boundary, flow direction raster data is used as a base map. DEM derivatives extracted from the CartoSAT-1 DEM are drainage, slope, hill shade, and contour.

3.4.2 Drainage network map

The drainage network of the Gurpur watershed is extracted from DEM using a series of geoprocessing tools in Arc GIS 10.2. The output of this method is the basis for creating a stream/drainage network grid with stream order (Strahler 1964). As pointed out, the Strahler's classification system designates a segment with no tributaries as a first-order stream. Whenever two same stream order joins, it will form a higher stream order and so on.

Figure 3.4 represents the drainage map of the Gurpur watershed with different stream orders. The highest stream order identified is the 7th order. The drainage pattern can be identified as a dendritic drainage pattern.

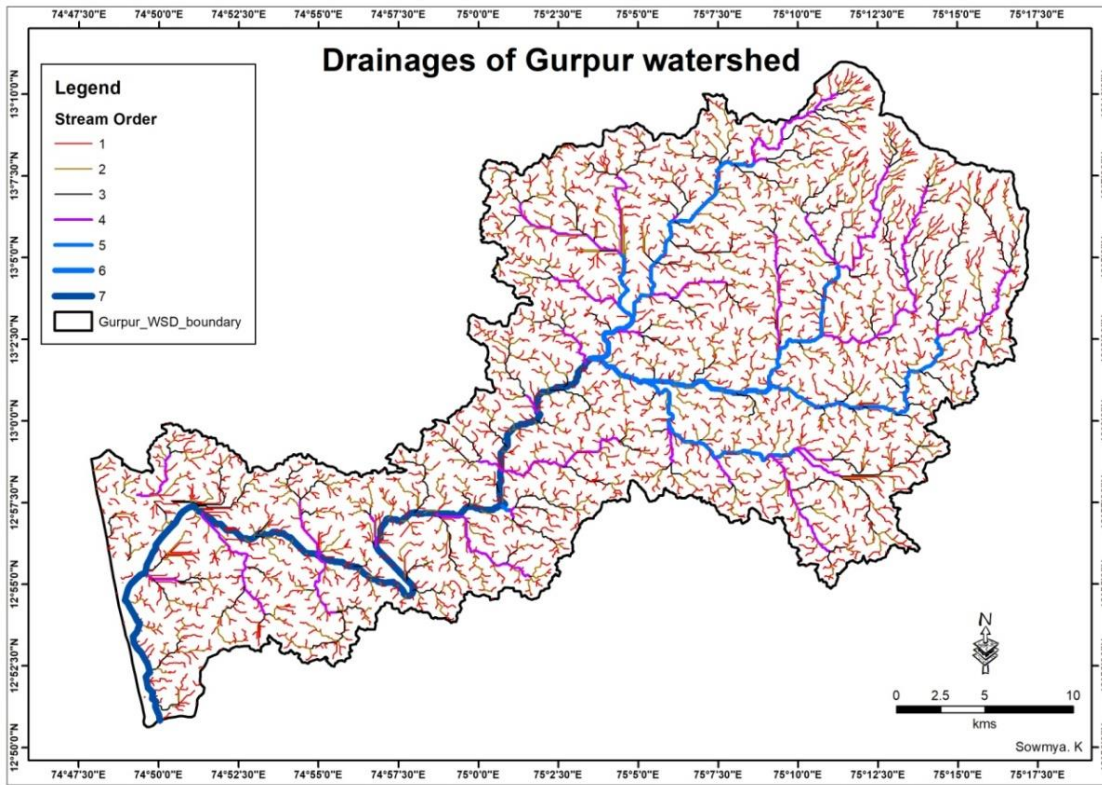


Figure 3.4 Drainage map of Gurpur watershed

3.4.3 Slope map

A slope is a slanting surface at an angle of less than 90° to a flat surface. Slope provides a basis so that by successive combination into layer units, general geomorphology could be constructed. The slope is the measure of steepness or the degree of inclination of a feature relative to the horizontal plane. A slope map of the study area is calculated based on DEM data using the spatial analyst tool in ArcGIS 10.2 (Figure 3.5). A slope grid is identified as “the maximum rate of change in value from each cell to its neighbours” (Burrough 1986). It is observed that most of the low land and parts of midland show a 0-1% slope. The high land (Ghats) shows a 35-50% of slope (Table 3.4). The remaining nearly half of the area is covered by other slope categories. The slope is having an inverse relation with groundwater potential. An increase in slope increases runoff and thus decreases the infiltration and affects groundwater potential.

The slope is a necessary terrain parameter for land utilization, land availability, and land capability assessment rather than Aspect and Altitude. Following All India Soil and Land Use Survey guidelines on slope categories are used, and the slope map with the following slope categories has been prepared.

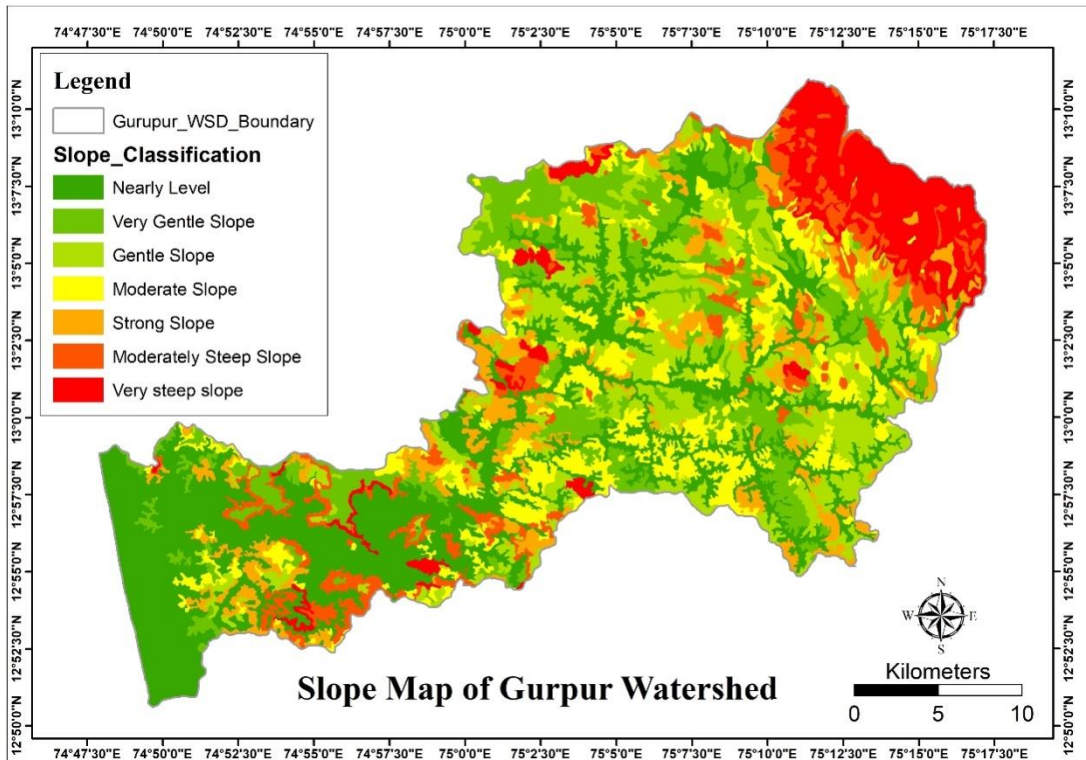


Figure 3.5 Spatial distribution of slope classes in Gurpur watershed.

Table 3.4 Categories of slope and their corresponding slope percentage.

Sl. No.	Slope Categories	Slope (%)	Area (km ²)	Area (%)
1	Nearly Level	0-1	262.32	30
2	Very Gentle Slope	1-3	122.52	14
3	Gentle Slope	3-5	144.33	16
4	Moderate Slope	5-10	106.35	12
5	Strong Slope	10-15	87.12	10
6	Moderately Steep Slope	15-35	71.01	8
7	Very Steep Slope	35-50	84.06	10
TOTAL			877	100

Also, the slope theme is prepared using the CartoSAT DEM and from topo sheets. The similarity of both the layers is observed and utilized in the MCDM technique for integration and preparation of GWPZ, GRPZ, and site suitability for ARS.

3.4.4 Hill shade map

The Hill shade tool provides the hypothetical illumination values for each cell in raster data. It does this by setting a position for a hypothetical light source and calculating the illumination values of each cell in relation to neighbouring cells. It enhances the visualization effects by using transparency and overlaying on other thematic layers. It gives the 3D impression depending upon the angle of illumination (Figure 3.6).

3.4.5 Contour map

A contour line is a function that joins the point of equal value. The contour interval of a contour map is the difference in elevation between successive contour lines. The contour range from 0 to 61m and 61 to 153m covers most of the study area, i.e., low land and midland region (Figure 3.7). There is a sudden increase in contour line intensity due to the Western Ghats. The range of contour intervals used in the study can be seen in Figure 3.7.

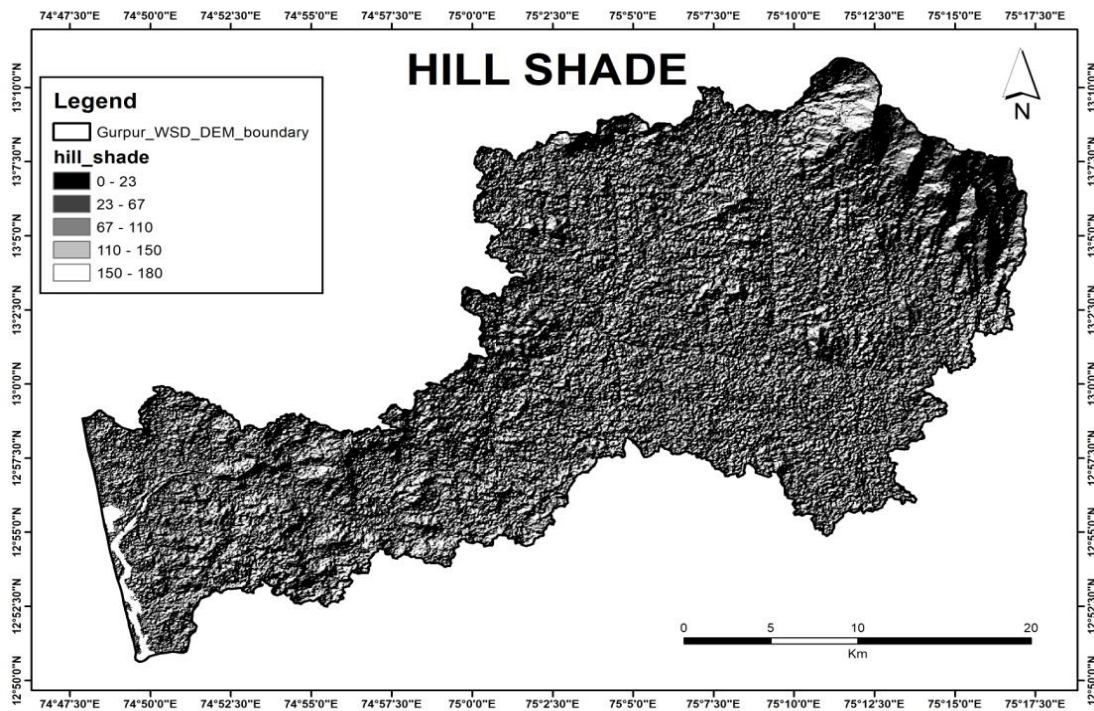


Figure 3.6 The hill shade map of Gurgur watershed

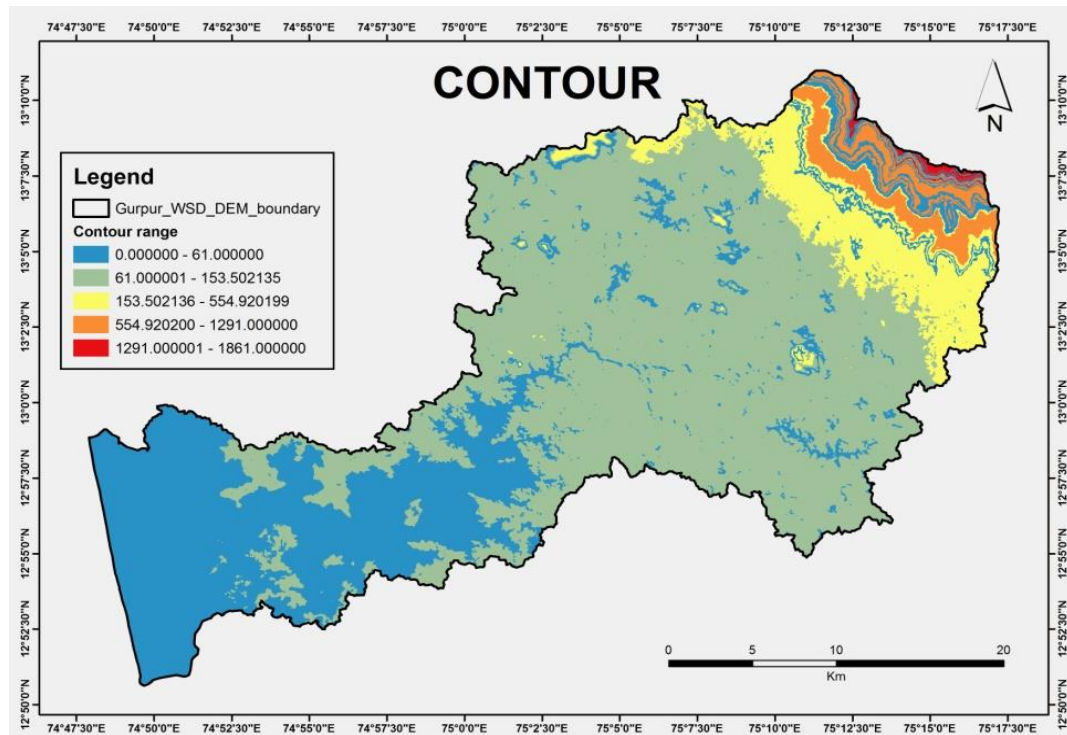


Figure 3.7 The filled contour map of Gurpur watershed.

3.5 Morphometric analysis

The geomorphology of any drainage basin can be quantitatively explained using morphodynamic evaluation of drainage data (Magesh et al. 2012). Remote sensing and GIS techniques are proven efficient tools for delineating, updating, and morphometric analysis of drainage basins. Various important hydrologic phenomena can be correlated with the physiographic characteristics of drainage basins such as size, shape, the slope of drainage area, drainage density, size, and length of the tributaries. The remote sensing data can be used in conjunction with conventional data to delineate characterization, priority evaluation, problem identification, assessment of potentials and management needs, identification of erosion-prone areas, evolving water conservation strategies, selection of sites for check dam and reservoirs.

3.5.1 Materials and methodology

Extraction of drainage network and assigning the stream order from published SOI toposheets and georeferenced satellite data for a large area manually is a time-consuming and tedious exercise. To issue can be avoided using automatic extraction techniques for evaluating a basin's morphometric parameters, i.e., extraction of River

basin/watershed boundary and extraction of drainage/stream network. Scanned SOI toposheets number 48K/15, 48K/16, 48O/3, 48O/4 of scale 1:50000 are georeferenced and projected to the regional projection (World Geodetic System (WGS) 1984, Universal Transverse Mercator (UTM) zone 43 N) using Arc GIS 10.2. The essential features were digitized to prepare the base map. The DEM of 30 m resolution of the study area is used. Other DEM derivatives such as slope and aspect were extracted using hydrology tools available in ArcGIS 10.2 software. The extraction of the basin was carried out by using flow direction. In the extraction of the drainage system, the flow direction and flow accumulation map were first extracted using various geoprocessing tools, and using these maps drainage map was extracted. It was then followed by stream ordering based on Horton’s law. According to this law un-branched stream is termed a first-order stream. When two first-order streams join, it is designated as second-order, followed by two second-order streams joining to form third order and so on. The number of streams from each order was recorded.

Morphometric parameters under linear, aerial, and relief were computed using standard methods and formulae. The fundamental parameter, namely, stream length, area, perimeter, number of streams, stream length, and basin length, are derived from the drainage layer. The values of morphometric parameters, namely; bifurcation ratio, drainage density, stream frequency, form factor, texture ratio, elongation ratio, circularity ratio, are derived. Table is prepared based on the formulae suggested (Horton 1945; Miller 1953; Schumm 1956). The formulae used in this study are prepared from Microsoft Excel 2007 to get final results. Therefore, the change in any of the values reflects in all the associated formulae. Also, excel formulae are more effective in time management rather than traditional methods.

Table 3.5 Formulae adopted for computation of Morphometric Parameters

	Sl. No.	Morphometric Parameter	Formula	References
LINEAR	1	Stream Order (N_u)	Hierarchical rank	(Strahler 1964)
	2	Stream Length (L_u)	Length of the stream	(Horton 1945)
	3	Mean stream length (L)	$L_{sm} = L_u / N_u$ Where L_u = Mean stream length of a given order (km), N_u Number of stream segment.	(Horton 1945)
	4	Stream length	$Rl = L_u / L_{u-1}$	(Horton 1945)

		ratio (Rl)	Where L_u = Total stream length of order (u), L_{u-1} = The total stream length of its next lower order.	
	5	Bifurcation ratio (Rb)	$Rb = N_u / (N_{u+1})$ N_u = Total no. of stream segments of order 'u'	(Schumm 1956)
	6	Mean bifurcation ratio (Rbm)	Rbm = Average of bifurcation ratios of all orders.	(Strahler 1957)
AERIAL	7	Drainage density (Dd)	$D = \Sigma Lu / A$ ΣLu = Total stream length of all orders A = Area of the basin (km ²)	(Horton 1932)
	8	Stream frequency (Fs)	$Fs = \Sigma Nu / A$ ΣNu = Total number of streams of all orders A = Area of the basin (km ²)	(Horton 1932)
	9	Texture ratio (T)	$T = \Sigma Nu / P$ ΣNu = Total number of streams of all orders P = Perimeter of the basin	(Horton 1945)
	10	Circularity ratio (Rc)	$Rc = 4 * \pi * A / P^2$ Where, Rc = Circularity ratio; π = 'Pi' value i.e. 3.14; A = Area of the basin (km ²); P = Perimeter (km)	(Miller 1953)
	11	Form factor (Ff)	$Ff = A / Lb^2$ A = Area of the basin (km ²) Lb^2 = Square of the basin length	(Horton 1932)
	12	Elongation Ratio (Re)	$Re = 2 \sqrt{A / \pi} / Lb$ Where, Re = Elongation Ratio A = Area of the Basin (km ²) π = 'Pi' value i.e., 3.14 Lb = Basin length	(Schumm 1956)
	13	Compactness Coefficient (Cc)	$Cc = Pc / P_u$ Where P_c = Perimeter of the watershed; P_u = Perimeter of the circle of watershed area	(Gravelius 1914)
	14	Length of overland flow (Lg)	$Lg = 1 / D * 2$ Where, Lg = Length of overland flow, D = Drainage density	(Horton 1945)
	15	Shape factor (Bs)	$Bs = L^2 / A$ Where, L = Basin length (km), A = Area of basin	(Horton 1932)
	16	Constant of channel maintenance (C)	$C = 1 / Dd$ Where Dd = Drainage density.	(Schumm 1956)
RELIEF	17	Basin Relief	It is the vertical distance	(Schumm 1956)

		(Bh)	between the lowest and highest points of the basin.	
	18	Relief Ratio (Rh)	Rh=Bh/Lb, Where, Bh= Basin relief, Lb= Basin length	(Schumm 1956)

3.5.2 Results and discussions on linear, aerial & relief parameters

The basic and linear parameters are tabulated in (Table 3.6&Table 3.7). The areal parameters are tabulated in Table 3.9, and relief parameters are recorded in Table 3.10.

Table 3.6 Basic morphometric parameters of Gurpur watershed.

Sl. No	Parameters	Results
1	Watershed Area (A)	877 Km ²
2	Basin Length (L _b)	61.60 Km
3	Perimeter (P)	205.48 Km
4	Stream Number (N _u)	
	I	2796
	II	1345
	III	660
	IV	31
	V	6
	VI	2
	VII	1
	$\sum N_u$	4841
5	Stream Length (L _u)	
	I	1144.686 km
	II	532.631 km
	III	252.653 km
	IV	142.166 km
	V	56.809 km
	VI	15.451 km
	VII	55.456 km
	$\sum L_u$	2199.852 km

The total area of the watershed is 877 Sq.km (Table 3.9).It is the total length of the drainage basin boundary. The perimeter of the watershed is 205 km. It is the maximum length of the basin measured parallel to the mainstream. The basin length of the main watershed is 61.60 km.

Stream order is assigned based on a hierarchical ranking of streams. Strahler's method was applied for stream ordering. In the watershed, usually number of streams decreases as stream order increases (Table 3.7)

The number of drainages of different stream orders in a micro-watershed was counted, and their lengths were measured. In the watershed, usually, the length of the stream decreases as stream order increases.

It is defined as the ratio of the number of stream segments of a given order to the following higher-order segments (Schumm 1956). The R_b indicates the complexity and degree of dissection of a drainage basin. The lower values of R_b are characteristics of the sub-watersheds, which have suffered fewer structural disturbances (Strahler 1964). The bifurcation ratio of the watershed varies from 2.0 to 21.29. The mean bifurcation ratio of the watershed is 5.93.

Drainage density is the ratio of total stream length to the basin's total area (Horton 1932). The density factor is related to climate, type of rocks, relief, infiltration capacity, vegetation cover, surface roughness, and runoff intensity index. The lower drainage density of any watershed indicates that it has permeable subsurface material, good vegetation cover, and low relief, and vice versa. The Cartosat-1 DEM data from the Bhuvan website is used in the present study, along with the drainage layer digitized over the Toposheet for better accuracy. Drainage density is calculated as the “ratio of the total length of streams of all orders within the basin to the basin area” (Reddy 2004) and expressed as km/km^2 .

The drainage density varies from 0.02 km^{-1} to 1.31 km^{-1} . The mean drainage density (D_d) for the Gurpur watershed is 0.36 km^{-1} as the total area of the catchment is 878 km^2 , and the total length of the drainage is 1442 km (Figure 3.8 & Table 3.8). Drainage density is grouped into five classes: Very High, High, Moderate, Low, and Very Low classes. The higher weightage is given to the Low and Very low drainage density regions. The very low and low drainage density regions result from lesser slope and, therefore, more significant infiltration and groundwater potentiality. Therefore the relationship between D_d , slope, infiltration, and groundwater potentiality can be expressed as an inverse relationship, i.e., “Lesser the drainage density, greater the possibility of groundwater resources.” The orientation and style of the drainages have a relationship with lineaments as they are associated with structural complexity (Shahzad et al. 2009). The drainage density from “very low” to “moderate” categories covers more than 85% of the total area (Table 3.8); therefore, the probability of groundwater recharge is more.

The total number of drainages of all orders per unit area is called stream frequency (Horton 1932). Stream frequency is inversely related to permeability, infiltration capacity and directly related to the relief of watersheds. The F_s of the watershed is 5.52.

The form factor is the ratio between basin area and the square of basin length (Horton 1932). The value of R_f is always less than 0.78 in a perfectly circular basin. The higher values of form factors have high peak flows of shorter duration, and low values of form factors have lower peak flow for a shorter duration. The watershed shows a form factor of 0.23 means the watershed is in sub-circular shape.

The R_c is the ratio of the area of the basins to the area of the circle having the same circumference as the perimeter of the basin (Miller 1953). It is mainly concerned with the length and frequency of streams, geological structures, land use/land cover, climate, relief, and slope of the basin. Higher R_c indicates the circular shape of the watershed and the moderate to high relief and permeable surface. The Circularity ratio of the watershed is 0.26. It indicates a more or less circular shape.

It is defined as the ratio of the diameter of a circle having the same area as the basin and maximum basin length. The watershed shows lower elongation ratio values that are highly susceptible to erosion, and the higher values indicate high infiltration capacity and low runoff. The present study area shows an elongation ratio of 4.26 (Table 3.9).

The drainage texture is the total number of drainages of all orders per perimeter of that watershed (Horton 1945). The drainage texture depends on the climate, rainfall, vegetation, rock and soil type, infiltration capacity, relief, and stage of development of a basin (Smith 1950). The $d_t < 2$ indicates very coarse, between 2 and 4 is related to coarse, between 4 and 6 is moderate, between 6 and 8 is fine, and >8 is very fine drainage texture. The drainage texture of the watershed is 23.61, i.e., the watershed is grouped under very fine texture (Table 3.9).

Table 3.7 Morphometric analysis of basic and linear parameters of Gurpur watershed.

	A	B	C	D	E	
1	BASIC PARAMETERS	Parameter	Sl. No.	order	Results	
2		Basin Area	1		877	
3		Basin perimeter	2		205	
4		stream order		3	I	2796
5				4	II	1345
6				5	III	660
7				6	IV	31
8				7	V	6
9				8	VI	2
10				9	VII	1
11		10	ΣNu		4841	
12	stream length		11	I	1144.69	
13			12	II	532.63	
14			13	III	252.65	
15			14	IV	142.17	
16			15	V	56.81	
17			16	VI	15.45	
18			17	VII	55.46	
19		18	ΣLu		2199.85	
20		Basin length	19		61.60	
21	LINEAR PARAMETERS	mean stream length	20	I	0.41	
22				21	II	0.40
23				22	III	0.38
24				23	IV	4.59
25				24	V	9.47
26				25	VI	7.73
27				26	VII	55.46
28			27	Avg.	11.20	
29		stream length ratio		28	I	0.97
30				29	II	0.97
31			30	III	11.98	
32			31	IV	2.06	
33			32	V	0.82	
34		33	VI	7.18		
35		mean stream length ratio	34	Avg.	4.00	
36	Bifurcation ratio		35	I	2.08	
37			36	II	2.04	
38			37	III	21.29	
39			38	IV	5.17	
40			39	V	3.00	
41		40	VI	2.00		
42		mean bifurcation ratio	41	Avg.	5.93	

Table 3.8 Drainage density and corresponding area statistics.

Sl. No.	Drainage Density Categories	DD Range (km/km ²)	Area (km ²)	Percentage (%)
1	Very Low	0 – 1.15	222.95	25
2	Low	1.16 – 2.30	314.98	36
3	Moderate	2.31 – 3.46	235.93	27
4	High	3.47 – 4.61	74.68	09
5	Very High	4.62 – 5.77	29.26	03
	Total		877	100

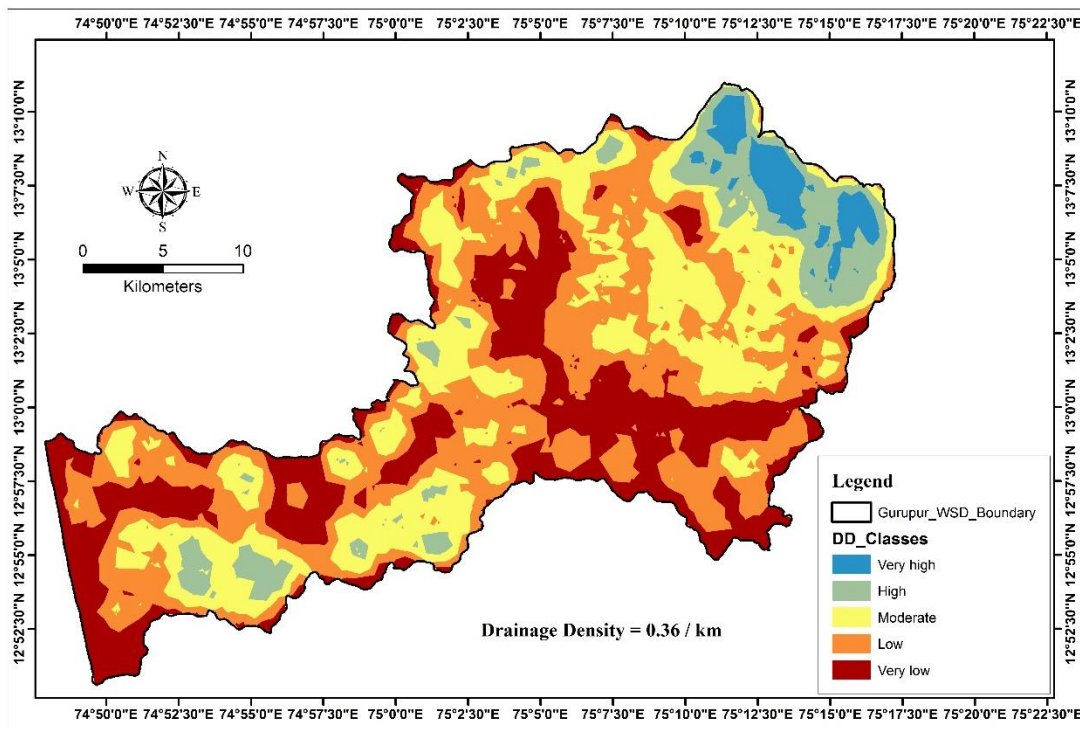


Figure 3.8 The spatial distribution of drainage density in Gurpur watershed.

According to (Gravelius 1914), the compactness coefficient of a watershed is the ratio of the perimeter of the watershed to the circumference of the circular area, which equals the area of the watershed. The Compactness Coefficient of a watershed is directly related to the infiltration capacity of the watershed. The C_c of the watershed shows a value of 1.95.

The areal morphometric parameters provide a measurement of basin shape irregularity. The basin would be a perfect circle if the shape factor = 1, successively, lower factors represent a more convoluted flow, and close to 0 = approaching a line.

It is also the area required to maintain one linear kilometre of a stream channel. Generally, the higher the C values of the basin, the higher the permeability of the rocks of that basin and vice-versa (Rao 2009). The C varies from 0.77 to 56.76, with an average of 14.29 indicating higher permeability (Table 3.9).

3.6 Land Use/Land Cover Map

The Land Use of a region results from the interaction of various factors such as physical, economic, and social, which shows the extent to which man has been able to utilize the land resources gainfully. Land Cover refers to anything on the surface which is not subjected to anthropogenic action like a forest, rivers, different types of rock exposures, and others. The land use/land cover analysis is essential to know the spatial distribution of land resources.

The area of interest (AOI) or training sites are selected on the LISS-IV imagery. Those Training Sites are verified on SPOT imagery of 2.5m resolution and verified by several field visits. Based on the ground verification, the boundaries of the lu/lc units were finalized, and then the mapping is carried out (Table 3.11).

The lu/lc features can be spatially interpreted (Figure 3.9), which indicates that about 45% of the total area is covered by forest and forest plantation. More than 10% of the area is identified as built-up land. Also, the agricultural land and plantations together constitute 35% of the total area.

The accuracy assessment is the important step in any classification process. The objective is the quantitative assessment of the pixels, which are sampled from the satellite imagery. These pixels could be identified on google imagery or verified by field visits. A total of 300 locations (points) were selected using the ArcGIS “Create random points” sampling tool. Then the locations were verified on google map. That is, out of 300 random sampling points, 263 points are found to be accurate, whereas 37 are found to be error prone. The details can be seen in the confusion matrix table. The accuracy was found to be 87.6%.

Table 3.9 Morphometric analysis of areal parameters.

	A	B	C	D	E
	AREAL PARAMETERS	Parameter	Sl. No.	order	Results
1		form factor	42		0.23
2		elongation ratio	43		4.26
3		circularity ratio	44		0.26
4		shape factor	45		4.33
5		compactness coefficient	46		1.95
6		Mean drainage density	54	Avg.	0.36
7		stream frequency	55		5.52
8		drainage texture	56	I	1.45
9			57	II	23.88
10			58	III	10.78
11			59	IV	7.20
12			60	V	3.35
13			61	VI	1.59
14			62	VII	0.89
15		mean drainage texture	63	Avg.	7.02
16		texture ratio	64		23.61
17		constant of channel maintenance	65	I	0.77
18			66	II	1.65
19			67	III	3.47
20			68	IV	6.17
21			69	V	15.44
22			70	VI	56.76
23			71	VII	15.81
24		length of overland flow	72	I	0.38
25			73	II	0.82
26			74	III	1.74
27			75	IV	3.08
28			76	V	7.72
29			77	VI	28.38
30	78		VII	7.91	

Table 3.10 Morphometric analysis of relief parameters.

	A	B	C	D	E
1	RELIEF PARAMETER	Max elev.	79	-	1.884
2		Min elev.	80	-	0.001
3		basin relief	81	-	1.883
4		relief ratio	82	-	0.031

Table 3.11 The lu/lc and corresponding area statistics.

Sl. No.	lu/lc categories	Area (km ²)	Area (%)
1	Agricultural Land	122.27	14
2	Barren / Stoney Waste	28.03	03
3	Built-Up	93.87	11
4	Forest	378.58	43
5	Forest Plantation	20.50	02
6	Grassland	15.95	02
7	Industrial Area	7.51	0.8
8	Island	1.01	0.3
9	Plantation	182.33	21
10	Scrub Land	9.91	0.9
11	Waterbody	17.79	02
	Total	877	100

3.7 Soil resource map

The soil resource map consists of the systematic examination, description, classification, and mapping of soils of an area. In the present study, accurate data from NBSS/LUP, an autonomous organization under the Ministry of Agriculture GOI, and KSRSAC Bangalore is used and then vectorized to create thematic information. The soil type (Figure 3.11) and soil depth (Figure 3.12) data of the study area provide crucial information with respect to groundwater resources. About 75% of the total area is covered by fine and fine loamy soil types (Figure 3.12).

It is observed that the information related to the thickness of the soil is also important with respect to infiltration and groundwater resources. Most of the study area is covered with deeper soils with a thickness of 100cm. The area which extends towards the Udupi district covers some part of “moderately shallow” soils.

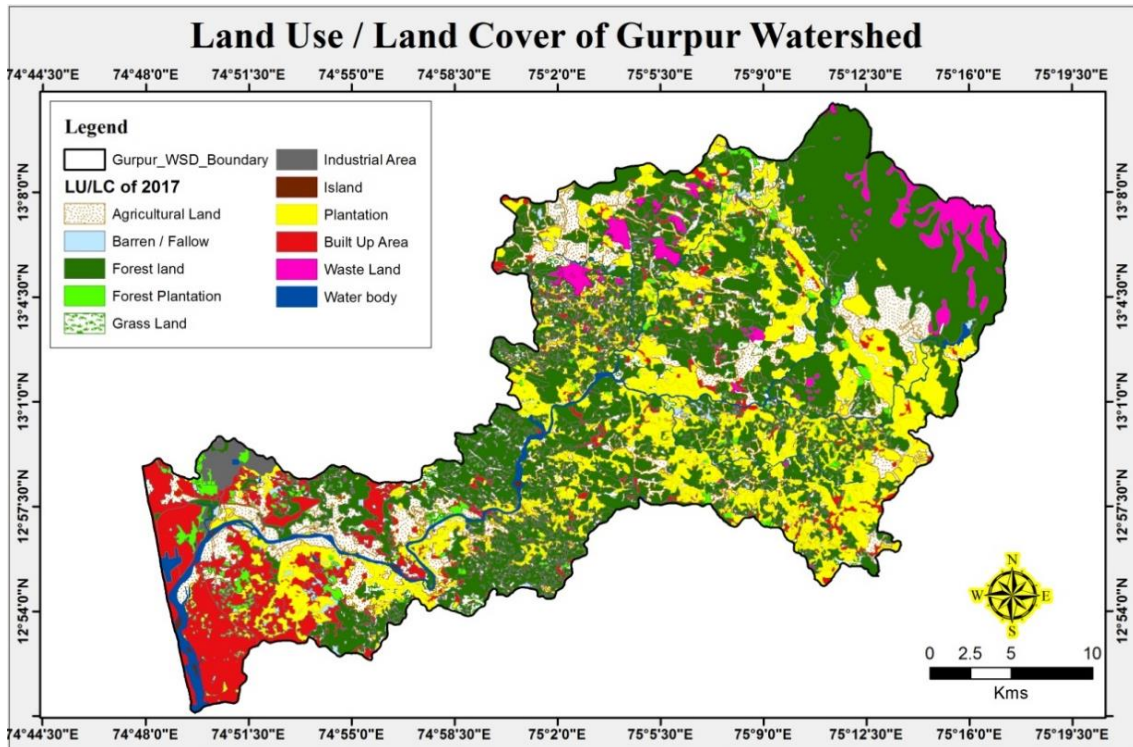


Figure 3.9 Spatial distribution of lu/lc categories in Gurpur watershed.

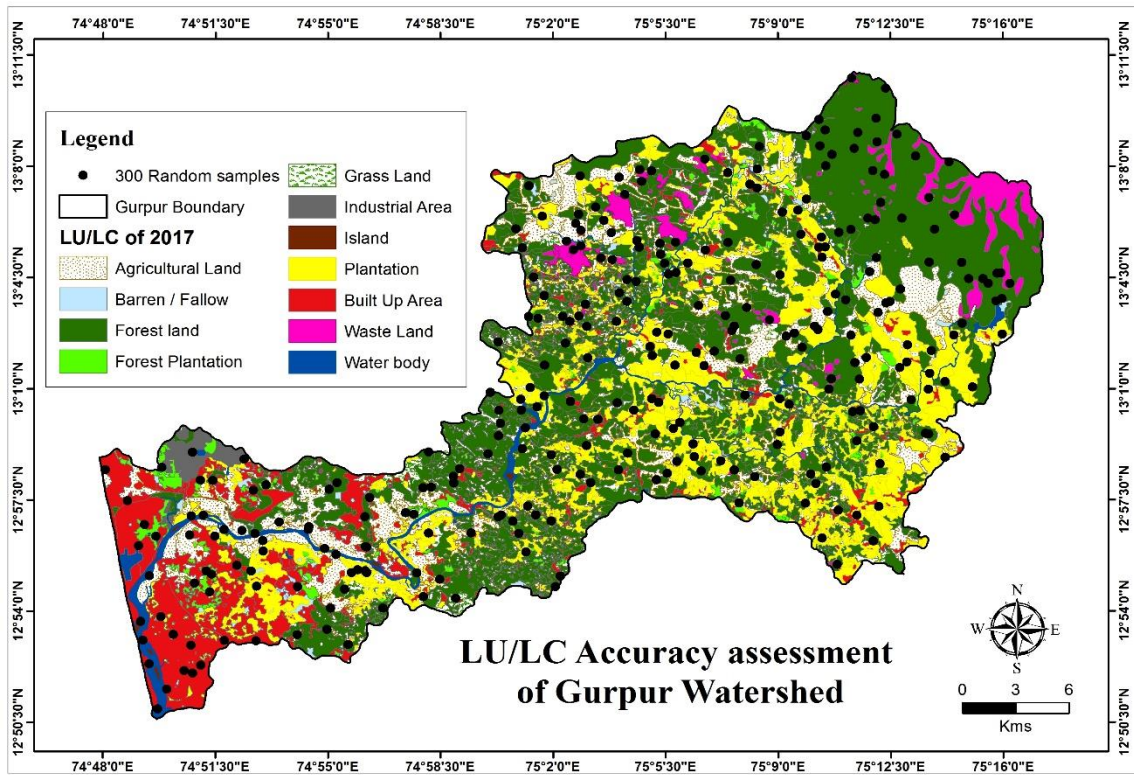


Figure 3.10 The lu/lc accuracy assessment using 300 random sampling

Table 3.12 Categories of soil types and corresponding area statistics.

Sl. No.	Soil Types	Area (km²)	Area (%)
1	Clayey Skeletal	35.96	04
2	Dyke Ridges	0.77	00
3	Fine	413.6	47
4	Fine loamy	246.1	28
5	Habitation Mask	14.68	02
6	Loamy	0.67	0
7	Loamy skeletal	140.27	16
8	Sandy	3.14	0
9	Waterbody mask	22.64	3
	Total	877	100

Table 3.13 Theoretical error matrix of lu\lc classification.

Sl. No.	LULC classification	Agricultural Land	Barren / Stony Waste	Built-Up	Forest	Forest Plantation	Grass Land	Industrial Area	Island	Plantation	Scrub Land	Waterbody	Total Samples	Error	Accurate
1	Agricultural Land			1	2		1			1			45	5	40
2	Barren / Stony Waste												10	0	10
3	Built-Up				2	1				4			23	7	16
4	Forest		2							9			128	11	117
5	Forest Plantation			2						4			12	6	6
6	Grass Land				2								5	2	3
7	Industrial Area												1	0	1
8	Island												1	0	1
9	Plantation	1			1								66	2	64
10	Scrub Land				1	1				1			1	3	-2
11	Waterbody			1									8	1	7
Total													300	37	263

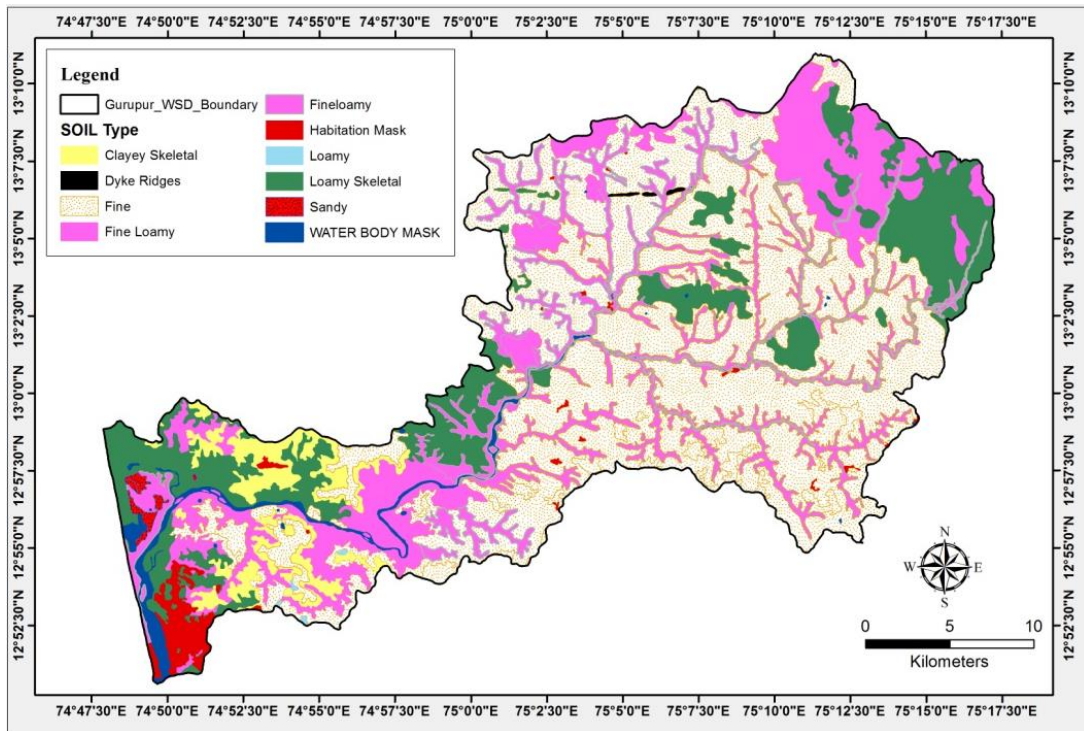


Figure 3.11 The classes of soil types in the study area.

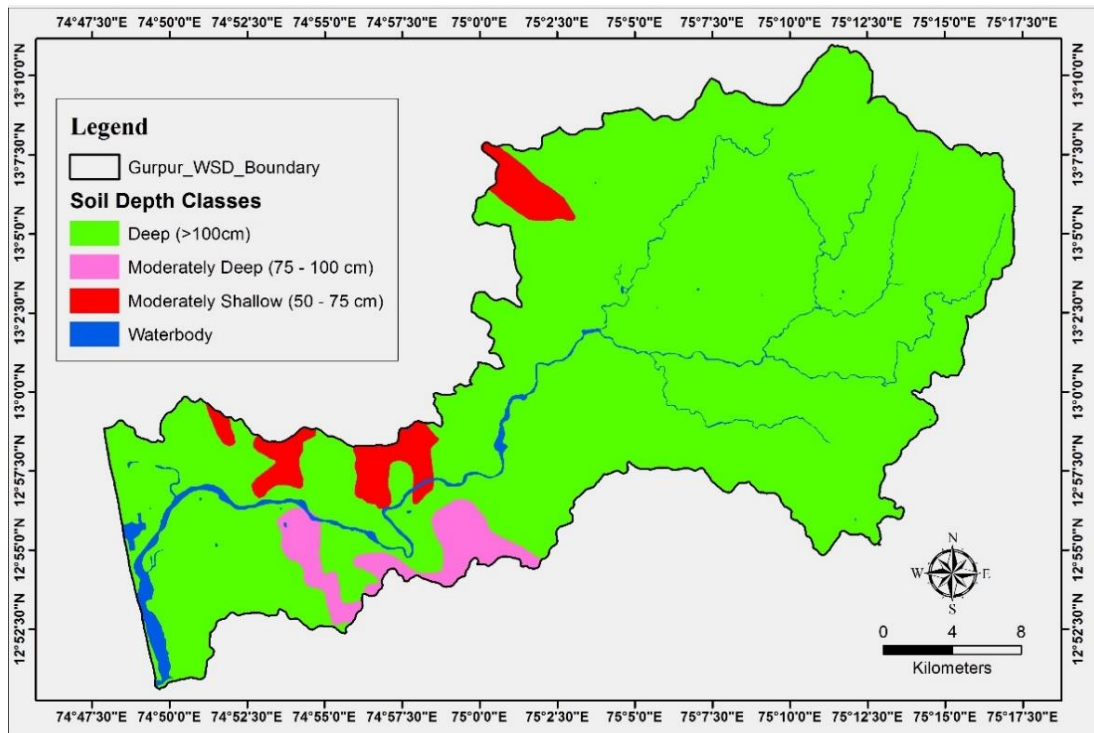


Figure 3.12 The classes of soil depth in the study area.

3.8 Summary

The groundwater is a natural resource influenced by the climate, geology, geomorphology, and drainage characteristics. Geological factors like lithology, stratigraphy and structures play an important role in providing boundary conditions for the aquifers. Remote sensing and GIS techniques are proven efficient tools for delineating, updating, and morphometric analysis of drainage basins. The major litho unit is PGC or Achaean MGTG. The Gurgur watershed is divided into high land, midland and low land (Ghats, hinterland, and coastal area) depending on terrain features and altitude. With the help of electrical resistivity data, the thickness of the weathered zone (depth to bedrock) is in the range of 20m to 40m from the surface. The CartoSAT-1 DEM data with a spatial resolution of 30m is used in the present study. The DEM derivatives like drainage network, slope, hill shade, and contour are extracted and utilized in the study.

Following the increasing use of GIS in analysing spatial data on diverse applications, this study shows that the GIS environment can also be efficiently used for landform and watershed studies. The morphometric analysis is carried out in terms of linear, aerial, and relief aspects. The Gurgur River is a 7th order stream. The “Nearly level” category of the slope is observed towards the beach, whereas a “very steep slope” is observed towards the Western Ghats. The dendritic drainage pattern is seen in the hilly and plateau parts of the drainage basin. The variation in stream length ratio is due to a change in slope and topography. The bifurcation ratio in the watershed indicates the normal watershed category, and the presence of moderate drainage density suggests that it has moderately permeable sub-soil and intermediate drainage texture. The lower values of the form factor of the sub-watersheds indicating the basins are elongated. A higher value of stream frequency is observed in the watershed, indicating low runoff, thick vegetation, and moderate relief. The result of morphometric analysis provides information about watershed development and areas vulnerable to land degradation. The study has strengthened the understanding of the drainage basin's hydrological, geological, and geomorphological characteristics. The lu/lc map reveals that forest, forest plantation covers about 56% of the total area. A plantation, which indicates more than half of the total area, is covered with vegetation.

Chapter 4

GROUNDWATER EXPLORATION

4.1 Introduction to groundwater exploration

The growing water demand for the increasing population can be met through GW's scientific exploration and exploitation. Though the direct approach of drilling provides first-hand information about GW, it is costly. Therefore, several indirect scientific methods are applied for GW exploration studies. Such studies include MCDM, AHP, WOA, and MCF. Saaty (1980) emphasized that the AHP method has numerous applications in natural resources, environmental, hydrogeological planning & management. The eigenvector of the square reciprocal matrix used to compare all possible pairs of criteria will be utilized for assigning weights (Chowdary et al. 2013). Several other suitability analysis methods are available; one of them is the “Weighted Overlay Analysis” which allows us to combine the weights and ranks of several different types of thematic information. The combination of multi-disciplinary fields like GIS, RS, and MCDM techniques is of great importance for GW studies. Therefore, Carver (1991) suggested that the potential use of a combined GIS-MCE approach for developing spatial decision support systems plays an important role.

4.2 Materials and methodology

4.2.1 Geophysical methods in groundwater exploration

The application of physical laws and principles for understanding the sub-surface of the earth is the concept behind geophysical techniques. Even though these are indirect methods, but scientifically they are reliable in probing subsurface formations and their geologic complexity. The role of geophysical techniques in exploration for GW, minerals & ores, oil, and petroleum are well known. There are several methods of geophysical exploration which are widely applicable for groundwater and sub-surface studies. Some of the important geophysical methods are gravity, seismic, magnetic, and electrical methods.

The seismic prospecting involves recording the time intervals and intensity of the earth's elastic wave energy (seismic waves), reflected from a targeted depth (Dobrin & Savit 1988). On the contrary, gravity and magnetic method involve measurement of the natural force field of the earth. The electrical and electromagnetic methods involve reflection and refraction principles, and the source can be either natural or artificial. The gravity or magnetic methods measure the combined contribution of all the levels of depth. At the same time, the seismic and electrical methods can give detailed and precise information of different depths. The seismic methods are highly helpful in probing greater depths. Therefore, the seismic method is widely applicable in oil and natural gas exploration. Whereas the electrical resistivity method is widely applicable in groundwater exploration.

4.2.2 Electrical resistivity method (ERM)

Our earth is heterogeneous in composition and thus shows a different range of electrical properties. The ER method works on the concept that the earth's heterogeneous sub-surface materials show electrical contrast. This electrical contrast can be either analysed by conductance (C) or resistance (R). The R can be obtained using Ohm's law,

$$R = \left(\frac{\Delta V}{I} \right) \quad \text{(equation 4.1)}$$

Where, $\Delta V = \text{Voltage}$ $I = \text{Current}$ $R = \text{Resistance}$

Vertical Electrical Sounding is the method that is based on the electrical conductivity or resistivity of the sub-surface materials. The measurement of potential difference (voltage) at the potential electrodes (M & N) is used to obtain apparent resistivity (ρ_a). The distance between the current electrodes (A & B) is used to obtain the targeted depth (Figure 4.1). The general formula for resistivity is,

$$\text{Resistivity}(\rho) = \frac{(\text{Resistance} * \text{Area of crosssection})}{\text{Length of the conductor}} \quad \text{(equation 4.2)}$$

The obtained ρ data is used to calculate apparent resistivity using Schlumberger's equation (equation 4.3). The formula for calculating ρ_a of Schlumberger array is,

$$\rho_a = \left[\frac{\pi \left[\left(\frac{AB}{2} \right)^2 - \left(\frac{MN}{2} \right)^2 \right]}{2 \left(\frac{MN}{2} \right)} \right] * R \quad \text{(equation 4.3)}$$

Where, ρ_a is the apparent resistivity.

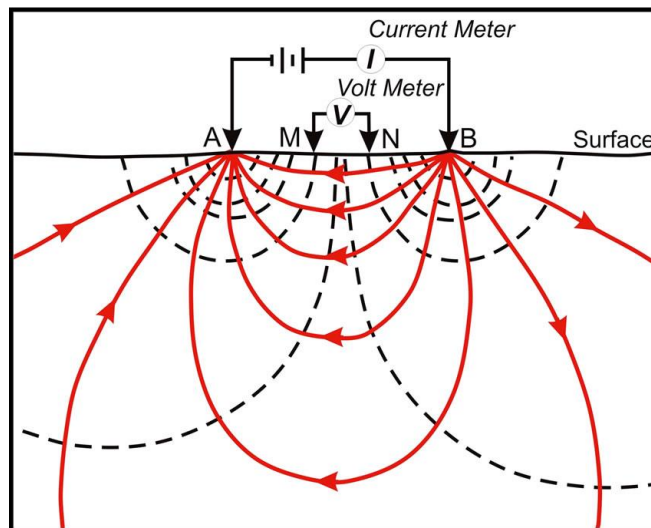


Figure 4.1 Schematic drawing of Electrical Resistivity principle(Clark & Page 2011)

The thickness of the material, composition, aquifer parameters (porosity, permeability, transmissivity, hydraulic conductivity), and associated structures plays a vital role in electrical resistivity observations. Water is a good conductor of electricity, so the presence of water gives relatively less resistance which could be the possible water source.

The ρ_a for each current electrode separation is calculated by multiplying the resistance value by Schlumberger configuration factor (Ramanuja 2012; Poongothai & Sridhar 2017).

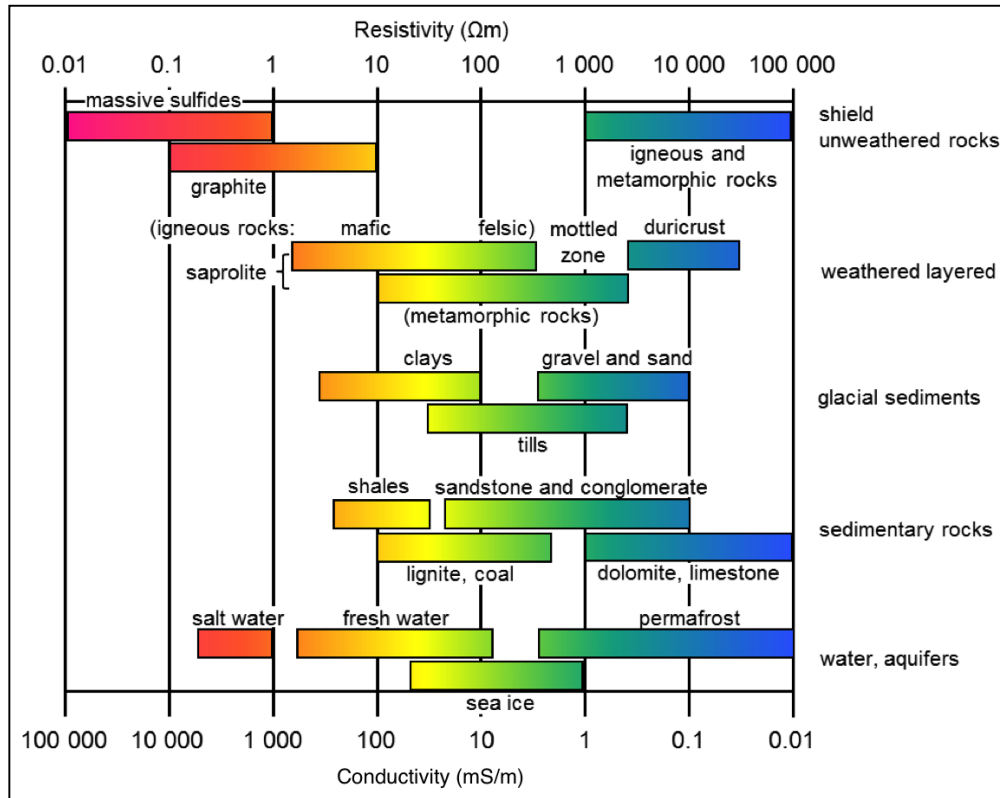


Figure 4.2 Typical resistivity values for different rocks (geosci.xyz)

The earth is heterogeneous in composition. Therefore all the materials and the rocks present in the subsurface must have different apparent resistivity (Figure 4.2).

4.2.2.1 ER method and configurations

In 1934, the VES was first presented by Schlumberger for 1-dimensional work. Later on, a wide variety of VES systems was presented, but the Schlumberger method is still accepted as the best method for depth probing (sounding) and depth profiling. Different Electrical Resistivity methods like Wenner array, Schlumberger, Pole-Pole, di-pole dipole, pole-dipole, half Schlumberger, square array method, etc., could be utilized the type of work to be conducted. For example, in Figure 4.3, it can be understood that the Schlumberger method is good in-depth probing while the Wenner method is suitable for lateral variations at the same depths (Loke 2001).

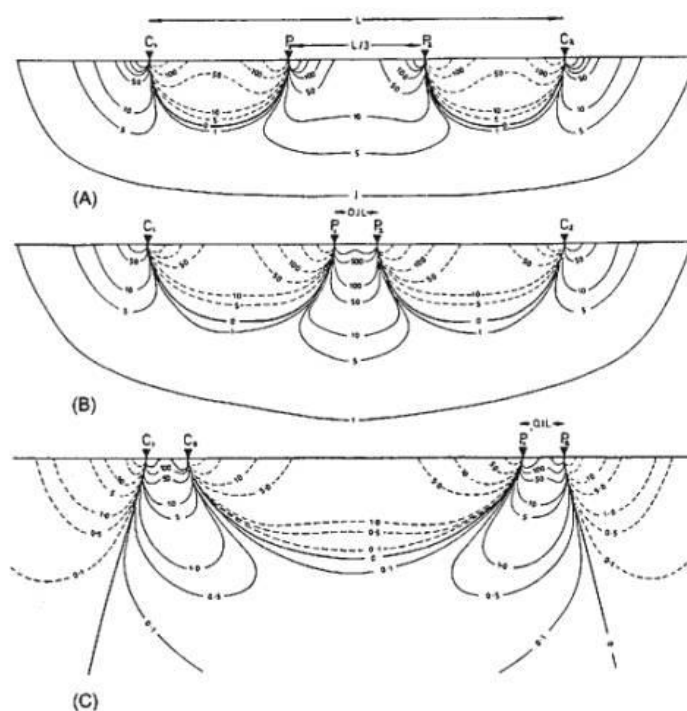


Figure 4.3 Wenner, Schlumberger and double di-pole arrays respectively

Horizontal profiling (HP) is one of the methods used to measure the resistivity variation along the length of the configuration. The HP method is used to measure the lateral variations of resistivity of the subsurface. Whereas depth probing is done using the VES method. The electrical resistivity instrument used in the study is a state-of-the-art, microprocessor-based signal stacking and signal enhancement resistivity meter. Signal Stacking Resistivity (SSR)-MP-ATS possess innovative features and advanced digital circuitry for data acquisition. The apparent resistivity is obtained directly along with its corresponding depth values in this instrument. The ISM and Java-based software ATS-3.0 is used for data plots and interpretation. The graph can either be obtained automatically with tolerance percentage or manually joining the segments. About 35 VES are carried out at selected locations in the study area using Schlumberger array with current electrode spacing $\left(\frac{AB}{2}\right)$ up to 200m.

4.2.2.2 Interpretation methods

There are different methods of analysing resistivity-sounding data, like qualitative and quantitative methods. Again, there are several methods in quantitative as well as

qualitative interpretation methods. A comparative study is carried out for both the interpretation techniques. In the present study, CMT and ISM are utilized for interpretation. The quantitative analysis technique, popularly known as the “Curve matching technique” is used in this study. However, VES data can be interpreted by different techniques to get a subsurface profile, layer thickness, and true resistivity. The confusion occurs during the selection of suitable methods of interpretation, as the accuracy of the result largely depends on the interpretation technique (Asije & Igwe 2014; Prabhu & Sivakumar 2018). Once the graph plots are ready, both qualitative and quantitative analyses are done. There are standard curves like H-type, A-type, K-type, Q-type, and those for several layered systems. These standard curves and set of curves provides the basic understanding of the curve matching technique.

The ISM is a direct method suggested by (Narayan & Ramanujachary 1967; Ramanuja 2012). For Schlumberger configuration, the plotting of ISM is done with respect to $\left(\frac{AB}{2}\right) / \rho_a$ in Y-axis against $\left(\frac{AB}{2}\right)$ in X-axis. The distance $\left(\frac{AB}{2}\right)$ is the half of current electrode spacing. The ISM method utilizes best fitting straight-line segments similar to CMT. But, when compared to CMT, the negative slope indicates the greater resistance in the ISM method. The exact thickness and depth of each layer are indicated with a sharp boundary. Once the profile line is ready, the slope for each segment is calculated, and the true resistivity is obtained. The ISM data obtained is then correlated with borehole log data.

4.2.2.2.1 Dar-Zarrouk parameters

Maillet (1947) suggested that the average geoelectrical properties of the subsurface formations can be outlined by parameters known as Dar-Zarrouk parameters. The surface resistivity and the thickness of different geoelectrical layers help obtain D-Z parameters. Several studies have been conducted on D-Z parameters and their relationship with aquifer parameters (Henriet 1976; Reghunath 1999; Utom et al. 2012; Batayneh 2013). The D-Z parameters coupled with pumping test results help establish empirical relationships and the hydraulic behaviour of the aquifers (Arétouyap et al.

2019). The layer resistivity (ρ) and layer thickness (h) are the important components of geoelectric layers. The different types of D-Z parameters are,

- A. Longitudinal unit Conductance (S)
- B. Transverse unit Resistance (TR)
- C. Aquifer Anisotropy (λ)

The S can be determined using the equation,

$$S = \sum_{i=1}^n \left(\frac{h_i}{\rho_i} \right) \quad (\text{equation 4.4})$$

Where h is layer thickness, and ρ is layer resistivity for 'n' number of layers.

The variation of the S value of each layer can be utilized qualitatively to identify the low resistivity materials and their thickness (Zohdy 1969). The high thickness of the layers is interpreted by large values, whereas smaller values of S can interpret the lesser thickness of the shallow basement.

The equation for TR is,

$$TR = \sum_{i=1}^n (h_i * \rho_i) \quad (\text{equation 4.5})$$

Where h is layer thickness, ρ is layer resistivity.

The λ can be determined using the equation,

$$\lambda = \sqrt{TR} * \left(\frac{S}{H} \right) \quad (\text{equation 4.6})$$

Where H is the total thickness

Usually, λ will be near to unity and exceeds for the rocks having high resistivity, indicating that lesser the λ greater will be the Porosity and permeability (Keller & Frischknecht 1966).

4.2.2.2.2 Hydraulic and geoelectric parameters

The ρ_a is used to extract the information like the aquifer layer resistivity (ρ_0) and layer thickness (Table 4.5). These form the base data to prepare the spatial distribution of

thematic layers like porosity, hydraulic conductivity, and transmissivity. The highly resistive subsurface medium shows an inverse relationship with the hydraulic flow (K) and electric current (ρ) passing horizontally in a typical unit column of an aquifer. Niwas & Singhal (1981) found that the electric current in the highly conductive medium will exhibit vertical flow, but hydraulic conductivity exhibits horizontal flow, indicating the direct relationship between ρ and K .

The hydraulic and geoelectric parameters of an aquifer and their relationship are controlled by the composition and subsurface lithology of the aquifers (Niwas & Lima 2003). If the aquifers transmit the maximum amount of water, it indicates the possibility for recharge potential, especially in humid regions. Less or no transmissivity of the aquifers below the groundwater table indicates either the poor hydraulic conductivity or the lack of potential recharge zone. The hydraulic conductivity (K) can be expressed as

$$K = [(8 * 10 - 6) * (e^{-0.0013\rho})] \quad \text{(equation 4.7)}$$

Consider the unit cross-section of an aquifer medium from top to bottom in the vertical prism form; the K obeys Darcy's law, and ρ in the aquifer medium obeys Ohm's law. These two laws are combined using prism form (Niwas & Singhal 1981). Therefore, for the K and ρ in a horizontal direction the equation for the T of the aquifer medium is given by

$$T = [(8 * 10 - 6) * (e^{-0.0013\rho})] * h \quad \text{(equation 4.8)}$$

Where ρ is bulk resistivity and h is the thickness of the aquifer medium.

The aquifer medium with uniform resistivity and saturated with water will be constant for either TR or S . Therefore,

$$T = S \quad \text{(equation 4.9)}$$

From equation 4.9, it is evident that the Transmissivity will be proportional to longitudinal unit conductance for the highly resistive aquifer medium. Also, for a highly conductive medium, the transmissivity is proportional to the transverse unit resistance (Niwas et al. 2011).

All the minerals and rocks have high resistivity except a few. Therefore the electric current passing through water-saturated pore spaces will exhibit less resistivity.

The Archie's law (Archie 1942) is modified by Winsauer & Shearin (1952) with the addition of lithology constant (a). From the modified Archie's law, the resistivity of the saturated clay-free material can be expressed as

$$\rho_0 = a \rho_w \emptyset^{-m} \quad (\text{equation 4.10})$$

Where, ρ_0 is the resistivity of water-saturated sand. The ρ_w is the resistivity of pore space water. The F is an intrinsic formation factor $\left(\frac{\rho_0}{\rho_w}\right)$ that includes all the properties of the material influencing electrical current flow. The relationship between F and \emptyset was first postulated by Humble oil company. The constants a and m are empirical with values 1 and 2, respectively, for a general average of typical reservoir rocks (Winsauer & Shearin 1952). The ρ_w can be measured using the equation

$$\rho_w = \left(\frac{10000}{EC}\right) \quad (\text{equation 4.11})$$

Where EC is the Electrical Conductivity ($\mu\text{S/cm}$) of the water sample of the aquifer. The porosity (\emptyset) can be obtained through the equation

$$\emptyset = \left(\frac{a}{F}\right)^{\frac{1}{m}} \quad (\text{equation 4.12})$$

Where m is the material constant and a is an empirical lithology constant.

4.2.3 Geoinformatics and GW exploration

The RS and GIS have a major role in hydrogeology and water resource development, especially the monitoring and generating spatial and temporal data. Hydrological, structural, geological, geomorphological, slope, drainage analysis, and delineation of land features are necessary for the preparation, prediction, and management of groundwater resources. The IRS satellite imagery/data and topographic maps of the scale 1:50,000 are used to develop integrated groundwater potential zones using the WOA method and provide the zones with good, moderate, poor, and very poor categories. These thematic layers are considered as the influencing factors for groundwater occurrence and movement. The merits and demerits of the features and their influence over groundwater occurrence are exactly the points of consideration for

assigning suitable weights (Jaiswal et al. 2003). The final map is obtained by multiplying individual ranks of the thematic layers with the weightage assigned.

Remote Sensing technology has proved itself as an effective and very important tool in natural resource mapping all over the globe. Because of the bird-eye-view, cost-effectiveness, and its applicability in identifying ground and soil features, satellite imagery is increasingly used in groundwater exploration, which provides the direct or indirect indications for the presence of groundwater or, let's say, the zones for groundwater availability. Satellite images are available as a small, medium, and large-scale data products based on the needs and necessity of the kind of work. The visual interpretation techniques are adopted to map lineaments and surface geological features, topography. The multi-spectral and hyper-spectral imageries provide data in many bands of the electromagnetic spectrum. These unique band data can be used to analyse the same features at a different wavelength, thus uniquely responding to it. As a result, the spatio-temporal information of large and even inaccessible locations can be utilized easily and thus forms the baseline information (Jha & Peiffer 2006; Jha et al. 2007; Kumar & Kumar 2010; Yousef et al. 2015). The GIS is an effective framework for ease and efficient handling of large and complex spatial data, integration, and analysis (Becker 2006; Thapa et al. 2017).

4.2.3.1 Thematic information database creation

Groundwater potential zonation studies are based on integrating several surfaces and sub-surface indicative features (thematic information), either by direct or indirect scientific methods. Quantitative and qualitative methods assess the determination of the groundwater potentiality in an area. The surface features or parameters can be easily accessible through remote sensing and field verification. In contrast, the sub-surface parameters are possible through OB wells, electrical resistivity methods, and direct observations in the possible exposures. The remotely sensed data is used for lu/lc and lineament mapping. Also, the geomorphological mapping and drainage basin analysis add up for it. The present work attempts to establish the relation between electrical resistivity method, RS, and GIS-based methodology in groundwater potential zone identification and mapping. The understanding of geological, structural,

geomorphological characteristics is necessary for assigning Rank/Weight. The thematic information used in this study is briefly introduced as follows.

A slope is a slanting surface at an angle of less than 90^0 to a flat surface. Slope provides a basis so that by successive combination into layer units, general geomorphology could be constructed. Following guidelines of the All India Soil and Land Use Survey on slope categories are used to categorize the slope map in the study. The slope theme is prepared using the CartoDEM and utilized in the MCDM technique for integration and preparation of GWPZ. The slope is having an inverse relation with groundwater potential. An increase in slope increases runoff and baseflow, thus decreasing the infiltration and affecting groundwater potential. Therefore ranking of 5 is given to the lowest slope categories and 1 for the highest slope.

The land use of a region results from the interaction of various factors such as physical, economic, and social factors, which shows the extent to which man has been able to utilize the land resources gainfully. The land cover refers to anything on the surface that is not subjected to anthropogenic action like forests, rivers, and different rock exposures. In the LISS IV multi-spectral imagery, the vegetation shows red colour in the FCC combination (Figure 1.1). The land use/land cover analysis is essential to know the spatial distribution of land resources. In this study, Level-I classification of the NRSC for lu/lc is used. The waterbody is given a high weightage of 5, and agricultural land is given 4. The dykes are hard rocks and unable to infiltrate GW but can be used as sub-surface barriers to arrest the flow of GW. Therefore, with respect to GW potentiality studies, dykes are given low weights, and with respect to GW recharge, the dykes are given high weightage.

The present study utilizes already available authentic soil types map collected from NBSS/LUP Bangalore and later georeferenced and vectorized in GIS environment. A higher ranking is given to soil types that can infiltrate more water, as shown in Figure 4.10b.

The CartoDEM data available from the Bhuvan website is used to prepare the drainage layer using which the drainage density thematic map is done and converted into a vector format. Drainage density is calculated as the “ratio of the total length of

streams of all orders within the basin to the basin area”(Reddy 2004) and expressed as km/km^2 .

The higher ranking is given to the very low and low drainage density regions due to the lesser slope and greater infiltration and groundwater potentiality. Shahzad et al. (2009) opined that the orientation and style of the drainages have a relationship with lineaments as they are associated with structural complexity. Generally, lineaments are associated with weathering and therefore increases porosity and permeability. Hence, lineament density and groundwater potential have a direct relationship (Hardcastle et al. 1995). Therefore, ranking of 1 and 3 are given to low and high lineament density classes, respectively.

The geomorphology maps and data were collected from GSI and KSRSAC organizations. The available relief information in the topo maps is verified with the LISS-IV imagery. Training sites for different litho-geomorphic units were selected and field verified. These are utilized in the preparation of spatial distribution of geomorphology thematic information. The satellite imagery provides useful information in mapping geomorphology, which along with the electrical resistivity data, helps verify and correlate the information on the depth of weathered zone, type of associated material, nature of the environment, agent of weathering, etc. The highest rank of 5 is given for plains, and the least rank of 1 is given for structural hills.

Lithology map for the study area was geo-referenced, and screen digitized from GSI published map with 1:50,000 scale. The characteristics of rocks in compactness, density, weathering status, composition, joints, and fractures play a vital role in weightage assignment for lithology. A ranking of 4 is given to alluvium or beach sand, whereas 1 is given to hard and indurated gneissic rock.

The rainfall data is collected from the IMD website, DMG Mangaluru, CGWB, KSNDMC, and Statistical Department. The rainfall data was sorted station-wise along with their coordinate information using Microsoft Excel 2013. The average annual rainfall for 19 years from 1999-2016 is tabulated and connected with associated point features of rain gauge stations in the GIS environment. The Geostatistical analyst tool is used to prepare the isohyetal map for rainfall distribution over 19 years. Later it is exported to a shapefile of polygon features and used for integration purposes so that the

accuracy of the groundwater potentiality can be increased. The rainfall is having a direct relationship with groundwater potentiality. Therefore highest ranking of 3 is given to the high rainfall distribution class and the lowest of 1 to the low rainfall distribution class.

The GWC map of the Gurple watershed is prepared using the groundwater level OB wells data obtained from DMG and CGWB. At first, the GPS coordinates of the well locations are attributed to groundwater level data for 2017 and transferred into the GIS platform. The groundwater level is considered as average, for the peak months of Phase-I (post-monsoon, December 2016) and Phase-III (pre-monsoon, March 2017) seasons. And finally, the GW contours thematic layer is prepared using the IDW method.

About 35 VES Soundings have been conducted using Schlumberger 1D method within the study area. The obtained apparent resistivity data is interpreted using the ISM technique. It is simple to operate and gives good results. In this method, the plotting is made by electrode space 'a' in X-axis and electrode separation divided by apparent resistivity values in Y-axis. The point of intercept gives the depth of various interfaces. The results obtained from ISM are used to prepare depth to bedrock (weathered zone thickness) thematic layer. The weathered zone hosts groundwater in its secondary porosity (like fissures, fractures, and pore spaces) of the weathered rocks (Gurumurthy 2013). The landscape of the study area along the coast is the reflectance of extensive tertiary denudation, which leads to the formation of laterites. The extent of weathering along with depth to bedrock forms the potential aquifers. Closer the bedrock depth from the ground, thinner will be the weathered zone, thus directly affecting groundwater potentiality.

The hydraulic and geoelectric parameters can also be calculated and utilized for GW studies. If the aquifers transmit the maximum amount of water, it indicates that recharge potential is high, especially in humid regions. Less or no transmissivity of the aquifers below the groundwater table indicates either the poor hydraulic conductivity or the lack of potential recharge zone. And thus, the highest ranking of 3 is given to the high transmissivity class. Poor hydraulic conductivity indicates a lack of potential aquifer zones. Therefore ranking of 3 is given to the high K class. The porosity is having

a direct relationship with groundwater potentiality. An increase in porosity, especially effective porosity, increases the groundwater potentiality. Thus, the highest ranking of 3 is given to the high porosity class.

4.2.4 Integrated approach for GW exploration

The integration of several methodologies for obtaining better results is a trending development in recent studies. Several studies have been carried out using the integrated approach (Khan & Moharana 2002; Anomohanran 2011; Bhattacharya et al. 2020; Warsi et al. 2020). The geospatial studies integrated with geophysical, geological, geomorphological, hydrological, socio-economical, geochemical can be used for integrated studies. The weighted overlay index (or the weighted index overlay) is an important technique used in the integrated approach (Gyeltshen et al. 2020). The weighted overlay analysis is one of the important methods used for modelling suitability. The WOA is used to solve multi-criteria problems such as site selection and suitability models (How Weighted Overlay works-ArcGIS Help). The WOA method is utilized in this study.

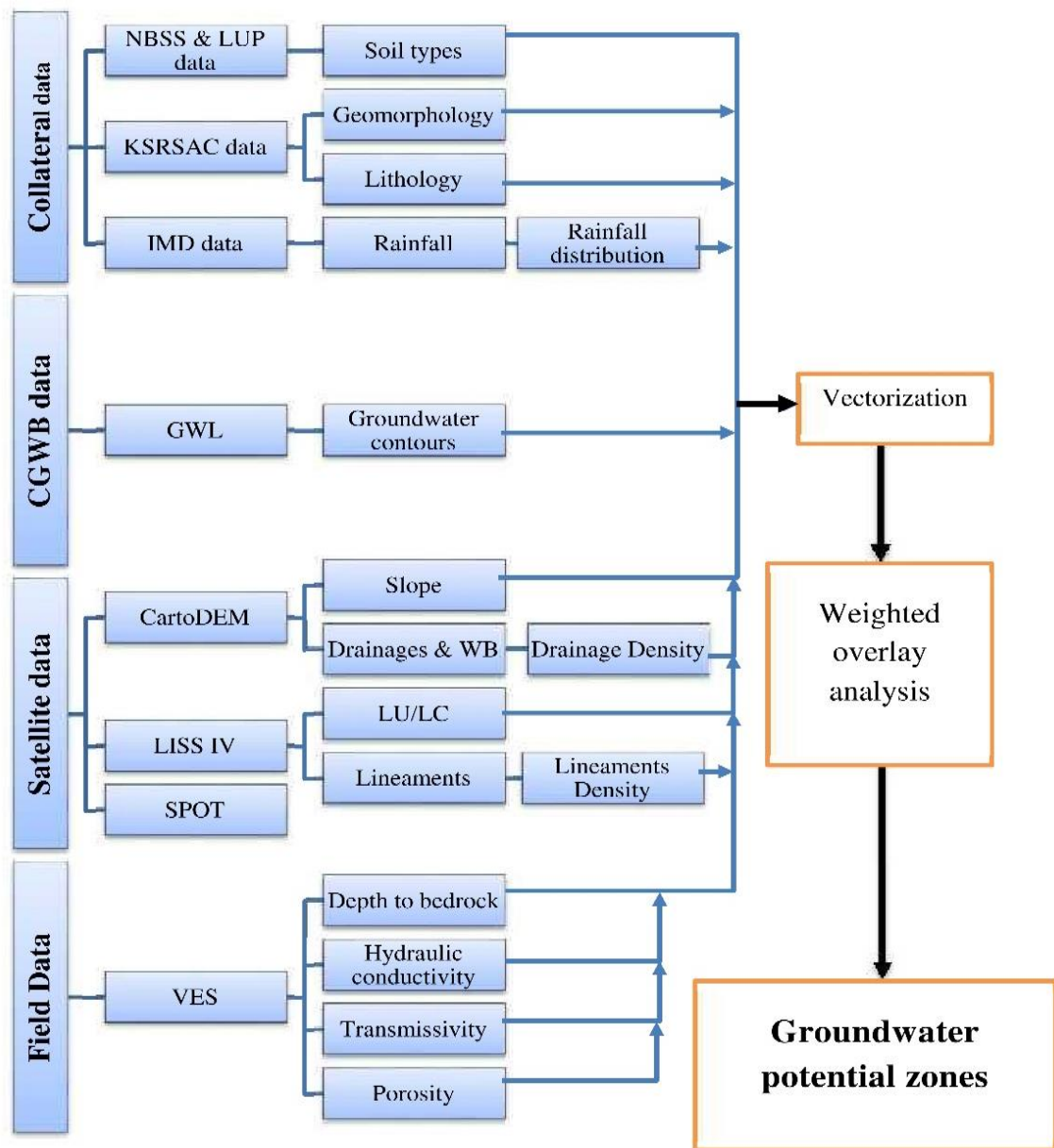


Figure 4.4 Flow chart for groundwater potential zones mapping.

4.3 Results and discussion

4.3.1 Qualitative and Quantitative VES analysis – ISM

The 35 soundings measurement is interpreted using the direct method, a quantitative interpretation method, and the statistics shown in (Table 4.1). The graphs and geoelectric section of the soundings are prepared and interpreted using ISM (Figure 4.5). The top layer resistivity is found to be in the range of 74 Ωm (VES 5) to 5458 Ωm .

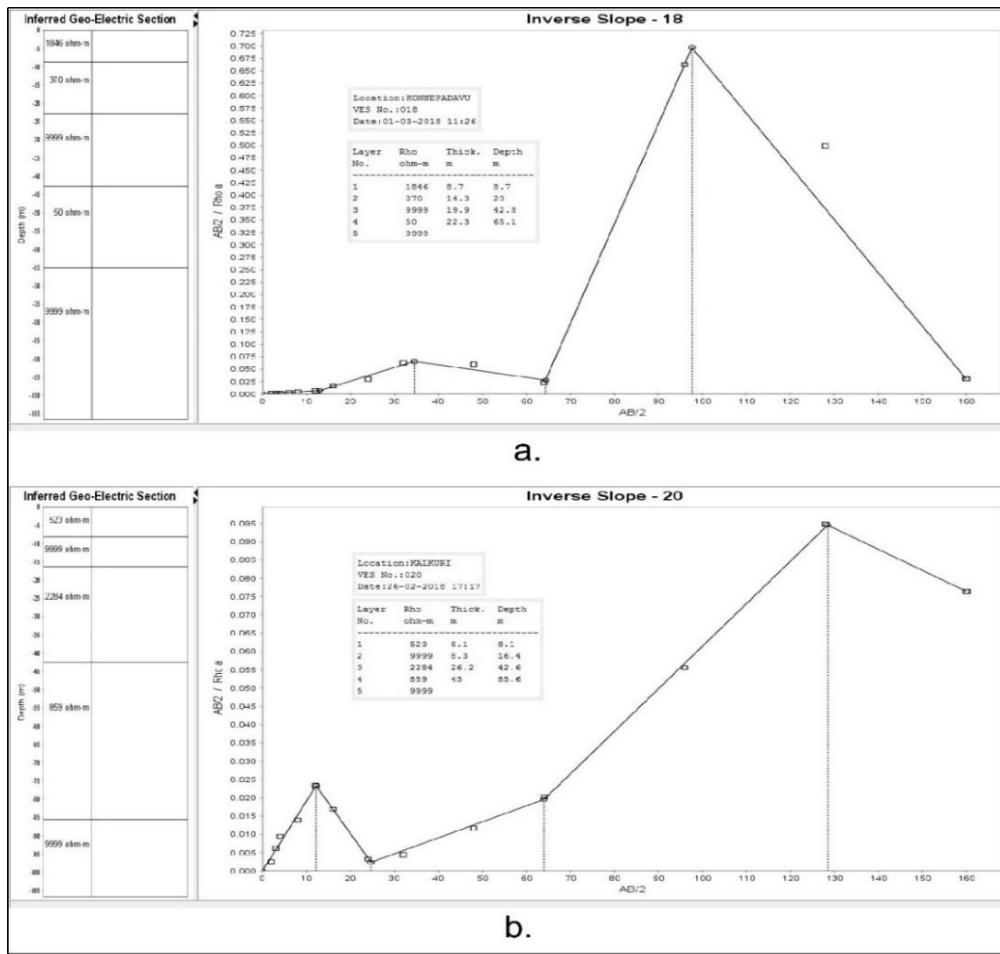


Figure 4.5 Selected graphs for ISM interpretation

(VES 33) and the thickness is from 1.3m (VES 7) to 21.6m (VES 19). The selected graphs VES-18 and VE-20 are shown here for representation purposes. The overall resistivity values are in the range of 14 Ω m (VES 3) to 7958 Ω m (VES 31). The thicknesses of the geoelectrical layers are found to be in the range of 1.3m (VES 23) – 76.2m (VES 11). The depth to bedrock varies from 3.7m (VES 2) to 44.4m (VES 10). The overall aquifer thickness (h) varies from 19.5m (VES 19) to 149.5m (VES 15).

The spatial distribution of depth to bedrock is prepared using the VES data and ISM technique. The depth to bedrock ranging from 9.2m – 25.5m covers a maximum study area of more than 70% (622.46 km^2). The shallow basement covers 6% (57.01 km^2) of the study area. The deeper basement covers 4% (32.33 km^2).

Table 4.1 Quantitative analysis of VES data interpreted using Inverse Slope Method

Sl.No.	VES No.	Location	No. of Layers	Depth to Bedrock	Aquifer Thickness (h)
1	1	Kulai	2	4.9	67.8
2	2	Tokuru 62	4	3.7	125.7
3	3	Kunjathbailu	3	15	61.7
4	4	Bondel	4	20.8	64.2
5	5	Bajpegama	4	5.1	94.3
6	6	Moodushedde	4	5.3	101.4
7	7	Paldaane/Kudupu	5	41.8	102.3
8	8	Fermai	4	33.5	108.1
9	9	Addoor	5	42.7	38.4
10	10	Gurpura	4	44.4	85.6
11	11	Ganjimatha	4	31	100.4
12	12	Kaavagudde	4	32.9	72.1
13	13	Benjanapadavu	5	12.1	95
14	14	Loretto	4	15.9	116.4
15	15	Varmala	5	40.5	149.5
16	16	Kuppepadavu	4	17.1	112.9
17	17	Iruvailu	4	16.2	49.7
18	18	Konnepadavu	5	23	22.3
19	19	Raayi	4	21.6	19.5
20	20	siddakatte	5	16.4	69.2
21	21	Pucchamogaru	4	42.7	53.1
22	22	Kallabettu	3	16.1	96.7
23	23	Maarnad	5	7.6	30.6
24	24	Maroor	5	16.2	26.5
25	25	Padanthadka	4	42.1	94.6
26	26	Vamanapadavu	5	43.0	21.3
27	27	Nadubottu	5	8.9	56.1
28	28	Gardady	4	10.7	75.6
29	29	Moodukodi	4	16.5	69.2
30	30	Pillya	4	11	41.7
31	31	Sulkeri	5	8.9	60.2
32	32	Kashipatna	3	17.3	47.4
33	33	Naravi	4	4.1	82.1
34	34	Hosmar	4	15.9	61.9
35	35	Eedu	5	7.8	66.7

Shallow depth to bedrock can be seen in and around ghats, extending to midland and in parts of low lands. The deeper basements are interpreted in the midlands of the study area. The single-layer sandwiched between two highly resistive rocks is indicated by a single resistivity value (Figure 4.5a). The multi-layered (Figure 4.5b) aquifer formation shows the number of layers sandwiched between hard rock layers. In such cases, the average resistivity and total thickness of all layers of the aquifer are

considered. Likewise, the aquifer resistivity and thickness for the 35 VES locations are considered and utilized to analyse the hydraulic and geoelectric parameters.

4.3.2 Qualitative and Quantitative VES analysis - CMT

The results were interpreted both quantitatively as well as qualitatively. The quantitative interpretation provides the details of the number of layers and their true resistivity, the thickness of the layer, and the depth encountered. Whereas the qualitative interpretation is made using the curve matching technique (Barseem et al. 2015) gives information about the curve type and layered formation. Selected plots of each typical curve type obtained in the present study are shown below. Based on these curve types, the lithology and groundwater potential is interpreted. The curve types are generated for all the 35 VES locations (Table 4.2, and Figure 4.6). Only the representative curves are explained and shown below. The curve types of all the 35 VES locations can be seen in Appendix B. The curves are interpreted based on the resistivity values rather than the graphs obtained.

4.3.2.1 A-type and AA-type curves

The A-type curves are characterized by the low to high resistivity for three-layered formations ($\rho_1 < \rho_2 < \rho_3$), whereas the AA-type curves are characterized by four-layered formations with low to very high resistivity values ($\rho_1 < \rho_2 < \rho_3 < \rho_4$) respectively. Table 4.3 shows the resistivity sequence of the A-type and AA type curves, respectively.

The VES location for 4, 19, 31, and 32 are selected nearby the gneissic outcrop within the study area. The topsoil resistivity is ranging between 126 Ωm to 2122 Ωm representing the clay material. Whereas the VES 01 showing top soil resistivity of 2122 Ωm represents Laterite in dry condition. The overall layer resistivity for these curve types varies from 126 Ωm to 12154 Ωm . The thickness varies from 0.92 m to 30.7 m.

In AA type curves, the top layer thickness varies from 1m to 8m, with low resistivity represents the possibility of groundwater (unconfined), whereas the 2nd layer with high resistivity represents the hard rock at a depth of 12m. The 3rd layer with relatively low resistivity represents the fractured zone at a depth of 24m with a probable

groundwater source (confined). The 4th layer is having relatively high resistivity indicating fewer chances of groundwater occurrence.

Table 4.2 Curve types for qualitative interpretation of VES

VES no's	Curve Type	Curve Characteristics	No. of Layers	Resistivity (ρ) range (Ωm)	Thickness range (m)
31, 32	A	$\rho_1 < \rho_2 < \rho_3$	3	126 - 8927	1 – 30.7
4, 19, 22	AA	$\rho_1 < \rho_2 < \rho_3 < \rho_4$	4		
2	AK	$\rho_1 < \rho_2 < \rho_3 > \rho_4$	4	22.8 – 2181	2.06 – 12.1
7, 14, 17, 25, 26	H	$\rho_1 > \rho_2 < \rho_3$	3	29.7 - 9400	1.73 – 45.8
6, 15, 30, 34	HA	$\rho_1 > \rho_2 < \rho_3 < \rho_4$	4	103 – 8927	1.16 – 10.4
5, 8, 20	HK	$\rho_1 > \rho_2 < \rho_3 > \rho_4$	4	6.08 – 9207	1 – 49.9
9, 12, 23	HKA	$\rho_1 > \rho_2 < \rho_3 > \rho_4 < \rho_5$	5	193 – 8304	1 – 32.4
11, 16	KH	$\rho_1 < \rho_2 > \rho_3 < \rho_4$	4	396 – 9590	2.01 – 23.2
1	K	$\rho_1 < \rho_2 > \rho_3$	3	118 – 5512	0.53 - 1
10, 33	KQ	$\rho_1 < \rho_2 > \rho_3 > \rho_4$	4	227 – 9237	1 – 25.7
3, 24, 27, 29, 35	QH	$\rho_1 > \rho_2 > \rho_3 < \rho_4$	4	5.13 – 8927	0.42 – 35.1
13	QKA	$\rho_1 > \rho_2 < \rho_3 > \rho_4 < \rho_5$	5	706 – 8929	1.22 – 12.7
18, 21, 28	QQ	$\rho_1 > \rho_2 > \rho_3 > \rho_4$	4	25.7 - 3565	1.21 – 61.2

4.3.2.2 AK-type curves

The VES-02 shows resistivity sequence for AK-type curves that are $\rho_1 < \rho_2 < \rho_3 > \rho_4$ and the typical curve can be seen in (Figure 4.6). The resistivity of the top layer is 63.9 Ωm , interpreted as clay material. The resistivity of the 2nd layer drastically increases, and so also for the 3rd layer. The 3rd layer shows a thickness of 22.8m. The resistivity of the 4th layer relatively decreases, which could be interpreted as favourable for GW potential.

4.3.2.3 H-type curves

The typical H-type curve shows the resistivity sequence of $\rho_1 > \rho_2 < \rho_3$ and can be seen in (Figure 4.6). In the present study, VES 7, 14, 17, 25, and 26 exhibits H-type curve. This type of curve represents 3 layered formations in which the 2nd layer exhibits relatively low resistivity indicating a probable groundwater source with the thickness varying from 36.7m (VES 17) to 45.8m (VES 25). These formations' resistivity ranges from 482 Ωm (VES 26) to 9207 Ωm (VES 17). These formations' thickness ranges from 1.82m (VES 26) to 45.8m (VES 25).

4.3.2.4 HA-type curves

The resistivity sequence for this type of curve is $\rho_1 > \rho_2 < \rho_3 < \rho_4$ and the selected representative curve can be seen in (Figure 4.6). The VES 6, 15, 30, and 34 are showing HA-type curves. The topsoil resistivity ranging from 409 – 9367 Ωm with thickness ranging from 1m to 3.16m can be interpreted as clay material. In contrast, the VES 21 showing layer resistivity of 9367 Ωm is because of the lateritic topsoil with the dry condition.

In the present study, the HA-type curves are exhibiting the layer resistivity from 6.08-39599 Ωm . The layer thickness varies in the range of 0.89m to 69.1m and the depth of the maximum investigation. The layer sequence shows relatively low resistivity for the 2nd layer sandwiched between the 1st and 3rd layer indicates the groundwater source for which the thickness varies from 0.89m (VES 06) to 7.87m (VES 34). But the resistivity increases continuously after the second layer, which can be interpreted as massive hard rock.

4.3.2.5 HK-type curves

The resistivity sequence for this type of curve is $\rho_1 > \rho_2 < \rho_3 > \rho_4$ and the selected representative curve can be seen in (Figure 4.6). The VES 5, 8, and 20 are showing HK-type curves. The layer resistivity varies from 78 Ωm (VES 08) to 9207 Ωm (VES 20). The thickness varies from 1m (VES 20) to 49.9m (VES 08). Here the 4th layer resistivity is gradually decreasing, which indicates the presence of good groundwater potential.

4.3.2.6 HKA-type curves

The resistivity sequence for this five layered formation is $\rho_1 > \rho_2 < \rho_3 > \rho_4 < \rho_5$ and the selected representative curve can be seen in (Figure 4.6). The VES 9, 12, and 23 are showing HKA-type curves. The layer resistivity varies from 193 Ωm (VES 23) to 8304 Ωm (VES 09). The thickness varies from 0.6m (VES 09) to 32.6m (VES 12). These formations are similar to the four-layered HK-type curves, whereas the 5th layer resistivity is increasing, interpreted as massive hard rock. Thus the 2nd and 4th layers are interpreted to be a good source of groundwater potential.

4.3.2.7 K-type curve

The K-type curve is a 3-layered formation with the resistivity sequence of $\rho_1 < \rho_2 > \rho_3$ and can be seen in VES-01. Here the layer resistivity of the 2nd layer is higher compared to the 1st and 3rd layers. This could be interpreted as wet soil of laterite, followed by hard rock and the fractured zone. The layer resistivity is varying from 396 Ωm to 9590 Ωm . Freshwater generally has a resistivity range of 01 Ωm – 100 Ωm , and for saltwater, the resistivity range is 0.1 Ωm – 1 Ωm . Therefore, this VES location may not yield sufficient GW.

4.3.2.8 KH-type curve

The resistivity sequence for this four-layered formation is $\rho_1 < \rho_2 > \rho_3 < \rho_4$ and the curve can be seen in Figure 4.6. The VES 16 shows the KH-type curve. The layer resistivity is varying in the range of 118 Ωm to 3731 Ωm . The thickness varies from 2.56m to 18.7m. In this curve type, the resistivity of the 2nd and 4th layers is higher than the 1st and 3rd layers indicating that the 3rd layer is a good source of groundwater.

4.3.2.9 KHA-type curve

The resistivity sequence for this five layered formation is $\rho_1 < \rho_2 > \rho_3 < \rho_4 < \rho_5$ and the curve can be seen in Figure 4.6. The VES 11 shows the KHA-type curve. The layer resistivity is varying in the range of 1009 Ωm to 9906 Ωm . The thickness varies from 2.31m to 24.5m. This curve type is similar to the KH-type curve, whereas the resistivity of the 5th layer is higher than the 4th layer indicating the hard rock formation up to the maximum depth of investigation. The 3rd layer with relatively less resistivity (1009 Ωm) and thickness of 15m can be interpreted as a good source of groundwater.

4.3.2.10 KQ-type curve

The resistivity sequence for this four-layered formation is $\rho_1 < \rho_2 > \rho_3 > \rho_4$ and the curve is as shown in (Figure 4.6). The VES 33 shows the KQ-type curve. The layer resistivity is varying in the range of 428 Ωm to 9539 Ωm . The thickness varies from 0.76m to 30.7m. In this curve type, the resistivity of the first 3 layers gradually increases, and for the 4th layer, the resistivity decreases drastically. Therefore, the 4th

layer, which has a layer resistivity of 428 Ωm with the thickness extending up to the maximum depth of investigation, can be interpreted as a good groundwater source.

The plots prepared using CMT are qualitative. The 10 plots shown in Figure 4.6 are just the representative plots for the 35 VES locations. That means the VES locations shows similar to those plots and the interpretation is completely based on types of curves obtained.

Table 4.3 Resistivity and thickness of layers for quantitative interpretation of VES

Sl. No.	VES No.	Location	Curve Type	ρ_1	ρ_2	ρ_3	ρ_4	ρ_5	h1	h2	h3	h4
1	1	Kulai	K	396	9590	1052	-	-	1	0.53	-	-
2	2	Tokuru 62	AK	50.5	2181	22.8	554	-	2.06	5.13	12.1	-
3	3	Kunjathbailu	QH	2551	53	5.13	34.5	-	1	4.57	4.09	-
4	4	Bondel	AA	290	599	137	6896	-	3.17	9	11.9	-
5	5	Bajpegrama	HK	409	32.6	2559	6.08	-	1.33	2.79	11.1	-
6	6	Moodushedde	HA	2394	797	4497	-	-	1.48	3.59	-	-
7	7	Paldaane/Kudupu	H	1325	269	9019	-	-	6.75	15.2	-	-
8	8	Fermai	HK	5911	1147	6460	78.1	5630	1.12	8.57	11	49.9
9	9	Addoor	HKA	2128	277	5846	682	8304	1	0.6	0.8	31.1
10	10	Gurpura	KQ	914	9169	605	3588	227	1	2.23	7.2	23.3
11	11	Ganjimatha	KH	2246	3884	985	5512	-	2.01	3.97	23.2	-
12	12	Kaavagudde	HKA	526	347	872	254	7968	1	6.05	5.09	32.4
13	13	Benjanapadavu	QKA	5269	1260	2589	706	8929	1.22	4.3	9.27	12.7
14	14	Loretto	H	1708	25.7	9400	-	-	1.73	3.71	-	-
15	15	Varmala	HA	625	216	5109	-	-	1.16	10.4	-	-
16	16	Kuppepadavu	KH	719	3731	118	861	-	2.56	2.95	18.7	-
17	17	Iruvailu	H	1536	612	9207	-	-	7.06	36.7	-	-
18	18	Konnepadavu	QQ	2132	663	25.7	-	-	5.54	58.8	-	-
19	19	Raayi	AA	157	1271	514	1456	466	1	1.65	16	30.7
20	20	siddakatte	HK	1274	251	9207	538	-	1	3.25	11	-
21	21	Pucchamogaru	QQ	3401	424	1472	416	120	2.08	1.21	14.4	61.2
22	22	Kallabettu	AA	1413	5367	567	5282	-	1	1.16	1.77	-
23	23	Maarnad	HKA	2256	193	1956	197	2311	1	1.11	3.66	18.2
24	24	Maroor	QH	4965	205	1281	278	6497	1	0.42	6.8	17.4
25	25	Padanthadka	H	2723	1133	5775	-	-	2.17	45.8	-	-
26	26	Vamanapadavu	H	750	482	3463	-	-	1.82	37.9	-	-
27	27	Nadubottu	QH	2030	5015	354	7646	-	3.16	2.89	35.1	-
28	28	Gardady	QQ	3769	1582	204	1088	86.5	2.67	4.37	11.6	30.7
29	29	Moodukodi	QH	3672	7234	217	6755	-	3.93	14.2	27.5	-
30	30	Pillya	HA	961	103	8927	-	-	1.68	2.66	-	-
31	31	Sulkeri	A	126	1525	8927	-	-	1	20	-	-
32	32	Kashipatna	A	1104	853	2855	-	-	8.08	14.9	-	-
33	33	Naravi	KQ	1651	5890	9237	816	-	1	5.61	25.7	-
34	34	Hosmar	HA	1266	632	5374	-	-	1.32	7.87	-	-
35	35	Eedu	QH	1285	2807	135	8927	-	1.29	2.28	42	-

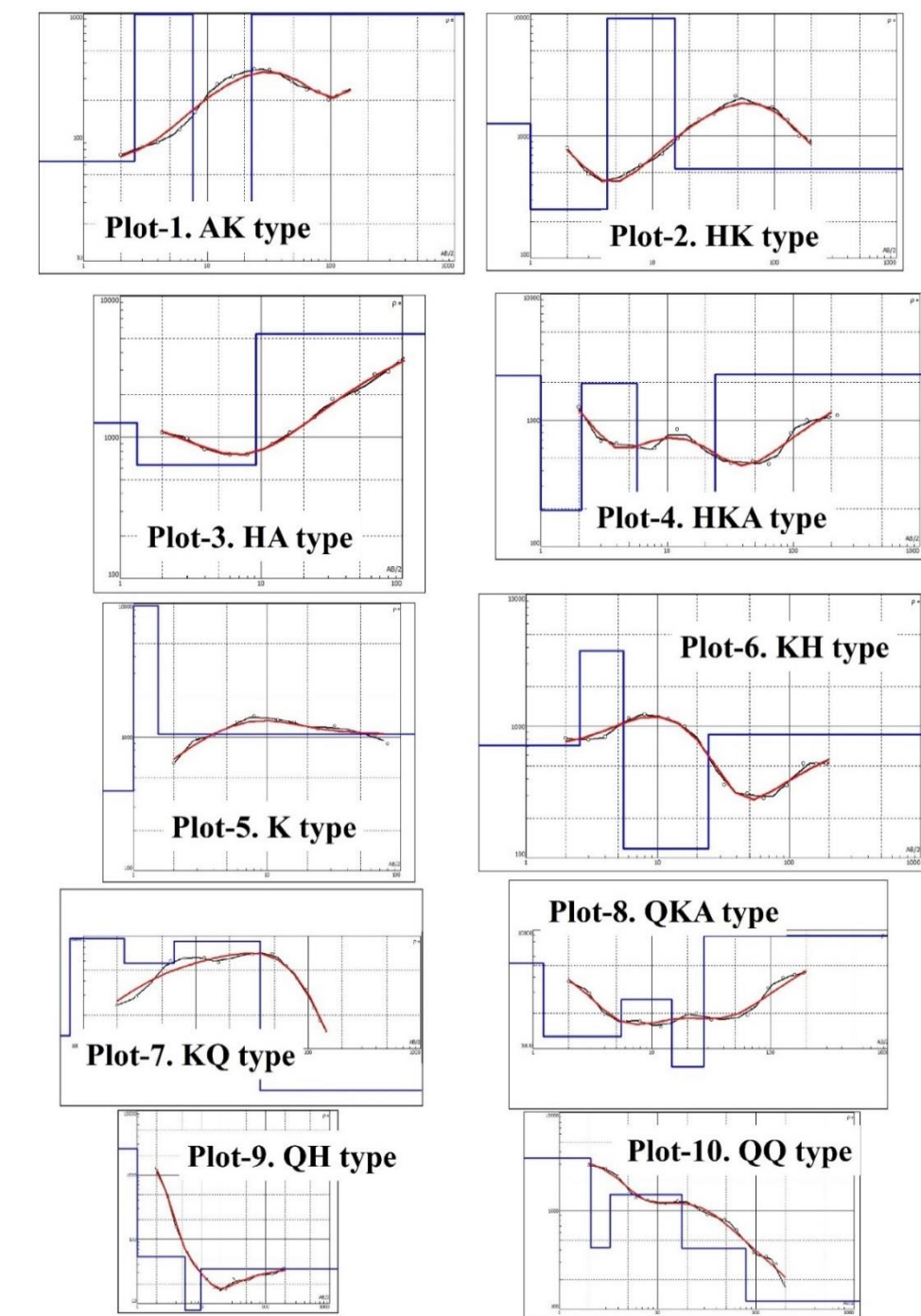


Figure 4.6 Selected plots of each curve types obtained using CMT

4.3.2.11 QH-type curves

The resistivity sequence for this four-layered formation is $\rho_1 > \rho_2 > \rho_3 < \rho_4$ and the curve type is shown in Figure 4.6. The VES 3, 24, 27, 29, and 35 show the QH-type

curve. The layer resistivity varies from 5.13 Ωm (VES 03) to 9019 Ωm (VES 07). The thickness varies from 0.42m (VES 24) to 42m (VES 35). In this curve type, the resistivity of the first 3 layers gradually decreases, and for the 4th layer, the resistivity increases. Therefore the 3rd layer, which is having a layer resistivity of 5.3 Ωm (VES 03) to 354 Ωm (VES 27) with the thickness extending from 4m (VES 03) up to 42m (VES 35), can be interpreted as a good source of groundwater potential. The 4th layer with relatively high resistivity can be interpreted as hard rock formation, which extends up to the maximum depth of investigation.

4.3.2.12 QKA-type curve

The resistivity sequence for this five layered formation is $\rho_1 > \rho_2 < \rho_3 > \rho_4 < \rho_5$ and the curve can be seen in (Figure 4.6). The VES 13 shows the QKA-type curve. The topsoil with a resistivity of 5269 Ωm and thickness of 1.22m can be interpreted as Laterite due to its high resistivity. The layer resistivity is varying in the range of 706 Ωm to 8929 Ωm . The thickness varies from 1.22m to 12.7m. This curve type exhibits the layer sequence such that the 2nd and 4th layers resistivity is relatively low compared to the 1st, 3rd, and 5th layers. Thus, the 2nd and 4th layers are interpreted as a good source of groundwater.

4.3.2.13 QQ-type curves

The resistivity sequence for this four-layered formation is $\rho_1 > \rho_2 > \rho_3 > \rho_4$ and the curve can be seen in Figure 4.6. The VES 18, 21, and 28 show the QQ-type curves. The layer resistivity varies from 25.7 Ωm (VES 18) to 3565 Ωm (VES 28). The thickness varies from 1.21m (VES 21) to 105m (VES 28). In these curve types, the resistivity of all four layers gradually decreases up to the maximum depth of investigation. The 4th layer resistivity varies from 25.7 Ωm (VES 18) to 109 Ωm (VES 28), indicating a probable groundwater source. Therefore these curve types can be interpreted to be a good source of groundwater potential.

Table 4.4 Resistivity and thickness of layers for quantitative interpretation of VES

Sl. No.	VES No.	Location	Curve Type	ρ_1	ρ_2	ρ_3	ρ_4	ρ_5	h1	h2	h3	h4
1	1	Kulai	K	396	9590	1052	-	-	1	0.53	-	-
2	2	Tokuru 62	AK	50.5	2181	22.8	554	-	2.06	5.13	12.1	-
3	3	Kunjathbailu	QH	2551	53	5.13	34.5	-	1	4.57	4.09	-
4	4	Bondel	AA	290	599	137	6896	-	3.17	9	11.9	-
5	5	Bajpegrama	HK	409	32.6	2559	6.08	-	1.33	2.79	11.1	-
6	6	Moodushedde	HA	2394	797	4497	-	-	1.48	3.59	-	-
7	7	Paldaane/Kudupu	H	1325	269	9019	-	-	6.75	15.2	-	-
8	8	Fermai	HK	5911	1147	6460	78.1	5630	1.12	8.57	11	49.9
9	9	Addoor	HKA	2128	277	5846	682	8304	1	0.6	0.8	31.1
10	10	Gurpura	KQ	914	9169	605	3588	227	1	2.23	7.2	23.3
11	11	Ganjimatha	KH	2246	3884	985	5512	-	2.01	3.97	23.2	-
12	12	Kaavagudde	HKA	526	347	872	254	7968	1	6.05	5.09	32.4
13	13	Benjanapadavu	QKA	5269	1260	2589	706	8929	1.22	4.3	9.27	12.7
14	14	Loretto	H	1708	25.7	9400	-	-	1.73	3.71	-	-
15	15	Varmala	HA	625	216	5109	-	-	1.16	10.4	-	-
16	16	Kuppepadavu	KH	719	3731	118	861	-	2.56	2.95	18.7	-
17	17	Iruvailu	H	1536	612	9207	-	-	7.06	36.7	-	-
18	18	Konnepadavu	QQ	2132	663	25.7	-	-	5.54	58.8	-	-
19	19	Raayi	AA	157	1271	514	1456	466	1	1.65	16	30.7
20	20	siddakatte	HK	1274	251	9207	538	-	1	3.25	11	-
21	21	Pucchamogaru	QQ	3401	424	1472	416	120	2.08	1.21	14.4	61.2
22	22	Kallabettu	AA	1413	5367	567	5282	-	1	1.16	1.77	-
23	23	Maarnad	HKA	2256	193	1956	197	2311	1	1.11	3.66	18.2
24	24	Maroor	QH	4965	205	1281	278	6497	1	0.42	6.8	17.4
25	25	Padanthadka	H	2723	1133	5775	-	-	2.17	45.8	-	-
26	26	Vamanapadavu	H	750	482	3463	-	-	1.82	37.9	-	-
27	27	Nadubottu	QH	2030	5015	354	7646	-	3.16	2.89	35.1	-
28	28	Gardady	QQ	3769	1582	204	1088	86.5	2.67	4.37	11.6	30.7
29	29	Moodukodi	QH	3672	7234	217	6755	-	3.93	14.2	27.5	-
30	30	Pillya	HA	961	103	8927	-	-	1.68	2.66	-	-
31	31	Sulkeri	A	126	1525	8927	-	-	1	20	-	-
32	32	Kashipatna	A	1104	853	2855	-	-	8.08	14.9	-	-
33	33	Naravi	KQ	1651	5890	9237	816	-	1	5.61	25.7	-
34	34	Hosmar	HA	1266	632	5374	-	-	1.32	7.87	-	-
35	35	Eedu	QH	1285	2807	135	8927	-	1.29	2.28	42	-

4.3.3 Hydraulic and Goelectric parameters

The aquifer parameters (Figure 4.7) and (Table 4.4) are inferred using the aquifer layer resistivity (ρ_0) and thickness (h).

Table 4.5 Aquifer hydraulic and goelectric parameters of 35 VES locations

VES No.	VES Location	ρ_0 [ohm-m]	ρ_w [ohm-m]	F	K [m/day]	T [m ² /day]	Φ [%]
1	Kulai	1776	16.84	105.49	0.07	4.66	9.74
2	Tokuru 62	225	20.70	10.87	0.52	64.85	30.33
3	Kunjathbailu	144	39.06	3.69	0.57	35.37	52.08
4	Bondel	3163	44.44	71.17	0.01	0.73	11.85
5	Bajpegrama	617	49.02	12.59	0.31	29.23	28.19
6	Moodushedde	3022	74.07	40.79	0.01	1.38	15.66
7	Paldaane/Kudupu	4211	99.01	42.53	0.00	0.30	15.33
8	Fermai	369	91.74	4.02	0.43	46.25	49.86
9	Addoor	973	38.31	25.40	0.20	7.49	19.84
10	Gurpura	572	38.17	14.99	0.33	28.13	25.83
11	Ganjimatha	3486	42.55	81.91	0.01	0.75	11.05

12	Kaavagudde	500	153.85	3.25	0.36	26.02	55.47
13	Benjanapadavu	4548	142.86	31.84	0.00	0.18	17.72
14	Loretto	759	40.00	18.98	0.26	29.99	22.96
15	Varmala	1600	131.58	12.16	0.09	12.91	28.68
16	Kuppepadavu	325	35.46	9.16	0.45	51.17	33.05
17	Iruvailu	258	43.29	5.95	0.49	24.58	41.00
18	Konnapadavu	210	48.31	4.35	0.53	11.73	47.96
19	Malanturuguttu	586	35.84	16.35	0.32	6.29	24.73
20	Kalkuri/siddakatte	1572	60.24	26.09	0.09	6.20	19.58
21	Pucchamogaru	517	138.89	3.72	0.35	18.74	51.83
22	Kallabettu	5000	52.08	96.00	0.00	0.10	10.21
23	Maarnad	2703	48.08	56.21	0.02	0.63	13.34
24	Maroor	55	29.67	1.84	0.64	17.06	73.79
25	Padanthadka	1289	32.05	40.20	0.13	12.25	15.77
26	Vamanapadavu	1893	91.74	20.63	0.06	1.26	22.01
27	Nadubottu	1495	86.96	17.19	0.10	5.55	24.12
28	Gardady	301	32.36	9.29	0.47	35.36	32.82
29	Moodukodi	1068	55.87	19.11	0.17	11.94	22.88
30	Pillya	101	57.47	1.76	0.61	25.28	75.43
31	Sulkeri	4470	243.90	18.33	0.00	0.12	23.36
32	Kashipatna	1540	75.76	20.33	0.09	4.43	22.18
33	Naravi	1819	42.92	42.37	0.06	5.34	15.36
34	Hosmar	4190	263.16	15.92	0.00	0.18	25.06
35	Eedu	313	178.57	1.75	0.46	30.70	75.57

4.3.3.1 Transmissivity (T)

If the aquifers transmit the maximum amount of water, it indicates good recharge potential, especially in humid regions. Less or no transmissivity of the aquifers below the groundwater table indicates either the poor hydraulic conductivity or the lack of potential recharge zone. The T for individual locations varies from 0.1 m²/day (VES-31) to 64.2 m²/day (VES-02) with an average of 15.91 m²/day. The T classes used in this study are shown in (Figure 4.7 & Figure 4.10).

4.3.3.2 Hydraulic Conductivity (K)

Poor hydraulic conductivity indicates a lack of potential aquifer zones. Therefore ranking of 3 is given to the high K class. The K varies in the range of 0.001 m/day (VES-22) to 0.64m/day (VES-24) with an average of 0.24 m/day (Table 4.5).The spatial distribution of the K thematic layer can be seen in Figure 4.7.

4.3.3.3 Porosity (Φ)

The spatial distribution of porosity can be seen in Figure 4.7. The porosity is having a direct relationship with groundwater potentiality. The porosity varies between 9.7% (VES-01) to 55.9% (VES-24), with an average of 28.36% for the shallow coastal aquifer.

4.3.3.4 Formation factor

The F ranges from 1.75 (VES 35) to 105.49 (VES 01), with an average of 26.08.

4.3.4 Dar-Zarrouk parameters

The surface resistivity and the thickness of different geoelectrical layers help obtain D-Z parameters. The D-Z parameter (Table 4.6) like S is found to be in the range of 0.01 Ohm-1 (VES 26) to 0.56 Ohm-1 (VES 02) with an average of 0.13 Ohm-1. The TR is in the range of 1444.25 Ω .m² (VES 24) to 483500 Ω .m² (VES 22). The λ is ranging from 0.11 (VES 26) to 0.75 (VES 02) with an average of 0.32.

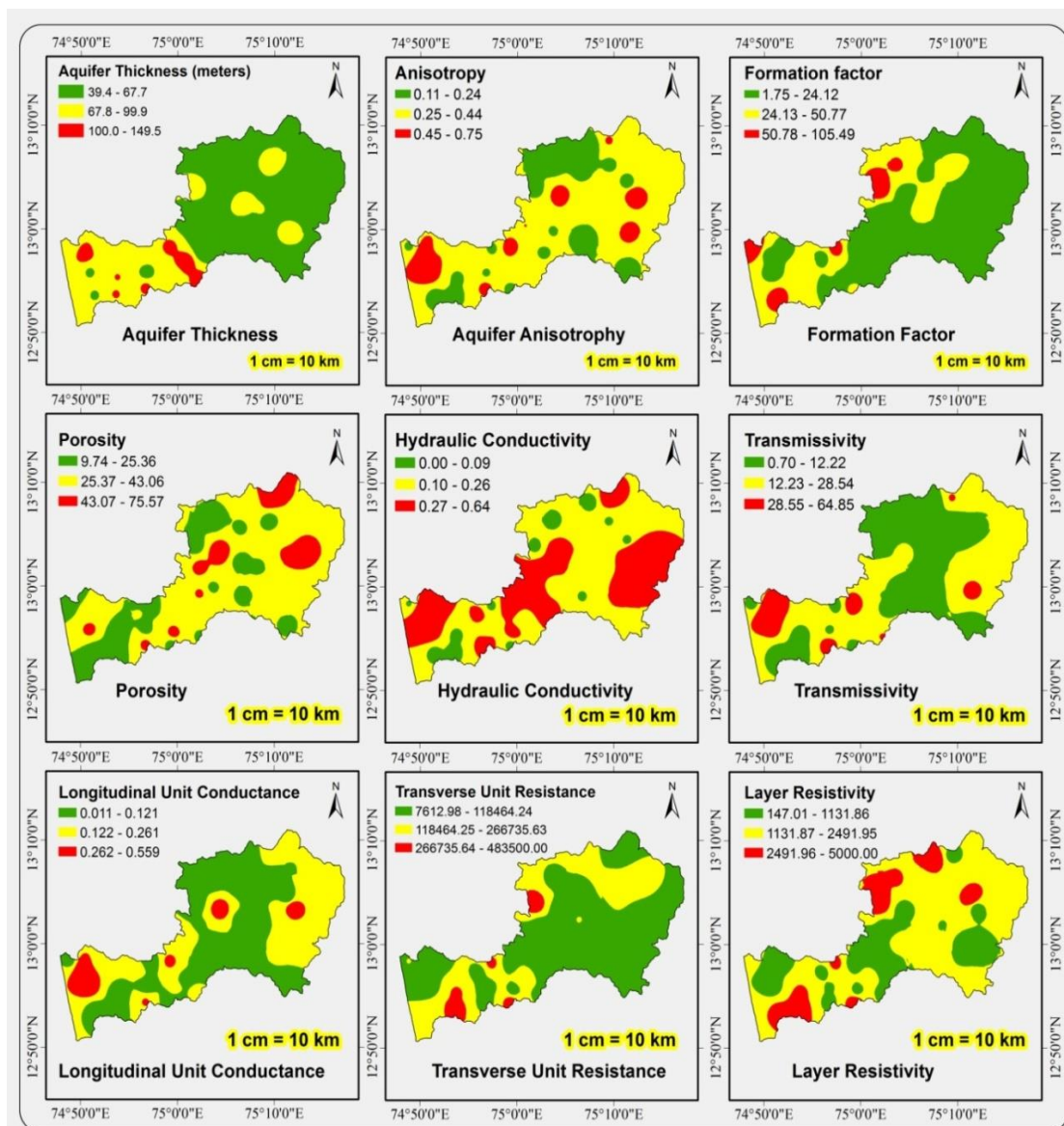


Figure 4.7 Spatial distribution maps of the aquifer parameters

Table 4.6 The Dar-Zarrouk parameters for 35 VES locations

VES No.	VES Location	ρ_0 [ohm-m]	ρ_w [ohm-m]	S [Ohm ⁻¹]	TR [Ohm.m ²]	λ
1	Kulai	1776	16.84	0.04	120412.80	0.20
2	Tokuru 62	225	20.70	0.56	28282.50	0.75
3	Kunjathbailu	144	39.06	0.43	8884.80	0.65
4	Bondel	3163	44.44	0.02	203064.60	0.14
5	Bajpegrama	617	49.02	0.15	58183.10	0.39
6	Moodushedde	3022	74.07	0.03	306380.10	0.18
7	Paldaane/Kudupu	4211	99.01	0.02	430785.30	0.16
8	Fermai	369	91.74	0.29	39888.90	0.54
9	Addoor	973	38.31	0.04	37363.20	0.20
10	Gurpura	572	38.17	0.15	48963.20	0.39
11	Ganjimatha	3486	42.55	0.03	349944.20	0.17
12	Kaavagudde	500	153.85	0.14	36050.00	0.38
13	Benjanapadavu	4548	142.86	0.02	432060.00	0.14
14	Loretto	759	40.00	0.15	88347.60	0.39
15	Varmala	1600	131.58	0.09	239200.00	0.31
16	Kuppepadavu	325	35.46	0.35	36654.87	0.59
17	Iruvailu	258	43.29	0.19	12797.75	0.44
18	Konnepadavu	210	48.31	0.11	4683.00	0.33
19	Malanturuguttu	586	35.84	0.03	11427.00	0.18
20	Kalkuri/siddakatte	1572	60.24	0.04	108747.80	0.21
21	Pucchamogaru	517	138.89	0.10	27452.70	0.32
22	Kallabettu	5000	52.08	0.02	483500.00	0.14
23	Maarnad	2703	48.08	0.01	82696.50	0.11
24	Maroor	55	29.67	0.49	1444.25	0.70
25	Padanthadka	1289	32.05	0.07	121892.10	0.27
26	Vamanapadavu	1893	91.74	0.01	40320.90	0.11
27	Nadubottu	1495	86.96	0.04	83869.50	0.19
28	Gardady	301	32.36	0.25	22717.80	0.50
29	Moodukodi	1068	55.87	0.06	73871.00	0.25
30	Pillya	101	57.47	0.41	4211.70	0.64
31	Sulkeri	4470	243.90	0.01	269073.93	0.12
32	Kashipatna	1540	75.76	0.03	72996.00	0.18
33	Naravi	1819	42.92	0.05	149298.85	0.21
34	Hosmar	4190	263.16	0.01	259361.00	0.12
35	Eedu	313	178.57	0.21	20854.87	0.46

4.3.5 Correlation studies

The correlation matrix or regression equations (Figure 4.9) for the aquifer parameters are obtained. It is observed that the correlation for K with respect to ϕ , T , S , and λ shows a positive and good correlation (>0.7). The correlation for K to ρ_0 and TR shows good but negative correlation, indicating their inverse relationship.

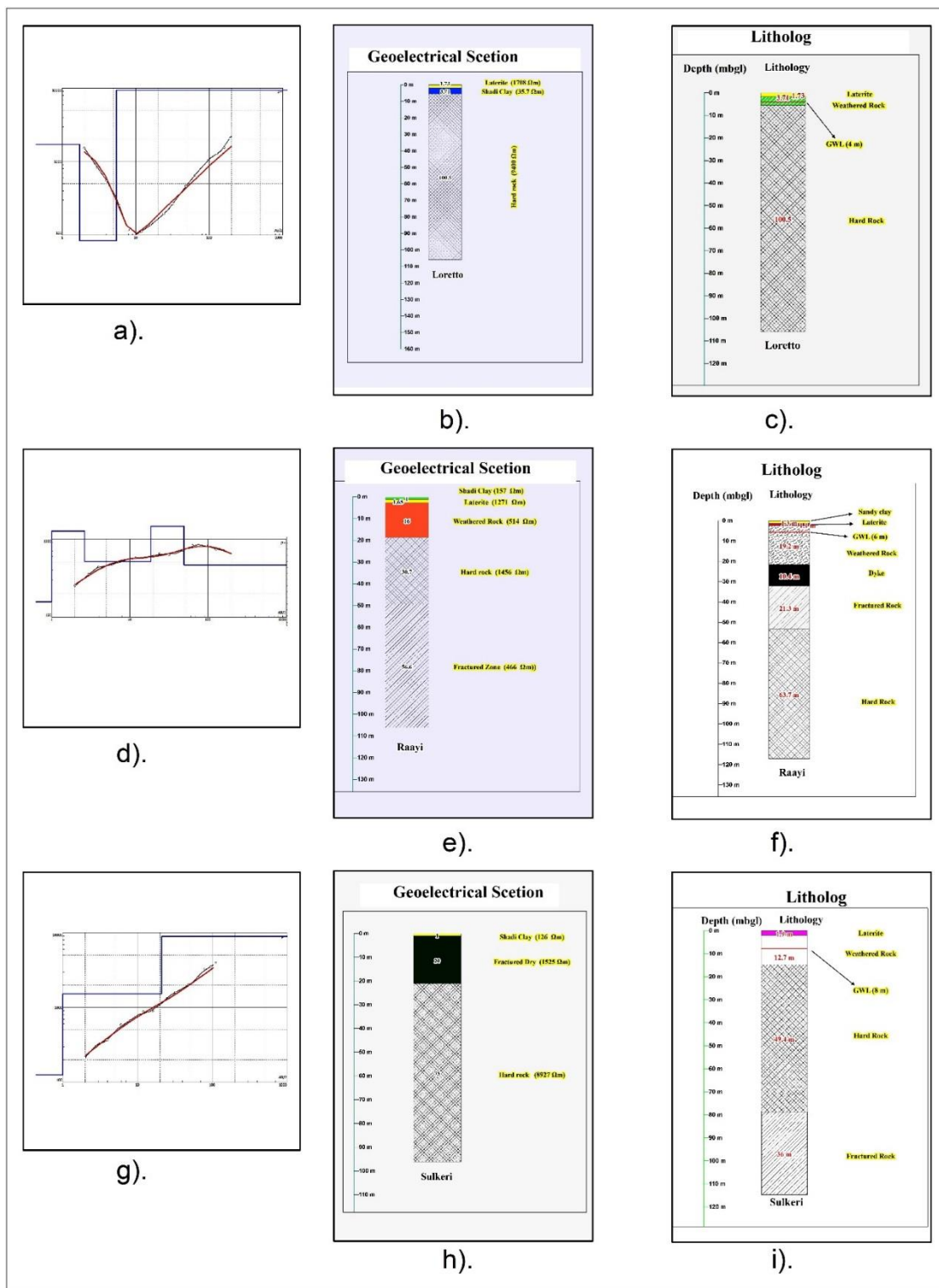


Figure 4.8 Correlative studies of CMT results with respect to the borehole lithology

The F shows moderate correlation with all the parameters except for ϕ . The correlation equations are as follows,

$$K = 0.318 \ln(\phi) - 0.799 \quad \text{(equation 4.13)}$$

$$K = -0.15 \ln(F) + 0.665 \quad \text{(equation 4.14)}$$

$$T = -7.25 \ln(F) + 32.45 \quad \text{(equation 4.15)}$$

$$T = 15.94 \ln(\phi) - 38.29 \quad \text{(equation 4.15)}$$

The logarithmic regression equation (Figure 4.9) for K to ϕ shows good correlation with $R^2 = 0.73$ (equation 4.13) and for K to F the $R^2 = 0.73$ (equation 4.14). The regression equations for T shows moderate correlation of $R^2 = 0.5$ for ϕ (equation 4.16) and the $R^2 = 0.5$ for F (equation 4.15).

Table 4.7 Correlation matrix of hydraulic and geoelectric parameters for 35 VES locations

	ρ_o	h	ρ_w	S	TR	λ	F	K	T	ϕ
ρ_o	1									
h	0.17	1								
ρ_w	0.42	0.01	1							
S	-0.64	0.12	-0.28	1						
TR	0.92	0.43	0.31	-0.51	1					
λ	-0.74	0.16	-0.29	0.98	-0.57	1				
F	0.63	0.14	-0.25	-0.51	0.61	-0.57	1			
K	-0.84	-0.17	-0.28	0.86	-0.73	0.91	-0.67	1		
T	-0.70	0.35	-0.24	0.84	-0.56	0.89	-0.54	0.77	1	
ϕ	-0.63	-0.26	0.16	0.69	-0.56	0.73	-0.69	0.83	0.51	1

Also, correlation studies are conducted for the geoelectric layers interpreted from ISM.

In this study, up to 6-layered formations are observed. The layered formations are correlated with three borehole data (Table 4.7) and (

Figure 4.8), which shows a good correlation. The TR shows good correlation with ρ_o .

The S shows good correlation with λ , K , and T . The K shows good correlation with λ ,

T , S and ϕ .

4.3.6 Thematic database creation

A total of 13 necessary thematic layers include drainage density, groundwater contours, depth to bedrock, slope, lithology, geomorphology, lu/lc, soil type, rainfall distribution, lineament density, porosity, transmissivity, and hydraulic conductivity are used in the integration for GWPZ. This integration of thematic layers gives us a certain acceptable interpretation for the possibility of groundwater occurrence.

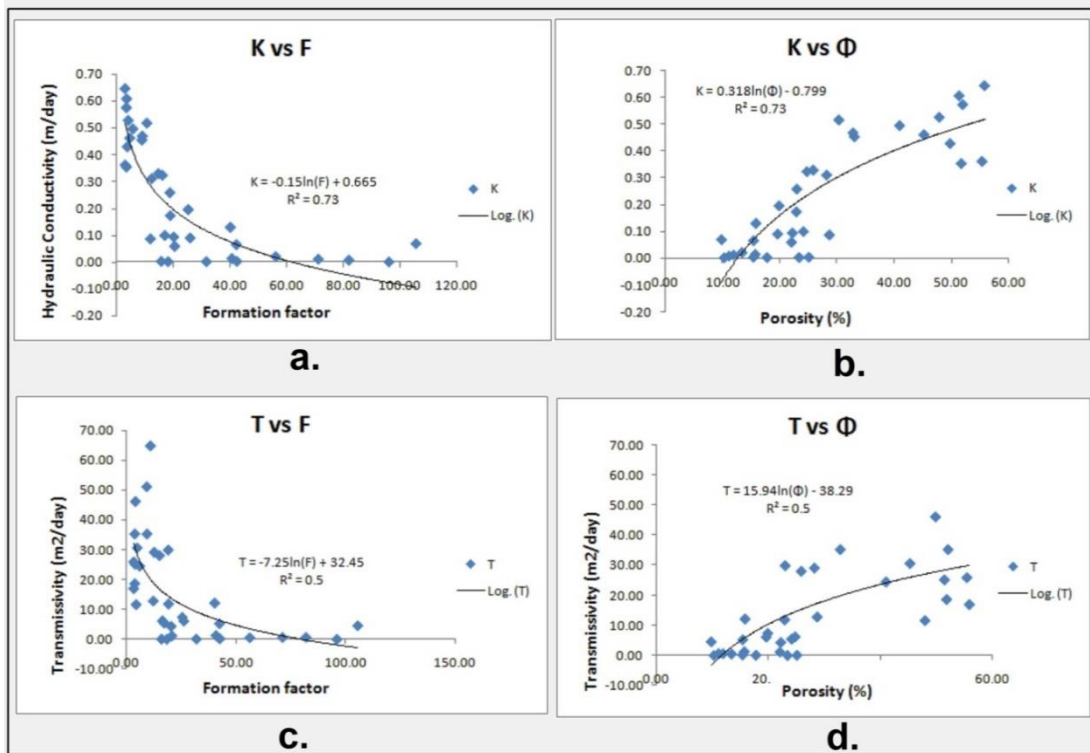


Figure 4.9 Regression equations for hydraulic and geoelectric parameters

4.3.6.1 Geomorphology

The available relief information in the topo maps is correlated with the LISS-IV imagery. The training sites for different litho-geomorphic units were selected and field verified.

The satellite imagery provides useful information in mapping geomorphology. The electrical resistivity data, helps verify and correlate the information on the depth of weathered zone, type of associated material, nature of the environment, agent of weathering, etc. The highest rank of 5 is given for plains, and the least rank of 1 is given for structural hills.

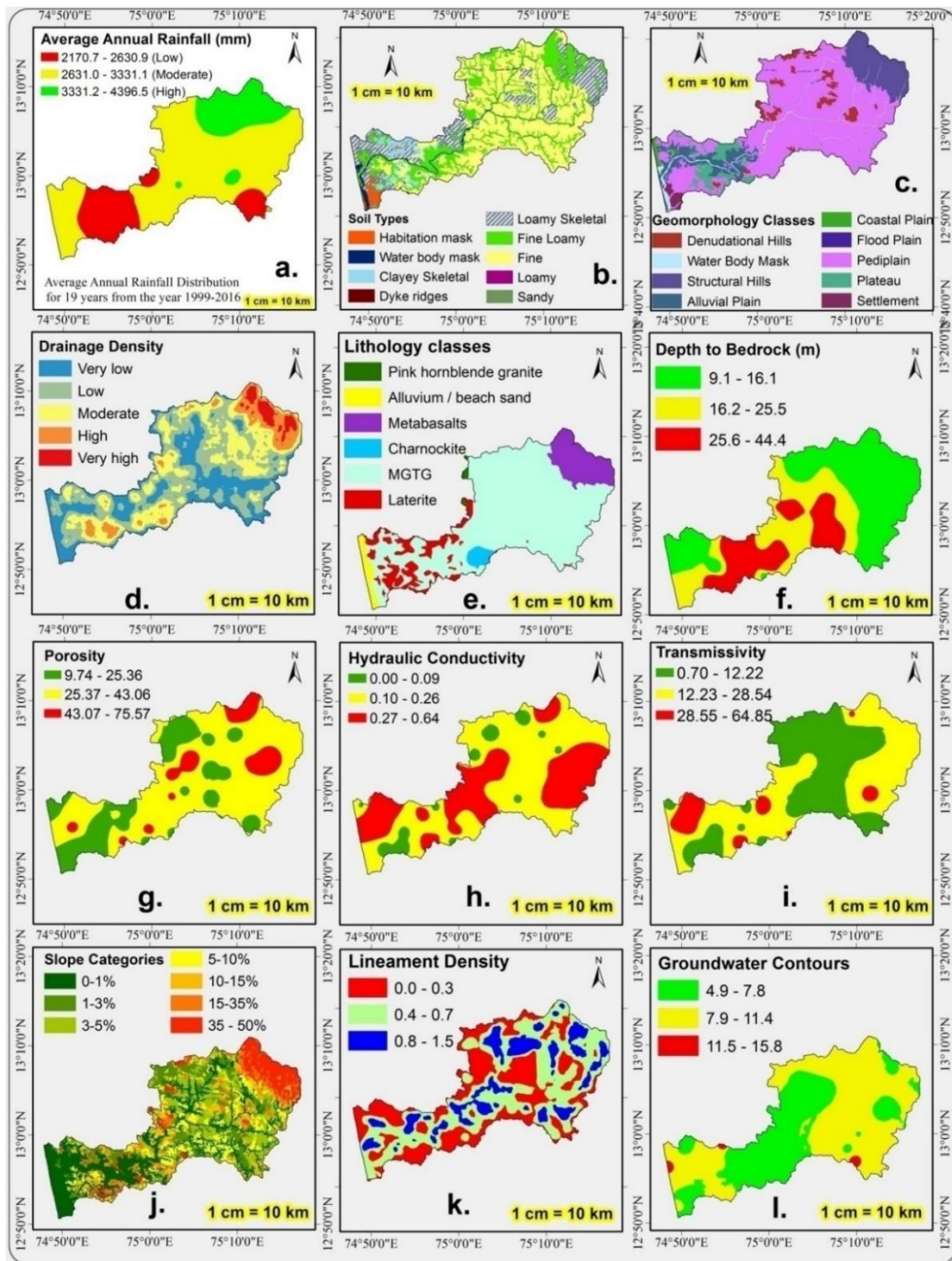


Figure 4.10 Thematic information used for preparation of GWPZ

4.3.6.2 Slope Map

The slope is one of the most important features for GW studies. The slope is having an inverse relation with groundwater potential. An increase in slope increases runoff and thus decreases the infiltration and affects groundwater potential. Therefore ranking of

5 is given to the lowest slope categories and 1 for the highest slope. It is observed that most of the low land region and parts of the midland region show 0-1% slope (263.3 km² of the total area). The high land (Ghats) shows 35-50% of the slope, about 84 km² (Figure 4.10). The slope has an inverse relation with groundwater potentiality, i.e., the greater the slope, the lesser the infiltration.

4.3.6.3 Land Use/Land Cover Map

The land use of a region results from the interaction of various factors such as physical, economic, and social, which shows the extent to which man has been able to utilize the land resources gainfully. Land cover refers to anything on the surface that is not subjected to anthropogenic action like forests, rivers, different rock exposures, etc. Vegetation shows red colour in FCC combination of the satellite imagery. The land use/land cover analysis is essential to know the spatial distribution of land resources. In this study, Level-I classification of the NRSC for lu/lc is used. Waterbody is given a high weightage of 5, Agricultural land is given 4, and for dykes it is 1 as they cannot infiltrate groundwater. The land cover includes the total vegetation cover, which is about 662.3 km² (more than 75% of the total area). The forest land and forest plantation cover 468.6 km². The agricultural land, industrial area, built-up, waterbody, and the wasteland cover about 17%, 2%, 18%, 3%, and 1% of the total area, respectively (Figure 4.11 & Table 3.11).

4.3.6.4 Soil Resources

The present study utilizes already available authentic soil-types map and later georeferenced and digitized (Figure 4.10) for integrated GW studies. A higher ranking is given to soil types that can infiltrate more water which can be seen in (Table 4.8). More than 75% of the study area (about 659 km²) is covered by fine and fine loamy soil types. Clayey soil covers 35.96 km² and sandy soil covers 3.14 km². Figure 4.10 & Table 4.8 shows the area statistics and the soil types found in the study area.

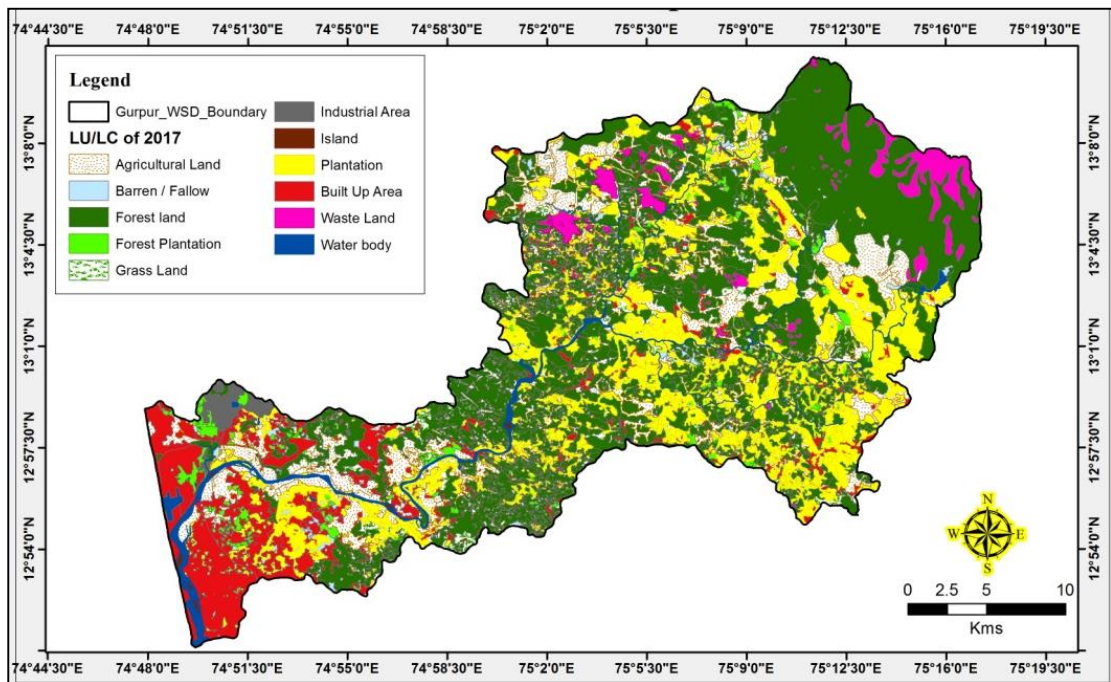


Figure 4.11 Land use / land cover thematic layer of Gurpur watershed

4.3.6.5 Lithology

The lithology map for the study area (Figure 4.10) was geo-referenced and screen digitized from GSI published map with 1:50,000 scale. The characteristics of rocks in compactness, density, weathering status, composition, joints, and fractures play a vital role in weightage assignment for Lithology. A ranking of 4 is given to alluvium or beach sand, whereas 1 is given to hard and indurated gneissic rock.

4.3.6.6 Lineament density

Generally, lineaments are associated with weathering and therefore increases porosity and permeability. Hence, lineament density and groundwater potential have a direct relationship (Hardcastle et al. 1995). Therefore, ranking of 1 and 3 are given to low and high lineament density classes, respectively (Figure 4.10). The geomorphology of the study area comprises Pediplain (about 66% of the study area, i.e., 579.66km²). Pediplain is the plain formed by the coalescence of pediments. It is mainly covered by lateritic soils and is associated with several inselbergs. Structural hills cover (105.17km²) about 12% of the total area. The coastal plain is covered by 6.6km² (about

1%) of the total area. The PGC rock of Archaean age is the major rock type found (about 75% of the study area, i.e., 657.6km²). The area statistics and ranking for lithology can be seen in (Table 4.8)

4.3.6.7 Drainage density

The CartoDEM data available from the Bhuvan website is used to prepare the drainage layer using which the drainage density layer is done and converted into a vector format. The drainage density for the Gurple catchment is found to be 1.64 per km as the total area of the catchment is 877 km² and the total length of the drainage is 1442 km. The higher ranking is given to the Very low and Low drainage density regions (Table 4.8) as they result from the lesser slope and, therefore, greater infiltration and groundwater potentiality.

The orientation and style of the drainages have a relationship with lineaments as they are associated with structural complexity (Shahzad et al. 2009). The drainage density is categorized into five classes (Figure 4.10). Very high (29.26 km²), High (74.68 km²), Moderate (235.94km²), Low (314.93km²), and Very low (222.56 km²). The ranks assigned and area statistics are provided in Table 4.8. The lineament density is classified into 3 classes' viz., Good (153.92 km²), Moderate (411.49 km²), and Low (312.33 km²). An increase in drainage density decreases groundwater potential, whereas increased lineament density increases groundwater potential. The ranks and weights for lineament density and drainage density are provided in Table 4.8.

4.3.6.8 Depth to Bedrock

About 35 Soundings have been conducted using Vertical Electrical Sounding (VES) with Schlumberger method within the present study. The obtained data is utilized to get apparent resistivity. The obtained apparent resistivity data is interpreted using ISM. It is simple to operate and gives good results (Narayan & Ramanujachary 1967). In this method, Plotting is made by electrode space 'a' in X-axis and electrode separation divided by apparent resistivity values in Y-axis. The point of intercept gives the depth of various interfaces. The results obtained from ISM are used to prepare depth to

bedrock thematic layer. The weathered zone hosts groundwater in its fissures, fractures, and pore spaces of the weathered rocks (Gurumurthy 2013).

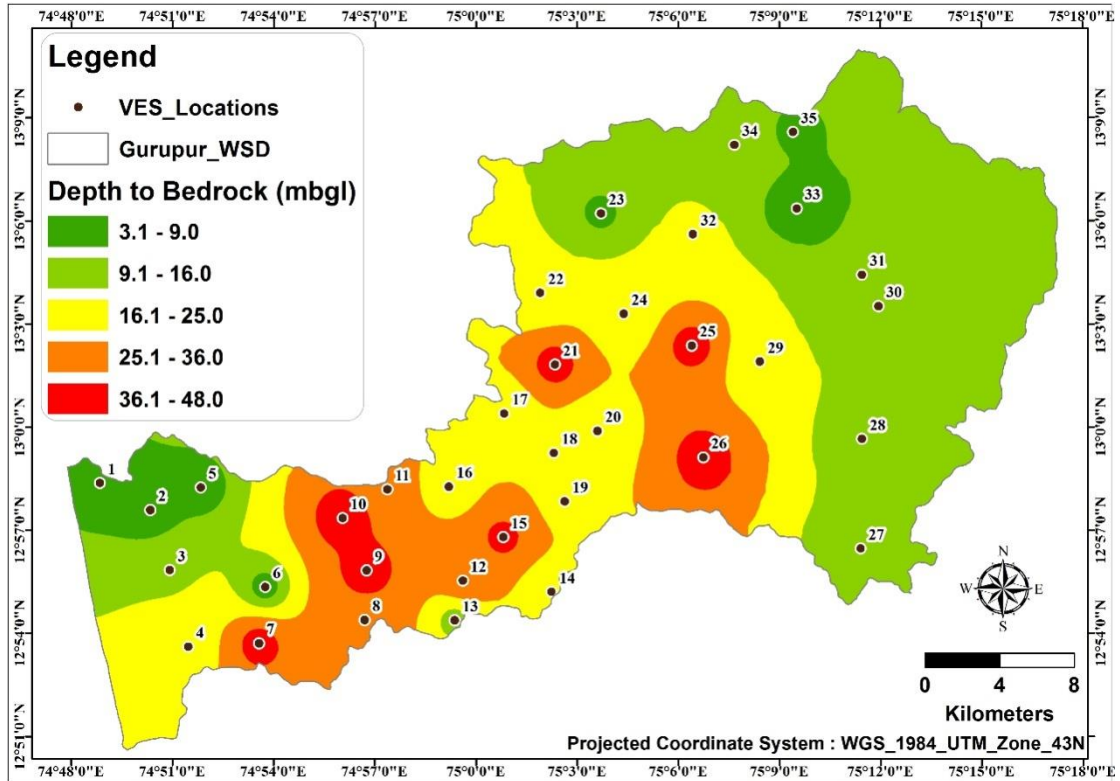


Figure 4.12 The spatial distribution of depth to bedrock (weathered zone thickness)

The present landscape along the coast is the reflectance of extensive tertiary denudation, which leads to the formation of laterites. The extent of weathering along with depth to bedrock forms potential aquifers. Closer the bedrock depth from the ground, thinner will be the weathered zone, thus directly affecting groundwater potentiality. The spatial distribution of depth to bedrock in the study area (Figure 4.12) shows the variation from 3.1m to 48m in the study area. Closer the bedrock depth from the ground, thinner will be the weathered zone, thus directly affecting groundwater potentiality. The ghats and the lowland region show the low depth to bedrock, whereas most of the midland and parts of low land shows moderate to high depths ranging from 16m – 48m. The depth to bedrock of all the 35 VES locations can be seen in Figure 4.12. The area statistics and rank assignments for depth to bedrock are given (Table 4.8).

4.3.6.9 Rainfall distribution

The average annual rainfall for 19 years from 1999-2016 is tabulated and connected with associated rain gauge station point features in the GIS environment. Using the geostatistical analyst tool, the isohyetal map for rainfall distribution over 19 years is prepared. Later, it is exported to a shapefile of polygon features and used for integration purposes so that the accuracy of the groundwater potentiality can be increased. Rainfall is having a direct relationship with groundwater potentiality. Therefore highest ranking of 3 is given to the high rainfall distribution class and the lowest of 1 to the low rainfall distribution class (Table 4.8).

The effects of moderate rainfall distribution can be seen in major parts of the study area (Figure 4.10), which is about 65% of the total area (575.3 km²). The classes with high and low rainfall distribution are having 17% and 18%, respectively.

4.3.6.10 Ground Water Contours

The groundwater contours are classified as high (8.1 km²), moderate (520.44 km²), and low (349.2 km²) categories (Table 4.8 & Figure 4.13).

4.3.7 Groundwater potentiality studies

Various works by researchers have established a close relationship between groundwater study, RS& GIS (Solomon & Quiel 2006; Babiker et al. 2007; Balakrishnan et al. 2011; Shekhar & Pandey 2015).

The suitability analysis like WOI is used for vector integration of all the thematic layers into a single GWPZ map. The weights for different themes are assigned based on their influence over the groundwater potential. Based on the evaluation of Ranking or the Weightage, the GWPZ are categorized.

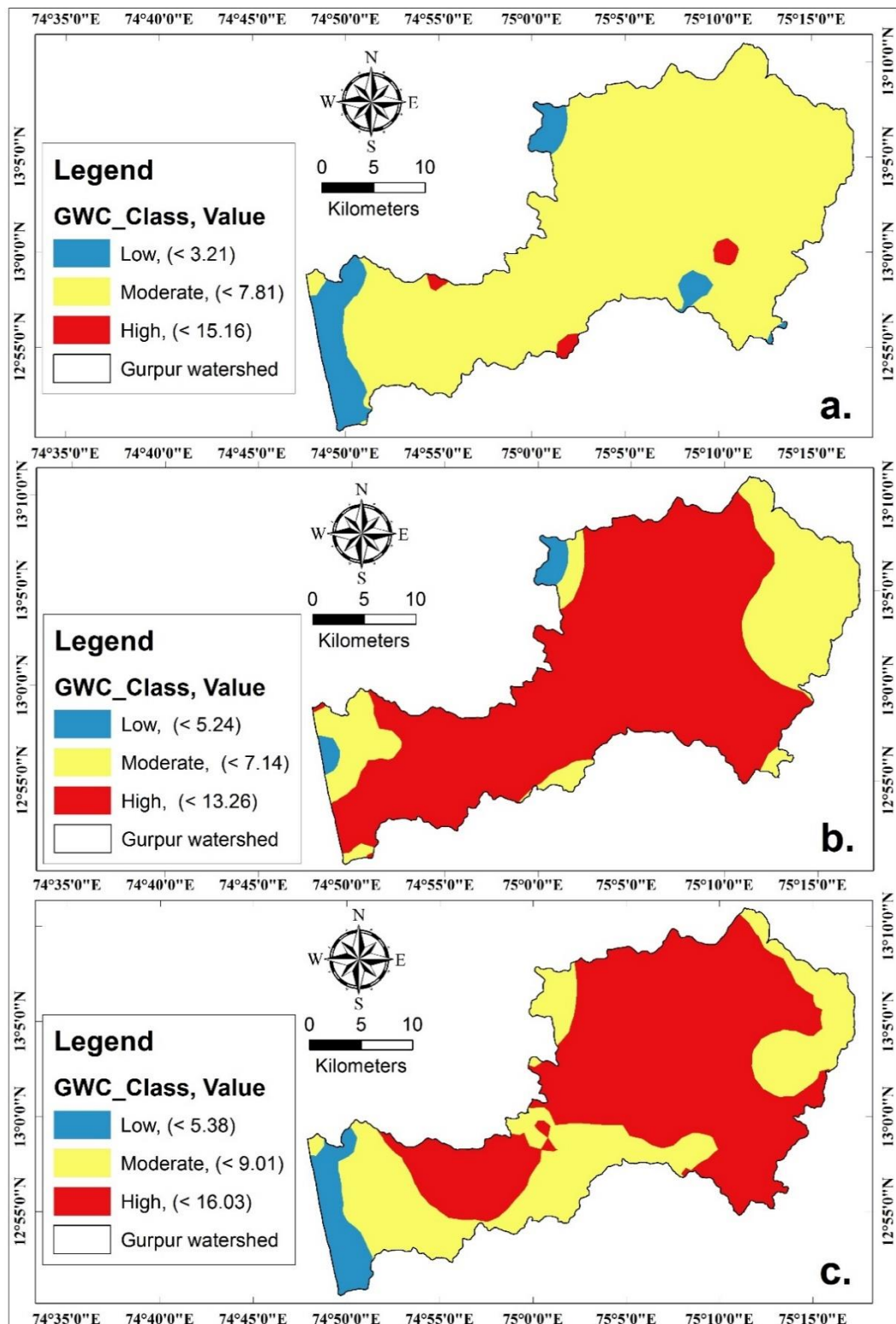


Figure 4.13 Spatial distribution of GWC of all the Three Phases

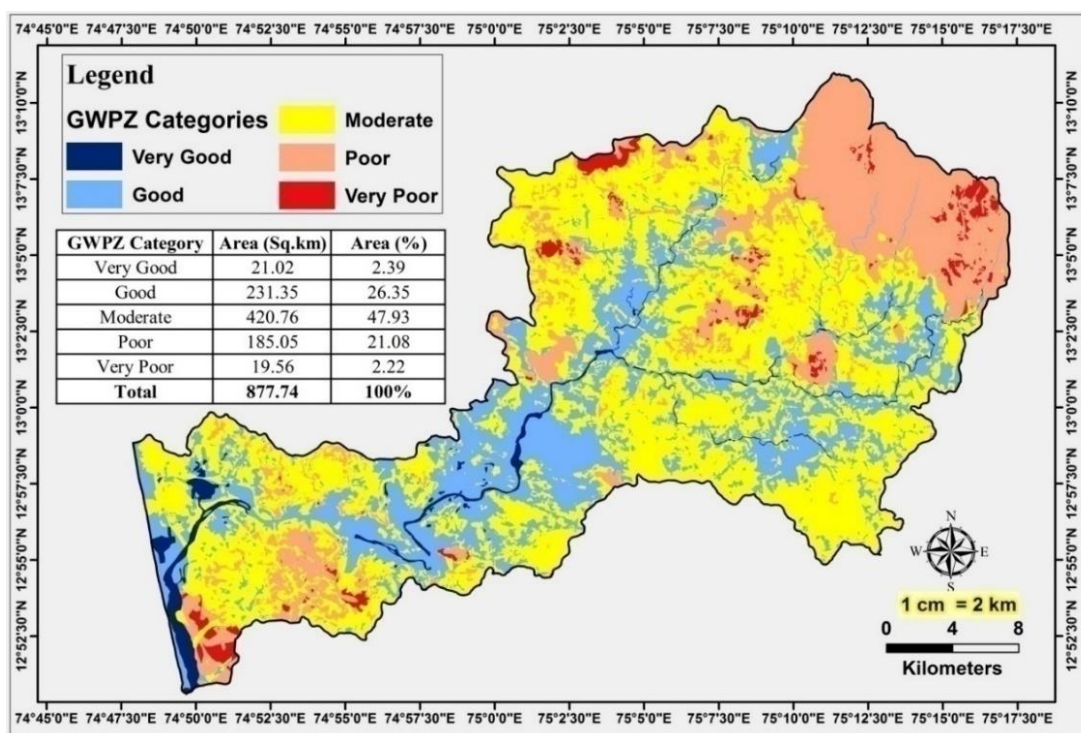


Figure 4.14 Spatial distribution of Groundwater Potential Zones prepared using CMT

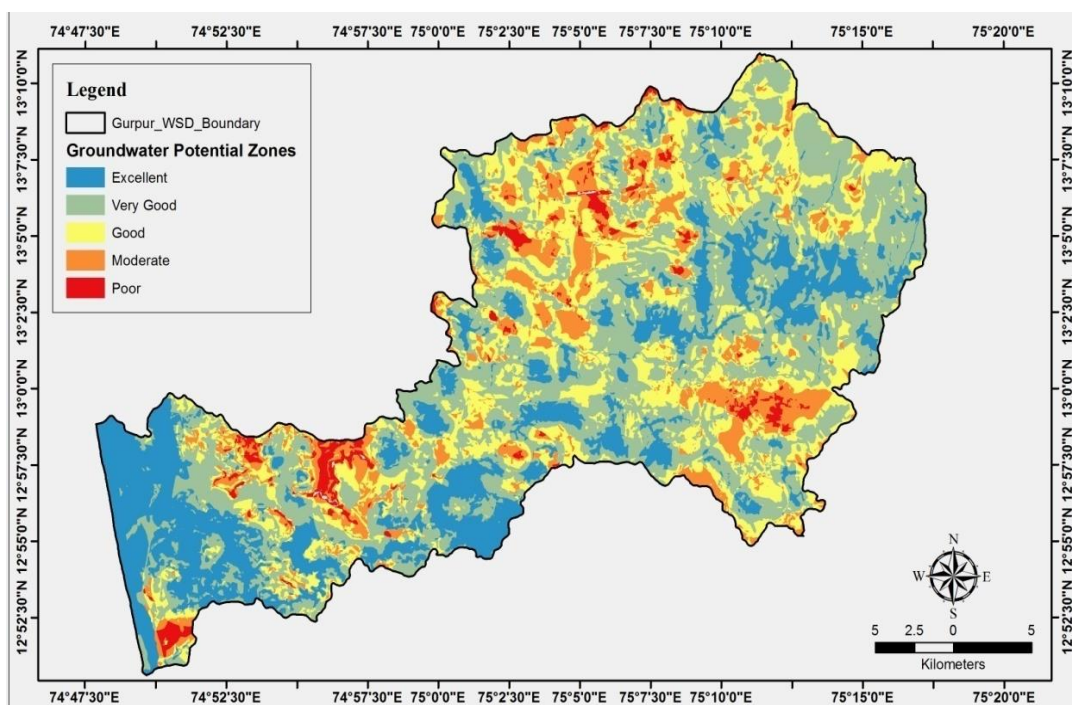


Figure 4.15 Spatial distribution of Groundwater Potential Zones prepared using WOI

Table 4.8 Weightage assignment for thematic layers used in the preparation of GWPZ

Sl.	Thematic	Classes	Area	Assigned	Assigned	Sl.	Thematic layer	Classes	Area	Assigned	Assigned
-----	----------	---------	------	----------	----------	-----	----------------	---------	------	----------	----------

No.	layer		(sq.km)	Ranks	Weights	No.			(sq.km)	Ranking	Weights
1	Lithology	Alluvium - Beach Sand	21.22	4	10	34	Slope	0-1	262.32	5	10
2	Lithology	Charnockite	17.29	2		35	Slope	1-3	122.53	5	
3	Lithology	Laterite	82.93	3		36	Slope	3-5	144.33	4	
4	Lithology	MGTG	657.6	1		37	Slope	5-10	106.35	4	
5	Lithology	Metabasalts	94.27	2		38	Slope	10-15	87.12	4	
6	Lithology	Pink Hornblende Granite	4.42	1		39	Slope	15-35	71.02	3	
7	LULC	Agricultural land	147.98	4	10	40	Slope	35-50	84.07	2	5
8	LULC	Forest land	286.32	4		41	Drainage density	Very low	222.56	5	
9	LULC	Forest plantation	182.32	3		42	Drainage density	Low	314.93	4	
10	LULC	Grassland	45.66	3		43	Drainage density	Moderate	235.94	3	
11	LULC	Industrial area	13.37	1		44	Drainage density	High	74.68	2	
12	LULC	River island	0.75	5		45	Drainage density	Very high	29.26	1	
13	LULC	Built-Up area	161.36	1		46	GW Contours	4.9 - 7.8	349.2	3	
14	LULC	Waste land	13.19	2		47	GW Contours	7.9 - 11.4	520.44	2	
15	LULC	Waterbody	26.76	5	48	GW Contours	11.5 - 15.8	8.1	1	10	
16	Geomorphology	Alluvial plain	63.95	5	15	49	Rainfall Distribution	Low	154.61	1	5
17	Geomorphology	Coastal plain	6.6	5		50	Rainfall Distribution	Moderate	575.31	2	
18	Geomorphology	Flood plain	0.75	5		51	Rainfall Distribution	High	147.9	3	
19	Geomorphology	Waterbody mask	22.63	5		52	Lineament Density	Low	312.33	3	
20	Geomorphology	Denudational hill	43.14	1		53	Lineament Density	Moderate	411.49	2	
21	Geomorphology	Pediplain	579.79	4		54	Lineament Density	High	153.92	1	
22	Geomorphology	Plateau	45.65	3		55	D2BR	Low	165.45	1	
23	Geomorphology	Settlement	10.06	1		56	D2BR	Moderate	570.18	2	
24	Geomorphology	Structural hills	105.17	1		57	D2BR	High	142.11	3	
25	Soil Types	Dyke ridges	0.77	1		58	Porosity	Low	216.52	1	
26	Soil Types	Habitation mask	14.69	1	59	Porosity	Moderate	567.72	2		
27	Soil Types	Clayey skeletal	35.96	2	60	Porosity	High	93.49	3		
28	Soil Types	Fine	413.61	3	5	61	Hydraulic Conductivity	Low	56.08	1	5
29	Soil Types	Fine loamy	246.06	3		62	Hydraulic Conductivity	Moderate	448.02	2	
30	Soil Types	Loamy	0.62	3		63	Hydraulic Conductivity	High	333.64	3	
31	Soil Types	Loamy skeletal	140.24	3		64	Transmissivity	Low	383.01	1	
32	Soil Types	Sandy	3.14	4		65	Transmissivity	Moderate	426.77	2	
33	Soil Types	Waterbody mask	22.64	5	66	Transmissivity	High	67.95	3	5	

The resultant map for the potential groundwater zones using weighted overlay index is shown in (Figure 4.15). The category with good to moderate groundwater potential zones together covers about 74% of the total area. The category with very good, poor, very poor groundwater potential zones covers 21.02 km², 185.05 km², and 19.56 km², respectively.

4.4 Summary and conclusion

This study involves the electrical resistivity method (VES) with Schlumberger configuration to investigate the groundwater potential in 35 locations. The study also provides a database for assessment, management, and suitable borehole drilling locations for GW extraction within the Gurpur watershed. This study can be replicated for other coastal shallow aquifers. Probing for greater depths was impossible in some VES locations because of the non-availability of open space on the surface. Therefore

in such locations maximum depth of investigation is considered as the lower basement of the aquifer. The VES with Schlumberger array was conducted for 35 locations within the Gurpur watershed to delineate potential groundwater zones in coastal shallow aquifers. The gneiss and Charnockite are the major rock types found in the study area. The topsoil mainly comprises red colour laterite and also reddish-yellow coloured laterite with clay.

The data obtained are interpreted using ISM of interpretation. Unlike the curve matching technique, the ISM gives sharp boundaries for different layers. The geoelectrical resistivity data is used for the identification of depth to bedrock. The data is also interpreted to get hydraulic conductivity, transmissivity, porosity, and formation factor. From the interpretation of the VES data, it is inferred that there are 05 three-layered formations, 24 four-layered, and 06 five-layered formations. In the study area, up to 5-layered formations are observed. The correlation for hydraulic and geoelectric parameters shows weak to good correlation. This method of calculating hydraulic parameters can be economical, time-saving, and an alternative for pumping tests.

The interpretation of 35 VES soundings using the curve matching technique yielded 13 different curve types. Based on the obtained results, the GWPZ is inferred. Based on the geo-electrical sections, the hydro-geological conditions were inferred to be laterite, sandy clay, fractured/weathered rock, and bedrock. The layer resistivity values are in the range of 5.3-39599 Ohm-m. The thickness of the geo-electrical layers was observed to be in the range of 0.42–105 m. The formations which come under the H, KH, KQ, QH, and QQ curve types show good groundwater potential, which covers about 43%. The formations which come under AK, HA, HK, QKA curve types exhibit moderate groundwater potential, which is about 34%. The formations that come under A, AA, K, and HKA curve types exhibit poor groundwater potential, which comprises about 23%. Geo-electrical resistivity data interpreted with CMT is correlated with the borehole lithologs inferred good correlation. Therefore this method is used for the identification of GRPZ.

Integration of remote sensing, GIS, and electrical resistivity data has been used to integrate 13 thematic layers to prepare GWPZ. The caution is warranted to interpret the features and their influence over GW. Else, the results may yield misleading

information. The groundwater potential zones are classified into 5 classes based on the integration of rank and weights assigned for different thematic layers. The zones associated with low slope, lateritic soil, high lineament density, forest or agricultural land, and coastal plain yields good groundwater potential. The areas associated with high slope, clayey soil, low lineament density, high drainage density, built-up land, and structural hills yield low groundwater potential. It is observed that the groundwater potential category with good and moderate zones together covers about 74% of the total area. These results provide a better hydrogeological understanding of the study area. Therefore, this methodology is suitable for identifying GWPZ in coastal aquifers, and this methodology can be extended to other areas.

Chapter 5

GROUNDWATER QUALITY

5.1 Introduction

Groundwater is a naturally occurring, renewable resource. But it is still a very rare commodity in certain parts of the world. Just as surface water, the groundwater is also over-exploited and polluted. Exploration, exploitation, and groundwater management are essential in the present scenario (Oseji 2010; Majumdar et al. 2016; Virupaksha & Lokesh 2019).

However, studies have not been carried out specifically to the Gurpur watershed using the WQI approach. Therefore, this study aims to utilize the data verified from the CCA method and study the drinking water quality using the WQI method for the Gurpur watershed in coastal Karnataka, India.

5.2 Materials and methods

5.2.1 Groundwater quality analysis

Groundwater samples in 51 locations are collected for dug wells such that the broader scenario of the study area can be understood. The GPS survey was conducted for selecting the sampling locations. The samples were collected in three phases (Phase I, II, III) during the peak of the seasons like monsoon (August-2017), post-monsoon (December-2017), and pre-monsoon (April-2018), respectively. The drinking water quality parameters are analysed in the Environmental Engineering laboratory (Table 5.1). The parameters like pH, TDS, and EC are analysed on the spot, whereas the remaining parameters are analysed in the laboratory. Initially, the sampling cans were washed and rinsed with de-ionized water. Later in the field, the sapling cans were rinsed with the groundwater sample and then tightly sealed after collection. The sampling was carried out very cautiously so that the errors due to sampling were minimized. The collected samples were numbered and brought back to the laboratory for further analysis.

5.2.2 Drinking water quality parameters

The parameters like pH, EC, and TDS were measured on the spot during sample collection. According to standard procedure, the laboratory analysis for the drinking water quality parameters is conducted (Bureau of Indian Standards 2012). The analysis for parameters like K^+ , Ca^{2+} , Mg^{2+} , TH, TA, SO_4^{2-} , NO_3^- , HCO_3^- , Cl^- , F^- and Fe^{2+} were conducted in the laboratory (Table 5.1).

Table 5.1 Drinking water quality parameters.

Sl. No.	Parameter	Instrument	Desirable limits (IS 10500:2012)	Permissible limits
1	pH	pH meter	6.5-8.5	6.5-8.5
2	EC	EC meter	300 μ S/cm	--
3	TDS	TDS meter	500 mg/l	2000 mg/l
4	Na^+	Flame Photometer	50 mg/l	--
5	K^+	Flame Photometer	50 mg/l	--
6	Fe^{2+}	UV Spectrophotometer	0.3 mg/l	--
7	NO_3^-	UV Spectrophotometer	45 mg/l	--
8	SO_4^{2-}	UV Spectrophotometer	200 mg/l	400 mg/l
9	TA	Titration	200 mg/l	600 mg/l
10	Mg^{2+}	Titration	30 mg/l	100 mg/l
11	Ca^{2+}	Titration	75 mg/l	200 mg/l
12	F^-	Ion Selective Electrode meter	1.0 mg/l	1.5 mg/l
13	Cl^-	Titration	250 mg/l	1000 mg/l
14	TH	Titration	200 mg/l	600 mg/l

5.2.3 Phases of groundwater quality studies

The groundwater quality studies are conducted in three different phases (phase-I in August-2017, phase-II in December-2017, and phase-III in April-2018). The reason for considering this methodology is that the coastal region of Karnataka is associated with heavy rainfall (average of 5000 mm/year). The water level is almost to the ground level and, in some cases, may overflow. Therefore groundwater quality during monsoon season (phase I) is pretty good. And, the concentrations of the dissolved ionic and non-

ionic constituents of the groundwater are considerably low. The studies on spatial and temporal changes of the groundwater quality in the study area are also carried out. The temporal studies are conducted to understand the change in the concentration of parameters in three different time intervals (seasons like the monsoon, post-monsoon, and pre-monsoon). The samples are collected in the peak time of each season and assumed that they represent the cumulative of the respective phases.

Phase-I was conducted during the peak monsoon season of August 2017. Phase – II was carried out during the peak of the post-monsoon season (December 2017). Phase – III was carried out during the peak of the pre-monsoon season (April 2018). The constituents and their concentrations are very low during phase-I. Therefore, to understand the complete scenario of spatial and temporal variation of the groundwater quality parameters, the studies are carried out from monsoon as the initial phase.

5.2.4 Drinking water quality parameters

The groundwater samples are collected and analysed with respect to drinking water standards (Bureau of Indian Standards 2012). The groundwater samples are analysed for ionic and non-ionic constituents.

5.2.4.1 Ionic constituents

The ionic constituents are mainly divided into cations (positive charge) and anions (negative charge). The Na⁺, K⁺, Ca²⁺, Mg²⁺, Fe⁺ are the cations, whereas the Cl⁻, SO₄²⁻, NO₃⁻, HCO₃⁻, CO₃²⁻ and F⁻ are the anions observed in the groundwater samples of the study area.

5.2.4.2 Non-ionic constituents

The non-ionic parameters can also affect the groundwater quality in significant proportions. Some important non-ionic parameters are pH, total dissolved solids, electrical conductivity, total hardness, and total alkalinity.

5.2.5 Water Quality Index method

The WQI effectively portrays the importance of complex water quality information simply and effectively to the concerned policymakers and the public. This methodology expresses the information of several water quality parameters into a single number or a category such as excellent, good, poor, very poor, and unfit for drinking (Table 5.2) so that even a layperson can understand the complexity of the water pollution in simple terms. There are more than 35 versions of WQI and several modifications are also being made (Debels et al. 2005; Uddin et al. 2021). The WQI, or in this case it is Groundwater Quality Index (GQI), can be obtained by Brown’s equation (Brown et al. 1972).

Brown’s WQI is one of the widely used WQI method. Few of the recent publications of reputed journals have used the same (Bawoke & Anteneh 2020; Lkr et al. 2020; Anonna et al. 2021). Brown’s equation is the modified WQI method of National Sanitation Foundation WQI method (USA) of 1965, which is again a modified version of Horton’s WQI (USA) of 1960. The methodology is given in equation (equation 5.14), (equation 5.15) & (equation 5.16). Later the obtained water quality data is utilized to prepare spatial distribution maps in the GIS environment.

Table 5.2 Criteria for GQI

WQI value	Water quality status
< 25	Excellent water
25 – 50	Good water
50 – 75	Poor water
75 – 100	Very poor water
> 100	Water unsuitable for drinking

5.2.6 QAP or CCA for water quality analysis

The quality assurance practices or checking the correctness of analysis constitutes the GW quality parameters like pH, EC, TDS, Major cationic, and anionic constituents. The following procedures for CCA are considered for general and drinking water quality (APHA 1999).

5.2.6.1 Anion – Cation Balance

The ACB is one of the most utilized CCA methods. The sums of anion and cation should be balanced (equation 5.4) and expressed in milliequivalents per litre (meq/l). The potable water always is electrically neutral. Thus the anions and cations should be balanced.

$$Cat\ ions = \left[\left(\frac{Ca}{20.1} \right) + \left(\frac{Mg}{12.2} \right) + \left(\frac{Na}{23} \right) + \left(\frac{K}{39.1} \right) + \left(\frac{Fe}{55.847} \right) \right] \quad (\text{equation 5.1})$$

$$An\ ions = \left[\left(\frac{TA}{50} \right) + \left(\frac{Cl}{35.46} \right) + \left(\frac{SO_4}{48.1} \right) + \left(\frac{NO_3}{2} \right) \right] \quad (\text{equation 5.2})$$

$$Cat\ ions = An\ ions \quad (\text{equation 5.3})$$

$$\text{Percentage difference} = 100 * \left(\frac{\sum\ cations - \sum\ anions}{\sum\ cations + \sum\ anions} \right) \quad (\text{equation 5.4})$$

The criteria of acceptance (Table 5.3) considered for the present work is ± 0.2 meq/l as the Total Anions (TAn) or the Total cations (TCat) are well within the range of 0-3 meq/l.

Table 5.3 Typical criteria for acceptance of percentage difference of ACB

Anion sum	Acceptable difference
0 – 3.0	± 0.2 meq/l
3.0 – 10.0	± 2 meq/l
10.0 – 800	± 5 meq/l

5.2.6.2 Total Dissolved Solids (TDS)

The Calculated TDS is tabulated using equation 5.5 for all the 51 samples. Later the results are considered for correlation studies.

$$TDS = [0.6 * (TA)] + [Na + K + Ca + Mg + Cl + SO_4 + SiO_3 + NO_3 + F] \quad (\text{equation 5.5})$$

The analysis for Measured TDS was conducted in the laboratory. The MTDS must always be equal to CTDS, provided analysis is done without any error. The concentration of MTDS should always be higher than that of CTDS because a major contribution may not have been considered for calculation. The acceptable ratio for TDS (equation 5.6) is considered for checking the correctness of the analysis.

$$1.0 < \frac{\text{measuredTDS}}{\text{calculatedTDS}} < 1.2 \quad (\text{equation 5.6})$$

5.2.6.3 Measured EC and Ion sums

The total anions or the total cations should be $\frac{1}{100}^{\text{th}}$ of the measured EC value. The acceptable criteria equation 5.7 gives the relationship of MEC with the TAn or TCat.

$$100 * TAn \text{ (or TCat)} = (0.9 - 1.1) * EC \quad (\text{equation 5.7})$$

The equation 5.7 can be re-written in a simpler notation as,

$$(0.9 * EC) \leq 100 * TAn \leq (1.1 * EC) \quad (\text{equation 5.8})$$

Where TAn (or TCat) is in meq/l

5.2.6.4 Calculated TDS to EC ratio

The ratio of CTDS to conductivity should always fall under the range of 0.55 to 0.7. The acceptable criteria are as follows,

$$0.5 < \frac{CTDS}{\text{conductivity}} < 0.7 \quad (\text{equation 5.9})$$

5.2.6.5 Total Hardness (TH)

The hardness is one of the important GWQ parameters helpful in the detection of pollution. The Sulphates and Chlorides together constitute Permanent Hardness, also known as non-carbonate hardness. The carbonates and bicarbonates together cause

Temporary Hardness. The TH expresses a direct relationship with Ca and Mg. The equation for Calculated TH (Sawyer 1959; Karanth 2008) is as follows,

$$\text{Calculated TH} = (2.497 * Ca) + (4.115 * Mg) \quad (\text{equation 5.10})$$

It is imperative, there must be a direct relationship between bicarbonates (TeH) and Calcium and Magnesium (Ca+Mg) ions (Prasad & Saxena 1980). TH must also be equal to the sum of TA, Sulphate, and nitrate.

$$TH = (TA + SO_4 + NO_3) \quad (\text{equation 5.11})$$

The equation 5.11 gives the relationship between the TA, Sulphate, and nitrate (values are in meq/l), correlating the Ca and Mg values using equation 5.10.

5.2.6.6 Chloride's relationship with Na and K

The total chloride present in the water sample taken for analysis must be equal to the sum of total Sodium and Potassium.

$$Cl = Na + K \quad (\text{equation 5.12})$$

The equation 5.12 gives a direct relationship between Na and K. The equations from equation 5.4 through equation 5.12 are connected somehow to quality assurance practices. Therefore these relationships can be sharply observed in the correlation tables. As mentioned above, the QAP or CCA method is utilized in confirming the quality of the data generated before using the data for GQI.

5.2.7 Computation of Water Quality Index (WQI)

There are several methods available from time to time for studying Water Quality Index. Water is a broader term for all types of water, including groundwater. Here the importance is given for groundwater. Therefore, from here on, the term Groundwater quality index is used instead of water quality index. The present study concentrates on the Weighted Arithmetic Index method for evaluating the GQI of the Gurgur watershed. The WQI can be calculated using Brown's equation (Brown et al. 1972).

$$GQI = \frac{\sum_{i=1}^{i=n} (Q_i * W_i)}{\sum_{i=1}^{i=n} W_i} \quad (\text{equation 5.13})$$

Where W_i is the Unit weight of i^{th} parameter and can be calculated using equation 5.15.

Also, the equation for Water quality rating Q_i is given by

$$Q_i = \left(\frac{V_i - V_0}{S_i - V_0} \right) * 100 \quad (\text{equation 5.14})$$

Where, V_i is the estimated concentration of i^{th} parameter. V_0 is the ideal standard value of the i^{th} parameter in pure water. $V_0 = 0$ (except pH = 7.0 moles/l and DO = 14.6 mg/l). S_i is recommended standard value of the i^{th} parameter.

The formula calculates the unit weight (W_i) for the i^{th} parameter.

$$W_i = \frac{K}{S_i} \quad (\text{equation 5.15})$$

Where, V_s is recommended standard value of the i^{th} parameter. K is proportionality constant.

The equation for K is given below,

$$K = \left(\frac{1}{\sum_{i=1}^{i=n} \left(\frac{1}{S_i} \right)} \right) \quad (\text{equation 5.16})$$

The Water Quality Rating and grading are assigned to the Weighted Arithmetic GQI method. Later utilizing the obtained data, the spatial distribution maps for important parameters are prepared in the GIS environment.

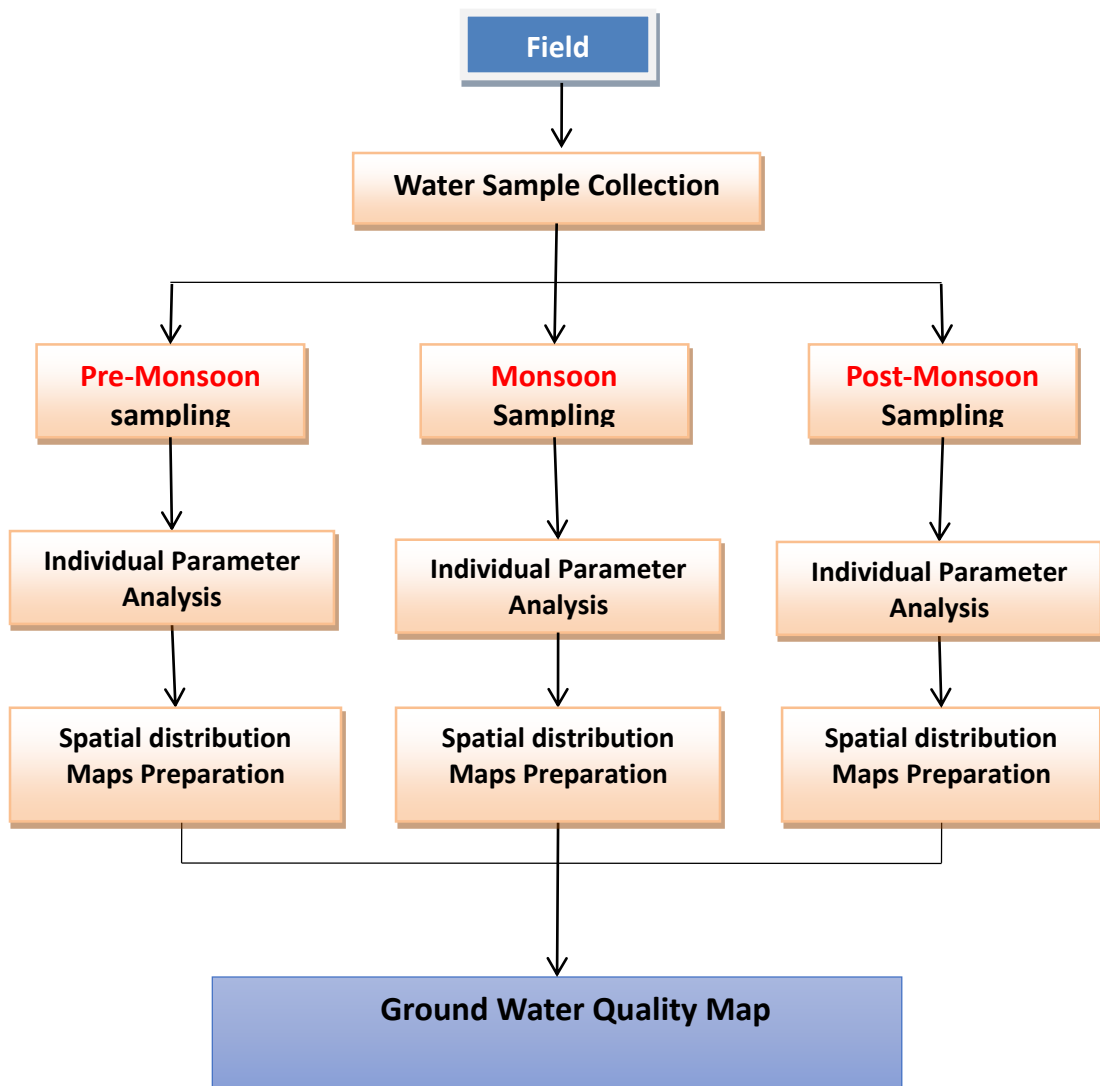


Figure 5.1 Flow chart for spatial distribution of groundwater quality parameters.

5.3 Results and discussion

5.3.1 Groundwater quality analysis for drinking purposes

The Gurpur watershed covers about 877 km² of area. Therefore, sampling locations were selected cautiously such that the broader scenario of the study can be observed. The groundwater quality studies are conducted in three different phases (phase-I in August-2017, phase-II in December-2017, and phase-III in April-2018). The study aims to analyse the spatial and temporal changes of the groundwater quality in the study area.

The temporal studies are conducted to understand the change in the concentration of parameters in three different time intervals. The spatial studies in groundwater quality are conducted to understand the spatial distribution of parameter concentrations. The results obtained are correlated by using the CCA method, which revealed the relationship between different parameters.

5.3.2 Drinking water quality parameters

The groundwater samples were collected in 51 locations throughout the Gurpur watershed. A total of 14 groundwater quality parameters are analysed in three phases concerning drinking water specifications. The acceptable limits and permissible limits of the drinking water quality parameters can be seen in Table 5.1. The spatial distribution maps for the drinking water quality parameters (Figure 5.2 & Figure 5.3) are prepared for spatial studies. These maps are prepared in a GIS environment using the IDW interpolation tool.

5.3.2.1 Ionic constituents

The ionic constituents are mainly divided into cations (positive charge) and anions (negative charge). The Na^+ , K^+ , Ca^{2+} , Mg^{2+} , Fe^+ are the major cations. The Cl^- , SO_4^{2-} , NO_3^- , HCO_3^- , CO_3^{2-} and F^- are the major anions analysed in the groundwater samples to drinking water standards.

5.3.2.1.1 Sodium

The sodium, also known as Natrium (Na), is one of the major cations found in groundwater due to weathering of rocks. The sewage and industrial waste also consist of Na, when leached to groundwater, may increase the Na concentration. The prolonged exposure to excess ingestion of the Na may cause high blood pressure, heart failure, stroke, cancers (stomach related), kidney diseases, osteoporosis, and kidney stones.

The highest value of Na in the study was 61.15 mg/l during phase-II (Table 5.4). It is within the permissible as well as desirable limits. The average range of value of the Na is 5.87 mg/l to 17 mg/l. The Na shows a positive and linear correlation with

potassium as well as Chloride. Therefore, an increase in Na and K increases the concentration of chloride.

5.3.2.1.2 Potassium

Like Na, the K is also a major cation found in freshwater. The K is good for health with a proper and natural diet. If consumed excessively, it may cause serious problems to human health like nausea, stomach problems, vomiting, intestinal problems, diarrhoea, skin burning sensation, body weakness, paralysis, irregular heartbeat.

There is no permissible limit for K, but only a desirable limit (Table 5.1). The average K value from the three phases ranges from 1.23 mg/l to 5.33 mg/l (Table 5.4). The K is having a relationship with only two other parameters, such as Na and Cl. Also, this relationship is a linear (direct) relationship, i.e., the increase in K concentration increases the Na and Cl concentrations.

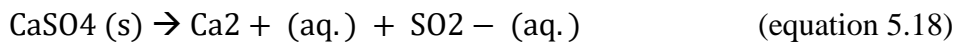
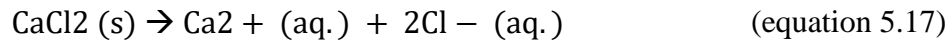
Table 5.4 Statistics of groundwater quality parameters for 51 samples

Sl. No.	Parameters	Units	Phase-I (Monsoon)			Phase-II (Post-monsoon)			Phase-III (Pre-monsoon)		
			Min.	Max.	Mean	Min.	Max.	Mean	Min.	Max.	Mean
1	pH	moles/l	4.20	7.20	5.55	4.30	7.30	5.57	5.20	7.80	6.49
2	EC	µs/cm	19.00	362.00	105.24	0.00	560.00	130.73	49.11	619.24	158.47
3	TDS	mg/l	12.73	242.54	70.51	0.00	375.20	87.59	30.03	350.54	91.43
4	Cl	mg/l	5.23	24.27	10.85	10.98	108.66	28.98	9.83	46.24	20.68
5	F	mg/l	0.00	0.21	0.08	0.10	0.74	0.24	0.17	1.46	0.57
6	TH	mg/l	0.09	43.83	11.62	3.81	247.62	55.24	5.74	271.54	53.79
7	Ca	mg/l	0.43	33.30	9.40	1.25	106.17	22.96	0.48	58.57	9.68
8	Na	mg/l	2.91	13.31	5.85	6.81	61.15	17.00	5.70	26.63	11.97
9	K	mg/l	0.29	2.89	1.23	1.92	19.06	5.33	0.63	5.79	2.52
10	Mg	mg/l	0.04	9.12	2.21	0.17	3.60	1.84	0.12	34.78	7.20
11	HCO₃	mg/l	0.09	43.83	11.62	2.59	246.25	53.79	0.25	236.65	45.91
12	Fe	mg/l	0.00	0.26	0.02	0.00	1.11	0.09	0.00	0.28	0.06
13	NO₃	mg/l	0.00	15.54	2.93	0.00	5.87	0.83	0.15	1.41	0.61
14	SO₄	mg/l	0.09	54.22	15.17	2.15	25.17	9.10	1.91	35.23	7.69

5.3.2.1.3 Calcium

Calcium is one of the major inorganic cations in freshwater and saline water as Ca²⁺ ions. Calcium is one of the most common constituents of rock-forming minerals like pyroxenes, amphiboles, plagioclase feldspar, and calcite. The majority of the calcium

present in the freshwater is due to the rocks like limestone (CaCO_3), dolomite ($\text{CaCO}_3 + \text{MgCO}_3$), gypsum ($\text{CaSO}_4 \cdot 2\text{H}_2\text{O}$), and other calcium-containing rocks dissolving in the water. The dissociation of salts such as calcium chloride and calcium Sulphate in the water yields calcium ions.



Note: the symbol (s) implies solid-state and (aq.) implies aqueous state.

The aquifers may allow the leaching of calcium from rocks into the groundwater. Though CaCO_3 is relatively insoluble, it may react with dissolved carbon-di-oxide (CO_2), forming carbonic acid. The minimum value of 0.43 mg/l (phase-I) and a maximum of 106.17 mg/l (phase-II) is observed (Table 5.4). The average value of calcium ions was 14.01 mg/l for all seasons, and it is way within the desirable limits (75 mg/l as per IS 10500:2012 regulations) of drinking water. Though the maximum value is greater than the desirable limit, it is still within the permissible limits of 200 mg/l (Table 5.1). It can be observed that the calcium ions are increasing in phase-II (post-monsoon season), which implies that the water quality is deteriorating in the post-monsoon season.

5.3.2.1.4 Magnesium

The Mg is the fourth most abundant cation in the human body. The lower or higher level of Mg concentrations in the human body may cause serious side effects. Therefore the diet should be properly balanced. Excessive Mg intake along with Sulphates may cause gastrointestinal dysfunctions, hyper-magnesaemia (decreased ability to excrete magnesium), diarrhoea, and abnormal kidney functions. Whereas low Mg concentrations in humans may cause hypertension, the onset of type-2 diabetes, cardiac arrhythmia, and coronary heart disease. The Mg works as an anti-inflammatory agent if treated with proper dosage. Therefore Mg is one of the important parameters to be included in regular diet and drinking purposes.

The average Mg level in the groundwater samples was in the range of 1.84 mg/l to 7.2 mg/l. But during Phase-III, only three samples (G37, G38 & G49) show a sudden deviation from the average value of Mg concentration (Table 5.4). This is mainly because of the saltwater intrusion during the pre-monsoon (April) season. The Mg values along with the Na, K, Cl, Mg, and Ca of the groundwater samples have drastically increased during Phase-III, suggesting the possibility of saltwater intrusion because seawater is the source of excessive ionic concentration. Therefore, it can be implied that the acute scarcity of water during summer leads to an overdraft of groundwater, leading to saltwater intrusion into freshwater aquifers.

5.3.2.1.5 Iron

Iron is one of the important minerals that are essential for human health. The lack of iron may lead to fatigue, anaemia, infections, and skin problems. The iron overload may cause hemochromatosis, which in turn may cause liver damage, heart and pancreas damage. Excessive iron may also cause skin wrinkles. The analysis for iron was carried out using Ultra Violet (UV) spectrophotometer at the wavelength of 510 nm.

The average value of iron was found to be in the range of 0.02 mg/l to 0.09 mg/l and is well within the permissible limits (Table 5.1 & Table 5.4). Phase-II is showing excessive iron values (greater than permissible limits) at four locations. It is observed that the concentration of the iron is extremely low and does not have any correlation with other parameters

Table 5.6, Table 5.7, Table 5.8 & Table 5.9).

5.3.2.1.6 Chloride

Chloride is one of the major anions in any of the water types. Usually, Cl is associated with cations as NaCl, KCl, or CaCl₂. The Cl is known for its organoleptic properties (the taste threshold is dependent on associated cations). Even the taste of the coffee varies with the water used, i.e., NaCl water or CaCl₂ water. The Cl is widely used in industries, fertilizers, bleaching liquids, water treatment, and food additives when associated with cations. There are no guidelines for the Cl levels and human health.

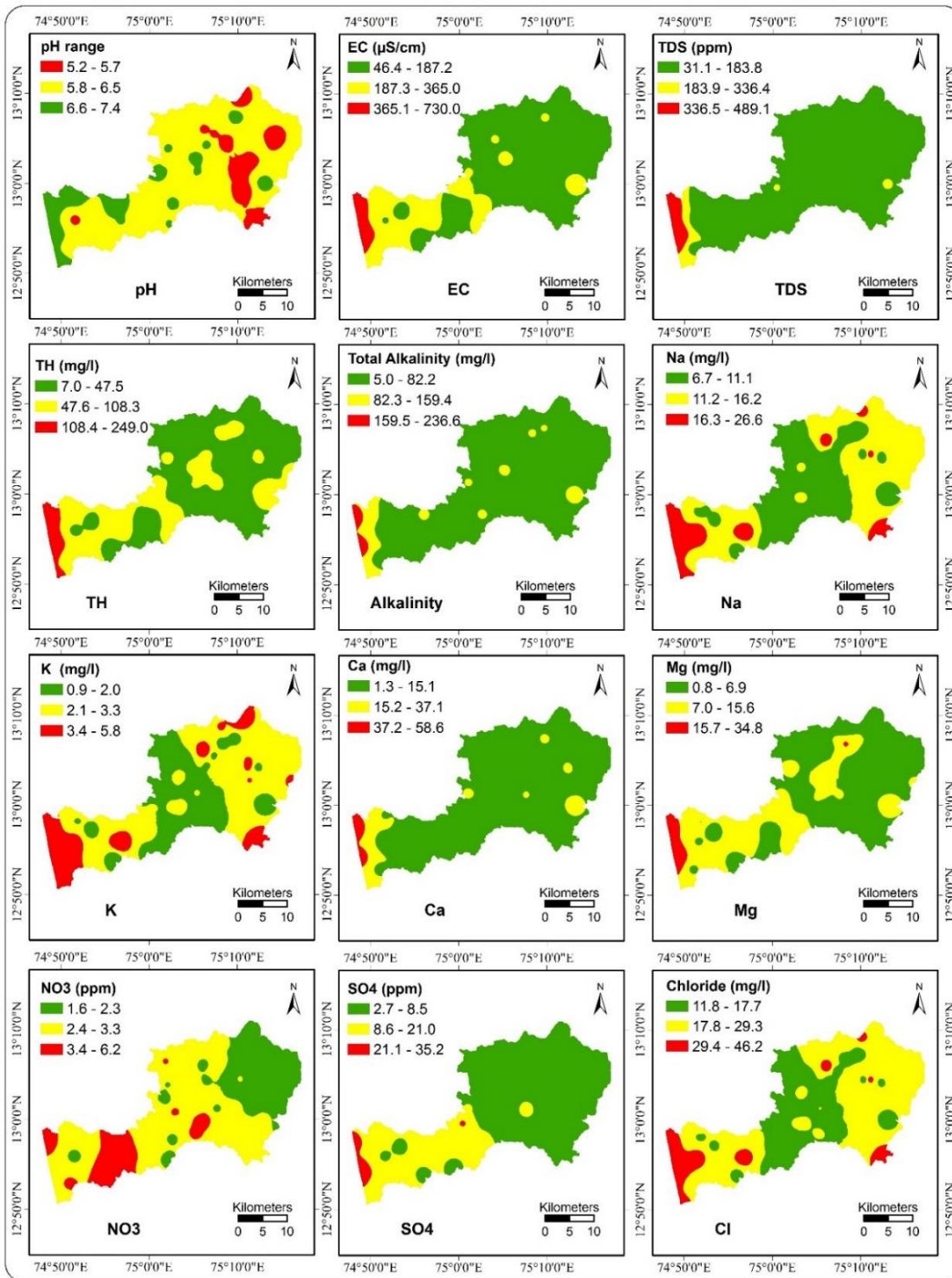


Figure 5.2 Spatial distribution maps of groundwater quality parameters.

The silver nitrate method of titration is used in the present study for measuring the Cl. The Cl increases electrical conductivity as well as the corrosiveness of the water. The Cl reacts with metal pipes and forms soluble salts of metals, which may cause serious health problems after ingestion. The chloride concentrations in the groundwater samples of all three phases are well within the desirable and permissible limits. The average Cl levels are in the range of 10.85 mg/l to 28.98 mg/l (Table 5.4). The Cl levels in the groundwater are one of the important indicators of saltwater intrusion analysis. It is observed that during phase-III, the effects of saltwater intrusion are seen in the groundwater samples nearer to sea. The Cl ions show a positive linear correlation with Na and K ions in the water samples.

5.3.2.1.7 Sulphate

Sulphates are the compound of sulphur and oxygen ions. The Sulphate levels in the drinking water are connected with the hardness of the water. Like the calcium and magnesium levels, the concentration of Sulphate affects the hardness and the taste of the water. The Sulphate analysis was carried out using UV spectrophotometer at the wavelength of 420 nm. The major source of Sulphates in the drinking water are sulphite ores, sedimentary rocks like shale, minerals like Epsom salt (magnesium Sulphate) and gypsum (calcium Sulphate), industrial or sewage treated water leaching into groundwater. The Sulphates, when combined with Ca or Mg, may cause hardness. The excessive use of a high concentration of SO₄ can cause diarrhoea and dehydration. The high concentration of SO₄ can cause corrosion of the pipes.

The SO₄ levels are well within the desirable and permissible limits (Table 5.1 & Table 5.4). The average levels (for 51 groundwater samples) of SO₄ are very high during phase-I and gradually decreasing towards phase-III. This is because SO₄ and NO₃ are used in artificial fertilizers and may have percolated into groundwater. The SO₄ shows a direct relationship with the NO₃, TH, and TA (Table 5.6, Table 5.7, Table 5.8 & Table 5.9).

5.3.2.1.8 Nitrate

Nitrates are the compound of nitrogen and oxygen ions. The nitrate analysis was carried out using UV spectrophotometer at two wavelengths of 220 nm and 275 nm. The absorbance of NO_3 is unique from the absorbance of organic matter at two different wavelengths. The major source of nitrate in drinking water is nitrogen-based fertilizers, and animal wastes infiltrate into water sources. The health issues like diarrhoea, dehydration, variation in the supply of oxygen in the blood are associated with nitrate. The high nitrate concentration can cause serious health issues, especially for infants and pregnant women.

The average value of nitrate for all three phases is found to be in the range of 0.83 mg/l to 2.93 mg/l (Table 5.4). It can be implied that nitrate concentration is observed mainly due to nitrate-based fertilizers. The nitrate does not show any correlation with other parameters.

5.3.2.1.9 Fluoride

The fluorine is highly reactive and therefore always be found in nature as fluoride. The higher concentrations of fluoride can be found in groundwater, especially in deeper aquifers. The excess and prolonged ingestion of fluoride from drinking water forms the equilibrium with the blood fluoride concentrations and then starts to incorporate into teeth and bones. Once the accumulation of fluoride ends, the fluoride starts to transport outside the body as excreta.

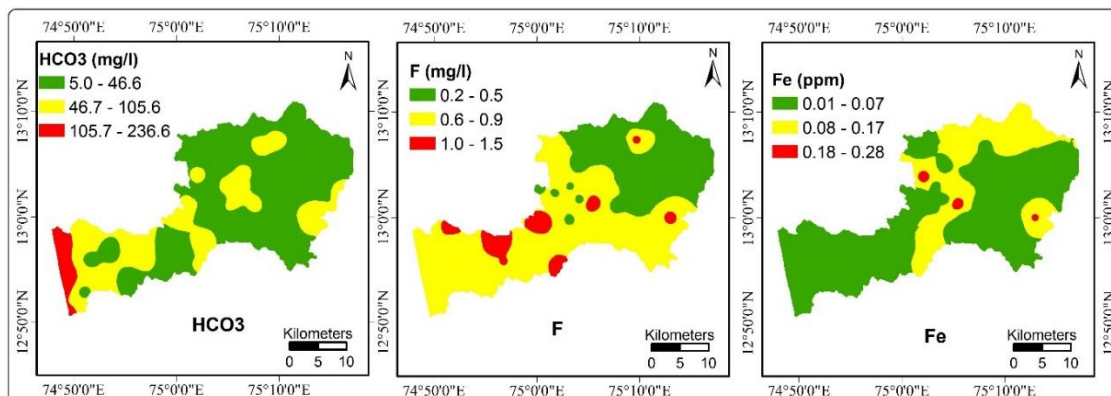


Figure 5.3 Spatial distribution maps of Bicarbonates, Fluoride and Iron.

The average fluoride value for all three phases is found to be in the range of 0.08 mg/l to 0.57 mg/l (Table 5.4). The maximum concentration of fluoride was observed in Phase-III during the study. The fluoride is not showing a correlation with any of the other parameters.

5.3.2.2 Non-ionic constituents

The non-ionic parameters can also affect the groundwater quality insignificant proportions. Some important non-ionic parameters are pH, total dissolved solids, electrical conductivity, total hardness, and total alkalinity. The parameter pH should always be approximately neutral (pH = 7) for drinking water. Even as light decrease can make the water acidic and unfit for drinking without treatment. The variation in the non-ionic constituents can also seriously affect health.

5.3.2.2.1 The pH

The pH of a solution is the negative logarithm of the hydrogen ion activity. The pH of the water is the measure of acid-base equilibrium, which depends on carbon-di-oxide (CO₂) and bicarbonates.

$$pH = -\log(H^+) \quad (\text{equation 5.19})$$

The pH has an inverse relationship with CO₂, i.e., an increase in CO₂ decreases the pH (acidic range). The corrosiveness of the water is mainly dependent on pH. Extensive exposure to extreme pH may induce serious health problems in humans as well as animals. The issues like eye irritation, itching of the skin, throat infections, increased blood pH, acidity, and gastro-intestinal irritation are associated with extremely low or high pH.

The permissible limit of pH is from 6.5-8.5 on the pH scale. The minimum value observed is 4.2 (phase-I). The average pH value of all three seasons is still outside the range of permissible limits. The maximum pH value of all three seasons is observed to be within the permissible limits. However, water needs to be treated before consumption where ever the pH is low.

5.3.2.2.2 Electrical conductivity

The EC is the measure of electrolytes (concentration of ions) in the water, through which the electrical flow can occur. The EC is usually measured as specific conductance. The specific conductance is the measure of electrical conductivity that is made at or corrected to 25°C. The unit for specific conductance is $\mu\text{S}/\text{cm}$ at 25°C. The EC has a direct relationship with electrolytes, i.e., the higher the electrolytes (ions) concentration, the higher the EC will be. The pure distilled water is having an EC value of 0.05 $\mu\text{S}/\text{cm}$. Also, the EC expresses the linear correlation with TDS. Therefore, an increase in EC implies more dissolved solids.

The EC is observed to be as low as 19 $\mu\text{S}/\text{cm}$ during phase-I. Temporally, the study's average EC values vary from approximately 100 to 160 $\mu\text{S}/\text{cm}$, which is within the desirable limits of EC (Table 5.1 & Table 5.4).

5.3.2.2.3 Total dissolved solids

The total dissolved solids are the measure of combined organic and inorganic substances dissolved in the liquid. The TDS is not a primary pollutant that affects human health but is used as an indicator for important characteristics of freshwater (drinking water).

The TDS value is observed within the desirable limits, let alone the permissible limits (Table 5.1 & Table 5.4). The TDS is gradually increasing from phase-I to Phase-III, indicating that it is due to a decrease in groundwater quantity in the aquifers. The irrigation practices and artificial fertilizers, leaching of soil contaminants, and discharge of sewage pollutants into groundwater may also increase the TDS in groundwater aquifers. The TDS will be high if the groundwater is static because of the time available for groundwater interaction with rocks and minerals of the aquifers. Whereas in the study area, because of the lateritic soils, the transmissivity of the groundwater is high, and thus the TDS value is comparatively less.

5.3.2.2.4 Total Alkalinity

The alkalinity measures a water's ability to resist the changes in pH upon adding the acids or bases. The term "alkaline" means the pH value greater than 7 on the pH scale of 0 – 14. The alkaline waters are associated with negative oxidizing reduction potential (ORP), i.e., anti-oxidizing agents. The possible health hazards of increased TA are reduced stomach acidity, reduced blood pH, gastrointestinal problems, and skin & eye irritation. The increased alkalinity may also cause Alkalosis (a medical condition), where the body is deprived of free calcium. The symptoms of alkalosis are vomiting, nausea, tremors in the hands.

The alkalinity having the pH range of 10.7 to 8.3 is called carbonate alkalinity. All the carbonate in the water sample is reacted during that time. Likewise, alkalinity having the pH range of 8.3 to 4.5 is called total alkalinity, at which point both the carbonates and bicarbonates are completely reacted. The pH value less than 4.5 indicates only carbonic acid and no traces of CO_3 or HCO_3 in the water.

The highest TA in the study area was during phase-II and is well within the permissible limits (Table 5.1&Table 5.4). It is observed that the TA values are drastically reduced around the pH of 4.5. It is also observed that all the groundwater samples analysed are found to be in bicarbonate alkalinity, i.e., there is no carbonate alkalinity ($\text{pH}>8.3$) in the samples.

5.3.2.2.5 Total Hardness

The total hardness is the measure of dissolved minerals of calcium and magnesium in the water sample. The hardness does not have harmful effects on human health but can seriously affect the industrial fitting, pipes, washing clothes, bathing, cooking.

The average total hardness of the water was found to be ranging from 9 – 23 mg/l. Therefore, most of the samples are considered as "soft" ($\text{TH} < 60$ mg/l) from all three phases of the study. The TH was found to be in the range of "moderate" (TH between 60 - 100 mg/l) only in two samples (G38 & G49 of phase-II) from the three phases. It is observed that the TH is having a linear and direct relationship with TA,

SO₄, and NO₃ in the water samples (Table 5.9). Also, it is observed that there is a linear and direct relationship between Ca and Mg ions (as CaCO₃).

5.3.3 Phases of groundwater quality studies

5.3.3.1 Phase-I (August – 2017)

Phase-I (August 2017) for groundwater sampling and analysis was conducted during peak monsoon season. The reason for considering this method of study is that the coastal region of Karnataka is associated with heavy rainfall, and the water level will be almost ground level. Therefore groundwater quality during this period is pretty good, and the concentrations of water quality parameters will be considerably low. Also, the study area is covered with lateritic soils, which have a very high permeability rate. Therefore, the groundwater level increases up to ground level and thus improves groundwater quality.

During phase-I (monsoon season), all the drinking water quality parameters show low concentrations. The pH, SO₄, and NO₃ are the only parameters that's how high concentrations (Table 5.4 & Table 5.7). The NO₃ is the only parameter that is higher than the acceptable limit without relaxation. The reason for these high concentrations is mainly because of pesticides and fertilizers leaching into the ground.

The lowest concentration of pH (4.2 moles/l) in all three phases was recorded with an average of 5.5 moles/l. The pH is the only parameter below (Acidic range) the acceptable limit of 6.5 to 8.5 moles/l.

5.3.3.2 Phase-II (December – 2017)

It is observed that few of the parameters show high concentrations in groundwater samples (Table 5.4&Table 5.8). The parameters like Ca, Na, K, Fe, Cl, HCO₃, and TA show high concentrations (more than the acceptable limit) in few locations. Yet, they are well within the permissible limits. The high concentrations of Na, K, and Cl are observed only in the locations nearer to sea, indicating the problem of saltwater

intrusion. Also, this problem continues to persist throughout phase-III. Total Alkalinity is the other parameter over the acceptable limit, but it is within the permissible limit.

5.3.3.3 Phase-III (April – 2018)

Phase-III recorded the highest pH value (7.8 moles/l), which is within the acceptable limits of drinking water quality. The average pH of 6.37 moles/l was observed in this phase, just below the specification required (Table 5.1). Most of the study area experiences pH in the acidic range (no relaxation). The reason for this might be the lateritic soils. The lateritic soils are the natural source of acidic pH levels in groundwater. Also, heavy metals like Lead, Iron, Zinc, and Manganese might cause acidity in drinking water. The imbalance in pH can cause several health issues like diarrhoea, vomiting, nausea, nervous system problems, liver & kidney problems. Therefore, there is a serious need to treat the pH of the groundwater before using it for drinking purposes.

The TH and Mg are just over the acceptable limit but are within the permissible limit (Table 5.1, Table 5.4). Though the fluoride concentration is also higher than the acceptable limit, it is within the permissible limit. Few locations have fluoride concentrations closer to permissible limits. Thus, there is a need for continuous monitoring.

5.3.4 Computation of Groundwater Quality Index

The weighted arithmetic WQI method is used in this study. In this method, the water quality is classified with respect to the degree of purity using water quality parameters. The WQI for all three phases is calculated, i.e., for phases I, II, and III (Table 5.2 & Table 5.5).

It is observed that the drinking water quality parameters other than pH are rated as “excellent category”. The very poor water quality rating for pH can also be confirmed from Table 5.4, in which pH is below the specified acceptable limits (6.5 to 8.5 moles/l). Even though the parameters like EC and TDS have a direct relationship, they show a very different water quality rating. The pH shows a poor rating of groundwater quality,

whereas the TDS shows an excellent groundwater quality rating. This variation is mainly due to the proportionality constant 'K', which is 5.9 for pH and 39.2 for TDS. The pH shows the GQI value of 91 (Table 5.5), which means it is nearly unsuitable for drinking. The parameter fluoride falls under "good water quality", but it is still of serious consideration. The fluoride concentrations are constantly increasing from phase-I to Phase-III (from almost nil to nearly over the permissible limit of 1.5 mg/l). This indicates a serious health concern due to excessive fluoride concentration in drinking water. It can be observed that there is an increase in serious health concerns during phase-II (Post-monsoon season) because of its reduced water quality (Figure 5.4). Especially, pH is the parameter leaning towards acidic range and renders as "unfit for drinking". This is happening mainly because of the laterite soil, which is acidic. Therefore, there is a need for continuous monitoring of the groundwater quality, especially for pH and fluoride.

5.3.5 Implementation of QAP

5.3.5.1 Correlation studies

The correlation studies were conducted to analyse the relationship between different parameters (

Table 5.6 through Table 5.9). A strong positive correlation (0.97 to 1.0) is observed between total cations and total anions in all three phases. This strong correlation shows the positive inter-relationship between all the ionic parameters. Also, total cations and total anions strongly correlate with MTDS, CTDS MTH, CTH, and TeH (equation 5.1 through equation 5.12). In a perfect scenario, the MTDS must be equal to CTDS. Hence there is little or no correlation between them. There is a very good positive correlation between the left-hand side and the right-hand side of the equations. Also, it can be observed that the inter-relationship between different equations shows a strong and positive correlation. The TH is equal to the sum of Ca and Mg and equal to TA, SO₄, and NO₃. Therefore a strong positive correlation is seen between different equations. The permanent hardness (SO₄ and Cl) show a moderate

correlation with all the equations, except for equation 9, which shows a good positive correlation.

Table 5.5 The GQI status for all the three phases of the study.

Sl. No.	GWS No.	GQI_R (P1)	GQI_R (P2)	GQI_R (P3)	GQ status (P1)	GQ status (P2)	GQ status (P3)
1	G1	21.57	46.04	59.77	Excellent	Good	Poor
2	G2	17.76	14.06	31.79	Excellent	Excellent	Good
3	G3	81.54	93.88	29.57	Very Poor	Very Poor	Good
4	G4	20.21	32.77	32.67	Excellent	Good	Good
5	G5	7.35	17.24	27.05	Excellent	Excellent	Good
6	G6	71.87	78.87	12.75	Poor	Very Poor	Excellent
7	G7	2.44	9.39	61.10	Excellent	Excellent	Poor
8	G8	18.69	19.46	25.27	Excellent	Excellent	Good
9	G9	20.34	20.29	20.95	Excellent	Excellent	Excellent
10	G10	9.56	9.11	14.33	Excellent	Excellent	Excellent
11	G11	23.00	32.22	50.18	Excellent	Good	Poor
12	G12	13.19	11.29	15.30	Excellent	Excellent	Excellent
13	G13	12.68	12.85	21.81	Excellent	Excellent	Excellent
14	G14	21.97	21.49	16.69	Excellent	Excellent	Excellent
15	G15	13.35	11.95	14.05	Excellent	Excellent	Excellent
16	G16	4.54	96.16	46.82	Excellent	Very Poor	Good
17	G17	4.66	299.05	74.90	Excellent	Unfit for drinking	Poor
18	G18	14.72	13.78	20.63	Excellent	Excellent	Excellent
19	G19	20.92	19.73	45.49	Excellent	Excellent	Good
20	G20	19.10	16.87	25.38	Excellent	Excellent	Good
21	G21	32.49	30.64	20.06	Good	Good	Excellent
22	G22	4.47	263.95	50.39	Excellent	Unfit for drinking	Poor
23	G23	28.84	36.17	38.01	Good	Good	Good
24	G24	15.21	14.06	35.40	Excellent	Excellent	Good
25	G25	15.58	16.30	21.21	Excellent	Excellent	Excellent
26	G26	39.40	36.37	17.16	Good	Good	Excellent
27	G27	17.58	22.03	22.97	Excellent	Excellent	Excellent
28	G28	17.66	16.94	22.52	Excellent	Excellent	Excellent
29	G29	19.63	18.70	16.28	Excellent	Excellent	Excellent
30	G30	12.64	22.59	90.31	Excellent	Excellent	Very Poor
31	G31	10.86	30.69	14.57	Excellent	Good	Excellent
32	G32	22.10	20.27	15.69	Excellent	Excellent	Excellent
33	G33	14.63	35.27	20.66	Excellent	Good	Excellent
34	G34	12.05	15.74	17.02	Excellent	Excellent	Excellent
35	G35	8.71	14.54	23.96	Excellent	Excellent	Excellent
36	G36	19.57	21.87	18.50	Excellent	Excellent	Excellent
37	G37	19.54	33.47	9.33	Excellent	Good	Excellent

38	G38	1.00	3.37	16.13	Excellent	Excellent	Excellent
39	G39	1.07	114.68	13.28	Excellent	Unfit for drinking	Excellent
40	G40	3.92	10.76	23.27	Excellent	Excellent	Excellent
41	G41	11.45	5.52	19.62	Excellent	Excellent	Excellent
42	G42	9.07	12.49	31.63	Excellent	Excellent	Good
43	G43	6.82	5.63	13.28	Excellent	Excellent	Excellent
44	G44	14.96	16.72	18.97	Excellent	Excellent	Excellent
45	G45	10.78	34.22	14.12	Excellent	Good	Excellent
46	G46	27.50	32.49	16.94	Good	Good	Excellent
47	G47	46.14	54.40	16.79	Good	Poor	Excellent
48	G48	12.17	12.36	13.25	Excellent	Excellent	Excellent
49	G49	0.49	3.88	13.80	Excellent	Excellent	Excellent
50	G50	14.25	13.79	18.62	Excellent	Excellent	Excellent
51	G51	14.46	15.32	18.05	Excellent	Excellent	Excellent

Table 5.6 Correlation studies for QAP equations.

GWQ parameters	Na+K	Cl	TA+SO ₄ +NO ₃	TH	Ca+Mg
Na+K	1				
Cl	1	1			
TA+SO ₄ +NO ₃	0.20	0.20	1		
TH	0.19	0.19	0.99	1	
Ca+Mg	0.19	0.20	0.98	1	1

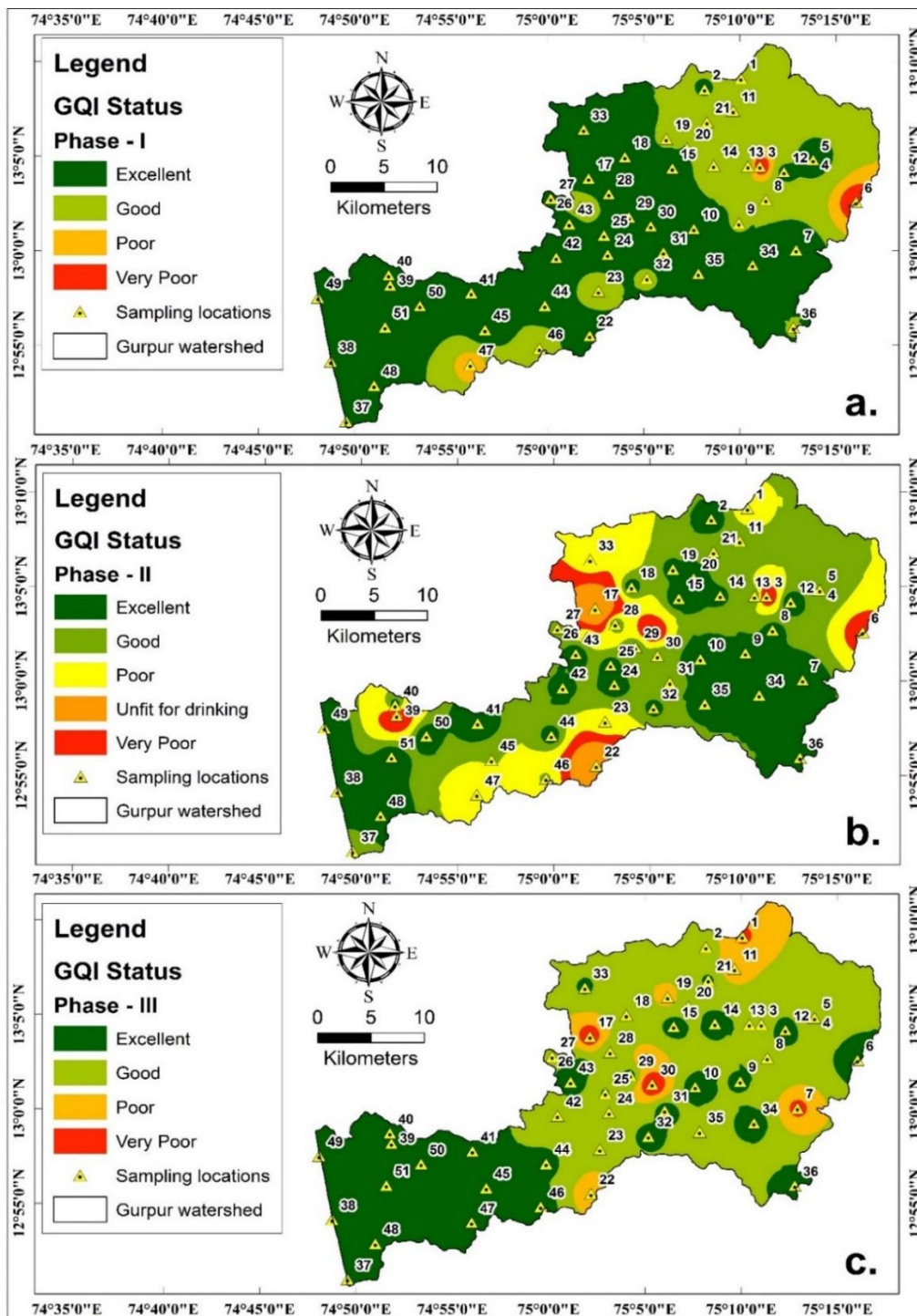


Figure 5.4 Spatial distribution maps of GQI for three phases.

Table 5.7 Correlation matrix for Phase-I Groundwater quality data (August-2017)

	pH	EC	M_TDS	TH	Ca+	Mg2+	Na+	K+	Fe+	Cl-	HCO3-	TA	SO42-	NO3-	F-	T_Cat	T_An
pH	1.00																
EC	0.79	1.00															
M_TDS	0.79	1.00	1.00														
TH	0.41	0.32	0.32	1.00													
Ca+	0.42	0.34	0.34	0.90	1.00												
Mg2+	0.04	0.01	0.01	0.36	-0.08	1.00											
Na+	0.13	0.13	0.13	0.17	0.30	-0.25	1.00										
K+	0.09	0.10	0.10	0.12	0.23	-0.23	0.97	1.00									
Fe+	0.05	-0.03	-0.03	0.04	0.10	-0.13	0.25	0.22	1.00								
Cl-	0.13	0.13	0.13	0.19	0.30	-0.22	1.00	0.97	0.23	1.00							
HCO3-	0.93	0.84	0.84	0.52	0.51	0.07	0.13	0.06	0.05	0.14	1.00						
TA	0.93	0.84	0.84	0.52	0.51	0.07	0.13	0.06	0.05	0.14	1.00	1.00					
SO42-	-0.20	-0.24	-0.24	0.78	0.67	0.35	0.11	0.09	0.00	0.13	-0.13	-0.13	1.00				
NO3-	-0.16	-0.18	-0.18	0.73	0.60	0.38	0.04	0.05	0.08	0.05	-0.10	-0.10	0.88	1.00			
F-	-0.29	-0.36	-0.36	-0.15	-0.08	-0.15	-0.01	-0.04	-0.08	-0.02	-0.38	-0.38	0.12	0.04	1.00		
T_Cat	0.41	0.33	0.33	0.96	0.90	0.25	0.45	0.39	0.11	0.47	0.50	0.50	0.74	0.67	-0.13	1.00	
T_An	0.25	0.18	0.18	0.96	0.87	0.32	0.35	0.31	0.11	0.37	0.34	0.34	0.85	0.83	-0.08	0.97	1.00

Table 5.8 Correlation matrix for Phase-II Groundwater quality data (December-2017)

	pH	EC	M_TDS	TH	Ca+	Mg2+	Na+	K+	Fe+	Cl-	HCO3-	TA	SO42-	NO3-	F-	T_Cat	T_An
pH	1.00																
EC	0.78	1.00															
M_TDS	0.78	1.00	1.00														
TH	0.76	0.92	0.92	1.00													
Ca+	0.75	0.91	0.91	0.99	1.00												
Mg2+	0.07	0.06	0.06	0.04	-0.05	1.00											
Na+	-0.39	-0.07	-0.07	0.03	0.03	0.02	1.00										
K+	-0.37	-0.07	-0.07	0.02	0.02	0.06	0.95	1.00									
Fe+	0.32	0.13	0.13	0.18	0.19	-0.13	-0.26	-0.24	1.00								
Cl-	-0.38	-0.07	-0.07	0.03	0.03	0.02	1.00	0.96	-0.26	1.00							
HCO3-	0.76	0.92	0.92	1.00	0.99	0.04	0.03	0.02	0.18	0.03	1.00						
TA	0.76	0.92	0.92	1.00	0.99	0.04	0.03	0.02	0.18	0.03	1.00	1.00					
SO42-	0.59	0.74	0.74	0.78	0.82	-0.11	-0.06	-0.08	0.26	-0.05	0.78	0.78	1.00				
NO3-	0.18	0.60	0.60	0.48	0.49	0.07	0.26	0.21	-0.18	0.25	0.48	0.48	0.38	1.00			
F-	0.54	0.40	0.40	0.37	0.36	0.10	-0.25	-0.27	0.26	-0.25	0.37	0.37	0.32	-0.07	1.00		
T_Cat	0.53	0.80	0.80	0.91	0.91	0.03	0.43	0.41	0.06	0.43	0.91	0.91	0.71	0.54	0.23	1.00	
T_An	0.53	0.81	0.81	0.91	0.91	0.03	0.43	0.40	0.06	0.43	0.91	0.91	0.71	0.57	0.23	1.00	1.00

Table 5.9 Correlation matrix for Phase-III Groundwater quality data (April-2018)

	pH	EC	TDS	TH	Ca+	Mg2+	Na+	K+	Fe2+	Cl-	HCO3-	TA	SO42-	NO3-	F-	T_Cat	T_An
pH	1.00																
EC	0.73	1.00															
TDS	0.73	1.00	1.00														
TH	0.79	0.93	0.93	1.00													
Ca+	0.75	0.88	0.88	0.96	1.00												
Mg2+	0.75	0.88	0.88	0.93	0.79	1.00											
Na+	-0.14	0.31	0.31	0.19	0.21	0.14	1.00										
K+	-0.15	0.25	0.25	0.17	0.20	0.11	0.96	1.00									
Fe+	0.23	0.04	0.04	0.08	0.01	0.16	-0.15	-0.14	1.00								
Cl-	-0.14	0.30	0.30	0.19	0.21	0.14	1.00	0.97	-0.15	1.00							
HCO3-	0.80	0.93	0.93	0.98	0.93	0.94	0.19	0.17	0.12	0.19	1.00						
TA	0.80	0.93	0.93	0.98	0.93	0.94	0.19	0.17	0.12	0.19	1.00	1.00					
SO42-	0.56	0.84	0.84	0.77	0.71	0.75	0.28	0.25	-0.11	0.28	0.73	0.73	1.00				
NO3-	0.16	0.21	0.21	0.14	0.11	0.16	0.15	0.15	-0.27	0.15	0.17	0.17	0.24	1.00			
F-	0.69	0.48	0.48	0.47	0.39	0.51	-0.17	-0.19	0.36	-0.18	0.47	0.47	0.45	0.22	1.00		
T_Cat	0.70	0.93	0.93	0.97	0.93	0.91	0.41	0.38	0.05	0.41	0.96	0.96	0.78	0.16	0.40	1.00	
T_An	0.70	0.94	0.94	0.96	0.91	0.91	0.42	0.39	0.06	0.42	0.97	0.97	0.80	0.22	0.42	0.99	1.00

5.4 Summary

Groundwater samples in 51 locations were collected from dug wells in the Gurpur watershed of Coastal Karnataka. The samples were collected in three phases (Phase I, II, III) during the peak seasons of Monsoon (August-2017), Post-Monsoon (December-2017), and Pre-Monsoon (April-2018), respectively. A total of fourteen drinking water quality parameters were analysed, out of which the parameters like pH, EC, and TDS were measured on the spot during sampling. Even though the health of human beings is not affected directly by the pH, careful attention is still required.

In the present study, several methods are applied for checking the correctness of the analysis to verify the quality of the data generated from water quality analysis. The groundwater quality index studies are conducted individually for all 51 samples. The major inference from the GQI studies is that phase-II is the most affected phase with reduced water quality. The parameters like pH, Fe, SO₄, NO₃, and Cl are of major concern as they exceed the desirable limits (but are within the permissible limits). The correlation studies for understanding the relationship between different parameters of drinking water quality are attempted. It can be concluded that there is a strong positive correlation between different equations used to check the correctness of the analysis. Hence the CCA method is useful in verifying the data before using it for GQI studies. The weighted arithmetic GQI method is used in this study. It is observed that the drinking water quality for the variables like TDS, Cl, TH, Ca, Na, K, Mg, TA, Fe, NO₃, and SO₄ are rated as “excellent water quality” category. The EC and pH fall under “poor” and “very poor” water quality, respectively.

Chapter 6

GROUNDWATER RECHARGE

6.1 Introduction

Water is one of the most fundamental resources of any country. Water is not just a renewable resource. It is the resource that supports life on earth. Therefore, the need for the increasing demand for this vital resource is felt instantly. Our earth's surface is mostly covered with water. But, about 97% of the earth's water is saline. Thus, it cannot be utilized without proper treatment (desalination). But desalination process is not economical for large-scale supply. The remaining 3% constitutes freshwater. Out of this freshwater, the glaciers alone cover 68.7%, which is also inaccessible. Next to glaciers, the groundwater comprises 30.1% of freshwater. But it is difficult to explore and exploit economically because of the earth's heterogenetic sub-surface and complexity. Therefore, the remaining 0.9% of freshwater is easily available, comprising surface runoff, evapotranspiration, soil moisture, but it is insufficient to meet the growing population's basic needs. Also, the natural distribution and availability of this freshwater resource are extremely uneven and highly unpredictable. Therefore, freshwater resources can be considered as limited resources even though they are renewable. Thus, acute scarcity of freshwater is experienced during non-monsoon seasons. Therefore, scientific exploration, exploitation, conservation, recharge, and proper planning and management are much needed to meet the water requirements of any nation.

The total water resources of India are estimated to be about 1880 km³. Due to spatial and temporal variations of precipitation, topographical, and other constraints, only 690 km³ of surface water resources are considered available. With the increase in population, adoption of intense agricultural practices, industrialization, and urbanization, water requirements have considerably increased, and scarcity of this resource is felt. The available water resources must be judiciously used, apart from the control of water wastage in various usages.

The study area comes under the Udupi and Dakshina Kannada districts on the west coast of India, which receives nearly 3000-5000 mm of average annual rainfall. Despite such high rainfall, it is observed that there is acute water scarcity in the months of summer. But, the groundwater table is almost to the surface (in some cases overflowing) during monsoon season. This is mainly because the rivers are seasonal as well as tidal. Also, the high porosity of lateritic rock formations is not suitable for storing and recharging for a longer duration. The chief occupation of the people here is mainly agriculture and fishing. The population of the district has been on a steep rise in recent years. The population density along the coast has considerably increased from 229/sq.km in 1970 to 281/sq.km in 1981 due to several developmental activities in agriculture, industry, commerce, and trade programs.

The surface water is available in rivers, rivulets, and creeks, which flow only during the rainy season and for few months during the post-monsoon period. Therefore, priority is given to the areas with deeper aquifers and post-monsoon season for groundwater recharge. Whereas the shallow aquifers which are having shallow water levels are usually not given priority. But in the present case, there is a need for looking into the shallow aquifers because lateritic soils have higher infiltration and permeability. Thus, water conservation and recharge plans are required to be efficiently utilized during non-monsoon seasons. There is a need for understanding the runoff for realistic assessment and quantification of the surface and groundwater. The complexity of the aquifers and subsurface can mislead to propose improper recharge structures (Todd & Mays 2005).

Community participation should be encouraged to plan, implement, and maintain public resources to improve the situation. Attention should also be given to combat the drinking water problem in rural areas by taking mitigative measures such as artificial groundwater recharge.

The groundwater recharge estimation can be classified as direct recharge (diffuse from recharge structures) and indirect recharge (from rivers and channels) depending upon the percolation of the surface water into groundwater.

Artificial Recharge is a means of infiltrating the surface runoff artificially into aquifers. In this regard, the selection of suitable methods and sites for groundwater recharge requires a detailed study. The need for water management and construction of small water harvesting structures is imminent and is gaining many scopes nowadays (Kumar & Rameshwar 2008). Thus, the present study aims to study the groundwater recharge potential of the study area and identify the sites for Artificial Recharge Structures that are location-specific and are suggested based on the application of multi-disciplinary fields like Geo-physics, RS, and GIS. The relationship between GIS and artificial recharge structures can be found in various literature (Shankar & Mohan 2005; Patil & Mohite 2014; Selvam et al. 2017).

6.2 Objectives of the study

The proposed work includes a detailed study of the hydrogeological and geophysical characters of the aquifers in the study area. The data generated helps

1. To study the groundwater recharge potentiality in the study area.
2. For selecting the suitable methods for groundwater recharge.
3. To identify the sites for Artificial Recharge Structures using site specific approach.
4. To study the groundwater budget of the study area.
5. To assess the aquifer parameter and to know the groundwater status of the area.
6. To draft proper and effective water management plans.

6.2.1 Geology

Laterites are highly porous and permeable. The aquifers in the area get fairly recharged during the rainy season, but since laterites are highly permeable, base flow is high, and hence the groundwater gets discharged gradually to the sea. The granitic gneisses, although impervious, have secondary porosity due to fractures and joints. These are occasionally intruded by dolerite dykes, which sometimes act as barriers to the groundwater flow. A

thin layer of lithomargic clay exists between laterite and granitic gneiss. Towards the coast, a small patch of alluvium consisting of sand, silt, and clay is present, which has high porosity but tapping water from this formation may yield saline water or aid in the saltwater intrusion. More detailed geology of the study area is explained in chapter 3, “Geology and Geomorphology”.

6.2.2 Groundwater Recharge Potential zones (GRPZ)

A total of 9 thematic layers like groundwater potential zones, geomorphology, land use/land cover (lu/lc), depth to bedrock, lineament density, groundwater fluctuation, slope (percentage), drainage order, and soil depth are used for integration and resultant GRPZ. This methodology is similar to the preparation of groundwater potential zones (chapter 4, “groundwater exploration studies”). But in this case, the theme weights and class ranks are given priority based on the Recharge potential. The GRPZ thematic layer is then overlaid by drainage and waterbodies thematic layer to propose the site suitability for ARS. Different artificial recharge structures can be proposed based on location, terrain conditions, hydrological and hydrogeological characteristics.

The present work attempts to establish the relation between the Electrical Resistivity method and RS &GIS-based methodology for groundwater recharge potential zone mapping in the Gurpur watershed of coastal Karnataka, India. Understanding geological, structural, geomorphological characteristics and their relationship with groundwater is necessary as it is the base for assigning ranks and weights. 13 thematic layers are used for integration purposes. (Venkateswara Rao & Briz-Kishore 1991) suggested that sum of the product of normalized weights (subscript w) of the thematic layers with their respective ranks (subscript r) of the classes forms the Groundwater Recharge Potential Index as given in the equation below;

$$\begin{aligned} \text{GRPI} = & [(GWPZ_w) * (GWPZ_r)] + [(GWC_w) * (GWC_r)] \\ & + [(LULC_w) * (LULC_r)] + (DO_w) * (DO_r) + [(SI_w) * (SI_r)] + [(Gm_w) * (Gm_r)] \\ & + [(SD_w) * (SD_r)] + [(DBR_w) * (DBR_r)] + [(LD_w) * (LD_r)] \end{aligned} \quad \text{(equation 6.1)}$$

Where, GWPZ-Groundwater Potential Zones, GWC-Groundwater contours, LULC-Land Use & Land Cover, DO-Drainage Order, SI-Slope, Gm-Geomorphology, SD-Soil depth, DBR-Depth to bedrock, LD-Lineament density.

The suitability analysis like WOI is used for vector integration of all the thematic layers into a single GRPZ map. The weights for different themes are assigned based on their influence over the groundwater potential. The merit and demerit of the features and their influence over groundwater occurrence are exactly the points of consideration for assigning suitable weights (Jaiswal et al. 2003). The final map is obtained by multiplying individual ranks of the thematic layers with the weightage assigned. The resultant map shows the groundwater recharge potential zones. The thematic layers used in integration are explained below in detail.

6.2.2.1 Groundwater Potential Zones (GWPZ)

Groundwater potential zonation means using the surface and sub-surface indicative parameters either by direct or indirect scientific methods for determining the potentiality of the groundwater zones in an area by quantitative and qualitative assessment. The surface features or parameters can be easily accessible through remote sensing and field verification. In contrast, the sub-surface parameters are possible through OB wells, ER methods, and direct observations in the possible exposures. GWPZ provides information on the best possible locations for groundwater tapping. If the GW potentiality is very high, then the possibility of recharge can also be very high. This shows the direct relationship between the two thematic layers. Therefore, a weightage of 20 is given for this thematic layer. The ranking of 5 is given to the “very high” category of groundwater potential zones. A ranking of 1 is given to the “very low” category of GWPZ.

6.2.2.2 Geomorphology

The geomorphology maps and data are collected from KSRSAC. A detailed explanation of geomorphology can be seen in chapter 3, “Geology and Geomorphology”. Geomorphology

plays an important role in GRPZ. Thus the weightage of 15 is given to this thematic layer. The features like alluvial plain and coastal plain are given a high ranking of 5 because the velocity of the water flow is greatly reduced due to plain land, which increases the recharge potential. The built-up land does not directly contribute to the recharge. But nowadays, rooftop rainwater harvesting is increasingly adopted for every house. So, either the rainwater can be stored or recharged to the nearest open wells or the bore wells. Therefore, in this study, the built-up area is given a ranking of 3. The water bodies are given the rank of 5 as they store and serve the purpose of recharge.

6.2.2.3 Land use/land cover

The detailed explanation of lu/lc can be seen in chapter 3, “Geology and Geomorphology”. The land use/land cover analysis is essential to know the spatial distribution of land resources and their influence on recharge potential. Agricultural land, forest land, and forest plantation are given the high rank of 5 and 4, respectively. The recharge is high in agricultural lands because of regular irrigation practices round the year. The forest land tends to recharge the groundwater naturally, and forest plantations are planted to reduce surface runoff to maximize recharge.

6.2.2.4 Depth to bedrock or weathered zone

The VES employing the Schlumberger method is used in the present study. About 35 Soundings have been conducted within the study area. This is utilized to get apparent resistivity data. The detailed methodology for electrical resistivity method, VES configurations, Inverse Slope Method is given in chapter 4, “groundwater exploration studies”. The categories with high depth to bedrock are given 5 because the higher the weathered zone thickness, the greater the recharge potential. This thematic layer shows a direct relationship with groundwater recharge potential.

6.2.2.5 Lineament density

Generally, lineaments are associated with the geodynamics and structural geology of the area. Therefore the continuous activity of building and breaking apart of the earth's crust leads to different types of folds, faults, joints, and unconformities. These geological features, which form linear or nearly linear features on the surface, are called lineament. A detailed explanation of LD can be seen in chapter 4, "groundwater exploration studies". The high lineament density indicates the high intensity of weathering and, therefore, the possibility of maximum effective porosity and permeability of the aquifers. Hence, lineament density and groundwater potential have a direct relationship (Hardcastle et al. 1995). Therefore, ranking of 2 and 4 are given to low and high lineament density classes, respectively. The LD is classified into 3 classes viz., Good (153.92 km²), Moderate (411.49 km²), and Low (312.33 km²).

6.2.2.6 Ground Water Fluctuation (GWF)

The GWF thematic layer for the Gurpur catchment is prepared using the observatory wells data and the water level data collected during field visits for pre-monsoon, monsoon, and post-monsoon seasons. The available OB wells data obtained from IMD is used in the study. The data is available in Microsoft excel comma-separated value format. This attribute data is converted into point shapefiles in the GIS platform. The average of 20 years of groundwater level data (from 1998 to 2018) is considered for Pre-Monsoon (January-May), Monsoon (June-August), and Post-Monsoon (September-December). The lowest groundwater level (GWL) is recorded as 1.22 mbgl in Ullala-A OB well during the 2006 post-monsoon season. The highest GWL, 11.7 mbgl is recorded in Bantwal during the 2007 pre-monsoon period. And finally, the GW fluctuation is prepared using the IDW method in the spatial analyst tools.

The Groundwater fluctuation is divided into 5 classes from "very low" to "very high". The GWF thematic layer plays an important role in demarcating recharge potential zones. The high fluctuation of GWL indicates a higher possibility of recharge capacity as well as groundwater storage. Therefore ranking of 5 is given for high GWF, and a ranking

of 2 is given for low fluctuation of GWL. From Figure 6.3, it is observed that most of the midland region is coming under the “high” and “very high” GWF categories. Therefore, the midland region should be given high priority for recharging the GW through artificial recharge structures. The subsurface water flow is towards the low land region where built-up land is high. Here the rainwater harvesting structures could be used effectively.

6.2.2.7 Slope

A slope is a slanting surface at an angle of less than 90° to a flat surface. A major portion of the earth's surface consists of the slope. Based on the All India Soil and Land Use Survey guidelines, the slope categories are prepared. The slope exhibits an inverse relationship with the recharge potential, i.e., the lesser slope means the lesser intensity of runoff, therefore, more time for infiltration. Thus the ranking of 5 is given to slope categories that are under 0 – 5 slope percentage. The ranking of 2 is given to the high slope category.

6.2.2.8 Drainage order and water bodies

The drainage network line features are prepared using DEM data in ArcMap and then converted into shapefiles. The detailed procedure for preparing drainage order thematic is given in chapter 3, “Geology and Geomorphology”. The study area consists of 7th order stream. This thematic layer is converted to polygon features using a 1m buffer for all the line features so that the drainage orders thematic layer can be used for integration. This is one of the important thematic layers which possess information about the possible recharge sites. The drainages up to 3rd order are spatial distributed and more in number, suitable for effective recharge. Therefore ranking of 5 is given to the drainages up to 3rd order. Also, these drainage orders are at a higher elevation, and so the groundwater flow is towards the higher order drainages. Though the 6th and 7th drainage orders could have a high volume of water, their spatial distribution is limited. Therefore they are assigned the ranking of 4, as they still hold good recharge capacity.

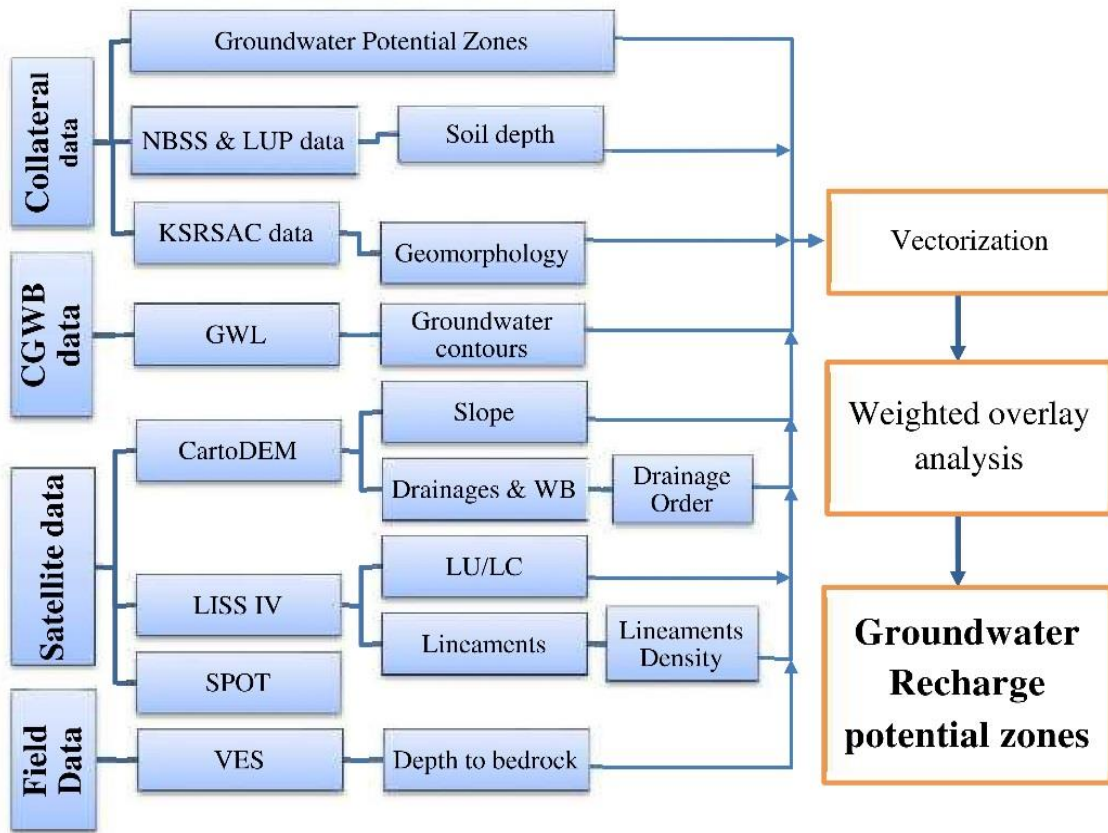


Figure 6.1 Flow chart for groundwater recharge potential zones mapping.

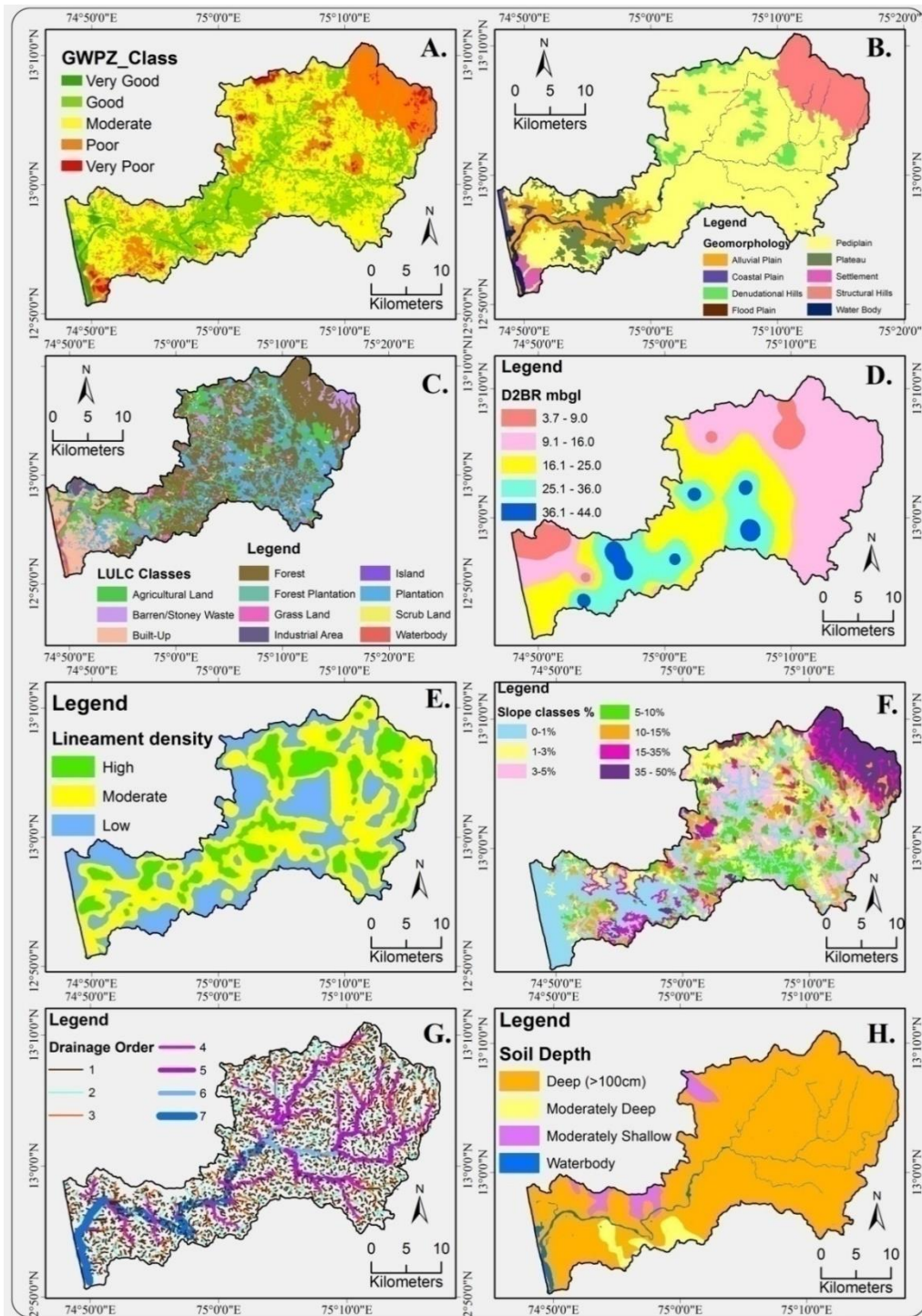


Figure 6.2 Thematic layers used in integration of GRPZ.

6.2.2.9 Soil Depth Map

A soil depth map of the study area, available as authentic data from NBSS/LUP, is used. It is georeferenced, vectorized, and provided attribute data in the ArcGIS environment. The study area possesses mostly the “deep” soil depth category, which almost covers 90% of the study area. A ranking of 4 is given for the deep soil depth class, and for waterbodies ranking of 5 is given. The soil depth thematic layer possesses a direct relationship with the recharge potentiality.

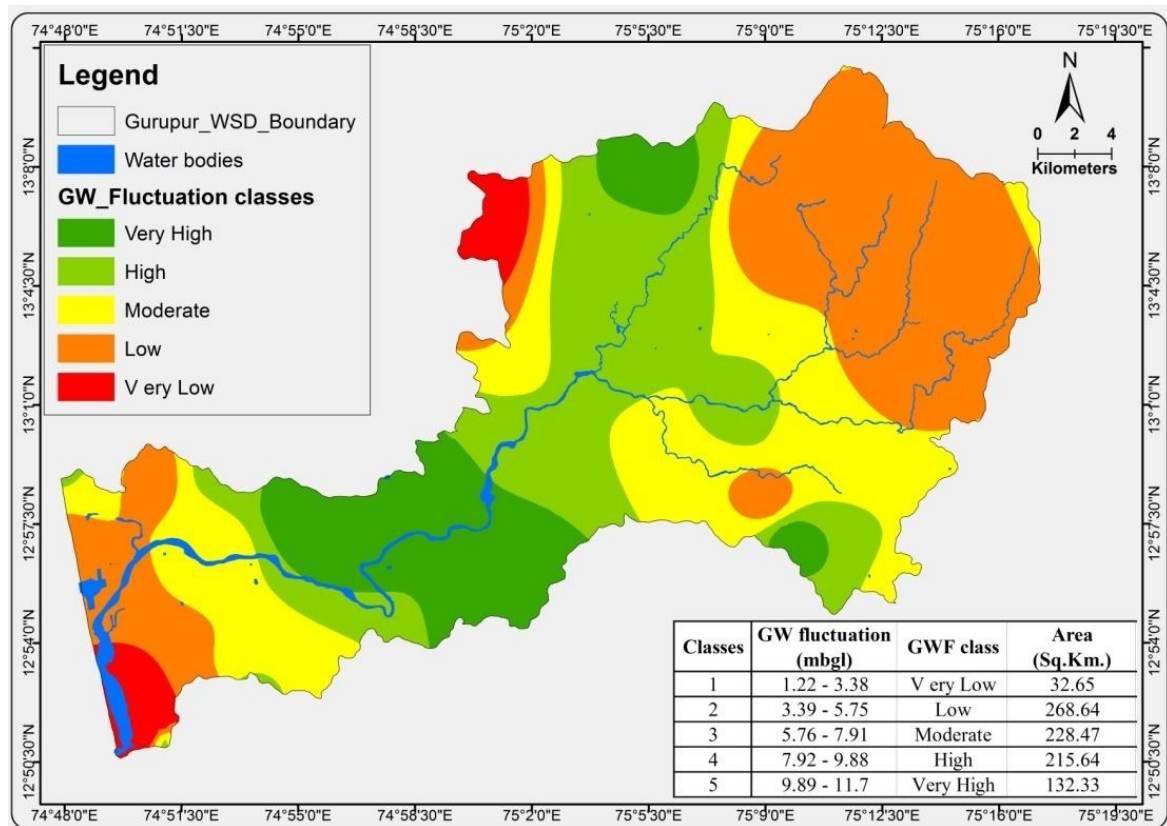


Figure 6.3 Groundwater fluctuation map (average for 20 years 1998-2018)

6.2.2.10 Groundwater recharge potential zones

The thematic layers like groundwater potential zones, geomorphology, lu/lc, depth to bedrock, lineament density, groundwater fluctuation, slope, drainage order, and soil depth are used to integrate and prepare GRPZ. The theme weights and class ranks are given priority based on the relationship of the individual thematic layers with respect to Recharge

potential. The results obtained indicate that about 27% of the study area is categorized under “high” and “very high” categories. The moderate category of GRPZ constitutes 32% of the study area. About 41% of the area is considered under “low” and “very low” categories. Based on these results, the site suitability of artificial recharge structures and conservation methods are proposed. The GRPZ with “very high” and “high” categories, which come in midlands, are prioritized. Because the GWF Figure 6.3 in midlands is very high, the construction of ARS is highly recommended. The ARS, like check dams, percolation ponds, farm ponds, could be constructed in these locations for better results.

Table 6.1 GRPZ weightage assignment and recharge ratio factors.

Sl. No	Thematic Layer	Classes	Area (Km ²)	Rank (Y)	Weights (X)	A = (X*Y)	B = $\sum(X*Y)$	Recharge Ratio %
1	GWPZ	Very Good	21.02	5	20	100	300	14.76
		Good	231.35	4		80		
		Moderate	420.76	3		60		
		Poor	185.05	2		40		
		Very Poor	19.56	1		20		
2	Geo-morphology	Alluvial plain	63.95	5	15	75	480	23.61
		Coastal plain	6.6	5		75		
		Flood plain	0.75	5		75		
		Waterbody	22.63	5		75		
		Denudational hill	43.14	2		30		
		Pediplain	579.79	4		60		
		Plateau	45.65	1		15		
		Settlement	10.06	3		45		
		Structural hills	105.17	2		30		
3	LULC	Agricultural land	147.98	5	15	75	450	22.13
		Forest land	286.32	4		60		
		Forest plantation	182.32	4		60		
		Grassland	45.66	3		45		
		Industrial area	13.37	1		15		
		River island	0.75	1		15		
		Built-Up area	161.36	3		45		
		Wasteland	13.19	4		60		
		Waterbody	26.76	5		75		
4	Depth to bedrock	Low	165.45	2	14	28	140	6.89
		Moderate	570.18	3		42		
		High	142.11	5		70		
5	Lineament Density	Low	312.33	2	11	22	99	4.87
		Moderate	411.49	3		33		
		High	153.92	4		44		
6	GW Fluctuation	Very Low	32.65	2	9	18	153	7.53
		Low	368.64	3		27		
		Moderate	228.47	3		27		

Chapter 6 - Groundwater Recharge

		High	215.64	4		36		
		Vey High	132.33	5		45		
7	Slope (%)	000-001	262.32	5	8	40	224	11.02
		000-003	122.53	5		40		
		003-005	144.33	5		40		
		005-010	106.35	4		32		
		010-015	87.12	4		32		
		015-035	71.02	3		24		
		035-050	84.07	2		16		
8	Drainage order	1st order	222.56	5	5	25	145	7.13
		2nd order	314.93	5		25		
		3rd order	235.94	5		25		
		4th order	74.68	3		15		
		5th order	29.26	3		15		
		6th order	74.68	4		20		
		7th order	29.26	4		20		
9	Soil Depth	Moderately Shallow (50 - 75 cm)	34.718	2	3	6	42	2.07
		Moderately Deep (75 - 100 cm)	31.347	3		9		
		Deep (>100cm)	788.39	4		12		
		Waterbody	23.282	5		15		
Total					100	ΣB = 2033.00	100.00	

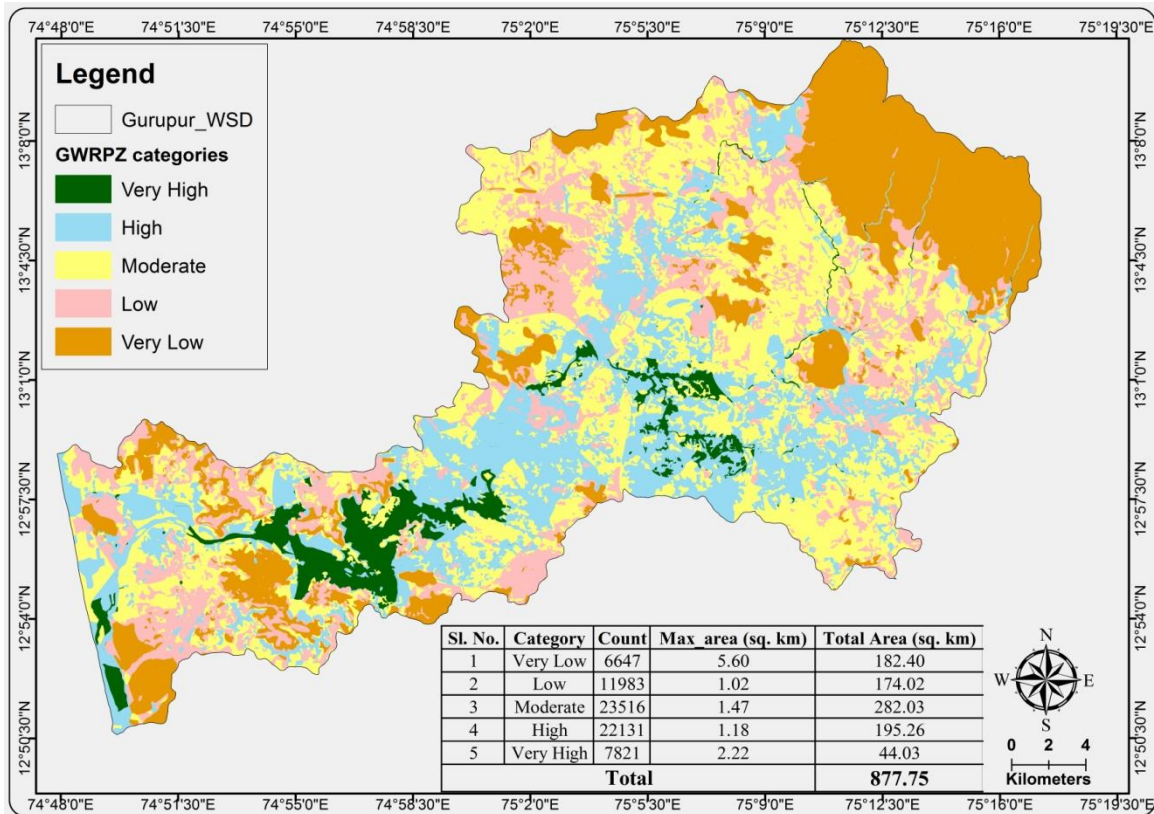


Figure 6.4 Groundwater recharge potential zones of Gurpur watershed.

6.2.3 Artificial recharge structures

Artificial recharge may be defined as the process of augmenting natural aquifers by artificial means. There are many methods of recharging groundwater viz., recharge wells, percolation tanks, sub-surface dams, check dams/vented dams, irrigation practices. Only sub-surface dams, check dams / vented dams are ideal methods in the study area. In addition to those, the water harvesting methods like roof-top rainwater harvesting, micro watershed practices may also directly or indirectly help in improving the groundwater levels.

Depending upon the hydrogeological framework, there are different types of artificial recharge techniques. The following are the broad classification of the artificial recharge techniques,

I. Direct Methods

A). Surface Spreading Techniques

- a. Flooding
- b. Ditch and Furrows
- c. Recharge Basins
- d. Runoff Conservation Structures
 - i. Bench Terracing
 - ii. Contour Bunds and Contour Trenches
 - iii. Gully Plugs, *Nalah* Bunds, Check Dams
 - iv. Percolation Ponds
- e. Stream Modification/Augmentation

B). Sub-surface Techniques

- a. Injection Wells (Recharge Wells)
- b. Gravity Head Recharge Wells
- c. Recharge Pits and Shafts

II. Indirect Methods

- A). Induced Recharge from Surface Water Sources;
- B). Aquifer Modification
 - a. Bore Blasting.
 - b. Hydro-fracturing.

III. Combination Methods

In addition to the above, groundwater recharge structures like Subsurface dykes (*Bandharas*) and Fracture Sealing Cementation techniques are also used to arrest subsurface flows.

6.2.3.1 Water conservation methods

In addition to artificial recharge of groundwater, the water conservation/water harvesting (WH) methods play a vital role in meeting the necessary water demand. There are three main categories of WH techniques that have been devised and perfected over the years. Each category has its subset of methods and techniques employed to get the maximum amount of benefit from each water source, be it floods water, rainfall or groundwater. The following are some water conservation methods that can be implemented to meet the water supply demand.

- I. Watershed Development
 - a) Contour bunding
 - b) Counter trenching
 - c) Land terracing
 - d) Gully plugging
 - e) Afforestation
 - f) Localized water conservation
- II. Adopting Modern Irrigation Practices
 - a) Drip irrigation
 - b) Sprinkler irrigation
 - c) Pot irrigation
 - d) Selection of water use efficiency crops
- III. Rooftop rainwater harvesting

Besides, there are some other methods of water conservation viz.,

- Conjunctive use
- Recycling of water
- Reducing water evaporation
- Educating people to avoid wastage of water through media, TV, NGOs.

Nowadays, Roof-top rainwater harvesting structures are being built widely in many places and supported by the state and central government to conserve the rainwater.

6.2.4 Site specific approach for proposing ARS

The spatial and thematic information generated like slope, soil type & depth, geomorphology, lithology, drainage density, lu/lc, GWPZ should have to be properly understood to know the effects of those thematic layers over the groundwater recharge. Then the integrated theme is overlaid by drainage and water bodies for site selection of ARS. Based on the terrain conditions, hydrological and hydrogeological characteristics, different artificial recharge structures can be proposed. Therefore, a detailed study on site-specific recharge structures and ideal water conservation techniques are discussed.

There are many site-specific artificial recharge methods available, which mostly depend on the lu/lc, geomorphology, soil depth, drainage order, lineament density, depth to bedrock (thickness of weathered zone), slope, and groundwater level of the area. Also, a new thematic layer is generated, i.e., groundwater potential zones resulting from the major and minor effects of all the above-mentioned thematic layers and others over groundwater

potentiality. Finally, a criterion is prepared using all the above-mentioned thematic layers to select the site specific recharge methods for groundwater recharge. Based on these criteria, it was found that the following recharge methods are ideal in the study area: The construction of check dams / vented dams, nala bunds, percolation tanks, farm ponds, contour trenching, subsurface dams, and using the available dug wells/bore wells, for recharging.

Water harvesting structures like reservoirs and tanks are silting up quickly due to accelerated topsoil erosion (adverse effects of deforestation, urbanization). The increasing number of bore wells and over-tapping of groundwater have caused a rapid decrease in the groundwater table. The combination of artificial recharge (groundwater) and rainwater harvesting (surface storage) is the only possible economic means of overcoming the existing water problems.

Artificial recharge techniques have been successfully implemented in sedimentary terrains with large aquifers. Such practices are rare in hard rock aquifers such as those prevalent in peninsular India, consisting of many arid and semiarid zones. Artificial recharge practices in granitic or hard rock terrain are prevalent from ancient times. The artificial recharge through percolation tanks/bunds is expected to reduce the evaporation losses.

The construction of subsurface dyke, a relatively recent concept in artificial recharge, has proved its efficacy in many locations in the hard rock terrain of India and is being practiced not only by governmental agencies but even by private agencies and landowners. Following are few important artificial recharge structures as well as water conservation techniques proposed for the study area.

6.2.4.1 Check dams

A check dam is a small barrier constructed across the flow direction of streams to recharge the groundwater. The restoration of low foot-print runoff harvesting vegetation on the hill slopes strengthens the source-sink relations and increases the streams' runoff (Stavi et al. 2020). The check dams could be constructed for storing and using the surface runoff for

irrigation, for reducing soil erosion, for sediment capture, for promoting surface vegetation and soil humidity. The harvested water could also be used for domestic and livestock needs. The check dams are economical and easy to install structures which are very effective in groundwater recharge. The check dams are proposed based on the site suitability approach in the Gurple watershed. The GRPZ thematic layer is also considered for prioritizing the proposed check dam sites. The details of the criteria used for proposed check dam sites are provided in Table 6.2.

6.2.4.2 Nala bunds

Nala bunds are constructed to arrest the velocity of the streams and increase the possibility of infiltration of the water. Nala bunds are also constructed to reduce soil erosion and reduce silting of artificial recharge structures. Due to the primary porosity of the lateritic rocks, the recharge to groundwater aquifers is significant. However, in hard rock stream beds, secondary porosity is less, and so is the percolation. Therefore, if these bunds are located adjacent to some marked discontinuities/lineaments/fractures, the recharge to deeper groundwater bodies may be quite significant even if the recharge occurs for a brief time.

6.2.4.3 Percolation tank

The percolation tanks are the small tanks constructed across the stream flow. These are mostly the spillway type of structures. The percolation tanks are most effective if associated with highly weathered and fractured zones. Therefore greater the lineament (fractures) density, the greater is the recharge through percolation tanks. These structures are best suitable for high slope regions with streams of 2nd to 4th order. Soil erosion is one of the major drawbacks of the construction of percolation tanks. The silt collected hinders the groundwater recharge and also leads to regenerated surface flow. Therefore the proposed percolation tanks should be closely associated with nala bunds. Most of the eroded soil and silt is trapped by nala bunds before entering the percolation tanks.

6.2.4.4 Farm pond

The farm ponds intend to recharge the nearby wells along with irrigation, cattle rearing purposes, etc. The farm pond can be of different sizes depending upon the space available and surface runoff. They can store the water for some time and can slowly recharge the groundwater. With proper maintenance and de-silting, these ponds can recharge a huge volume of groundwater. The farm ponds are usually associated with 1st or 2nd order drainages; therefore, they can be more in number and spatially distributed. The farm ponds associated with high lineament density can accelerate the process of recharge.

6.2.4.5 Contour trenching

The contour trenching is done to arrest the immediate flow of surface water downhill. Usually, these are suggested for greater slope areas, i.e., hilly terrains. The parallel trenches in the hilly regions along the regular elevation intervals reduce the water flow and store the water for some time, which serves the groundwater recharge. Therefore the vegetation downhill to those trenches can utilize the water in the form of soil moisture.

6.2.4.6 Rainwater harvesting

The demand for freshwater is increasing rapidly due to population growth, contamination, little availability of groundwater. Therefore, harvesting the surface water, especially rainwater (superior quality), properly and efficiently is highly suggested (Baby et al. 2019). The physical and chemical properties of rainwater are superior in quality to the surface runoff and groundwater, which are prone to contamination due to various reasons. It is documented that RWH was practiced by ancient Romans and Greeks (Phoca & Valavanis 1999). And Nowadays, the popularity and necessity of RWH have grown exponentially (Zhang et al. 2009).

Table 6.2 Site specific approach for selection of artificial recharge structures.

Sl. No	Recommendation	GWPZ	GW level (mbgl)	LULC	Drainage order	Slope	Geomorphology	Soil Depth	D2BR (m)	Lineament density
01	Check Dam	Very Poor - Moderate	7.9 - 15.8	Agricultural land Forest land Grassland Wasteland	2nd - 4th	0-15	Denudational hill Structural hills Pediplain	moderately shallow moderately deep deep	9-44	Moderate-High
02	Nala bunds	Very Poor - Moderate	4.9 - 7.8	Agricultural land Forest land Grassland Wasteland	1st - 2nd	15-50	Denudational hill Structural hills	deep	3.7 - 9	Moderate-High
03	Farm pond	Very Good - Poor	4.9 - 7.8	Agricultural land Forest land Grassland River Island	1st - 2nd	0 - 5	Alluvial plain Coastal plain Flood plain Pediplain Plateau	moderately shallow moderately deep deep	3.7 - 44	Low - Moderate
04	Contour Trenching	Very Good - Moderate	4.9 - 7.8	Agricultural land Forest land Grassland Wasteland	1st - 2nd	15-50	Denudational hill Structural hills	moderately shallow moderately deep deep	3.7 - 44	Low - Moderate
05	Percolation tank	Very Poor - Moderate	7.9 - 15.8	Wasteland Forest land Grassland	2nd - 4th	0 - 5	Alluvial plain Coastal plain Flood plain Pediplain	moderately deep deep deep	9 - 44	Low

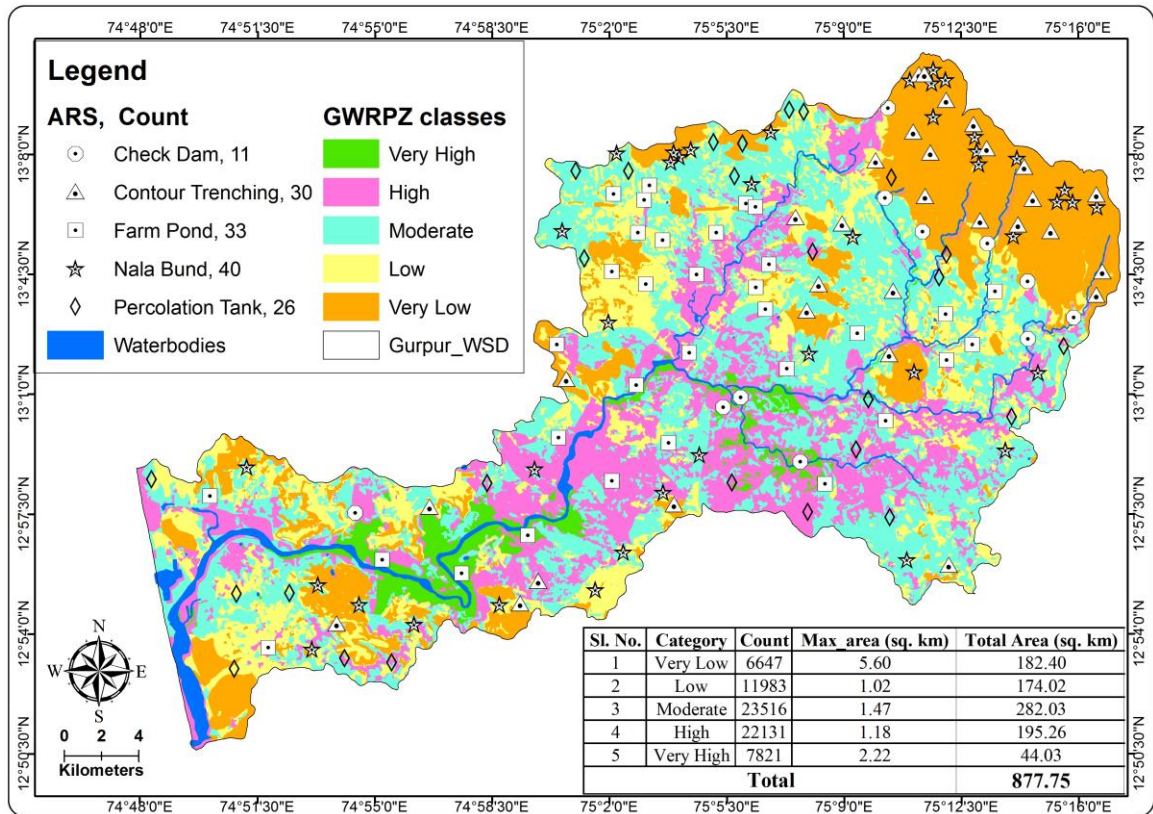


Figure 6.5 Proposed artificial recharge structures using GRPZ and site specific approach.

The rainwater can be collected on the ground and from roof surfaces. The rainwater could be directly used for drinking, and domestic purposes, provided proper mechanisms and filters are used. Once the rainwater falls on the ground and generates runoff, many considerations are to be made concerning the water quality. The parameters like organic matter & micro-organisms, fertilizers & pesticides, suspended minerals, acidity, etc., are considered. Therefore importance is given to rainwater harvesting with different screening and purification systems to store the water with superior quality.

The study area covers 161.37 km² of built-up (about 18%) area and experiences a very high precipitation intensity during monsoon. Therefore almost 600 million cubic meters (MCM) / year of rainfall could be encountered and collected if the rooftops are utilized one hundred percent. Also, if the storage capacity is exceeded, then the rainwater could be diverted to recharge the nearest dug wells/bore wells. This could replenish the shallow as well as the deeper aquifers.

6.2.4.7 Dug well / bore well recharge

The bore wells and dug wells are the primary water source for suburban and rural locations, where the government could not deliver surface water. The water table is lowering significantly every year due to the tapping of deeper aquifers through bore wells or tube wells. Therefore these aquifers need to be recharged during the rainy season. The rainwater and surface runoff could be diverted to recharge the nearest bore wells, which in turn replenish the deeper aquifers.

6.2.4.8 Quarry reservoirs

Laterite quarrying is one of the important mining activities in the study area. Most of the time, these quarries would cut the hilly terrains into flatlands. But the abandoned quarries could be used to store diverted water and eventually lead to groundwater recharge.

6.2.4.9 Subsurface dams / dykes

The subsurface dams are the barriers constructed to arrest the base flow. Generally, they are constructed at locations where the depth to bedrock is least. The reason for constructing these structures is to effectively arrest the groundwater flow on the downstream side and minimize the construction cost. The selection of such sites with the help of modern technology like remote sensing and GIS is the need of the hour. These methods help to bring out the geological and structural features in the area selected for artificial recharge.

6.2.4.10 Park recharge structures

The parks in the city corporation limits, institutes/organizations, agglomerates of apartments, or mansions and bungalows could be effectively used to divert the surface runoff for recharging the groundwater. If a large area is available in the park, then the basins (ponds/tanks) can be excavated, recharging and improving the park's aesthetic view. If the area available is less, then the dug well/bore well or recharge shafts can be used for recharging groundwater. The pits and trenches can be constructed along the borders of the park for accommodating infiltration. Also, the storage tank structures can be constructed within the park, which may be used for storing the rainwater harvested from nearby

rooftops. Therefore, these park structures could reduce urban flooding and divert the water for recharge.

6.2.4.11 Injection wells

The injection wells (also known as recharge wells) are the shafts/wells which directly allow the surface water to flow into groundwater aquifers. These are the only means of recharge, where the soil permeability is very less. Also, injection wells are widely used for controlling saltwater intrusion in coastal areas. The quality of the injected water is very important as it filters through the soil naturally during recharge. The suspended solids, clay content, organic and chemical impurities affect the efficiency and utilization of the aquifer. The water temperature used for recharge through injection wells is also a point of concern because the solubility of air increases with temperature decreases. Therefore, if the surface water at 10°C is injected into an aquifer with 20°C of temperature, it releases the saturated air into the aquifer. While some air escapes, most of it settles in the pore spaces, becoming tiny bubbles. This could seriously reduce the aquifer capacity. On the contrary, if the groundwater temperature is lower than the surface water, the saturated air in the groundwater is released. Therefore proper temperature is required for recharge through injection wells (USDA & NRCS 2010).

6.2.4.12 Soil Aquifer Treatment (SAT)

The treated water generated by the Sewage treatment plant (STP) could be used for domestic uses, irrigation, and as well as for recharging the groundwater. The usage of sewage-treated water slightly reduces the water demand, as this water can be available throughout the year. Wastewater reclamation is the most effective strategy in Water Ecosystem Impact reduction (Xiong et al. 2020). For recharging the treated water, first, quality analysis is to be done, especially for heavy metals, as they tend to pollute the aquifers in the long run. Then the SAT can be implemented by excavating infiltration ponds for the removal of nutrients and pathogens. The proof-of-concept experiments had shown that under normal recharge conditions, some of the pharmaceuticals, pathogens, and other organic wastewater compounds would prevail in the treated effluent after SAT (Cordy et

al. 2004). The soil adsorption capacity is finite, and considering the long-term SAT, the aquifers eventually become polluted (Vengosh & Keren 1996). Therefore proper planning and treatment should be conducted before the SAT because, in long term scenario, even the treated water could pollute the groundwater resources.

6.2.5 Recharge estimation methods

Recharge is defined as the water percolated to the groundwater body. But in recharge from rivers, it is considered the transmission loss (water that leaves the river downwards). The perched aquifers, evapotranspiration, water stored in unsaturated zones could make a huge difference between recharge and transmission loss (Hughes & Sami 1992). The recharge estimation methods are classified into five categories according to (Lerner et al. 1990), which are direct measurement, correlation methods, tracer techniques, Darcian approaches, and water balance methods. The direct measurements use lysimeters to measure percolation in open waters, whereas the correlation methods relate the recharge to easily accessible data like groundwater level fluctuation or river discharge. The groundwater response function yields similar results as in-unit hydrograph and could be a good example for the correlation method (Besbes et al. 1978). The estimation of recharge from precipitation has wide applicability of the tracer techniques (Sukhija et al. 1996). The Darcian methods include field data like hydraulic properties, flow net, infiltration equations, etc., but it is not easy to gather enough data to model reality. The water balance methods could use aquifer modelling, watershed modelling, watertable fluctuation to estimate the recharge. In the present study, few of the methods or approaches are used to estimate the groundwater recharge.

6.2.5.1 Groundwater recharge ratio

The recharge rate in the watershed can be found using the average of 20 years (from 1998 to 2018) rainfall is considered in Table 6.3. The details like coordinates of the rain gauge stations (RGS), RGS names, and rainfall statistics are given (Table 6.3).

Table 6.3 Rainfall statistics for 20 years from 1998 – 2018 for 12 rain gauging stations

Sl. No.	RGS	Elevation (m)	Longitude (Decimal degrees)	Latitude (Decimal degrees)	Avg. RF distribution (mm/year)	Min (mm)	Max (mm)
1	bajpe	101	74.883333	12.916667	3434.58	2192.60	4384.90
2	gurupur	80	74.916667	12.916667	3428.81	2340.00	4503.00
3	kavalakatte	110	75.183333	12.95	3134.51	1988.20	4416.20
4	mangaluru DCO	12.8	74.833333	12.85	3283.53	2819.40	4543.10
5	mangaluru RS	8.84	74.833333	12.883333	3412.82	2887.70	4094.00
6	naravi	100	75.15	13.133333	5277.98	4380.80	6661.20
7	panambur	114	74.833333	12.883333	3356.06	2381.70	4713.30
8	Pudu	60.96	75.1	12.933333	3416.15	2626.80	4317.61
9	sangabettu	80	75.05	12.983333	3881.98	2867.20	4836.80
10	sulkeri	110	75.183333	13.066667	4969.99	3867.80	6240.80
11	ullala	15	75	13	3084.66	2281.20	4334.20
12	venoor	100	75.15	13	3924.54	3178.80	4886.60
Average					3717.13		

The GRPZ is prepared by integrating 9 thematic layers with respect to their thematic weights and individual theme's rank assessment. The product of average annual rainfall, with its corresponding area factor and the recharge factor, gives the recharge rate in the watershed (Selvam et al. 2014). Based on these results, the GRPZ is deciphered into 5 classes from "very high" to "very low". The estimation of recharged volume (W) is calculated using the formula

$$W = P \times R \times A \quad (\text{equation 6.2})$$

Where, W = Recharge water (mm / year); P = Average precipitation (mm / year); R = Recharge ratio; A = area (in percentage)

Table 6.4 calculation of recharge rate factors and statistics.

Sl. No.	Category	Count	Max Area (sq. km)	Total Area (sq. km)	Area (%)	Recharge ratio (RR)	(Area*RR)
1	Very Low	6647	5.60	182.40	0.21	0.275	0.057
2	Low	11983	1.02	174.02	0.20	0.325	0.064
3	Moderate	23516	1.47	282.03	0.32	0.375	0.121
4	High	22131	1.18	195.26	0.22	0.425	0.094
5	Very High	7821	2.22	44.03	0.05	0.475	0.024
Total				877.75	1.00	1.88	0.36

Therefore,

$$W = (3262.7 * 10^6) * ((0.275 * 0.21) + (0.325 * 0.20) + (0.375 * 0.32) + (0.425 * 0.22) + (0.475 * 0.05))$$

$$W = (3262.7 * 10^6) * (0.36)$$

$$W = 1174.57 * 10^6 \text{ m}^3/\text{year}$$

$$W = 1174.57 \text{ MCM}/\text{year}$$

Also, equation 6.2 can be used to estimate recharge rate in mm per year (or percentage) with respect to the unit of the average precipitation considered (Table 6.5), which is as follows:

$$W = 3717.13 * 0.36$$

$$W = 1339.82 \text{ mm} / \text{year}$$

The recharge rate of the Gurgur watershed is 1174.57 MCM/year, which covers 36% of the total average annual rainfall of 20 years from 1998 to 2018.

Table 6.5 The rainfall to recharge rate calculations with corresponding units.

Ppt. (mm/year)	Recharge factor	Recharge (mm/year)	Recharge (%)
3717.13	0.36	1339.82	36.04

The results obtained are then compared with the proposed standards adopted by (UN 1967). This methodology yielded 36% recharge of total precipitation occurred.

6.2.5.2 Validation of the results

The groundwater recharge estimation can be classified as direct recharge (diffuse from recharge structures) and indirect recharge (from rivers and channels) depending upon the percolation of the surface water into groundwater. These methods are also used with different terminologies like localized or focused recharge (Lerner 1997) and also as direct (diffused) and localized (preferential flow) recharge estimation (Rushton 1997). The natural groundwater recharge can be estimated from several physical, geochemical, and inverse methods. The widely used empirical methods, rainfall infiltration method,

hydrodynamic method, and water balance method are employed to estimate groundwater recharge and validate the results.

6.2.5.3 The empirical relationships

The empirical relationships with the different aspects of recharge having physical meaning are considered in these methods. The relationships between precipitation and recharge are mainly considered because the runoff and recharge are closely associated with the amount and intensity of the rainfall. The natural groundwater recharge can be estimated using the following empirical formulae and guidelines (Groundwater Resource Estimation Committee 2009). Therefore the empirical relationships proposed (Bhattacharya et al. 1954; Rao 1970; Chaturvedi 1973; Sehgal 1973; Kumar & Seethapathi 2002) are used in this study to validate the results.

Chaturvedi in 1936 derived a relationship based on groundwater level and rainfall to estimate recharge in Ganga-Yamuna doab (Kumar 1996). The empirical relation is given by,

$$R_g = 2 * (P - 15)^{0.4} \quad \text{(equation 6.3)}$$

Where R_g is net recharge (in inches), and P is annual rainfall (in inches).

This formula helps understand the preliminary relationship between rainfall and recharge. Later this formula was updated in 1954 by U.P.I.R.I. as

$$R_g = 1.35 * (P - 14)^{0.5} \quad \text{(equation 6.4)}$$

Where R_g is net recharge (in inches), and P is annual rainfall (in inches).

The U.P.I.R.I formula was again updated as the Amritsar formula (Sehgal 1973). This formula is denoted by

$$R_g = 2.5 * (P - 16)^{0.5} \quad \text{(equation 6.5)}$$

Where R_g is net recharge (in inches), and P is annual rainfall (in inches).

Also, the relationships between rainfall and recharge for a particular climate and homogenous area were proposed by Krishna Rao in the 1970s (Kumar 1996). The Krishna Rao relationship was given by the following formula,

$$R_r = K * (P - X) \quad \text{(equation 6.6)}$$

Where R_r is groundwater recharge (mm), P is precipitation (mm), K is recharge coefficient, X is no. of point rainfall.

The following relations are suitable for different parts of Karnataka with different climatic conditions.

$$R_r = 0.20 * (P - 400) \text{ Where annual rainfall is between 400 to 600 mm}$$

$$R_r = 0.25 * (P - 400) \text{ Where annual rainfall is between 600 to 1000 mm}$$

$$R_r = 0.35 * (P - 600) \text{ Where annual rainfall is } >2000 \text{ mm}$$

Bhattacharya et al. (1954) also proposed the empirical relations for estimating recharge from rainfall alone.

$$R = 3.47 * (P - 38)^{0.4} \quad \text{(equation 6.7)}$$

Where R is groundwater recharge (inches), and P is precipitation (inches).

Later, Kumar & Seethapathi (2002) proposed a relationship for recharge estimation from rainfall in the upper Ganga canal command area (Kumar & Seethapathi 2002). This method considers the rainfall variability during the monsoon period.

$$R_g = 0.63 * (P - 15.28)^{0.76} \quad \text{(equation 6.8)}$$

Where R_g is groundwater recharge during monsoon (in inches) and P is mean rainfall in monsoon (in inches).

6.2.5.4 Rainfall Infiltration (RI) method

The Gurpur watershed is composed of hard rocks like granite and gneiss, which are highly impervious. Therefore, water can only be stored in cracks and fractures, creating secondary porosity (effective porosity). The storativity of these hard rock aquifers is mainly dependent on the weathering activity and associated lineaments. The relationships of recharge and rainfall in the rainfall infiltration method can be seen in the following formula,

$$\text{GWR} = A * \text{RFI} * P \quad (\text{equation 6.9})$$

Where GWR is the Groundwater Recharge, A is Area, RFI is the Rainfall infiltration factor, and P is the average annual rainfall.

For the Gurpur watershed:

$$\text{Area (A)} = 877.75 * 10^6 \text{ m}^2$$

Rainfall infiltration factor (RFI) = 0.005 which is 5.5% (Karanth 1994)

Average annual rainfall = 3.71713 m per year

Groundwater Recharge = 179.45 MCM per year

Therefore, the amount of groundwater recharge estimated using the rainfall infiltration method is 179.45 MCM for 20 years of average annual rainfall.

6.2.5.5 Hydrodynamic Method

The groundwater table fluctuation is the combined effect of many factors like infiltration, pumping/drafting, transmission losses, irrigation recharge, and groundwater withdrawal for irrigation. Therefore, the need for the network of representative OB wells, which gives practical and physical meaning to the groundwater level fluctuations in the field, is important. Based on the network of OB wells data, the quantitate changes in water level due to recharge or discharge could be measured (CBIP 1976; Adyalkar & Rao 1979).

The estimation of groundwater recharge using the hydrodynamic method is as follows,

$$\text{GWR} = \text{Area} * \text{Avg. Water level fluctuation} * \text{Specific Yield} \quad (\text{equation 6.10})$$

$$\text{Area (A)} = 877.75 * 10^6 \text{ m}^2$$

$$\text{Average GWF} = 6.64 \text{ m}$$

Specific yield = 0.2 is considered for the study area (Ministry of Water Resources & RDGR 2017)

$$\text{Groundwater Recharge} = 1165.65 \text{ MCM per year}$$

Therefore, the groundwater recharge estimated using the hydrodynamic method yielded the groundwater recharge of 1165.65 MCM for the average groundwater level fluctuation of 6.64m. This volume of groundwater is the dynamic portion of groundwater

that is practically available as a reserve. Also, the result obtained from the hydrodynamic method is yielding a similar result as that of the rainfall infiltration method. Also, the Groundwater Resource Estimation Methodology of the Ministry of water resources, GOI recommends that about 5% to 10 % of the total recharge could be lost as base flow discharge or evapotranspiration. Therefore, the average value mentioned earlier is considered in the study, i.e., 7.5%, which yields net GWR of 161.73 MCM per year.

6.2.5.6 Water table fluctuation method

The water table fluctuation method works under the assumption that the dynamic groundwater level is due to groundwater recharge alone, and then it moves to storage (Healy & Cook 2002).

$$q_w = S_y * \left(\frac{dh}{dt} \right) \quad \text{(equation 6.11)}$$

Where S_y is the Specific yield, h is the GW fluctuation, and t is the time.

$$\begin{aligned} \text{Therefore, the GWR} &= (0.2) * (6.64 / 1) \\ &= 1.328 \text{ m per year} \\ &= 1328 \text{ mm per year} \end{aligned}$$

The total dynamic GWR in the study area is estimated to be about 35.73% per year of the average annual rainfall for 20 years.

6.2.5.7 Water balance method

The mean temperature ($^{\circ}\text{C}$) is considered from the Panambur station within the study area. The mean temperature ($^{\circ}\text{C}$) for a monthly average of 30 years from 1981 to 2010 is considered and the average number of rainy days (IMD Bangalore).

The basic water balance equation considers the effects of rainfall, recharge, ET, and surface runoff. The water balance equation is as follows,

$$P = AET + Q + R_t \quad \text{(equation 6.12)}$$

Where P is the precipitation, AET is the actual evapotranspiration, Q is direct runoff, and Rt is total recharge (including base flow, soil moisture, and groundwater).

The soil water balance can be estimated using the Penman-Grindley method, similar to the water balance equation. But the only difference is that the PG method considers soil water storage (ΔS) instead of groundwater recharge. The equation for PG method (Penman 1950; Grindley 1967) for a uniform zone and certain time interval is as follows,

$$P = E_A + R + \Delta S \quad (\text{equation 6.13})$$

Where P is rainfall (in L), EA is actual ET (L), R is runoff (LL^{-2}), and ΔS is change in soil water storage. The Soil Moisture Deficit (SMD) is the total of Potential SMD and Groundwater recharge (ΔS).

Many researchers have worked on the SCS-CN method for estimating runoff (Nandagiri 2007; Suresh Babu & Mishra 2011; Soulis & Valiantzas 2012; Gundalia & Dholakia 2014; Mishra & Kansal 2014). The daily rainfall data of consecutive 5 years is averaged for all the rain gauge stations to get the mean daily rainfall. The 5 years mean daily rainfall is used to estimate the runoff and reduce possible errors due to various aspects. The runoff percentage estimated in the present study is 34.45% of the mean annual rainfall and is projected for the total annual mean rainfall of 30 years which yielded 1280.62 mm/year.

Evapotranspiration is also an important factor in the water balance equation. In coastal Karnataka, the average relative humidity (RH) is about 75.33% throughout the year. The RH increases up to 89% (July) during the monsoon season, which indicates the ET is an important factor of the water balance equation in the study area. In this present study, the AET is estimated using PET. The PET is estimated using one of the basic empirical equation by Thornthwaite (1948),

$$PET = 16 * \left(\frac{L}{12}\right) * \left(\frac{N}{30}\right) * \left(\frac{10 * T_d}{I}\right)^\alpha \quad (\text{equation 6.14})$$

Where PET is Potential ET, T_d is mean daily temperature, L is the average length of a day in a month (in hours), N is the number of days in a month and α is estimated to be 4.078 using the following equation,

$$\alpha = ((6.75 * 10^{-7}) * I^3) - ((7.71 * 10^{-5}) * I^2) + ((1.792 * 10^{-2}) * I) + 0.49239 \quad (\text{equation 6.15})$$

Where I is the Total heat index estimated to be 158.38 using the following equation,

$$I = \sum_{i=1}^{12} \left(\frac{Tm_i}{5} \right)^{1.514} \quad (\text{equation 6.16})$$

Where Tm_i is the monthly mean temperature of 12 months.

Therefore, the actual average evapotranspiration (AET) can be estimated using the following equation proposed by Chandrashekhar & Naganna (1979),

$$AET = \left(\frac{PET_{monthly}}{N} \right) * 2 * r \quad (\text{equation 6.17})$$

Where AET is actual ET, N is the number of days in the month, and r is the number of rainy days in the month.

The statistics of estimated PET, AET, and Climatological data are recorded in Table 6.6. The monthly mean of 30 years is used in the present study to estimate AET, and it was found to be 1224 mm/year (1.224 m³/year) which is 32.9% of the total precipitation.

Table 6.6 Climatological data for 30 years from 1981 to 2010

Sl. No.	Month	Avg. RH (%)	Mean Sunshine hrs. (L)	Temperature (°C)		T _d = Mean Temperature (°C)	mean monthly Rainfall (mm)	r = Mean monthly Rainy Days	Tot. Heat Index (equation 6.16)	PET (equation 6.14)	AET = ((PET/d)*2*r) (equation 6.17)
				Daily Min	Daily Max						
1	Jan	62	313	21	33.1	27.1	1.2	0.2	12.88	146.69	1.89
2	Feb	66	296	21.9	33.3	27.6	0	0	13.28	145.12	0.00
3	Mar	68	299	23.7	33.9	28.8	3.1	0.2	14.17	205.21	2.65
4	Apr	71	292	25	34.3	29.7	29.7	1.7	14.80	223.61	25.34
5	May	71	276	25	33.7	29.4	168.6	6.1	14.58	238.73	93.95
6	Jun	87	119	23.5	30	26.8	1079.6	23.9	12.67	158.26	252.16
7	Jul	89	94	23	28.7	25.9	1502	27.3	12.03	162.55	286.29
8	Aug	88	133	23	28.7	25.9	757.3	24.8	12.03	162.55	260.08
9	Sep	85	178	23.2	30	26.6	285.9	13.9	12.56	154.67	143.33
10	Oct	79	226	23.2	31.2	27.2	223.8	9.9	12.99	175.05	111.80
11	Nov	73	271	22.7	32.7	27.7	82.8	3.9	13.36	156.40	40.66
12	Dec	65	292	21.4	33.1	27.3	9.8	0.6	13.03	151.17	5.85
Annual		75.333	2789	23.1	31.9	27.5	3693.7	112.4	158.38	173.33	102

Table 6.7 The groundwater recharge estimated for 12 rain gauging stations (20 years data from 2008 to 2018) using empirical equations.

Sl. No.	RGS Name	Annual Rainfall	Chaturvedi	U.P.I.R.I	Bhattacharjee	Sehgal	Kumar & Seethapathi	Krishna Rao
		20 yrs avg.	Recharge (%)	Recharge (%)	Recharge (%)	Recharge (%)	Recharge (%)	Recharge (%)
1	Bajpe	3434.58	10.05	20.19	16.01	20.19	17.71	28.89
2	Gurupur	3428.81	10.05	20.20	16.02	20.20	17.72	28.88
3	Kavalakatte	3134.51	10.56	21.00	16.66	21.00	17.94	28.30
4	Mangaluru DCO	3283.53	10.30	20.58	16.33	20.58	17.83	28.60
5	Mangaluru RS	3412.82	10.08	20.24	16.06	20.24	17.73	28.85
6	Naravi	5277.98	7.90	16.66	13.02	16.66	16.52	31.02
7	Panambur	3356.06	10.17	20.39	16.17	20.39	17.77	28.74
8	Pudu	3416.15	10.08	20.23	16.05	20.23	17.73	28.85
9	Sangabettu	3881.98	9.39	19.13	15.14	19.13	17.39	29.59
10	Sulkeri	4969.99	8.17	17.13	13.42	17.13	16.69	30.77
11	Ullala	3084.66	10.65	21.14	16.77	21.14	17.98	28.19
12	Venoor	3924.54	9.33	19.04	15.06	19.04	17.36	29.65
Average		3717.13	9.73	19.66	15.56	19.66	17.53	29.19

The average total annual recharge (in inches) for 20 years from 1998 to 2018 is 26.96 inches. And the total recharge in percentage is about 18.56 %. Also, the groundwater recharge is estimated using few other methods. Therefore, the estimated GWR is considered an average of these methods.

Avg. of empirical methods = 18.56%

GWR using integration of thematic layers = 36.04%

GWR using water balance equation = 32.65%

GWR using water table fluctuation method = 31.36

Average GWR = $(18.56 + 36.04 + 32.65 + 31.36)/4$

Average GWR = 29.65% which is 1102.1 mm/year

Therefore, the percentage of error can be calculated from equation 6.18, and the formula for error percentage calculation is as follows,

$$Error (\%) = \frac{(A - B)}{(A + B)} * 100 \quad \text{(equation 6.18)}$$

Where, A is precipitation (3717.13 mm/year) and B = Q+AET+R (3606.72 mm/year) for the water balance equation (equation 6.12).

$$Error (\%) = \frac{(3717.13 - 3603.72)}{(3717.13 + 3603.72)} * 100$$

$$Error (\%) = 01.51 \%$$

Therefore, an error of 1.51 % is observed, which is very less, because few of the results are based on empirical methods. Also, the terminologies used in this context are broad; hence, further research is needed to reduce the error.

6.3 Summary

In this chapter, a few of the thematic information discussed in the earlier chapters are used directly to integrate groundwater recharge potentiality studies. The results indicate that 27% of the study area is having high and very high GRPZ. Therefore, these locations are more suitable for bigger recharge structures for maximum recharge. The low and very low categories of GRPZ are the least suitable. However, the smaller ARS

and recharge methods are most suitable for such locations as they are spatially distributed to cover the whole study area. The ARS like park recharge structures is more suitable for urban locations, whereas the check dams are more suitable for higher altitudes. Several recharge methods can be associated together to obtain the most efficient recharge in terms of volume. The recharge estimation methods yielded an average recharge of 29.93%, which is 1112.54 mm/year.

Chapter 7

SUMMARY AND CONCLUSIONS

The sustenance of life is dependent on the water. Statistically, water covers a large portion of the earth, but the actual availability of freshwater is a precarious point of concern. The surface water cannot tend to the needs of the growing population. Therefore, groundwater is considered one of the primary water sources. Though groundwater provides ease of access and availability, overexploitation has made it a scarce and unpredictable commodity. Therefore, numerous factors and their relationship that influence groundwater resources are to be studied to draft efficient management plans for groundwater exploration and exploitation. This study utilizes the relationship between geology, geomorphology, groundwater exploration, groundwater quality, and groundwater recharge to understand the groundwater availability scenario. The present work establishes the relation between electrical resistivity methods, RS, and GIS-based methodology for the identification and mapping of groundwater potential & recharge potential zones. The brief conclusions of the research work carried out are presented below.

- The climate, geology, geomorphology, and drainage characteristics are some of the factors which have influence groundwater availability. The climatic factors include hydrometeorological parameters like precipitation (rainfall), surface temperature, humidity, number of rainy days, and rainfall intensity. The geological factors include lithology, stratigraphy, and structures (like folds, faults, joints). These geological factors play an important role in providing boundary conditions for the geological units (aquifers). The geomorphological studies provide an understanding of the surface features, river morphometry, and terrain conditions. The hydro-geochemical studies provide information about the chemical interaction of water with aquifer litho-units and its quality for drinking purposes.
- The major litho unit is PGC or Achaean MGTG. The Gurple watershed is divided

into high land, midland and low land (ghats, hinterland, and coastal area) depending on terrain features and altitude. The major water-bearing capacity of the granitic-gneiss aquifers is due to secondary porosity (cracks and fractures). More than 75% of the study area is covered with fine and fine loamy soil types. Also, the soil depth in the study area is deeper (greater than 100 cm) soils and covers greater than 80% of the total area.

- The false-colour composite process of satellite imagery effectively classifies the vegetation and other important lu/lc features. This thematic information shows that greater than 50% of the total area is covered by vegetation (forest, forest plantation, and plantation). More than 10% of the area is identified as built-up land.
- There is increasing use of RS and GIS for spatial analysis on diverse applications. This study shows that the GIS can also be efficiently used for landform and watersheds studies. The Remote sensing and GIS techniques are also proven to be efficient in delineating, updating, and morphometric analysis of drainage basins.
- The groundwater is a natural resource influenced by the climate, geology, geomorphology, and drainage characteristics. The geological factors like lithology, stratigraphy, and structures play an important role in providing boundary conditions for the aquifers. The morphometric analysis has been carried out by measuring linear, aerial, and relief aspects of the Gurple watershed. The result of morphometric analysis provides information about watershed development and areas vulnerable to land degradation. The morphometric study helps in understanding the hydrological, geological, and geomorphological characteristics of the drainage basin.
- The sub-surface indicators like GW fluctuation and depth to bedrock play an important role in providing hydro-geological information of the study area and surface indicators.
- In MCA or WOI methods, more thematic information provides accurate results. Understanding geological, structural, geomorphological characteristics are

necessary as it is the basis for assigning Rank/Weights. It is necessary to consider maximum information available, especially information like sub-surface lithology, major and minor fractures, soil moisture, aquifer thickness, pumping test data yielding hydraulic conductivity, specific yield, etc. It can help provide more accurate results.

- The CartoSAT-1 DEM data with a spatial resolution of 30m is used in the present study. The DEM derivatives like drainage network, slope, hill shade, and contour are extracted and utilized in the study. The drainage order of up to the 7th order stream is delineated. Slope categories “nearly level” are observed towards the beach, whereas the “very steep slope” is observed towards the Western Ghats.
- It is observed that electrical resistivity methods are best suited for groundwater exploration and recharge studies compared to other geophysical methods. Though 1D studies (VES) can provide good results, they are still confined to depth alone. With the help of electrical resistivity data, the thickness of the weathered zone (depth to bedrock) is in the range of 20 - 40m from the surface.
- The formations which come under the H, KH, KHQ, KQ, QH, and QQ curve types shows good groundwater potential, which covers about 43% of the study area. The formations which come under AH, HA, HK, KHA, QKA curve types exhibits moderate groundwater potential, which is about 34%. The formations that come under A, AA, and HKA curve types exhibit poor groundwater potential, which comprises about 23%. Based on the Geo-electrical sections, the Hydro-geological layers were inferred, which are laterite, sandy clay, fractured/weathered rock, and hard rock.
- The inverse slope method is rather a direct method of interpretation compared to CMT. This method yields a slope based on the relationship between current electrode spacing and apparent resistivity. The ISM and CMT methods of interpretation yielded almost similar results. Therefore, the depth to bedrock and geoelectrical parameters, hydraulic parameters, and Dar-Zarrouk parameters are

calculated based on the data obtained from the interpretation of ISM.

- The data obtained are interpreted using the Inverse Slope Method of interpretation. The ISM gives sharp boundaries for different layers. The geoelectrical resistivity data is used for the identification of depth to bedrock. The data is also interpreted to get hydraulic conductivity, transmissivity, porosity, and formation factor. From the interpretation of the VES data, it is inferred that there are 05 three-layered formations, 24 four-layered, and 06 five-layered formations out of 35 soundings.
- The correlation for hydraulic and geoelectric parameters shows weak to good correlation. This method of calculating hydraulic parameters can be economical, time-saving, and an alternative for pumping tests. Geo-electrical resistivity data interpreted with CMT is correlated with the Borehole Lithologs, which gave a good correlation. Therefore this method is used for the identification of GRPZ.
- This study also aims at thematic database creation, and a total of 46 thematic layers are prepared and used in this study. The thematic layers prepared are lithology, geomorphology, DEM, drainages, slope, hill shade, contours, drainage density, lu/lc, soil types, soil depth, aquifer thickness, anisotropy, formation factor, porosity, hydraulic conductivity, transmissivity, longitudinal unit conductance, transverse unit resistance, layer resistivity, rainfall distribution, depth to bedrock, lineaments, lineament density, groundwater contours, groundwater potential zones using CMT, groundwater potential zones using WOI, groundwater recharge potential zones, and proposed locations of ARS. The thematic database created for groundwater quality is as follows, pH, electrical conductivity, total dissolved solids, total hardness, total alkalinity, sodium, potassium, magnesium, calcium, nitrate, Sulphate, iron, chloride, fluoride, bicarbonates, and GQI for three phases. This thematic database with WOI analysis helps understand the physical relation of the themes and deduce the suitable zones for groundwater exploration and recharge.
- The GWPZ thematic layer provides information about the suitable bore well locations for drilling and extraction of groundwater. A total of 13 thematic layers

are utilized for integration. The weights for different themes are assigned based on their physical influence over the groundwater potential. The category with “Very Good to Moderate” groundwater potential zones covers about 77% of the total area. The category with “Poor” and “Very Poor” groundwater potential zones covers 13% of the total area. The fact also remains that the sub-surface is highly heterogeneous and complex. Therefore this methodology serves as preliminary results before conducting direct drilling.

- The GRPZ thematic layer provides information about the suitable recharge methods and preferable locations for constructing ARS for effective recharge. The results obtained indicate that about 27% of the study area is categorized under “high” and “very high” categories. The moderate category of GRPZ constitutes 32% of the study area. About 41% of the area is considered under “low” and “very low” categories. The midlands are associated with high groundwater fluctuation. Therefore priority for ARS site selection is given to midlands.
- The implementation of the suggested methodology of ARS and water conservation techniques may help improve the groundwater recharge and slightly reduce the groundwater demand. Though several ARS are proposed, only the most impact-full locations & methods are suggested. A total of 11 check dams, 40 nala bunds, 33 farm ponds, 30 contour trenches and, 26 percolation tanks are suggested in this study. Also, the combination of these ARS may yield more recharge.
- Several groundwater recharge estimation methods are also discussed in the study. These estimation methods are correlation and water balance methods. Therefore, they could provide only the general idea of the recharge that could occur and not the real-time measurements.
- The groundwater quality with respect to drinking water standards is conducted in the study to understand the groundwater quality scenario. The samples were collected in three phases (Phase I, II, III) during the peak seasons like Monsoon (August-2017), Post-Monsoon (December-2017), and Pre-Monsoon (April-2018),

respectively.

- The major deduction from the GQI studies is that phase-II is the most affected phase with reduced water quality. The parameters like pH, Fe, SO₄, NO₃, and Cl are of major concern as they extend over the desirable limits (but within the permissible limits). From the correlation studies, it can be concluded that there is a strong positive correlation between different equations used to check the correctness of the analysis.
- The weighted arithmetic WQI method is used in this study. It is observed that the drinking water quality for the variables like TDS, Cl, TH, Ca, Na, K, Mg, TA, Fe, NO₃, and SO₄ are rated as “excellent water quality” category. It is observed that the groundwater quality parameter “pH” is the only outlier identified, which could affect human health. The variables EC falls under “poor” water quality conditions observed only at the sampling locations near the sea and during the summer. This could mean that the variation is due to saltwater intrusion.
- The study also provides a database for assessment, management, suitable borehole drilling locations for GW extraction in the Gurgur watershed. This study can be implemented for other coastal aquifers.

7.1 Limitations

- If associated with electrical cables, the sounding location, conductive materials, metal ore deposits, underground pipes, fences may influence the resistivity results. Therefore proper care must be taken for conducting VES. Otherwise, the distorted data may be misinterpreted.
- The apparent resistivity data obtained for any depth is not based on a single factor. It is based on the cumulative effects of heterogeneous sub-surface, obtained from reflection and refraction of electrical signals of several materials. Therefore, the research based on resistivity data is dependent on the interpretation method, in-depth knowledge of geology, terrain, and other aspects of the study area. Based on this

limitation, it can be safely assumed that the validation of electrical resistivity data with borehole lithology may increase the accuracy of the interpretation.

- Probing for greater depths was not possible in some VES locations because of the non-availability of the open space on the surface. Therefore in such locations maximum depth of investigation is considered as the lower basement of the aquifer.

7.2 Scope for future work

- The further implementation of 2D (imaging) and 3D (tomography) studies can significantly improve the results and less time-consuming compared to 1D (VES) studies. They also cover more area in less time compared to 1D studies.
- Further studies like Normalized Difference Vegetation Index (NDVI) and Normalized Difference Water Index (NDWI) can be incorporated as a thematic layer and integrated for water resources studies.
- Groundwater discharge data could also be used for further validation of runoff generated from the SCS-CN method.
- The field-generated data derived from pumping tests and soil moisture data can also be integrated for water resources study.
- The spatial distribution of thematic evapotranspiration information generated from satellite imagery of National Oceanic and Atmospheric Administration - Advanced Very High-Resolution Radiometer (NOAA-AVHRR) data could also be used for integration and water resource studies.
- The accuracy assessment for satellite imagery supervised classification can also be done using different error matrix methods including; commission and omission error, sensitivity and specificity, positive and negative predictive power, and kappa statistics.
- Sensitivity analysis could be conducted for the integration of thematic layers, so that the bias of the weights assigned can be understood.

REFERENCES

- Abrahams AD. 1984. Channel Networks: A Geomorphological Perspective. *Water Resour Res.* 20(2):161–188.
- Acharya T, Kumbhakar S, Prasad R, Mondal S, Biswas A. 2019. Delineation of potential groundwater recharge zones in the coastal area of north-eastern India using geoinformatics. *Sustain Water Resour Manag.* 5(2):533–540.
- Adimalla N, Qian H. 2019. Groundwater quality evaluation using water quality index (WQI) for drinking purposes and human health risk (HHR) assessment in an agricultural region of Nanganur, south India. *Ecotoxicol Environ Saf* [Internet]. 176:153–161. <https://www.sciencedirect.com/science/article/pii/S0147651319303276>
- Adyalkar PG, Rao SS. 1979. Hydrodynamic method of assessing groundwater recharge by precipitation in deccan trap terrain: a case study. *J Geol Soc India.* 20:134–137.
- Agarwal CS. 1998. Study of drainage pattern through aerial data in Naugarh area of Varanasi district, U.P. *J Indian Soc Remote Sens.* 26(4):169–175.
- Andrews RG. 1954. The use of relative infiltration indices in computing runoff. Fort Worth, Texas.
- Anomohanran O. 2011. Determination of groundwater potential in Asaba , Nigeria using surface geoelectric sounding. 6(33):7651–7656.
- Anonna TA, Ahmed Z, Alam R, Karim MM, Xie Z, Kumar P, Zhang F, Simal-Gandara J. 2021. Water Quality Assessment for Drinking and Irrigation Purposes in Mahananda River Basin of Bangladesh. *Earth Syst Environ* 2021 [Internet]. [accessed 2021 Dec 13]:1–12. <https://link.springer.com/article/10.1007/s41748-021-00274-x>
- Anwar K, Aggarwal V. 2015. Analysis of Groundwater Quality of Aligarh City, (India): Using Water Quality Index. *Curr World Environ.* 9(3):851–857.
- APHA. 1999. Standard Methods for the Examination of Water and Wastewater. Washington, DC.
- APHA, AWWA, WEF. 2012. Standard Methods for the Examination of Water and Wastewater. 22nd, illust ed. Rice EW., Baird; RB, Eaton; AD, Clesceri LS, editors. Washington, DC: American Public Health Association. https://beta-static.fishersci.com/content/dam/fishersci/en_US/documents/programs/scientific/technical-documents/white-papers/apha-water-testing-standard-methods-white-paper.pdf
- Archie GE. 1942. The Electrical Resistivity Log as an Aid in Determining Some Reservoir Characteristics. *Trans AIME* [Internet]. 146(01):54–62.

<http://www.onepetro.org/doi/10.2118/942054-G>

Arétouyap Z, Bisso D, Njandjock Nouck P, Amougou Menkpa LE, Asfahani J. 2019. Hydrogeophysical Characteristics of Pan-African Aquifer Specified Through an Alternative Approach Based on the Interpretation of Vertical Electrical Sounding Data in the Adamawa Region, Central Africa. *Nat Resour Res* [Internet]. 28(1):63–77. <http://link.springer.com/10.1007/s11053-018-9373-8>

Asadi SS, Rao BVTV, Raju M V, Sagar MA. 2011. Creation of Information System for Identification of Ground Water Pollution Prevention Zones Using Remote sensing and GIS : A Model Study. 1(2):145–151.

Asfahani J. 2016. Hydraulic parameters estimation by using an approach based on vertical electrical soundings (VES) in the semi-arid Khanasser valley region, Syria. *J African Earth Sci.* 117:196–206.

Asije E, Igwe O. 2014. Electrical Resistivity Investigation for Ground Water in Parts of Pegi, Federal Capital Territory, Nigeria. *IOSR J Appl Geol Geophys.* 2(6):27–32.

Avinash K, Jayappa KS, Deepika B. 2011. Prioritization of sub-basins based on geomorphology and morphometric analysis using remote sensing and geographic information system (GIS) techniques. *Geocarto Int.* 26(7):569–592.

Babiker IS, Mohamed MAA, Hiyama T. 2007. Assessing groundwater quality using GIS. *Water Resour Manag* [Internet]. 21(4):699–715. <http://link.springer.com/10.1007/s11269-006-9059-6>

Baby SN, Arrowsmith C, Al-Ansari N. 2019. Application of GIS for Mapping Rainwater-Harvesting Potential: Case Study Wollert, Victoria. *Engineering.* 11(01):14–21.

Balakrishnan P, Saleem A, Mallikarjun ND. 2011. Groundwater quality mapping using geographic information system (GIS): A case study of Gulbarga City , Karnataka , India. *African J Environ Sci Technol* [Internet]. 5(December):1069–1084. [http://www.academicjournals.org/AJEST/abstracts/abstracts/abstract2011/Dec/Balakrishnan et al.htm](http://www.academicjournals.org/AJEST/abstracts/abstracts/abstract2011/Dec/Balakrishnan%20et%20al.htm)

Balasubrahmanyam MN. 1978. Geochronology and Geochemistry of Archaean Tonalitic Gneisses and Granites of South Kanara District, Karnataka State, India. *Dev Precambrian Geol* [Internet]. 1:59–77. <https://www.sciencedirect.com/science/article/pii/S0166263508700926>

Barseem MS, El-Lateef TAA, El-Deen HME, Rahman AAAAA. 2015. Geoelectrical exploration in South Qantara Shark area for supplementary irrigation purpose-Sinai-Egypt. *Hydrol Curr Res* [Internet]. 6(2):207. <https://www.cabdirect.org/cabdirect/abstract/20163037808>

Basavaraddi SB, Kousar H, Puttaiah ET. 2012. Dissolved Oxygen Concentration - a Remarkable Indicator of Ground Water Pollution in and around Tiptur town , Tumkur District , Karnataka , India. Bull Environ Pharmacol Life Sci [Internet]. 1(3):48–54. www.bepls.com

Batayneh AT. 2013. The estimation and significance of Dar-Zarrouk parameters in the exploration of quality affecting the Gulf of Aqaba coastal aquifer systems. J Coast Conserv [Internet]. 17:623–635. <https://www.jstor.org/stable/42657050>

Bawoke GT, Anteneh ZL. 2020. Spatial assessment and appraisal of groundwater suitability for drinking consumption in Andasa watershed using water quality index (WQI) and GIS techniques: Blue Nile Basin, Northwestern Ethiopia. <http://www.editorialmanager.com/cogenteng> [Internet]. [accessed 2021 Dec 13] 7(1). <https://www.tandfonline.com/doi/abs/10.1080/23311916.2020.1748950>

Becker MW. 2006. Potential for Satellite Remote Sensing of Ground Water. Ground Water [Internet]. 44(2):306–318. <http://doi.wiley.com/10.1111/j.1745-6584.2005.00123.x>

Besbes M, Delhomme JP, De Marsily G. 1978. Estimating recharge from ephemeral streams in arid regions: A case study at Kairouan, Tunisia. Water Resour Res [Internet]. 14(2):281–290. <http://doi.wiley.com/10.1029/WR014i002p00281>

Bhattacharya AP, Jindal SR, Srivastava BP. 1954. Penetration of rainwater to groundwater table in Western U.P., India. -.

Bhattacharya S, Das Swarupa, Das Sandipan, Kalashetty M, Warghat SR. 2020. An integrated approach for mapping groundwater potential applying geospatial and MIF techniques in the semiarid region. Environ Dev Sustain.:1–16.

Bosznay M. 1989. Generalization of SCS Curve Number Method. J Irrig Drain Eng [Internet]. 115(1):139–144. <https://ascelibrary.org/doi/abs/10.1061/%28ASCE%290733-9437%281989%29115%3A1%28139%29>

Brown RM, McClelland NI, Deininger RA, O'Connor MF. 1972. A Water Quality Index — Crashing the Psychological Barrier. In: Indic Environ Qual [Internet]. Boston, MA: Springer US; p. 173–182. http://link.springer.com/10.1007/978-1-4684-2856-8_15

Bureau of Indian Standards. 2012. Indian Standard DRINKING WATER — SPECIFICATION. 2nd ed. New Delhi.

Burrough PA. 1986. Principles of Geographical Information Systems for Land Resources Assessment. New York: Oxford University Press.

Carver SJ. 1991. Integrating multi-criteria evaluation with geographical information systems. *Int J Geogr Inf Syst* [Internet]. 5(3):321–339. <http://www.tandfonline.com/doi/abs/10.1080/02693799108927858>

Carver SJ. 2017. Integrating multi-criteria evaluation with geographical information systems. 3798(June).

Cazier DJ, Richard H. Hawkins. 1984. Regional application of the curve number method. In: *water today and tomorrow* [Internet]. New York, N.Y.: ASCE; p. 710. <https://cedb.asce.org/CEDBsearch/record.jsp?dockkey=0041386>

CBIP. 1976. *Manual on ground water and tube wells*. New Delhi.

Central Ground Water Board. 2015. *Ground water year book karnataka (2014-15)*. (September).

Chakraborty D, Dutta D, Chandrasekharan H. 2005. Spatial modelling for hydrological response behaviour of an arid watershed, india-remote sensing and gis approach. *J Spat Hydrol*. 5(1).

Chandrasekharappa K. 1989. *Morphometric analysis of Nethravathi river basin, Karnataka, India*. [place unknown]: Mangalore University.

Chandrashekhar H, Naganna C. 1979. Evaluation of groundwater resources of the Chikkahagari basin, Karnataka, India. In: *Hydrol areas low Precip* [Internet]. Vol. 1979. Paris: International Association of Hydrological Sciences; p. 279–286. <http://agris.fao.org/agris-search/search.do?recordID=US201302186509>

Channel Networks: A Geomorphological Perspective - Abrahams - 1984 - *Water Resources Research* - Wiley Online Library. [accessed 2020 May 4]. <https://agupubs.onlinelibrary.wiley.com/doi/abs/10.1029/WR020i002p00161>

Chatterjee C, Jha R, Lohani AK, Kumar R, Singh R. 2001. Runoff curve number estimation for a basin using remote sensing and GIS. *Asian-Pacific Remote Sens GIS J*. 14:1–7.

Chaturvedi RS. 1973. *A Note on the Investigation of Ground Water Resources in Western Districts of Uttar Pradesh*. U.P.

Chowdary VM, Chakraborty D, Jeyaram A, Murthy YV NK, Sharma JR, Dadhwal VK. 2013. Multi-Criteria Decision Making Approach for Watershed Prioritization Using Analytic Hierarchy Process Technique and GIS. *Water Resour Manag*. 27(10):3555–3571.

Clark JA, Page R. 2011. Inexpensive Geophysical Instruments Supporting Groundwater Exploration in Developing Nations. *J Water Resour Prot* [Internet]. 3:768–780. <http://www.scirp.org/journal/jwarp>

Cordy GE, Duran NL, Bouwer H, Rice RC, Furlong ET, Zaugg SD, Meyer MT, Barber LB, Kolpin DW. 2004. Do Pharmaceuticals, Pathogens, and Other Organic Waste Water Compounds Persist When Waste Water Is Used for Recharge? *Groundw Monit Remediat* [Internet]. 24(2):58–69. <http://doi.wiley.com/10.1111/j.1745-6592.2004.tb00713.x>

Das B, Pal SC, Malik S, Chakraborty R. 2019. Modeling groundwater potential zones of Puruliya district, West Bengal, India using remote sensing and GIS techniques. *Geol Ecol Landscapes* [Internet]. 3(3):223–237. <https://www.tandfonline.com/doi/full/10.1080/24749508.2018.1555740>

Das S, Pardeshi SD. 2018. Comparative analysis of lineaments extracted from Cartosat, SRTM and ASTER DEM: a study based on four watersheds in Konkan region, India. *Spat Inf Res* [Internet]. 26(1):47–57. <https://link.springer.com/article/10.1007/s41324-017-0155-x>

Debels P, Figueroa R, Urrutia R, Barra R, Niell X. 2005. Evaluation of Water Quality in the Chillán River (Central Chile) Using Physicochemical Parameters and a Modified Water Quality Index. *Environ Monit Assess* 2005 1101 [Internet]. [accessed 2021 Dec 13] 110(1):301–322. <https://link.springer.com/article/10.1007/s10661-005-8064-1>

Department of Mines and Geology. 2011. Groundwater hydrology and groundwater quality in and around Bangalore city. Bangalore.

Dikshit KR. 1981. The Western Ghats: a geomorphic overview. In: Singh LR, editor. *New Perspect Geogr*. Allahabad, India: Thinkers Library; p. 1–25.

Dobrin MB, Savit CH. 1988. Introduction to geophysical prospecting. 4th ed. Singapore: McGraw-Hill Book Company.

Dornkamp JC, King C. 1971. Numerical analyses in geomorphology, an introduction. New York: St. Martins Press.

Durbude DG, Jain MK, Mishra SK. 2011. Long-term hydrologic simulation using SCS-CN-based improved soil moisture accounting procedure. *Hydrol Process* [Internet]. 25(4):561–579. <http://doi.wiley.com/10.1002/hyp.7789>

Durbude DG, Purandara BK, Sharma A. 2001. Estimation of surface runoff potential of a watershed in semi-arid environment - a case study. *J Indian Soc Remote Sens* [Internet]. 29(1–2):47–58. <https://link.springer.com/article/10.1007/BF02989914>

Ekwe AC, Onu NN, Onuoha KM. 2006. Journal of spatial hydrology: an official publication of Spatial Hydrology. *J Spat Hydrol* [Internet]. 6(2):121–132. <http://spatialhydrology.net/index.php/JOSH/article/view/61>

Fetter CW. 2001. Applied hydrogeology. 4th ed. New Jersey: Waveland Press, Inc.

-
- Friedman LC, Erdmann DE. 1982. Quality Assurance Practices for Analyses of Water and Fluvial Sediments [Internet]. Techniques. Washington: United States Government Printing Office.
https://books.google.co.in/books?hl=en&lr=&id=mIshclPp0wAC&oi=fnd&pg=PA1&dq=Quality+Assurance+Practices+for+Analyses+of+Water+and+Fluvial+Sediments&ots=kQP4I0cGZb&sig=LiP11qfwMFRfx_gjJrRGgv0VfVE#v=onepage&q=Quality Assurance Practices for Analyses of Water
- Gajendragad MR, Ranganna G. 1989. Environmental Pollution, Monitoring and mitigation with particular reference to water resources of Dakshina Kannada District. Mangalore Univ Decenn Vol.:349.
- Gidey A. 2018. Geospatial distribution modeling and determining suitability of groundwater quality for irrigation purpose using geospatial methods and water quality index (WQI) in Northern Ethiopia. *Appl Water Sci* [Internet]. 8(3):1–16.
<https://doi.org/10.1007/s13201-018-0722-x>
- Gravelius H. 1914. Morphometry of Drainage Bassins. Amsterdam: Elsevier.
- Grindley F. 1967. Estimation of soil moisture deficits. *Meteorol Mag.* 96(1137):97.
- Groundwater Resource Estimation Committee. 2009. Ground water resource estimation methodology. India.
- Gundalia M, Dholakia M. 2014. Impact of Monthly Curve Number on Daily Runoff Estimation for Ozat Catchment in India. *Open J Mod Hydrol.* 04(04):144–155.
- Gurumurthy GP. 2013. Major ion, trace element and organic carbon geochemistry of river Nethravati, Southwest coast of India. [place unknown]: Manipal University.
<https://shodhganga.inflibnet.ac.in/handle/10603/11638>
- Gurumurthy GP, Balakrishna K, Tripti M, Riotte J, Audry S, Braun JJ, Lambs L, Udaya Shankar HN. 2014. Sources of major ions and processes affecting the geochemical and isotopic signatures of subsurface waters along a tropical river, Southwestern India. *Environ Earth Sci.* 73(1):333–346.
- Gyeltshen S, Tran T V., Teja Gunda GK, Kannaujiya S, Chatterjee RS, Champatiray PK. 2020. Groundwater potential zones using a combination of geospatial technology and geophysical approach: case study in Dehradun, India. *Hydrol Sci J.* 65(2):169–182.
- Hardcastle KC, Groundwater G, Street W. 1995. Computer- Aided Method for Remotely Sensed Degree to which Fractured Bedrock is Fractured Degree to which Fractured Bedrock.
- Healy RW, Cook PG. 2002. Using groundwater levels to estimate recharge. *Hydrogeol J.* 10(1):91–109.

-
- Henriet JP. 1976. Direct applications of the dar zarrouk parameters in ground water surveys. *Geophys Prospect* [Internet]. 24(2):344–353. <http://doi.wiley.com/10.1111/j.1365-2478.1976.tb00931.x>
- Herman R. 2001. An introduction to electrical resistivity in geophysics. *Am J Phys* [Internet]. 69(9):943–952. <http://aapt.scitation.org/doi/10.1119/1.1378013>
- Hjelmfelt AT. 1991. Investigation of Curve Number Procedure. *J Hydraul Eng* [Internet]. 117(6):725–737. <https://ascelibrary.org/doi/abs/10.1061/%28ASCE%290733-9429%281991%29117%3A6%28725%29>
- Horton RE. 1932. Drainage basin characteristics. *Trans Am Geophys Union*. 13:350–361.
- Horton RE. 1945. Erosional development of streams and their drainage basins: Hydrophysical approach to quantitative morphology. *Bull Geol Soc Am*. 56:275–370.
- How Weighted Overlay works-ArcGIS Help. <https://desktop.arcgis.com/en/arcmap/10.3/tools/spatial-analyst-toolbox/how-weighted-overlay-works.htm>
- Hughes DA, Sami K. 1992. Transmission losses to alluvium and associated moisture dynamics in a semiarid ephemeral channel system in Southern Africa. *Hydrol Process* [Internet]. 6(1):45–53. <http://doi.wiley.com/10.1002/hyp.3360060105>
- IMD Bangalore. Climatological table from 1981 - 2010 [Internet]. <http://city.imd.gov.in/citywx/extreme/DEC/mangaluru2.htm>
- Jaiswal RK, Mukherjee S, Krishnamurthy J, Saxena R. 2003. Role of remote sensing and GIS techniques for generation of groundwater prospect zones towards rural development--an approach. *Int J Remote Sens* [Internet]. 24(5):993–1008. <https://www.tandfonline.com/doi/full/10.1080/01431160210144543>
- Jha MK, Chowdhury A, Chowdary VM, Peiffer S. 2007. Groundwater management and development by integrated remote sensing and geographic information systems: prospects and constraints. *Water Resour Manag* [Internet]. 21(2):427–467. <http://link.springer.com/10.1007/s11269-006-9024-4>
- Jha MK, Peiffer S. 2006. Applications of Remote Sensing and GIS Technologies in Groundwater Hydrology: Past, Present and Future [Internet]. 1st ed. Bayreuth, Germany: Bayreuth Center of Ecology and Environmental Research. http://www.bayceer.uni-bayreuth.de/bayceer/html/bfoe/bfoe112_order.pdf
- John EJ, Cheriyan KP. 1974. Geomorphological Studies of the estuary of the river Nethravathi, near Mangalore. In: *Coast Eng Con*. [place unknown]: ASCE; p. 1304–

1318.

Joseph Markose V, Dinesh AC, Jayappa KS. 2014. Quantitative analysis of morphometric parameters of Kali River basin, southern India, using bearing azimuth and drainage (bAd) calculator and GIS. *Environ Earth Sci.* 72(8):2887–2903.

Joshi DM, Singh Bhandari N, Kumar A, Agrawal N. 2009. Statistical analysis of physicochemical parameters of water of river Ganga in Haridwar district [Internet]. 2(3):579–587. <http://www.rasayanjournal.com>

Karanth KR. 1987. Ground water assessment, development, and management. New Delhi: Tata McGraw-Hill Pub. Co.

Karanth KR. 1994. Groundwater evaluation and development in Karnataka. In: Geo Karnataka. Ravindra BM, Ranganathan N, editors. Bangalore: KAGA.

Karanth KR. 2008. Groundwater assessment development and management. 12th ed. New Delhi: Tata McGraw-Hill Education.

Keller GV, Frischknecht FC. 1966. Electrical methods in geophysical prospecting. Oxford: Pergamon.

Khan MA, Moharana PC. 2002. Use of Remote Sensing and Geographical Information System in the delineation and characterization of ground water prospect zones. *J Indian Soc Remote Sens* [Internet]. 30(3):131–141. <http://link.springer.com/10.1007/BF02990645>

Krishnamurthy J, Srinivas G, Jayaram V, Chandrasekhar M. 1996. Influence of rock type and structure in the development of drainage networks in typical hard rock terrain. *ITCJ.* 3(4):252–259.

Kumar B, Kumar U. 2010. Integrated approach using RS and GIS techniques for mapping of ground water prospects in Lower Sanjai Watershed, Jharkhand. *Int J Geomatics Geosci* [Internet]. 1(3):587–598. <https://www.researchgate.net/publication/270759451>

Kumar CP. 1996. Assessment of Ground Water Potential. In: All India Semin small watershed Dev Organ by Indian Assoc Hydrol West Bengal Cent. Calcutta.

Kumar CP, Seethapathi P V. 2002. Assessment of Natural Ground Water Recharge in Upper Ganga Canal Command Area. *J Appl Hydrol Assoc Hydrol India* [Internet]. XV(4):13–20. <http://www.angelfire.com/nh/cpkumar/publication/ugcm.pdf>

Kumar MG, Agarwal AK, Bali R. 2008. Delineation of potential sites for water harvesting structures using remote sensing and GIS. *J Indian Soc Remote Sens* [Internet]. 36(4):323–334. <http://link.springer.com/10.1007/s12524-008-0033-z>

Kumar MG, Bali R, Agarwal AK. 2009. Integration of remote sensing and electrical sounding data for hydrogeological exploration - A case study of Bakhar watershed, India. *Hydrol Sci J.* 54(5):949–960.

Kumar MG, Rameshwar AKA. 2008. Delineation of Potential Sites for Water Harvesting Structures using Remote Sensing and GIS. 80(December):323–334.

LeCompte MD, Klinger JK, Campbell SA, Menke DW. 2003. Editor's Introduction. *Rev Educ Res.* 73(2):123–124.

Lerner DN. 1997. Too much or too little: recharge in urban areas. *Groundw urban Environ.* 1:41–47.

Lerner DN, Issar AS, Simmers I. 1990. *Groundwater Recharge*. 8th ed. Hannover, editor. West Germany : Verlag Heinz Heise: Taylor and Francis.

Lkr A, Singh MR, Puro N. 2020. Assessment of water quality status of Doyang River, Nagaland, India, using Water Quality Index. *Appl Water Sci* [Internet]. [accessed 2021 Dec 13] 10(1):1–13. <https://link.springer.com/article/10.1007/s13201-019-1133-3>

Loke MH. 2001. Tutorial : 2-D and 3-D electrical imaging surveys [Internet]. [place unknown]. www.geotomosoft.com

Magesh NS, Chandrasekar N, Soundranayagam JP. 2012. Delineation of groundwater potential zones in Theni district, Tamil Nadu, using remote sensing, GIS and MIF techniques. *Geosci Front* [Internet]. 3(2):189–196. <http://dx.doi.org/10.1016/j.gsf.2011.10.007>

Mahajan SH, Padmane ST, Patil SN, Gupta G, Erram VC. 2015. Geoelectric investigation to delineate groundwater potential and recharge zones in Suki river basin, north Maharashtra. *J Earth Syst Sci.* 124(7):1487–1501.

Maillet R. 1947. The fundamental equations of electrical prospecting. *GEOPHYSICS* [Internet]. 12(4):529–556. <http://library.seg.org/doi/10.1190/1.1437342>

Majumdar RK, Kar S, Panda A, Samanta SK. 2016. Hydrological characterization of Budge Budge and Dum Dum areas of south and north 24 Parganas districts, West Bengal using geoelectric and geochemical methods. *J Geol Soc India.* 88(3):330–338.

Merzi N, Aktas MT. 2000. Geographic information systems (GIS) for the determination of inundation maps of Lake Mogan, Turkey. *Water Int* [Internet]. 25(3):474–480. <https://www.tandfonline.com/doi/abs/10.1080/02508060008686856>

Miller VC. 1953. A quantitative geomorphic study of drainage basin characteristics in the Clinch mountain area Virginia and Tennessee. Tennessee.

Ministry of Water Resources, RDGR G. 2017. GEC (2015) Ground Water Resource

Estimation Committee [Internet]. New Delhi. http://cgwb.gov.in/Documents/GEC2015_Report_Final 30.10.2017.pdf

Mishra SK, Kansal AK. 2014. a Procedure for Determination of Design Runoff Curve. 34(3):46–56.

Mockus V. 1949. Estimation of total (and peak rates of) surface runoff for individual storms. Washington DC.

Mukate S, Wagh V, Panaskar D, Jacobs JA, Sawant A. 2019. Development of new integrated water quality index (IWQI) model to evaluate the drinking suitability of water. *Ecol Indic.* 101:348–354.

Mukherjee Sandip, Joshi PK, Mukherjee Samadrita, Ghosh A, Garg RD, Mukhopadhyay A. 2012. Evaluation of vertical accuracy of open source Digital Elevation Model (DEM). *Int J Appl Earth Obs Geoinf.* 21(1):205–217.

Van Mullem JA. 1991. Runoff and Peak Discharges Using Green-Ampt Infiltration Model. *J Hydraul Eng* [Internet]. 117(3):354–370. <https://ascelibrary.org/doi/abs/10.1061/%28ASCE%290733-9429%281991%29117%3A3%28354%29>

Musgrave W. G. 1955. How Much of the Rain Enters the Soil? In: *Yearb Agric* [Internet]. [place unknown]; p. 151–160. <https://naldc.nal.usda.gov/download/IND43894552/PDF>

Nandagiri L. 2007. Calibrating hydrological models in ungauged basins: possible use of areal evapotranspiration instead of streamflows. *Predict Ungauged Basins PUB Kick-off* ... [Internet].(November 2002):20–22. <http://ks360352.kimsufi.com/redbooks/a309/309032.pdf>

Narayan PVS, Ramanujachary KR. 1967. An inverse slope method of determining absolute resistivity. *Geophysics* [Internet]. 32(6):1036–1040. <http://library.seg.org/doi/10.1190/1.1439906>

Narayana AC, Suresh GC. 1989. Chemical quality of groundwater of Mangalore City, Karnataka. *J Environ Prot.* 31:228–236.

Nas B, Berktaş A. 2014. Groundwater Quality Mapping in Urban Groundwater Using GIS Groundwater quality mapping in urban groundwater using GIS. (November 2009).

Nayak TR, Jaiswal RK. 2003. Rainfall-runoff modelling using satellite data and GIS for Bebas river in Madhya Pradesh. *J Inst Eng India Civ Eng Div* [Internet]. 84:47–50. <https://pascal-francis.inist.fr/vibad/index.php?action=getRecordDetail&lang=en&idt=15079853>

Niwas S, Lima OA. 2003. Aquifer Parameter Estimation from Surface Resistivity Data.

-
- Ground Water [Internet]. 41(1):94–99. <http://doi.wiley.com/10.1111/j.1745-6584.2003.tb02572.x>
- Niwas S, Singhal DC. 1981. Estimation of aquifer transmissivity from Dar-Zarrouk parameters in porous media. *J Hydrol* [Internet]. 50:393–399. <https://www.sciencedirect.com/science/article/pii/0022169481900822>
- Niwas S, Tezkan B, Israil M. 2011. Aquifer hydraulic conductivity estimation from surface geoelectrical measurements for Krauthausen test site, Germany. *Hydrogeol J* [Internet]. 19(2):307–315. <http://link.springer.com/10.1007/s10040-010-0689-7>
- Ogrosky HO. 1956. Several Objectives in the field of hydrology. [place unknown].
- Okoli FU, Aiegbedion IP, Marcellinus LM, Oludiji SM, Idoko IA. 2019. Groundwater Potential Mapping In Ado Ekiti, Nigeria Using GIS And Remote Sensing Techniques. *Int J Adv Res Publ* [Internet]. 3(3):18–21. <https://www.researchgate.net/publication/331792355>
- Okoli FU, Campus E, Polytechnic KS. 2017. Mapping Groundwater Potential Zones in Enugu State using Remote Sensing and GIS Techniques. 5(1):33–46.
- Oseji JO. 2010. Geoelectric investigation of groundwater resources and aquifer characteristics in Utagba-Ogbe kingdom Ndokwa land area of Delta State , Nigeria. 2(April):38–46.
- Osibanjo O, Majolagbe AO. 2012. Physicochemical Quality Assessment of Groundwater Based on Land Use in Lagos city , Southwest , Nigeria. 02(02):79–86.
- Oyedotun TDT. 2020. Quantitative assessment of the drainage morphometric characteristics of Chaohu Lake Basin from SRTM DEM Data: a GIS-based approach. *Geol Ecol Landscapes* [Internet]. [accessed 2020 Oct 31]:1–14. <https://www.tandfonline.com/doi/full/10.1080/24749508.2020.1812147>
- Pandey A, Sahu AK. 2000. Generation of curve number using remote sensing and geographic information system. In: *Water Resour Map India Conf (Vol 6)*. -; p. 1–4.
- Pandit A, Heck HH. 2009. Estimations of Soil Conservation Service Curve Numbers for Concrete and Asphalt. *J Hydrol Eng* [Internet]. 14(4):335–345. <https://ascelibrary.org/doi/abs/10.1061/%28ASCE%291084-0699%282009%2914%3A4%28335%29>
- Partridge EA. 1908. The electron theory. *J Franklin Inst*. 165(5):385–396.
- Patel KM, Devatha CP. 2019. Investigation on leaching behaviour of toxic metals from biomedical ash and its controlling mechanism. *Environ Sci Pollut Res*. 26(6):6191–6198.

-
- Patil SG, Mohite NM. 2014. Identification of groundwater recharge potential zones for a watershed using remote sensing and GIS. *Int J GEOMATICS Geosci* [Internet]. 4(3):485–498. www.gdem.aster.ersdac.or.jp
- Paudyal R, Kang S, Sharma CM, Tripathi L, Sillanpää M. 2016. Variations of the Physicochemical Parameters and Metal Levels and Their Risk Assessment in Urbanized Bagmati River, Kathmandu, Nepal. *J Chem* [Internet]. 2016:1–13. <https://www.hindawi.com/journals/jchem/2016/6025905/>
- Penman HL. 1950. The water balance of the Stour catchment area. *J Inst Water Eng.* 4(6):457–469.
- Phoca I, Valavanis P. 1999. *Rediscovering Ancient Greece: Architecture and city planning*. Athens: Kedros Books.
- Ponce VM, Hawkins RH. 1996. Runoff Curve Number: Has It Reached Maturity? *J Hydrol Eng* [Internet]. 1(1):11–19. <https://ascelibrary.org/doi/abs/10.1061/%28ASCE%291084-0699%281996%291%3A1%2811%29>
- Poongothai S, Sridhar N. 2017. Application of Geoelectrical Resistivity Technique for Groundwater Exploration in Lower Ponnaiyar SubWatershed, Tamilnadu, India. In: *IOP Conf Ser Earth Environ Sci* [Internet]. Vol. 80. Tirumalaisamudram, Thanjavur, India: IOP Publishing; p. 12071. <https://iopscience.iop.org/article/10.1088/1755-1315/80/1/012071/pdf>
- Prabhu K, Sivakumar R. 2018. Geoelectrical resistivity survey for groundwater potential – A case study of Nandi river basin, Tamil Nadu, India. *Appl Ecol Environ Res.* 16(2):1961–1972.
- Pradhan Ratika, Pradhan Mohan P., Ghose M.K., Agarwal Vivek S., Agarwal Shakshi. 2010. Estimation of Rainfall Runoff using Remote Sensing and GIS in and around Singtam, East Sikkim-. *Int J Geomatics Geosci* [Internet]. 1(3):466–476. <http://www.indianjournals.com/ijor.aspx?target=ijor:ijggs&volume=1&issue=3&article=015>
- Prasad BN, Saxena M. 1980. Ecological study of blue green algae in river Gomati [India]. *Indian J Environ Health.* 22:151–168.
- Radhakrishna BP. 1967. The western ghats of Indian Peninsula. In: *Sem Geomor stud India*. University of Saugar; p. 4–14.
- Radhakrishna BP. 1989. Suspect tectonostratigraphic terrain elements in the Indian Subcontinent. *Jour Geol Soc India.* 34:1–24.
- Radhakrishna BP. 1993. Neogene uplift and geomorphic rejuvenation of the Indian

-
- Peninsula. *Curr Sci* [Internet]. 64(11):787–793. www.jstor.org/stable/24096189
- Radhakrishna BP, Vaidyanathan R. 1994. *Geology of Karnataka*. Bangalore: Geological Society of India.
- Raghavan BR. 1988. *Geomorphology and evolution of the Sita and Swarna River Basin, Karnataka, India*. [place unknown]: Mangalore University.
- Rahman A. 2008. A GIS based DRASTIC model for assessing groundwater vulnerability in shallow aquifer in Aligarh, India. *Appl Geogr*. 28(1):32–53.
- Ramanuja CKR. 2012. *Geophysical Techniques for Groundwater Exploration (with special reference to Resistivity Techniques)*. Hyderabad: Professional Books Publisher.
- Randolph J. 2009. *A Guide to Writing the Dissertation Literature Review*. *Pract Assessment, Res Eval*. 14:13.
- Ranganathan N, Jayaram S. 2006. *Geomorphology of Karnataka (South India)*. Bangalore: Karnataka Geologist's Association.
- Ranganna G, Lokesh KN, Gajendragad M, Chandrakanth G, Harshendra K, Ars AK, Kori MM. 1991. Studies on infiltration characteristics of Pavanje river basin in Dakshina Kannada District of Karnataka. *Hydrol J*. 14:33–40.
- Rao GT, Rao VVSG, Ranganathan K. 2013. Hydrogeochemistry and groundwater quality assessment of Ranipet industrial area, Tamil Nadu, India. (3):855–867.
- Rao K. 1970. Hydrometeorological aspects of estimating ground water potential. *Semin Gr Water Potential Hard Rock Areas*. 1(1):1–18.
- Rao NS. 2009. A Numerical Scheme for Groundwater Development in a Watershed Basin of Basement Terrain: A Case Study from India. *Hydrogeol J* [Internet]. 17:379–396. <https://www.jstor.org/stable/24096189?seq=1>
- Rawat KS, Mishra AK, Sehgal VK, Ahmed N, Tripathi VK. 2013. Comparative evaluation of horizontal accuracy of elevations of selected ground control points from ASTER and SRTM DEM with respect to CARTOSAT-1 DEM: a case study of Shahjahanpur district, Uttar Pradesh, India. *Geocarto Int* [Internet]. 28(5):439–452. <https://www.tandfonline.com/doi/abs/10.1080/10106049.2012.724453>
- Reddy PJR. 2004. *A text book of hydrology* [Internet]. [place unknown]: Laxmi Publications. https://books.google.co.in/books?hl=en&lr=&id=5BwmnVsO_noC&oi=fnd&pg=PA1&dq=Text+book+of+Hydrology&ots=MezSJ37nl2&sig=M939GAJ7QzmmhKJAYahDKFCWihVY#v=onepage&q=Text+book+of+Hydrology&f=false
- Reghunath R. 1999. *Hydrogeological studies of Nethravathi River basin Karnataka*

state India [Internet]. [place unknown]: Mangalore University. <http://hdl.handle.net/10603/131884>

Rushton K. 1997. Recharge of phreatic aquifers in (semi)arid areas [Internet]. 1st ed. Ian Simmers, editor. Rotterdam: Balkema, AA. [https://books.google.co.in/books?hl=en&lr=&id=3GhQDwAAQBAJ&oi=fnd&pg=PT225&dq=Rushton+K+\(1997\)+Recharge+from+permanent+water+bodies.+In:+Simmers+I+\(ed\)+Recharge+of+phreatic+aquifers+in+\(semi\)arid+areas.+AA+Balkema,+Rotterdam,+pp+215-255&ots=J5-E1NDOYv&sig](https://books.google.co.in/books?hl=en&lr=&id=3GhQDwAAQBAJ&oi=fnd&pg=PT225&dq=Rushton+K+(1997)+Recharge+from+permanent+water+bodies.+In:+Simmers+I+(ed)+Recharge+of+phreatic+aquifers+in+(semi)arid+areas.+AA+Balkema,+Rotterdam,+pp+215-255&ots=J5-E1NDOYv&sig)

Saaty TL. 1980. The analytic hierarchy process: planning, priority setting, resource allocation. New York: McGraw-Hill.

Sarkar D, Mondal P, Sutradhar S, Sarkar P. 2020. Morphometric Analysis Using SRTM-DEM and GIS of Nagar River Basin, Indo-Bangladesh Barind Tract. *J Indian Soc Remote Sens* [Internet]. 48(4):597–614. <https://link.springer.com/article/10.1007/s12524-020-01106-7>

Sawyer CN. 1959. Chemistry in sanitary engineering. *J Chem Educ.* 36(2):95.

Schumm SA. 1956. Evolution of drainage systems and slopes in badlands at Perth Amboy, New Jersey. *Bull Geol Soc Am.* 67:597–646.

Sehgal SR. 1973. Ground water resources of Punjab State-a recent study. In: CBI P Annu Res Sess. New Delhi: CBI and P Annual Research Session.

Selvam S, Magesh NS, Sivasubramanian P, Soundranayagam JP, Manimaran G, Seshunarayana T. 2014. Deciphering of groundwater potential zones in Tuticorin, Tamil Nadu, using remote sensing and GIS techniques. *J Geol Soc India.* 84(5):597–608.

Selvam S, Venkatramanan S, Sivasubramanian P, Chung SY, Singaraja C. 2017. Geochemical characteristics and evaluation of minor and trace elements pollution in groundwater of Tuticorin city, Tamil Nadu, India using geospatial techniques. *J Geol Soc India.* 90(1):62–68.

Senanayake IP, Dissanayake DMDOK, Mayadunna BB, Weerasekera WL. 2016. Geoscience Frontiers An approach to delineate groundwater recharge potential sites in Ambalantota, Sri Lanka using GIS techniques. *Geosci Front* [Internet]. 7(1):115–124. <http://dx.doi.org/10.1016/j.gsf.2015.03.002>

Shahzad F, Mahmood SA, Gloaguen R. 2009. Drainage network and lineament analysis: An approach for Potwar Plateau (Northern Pakistan). *J Mt Sci* [Internet]. 6(1):14–24. <http://link.springer.com/10.1007/s11629-009-0206-4>

Shankar RMN, Mohan G. 2005. A GIS based hydrogeomorphic approach for

identification of site-specific artificial-recharge techniques in the Deccan Volcanic Province. *J Earth Syst Sci* [Internet]. 114(5):505–514. <http://link.springer.com/10.1007/BF02702026>

Shekhar S, Pandey AC. 2015. Delineation of groundwater potential zone in hard rock terrain of India using remote sensing, geographical information system (GIS) and analytic hierarchy process (AHP) techniques. *Geocarto Int* [Internet]. 30(4):402–421. <http://dx.doi.org/10.1080/10106049.2014.894584>

Sherman LK. 1949. *The Unit Hydrograph Method in Physics of the Earth* [Internet]. OE Meinzer, editor. [place unknown]. [https://scholar.google.com/scholar_lookup?title=The unit hydrograph method%2C Physics of the Earth&author=LK. Sherman&publication_year=1949](https://scholar.google.com/scholar_lookup?title=The+unit+hydrograph+method%2C+Physics+of+the+Earth&author=LK.Sherman&publication_year=1949)

Shivanna AM, Nagendrappa G. 2015. Water Quality Index (WQI) Approach to Evaluate the Water Quality of Certain Tank Waters of Tiptur Taluk in Tumkur District, Karnataka, India. *Curr World Environ* [Internet]. 10(1):189–198. <http://dx>.

Shrestha AK, Basnet N. 2018. The Correlation and Regression Analysis of Physicochemical Parameters of River Water for the Evaluation of Percentage Contribution to Electrical Conductivity. *J Chem*. 2018:1–9.

Singhal DC, Niwas S, Shakeel M, Adam EM. 1998. Estimation of hydraulic characteristics of alluvial aquifers from electrical resistivity data. *J Geol Soc India*. 51(4):461–470.

Smith KG. 1950. Standards for grading texture of erosional topography. *Am J Sci* [Internet]. 248:655–668. https://s3.amazonaws.com/academia.edu.documents/2438559/9fjg8q78n4wux4l.pdf?response-content-disposition=inline%3Bfilename%3DPrinciples_of_geographical_information_s.pdf&X-Amz-Algorithm=AWS4-HMAC-SHA256&X-Amz-Credential=ASIATUSBJ6BAGXNF3PNQ%2F20200504%2F

Soil Conservation Service. 1985. *Hydrology, National Engineering Handbook* [Internet]. Washington, D.C: Springer, Dordrecht. https://link.springer.com/chapter/10.1007/978-94-017-0147-1_2

Solomon S, Quiel F. 2006. Groundwater study using remote sensing and geographic information systems (GIS) in the central highlands of Eritrea. *Hydrogeol J* [Internet]. 14(6):1029–1041. <http://link.springer.com/10.1007/s10040-006-0096-2>

Soulis KX, Valiantzas JD. 2012. SCS-CN parameter determination using rainfall-runoff data in heterogeneous watersheds-the two-CN system approach. *Hydrol Earth Syst Sci*. 16(3):1001–1015.

-
- Sreedhara Murthy TR, Raghavan BR. 1994. Geomorphic facets of Karnataka. In: Ravindra BM, Ranganathan N, editors. *Geo Karnataka*. Bangalore: K.A.G.A; p. 314–327.
- Srivastava VK, Giri DN, Bharadwaj P. 2012. Study and Mapping of Ground Water Prospect using Remote Sensing, GIS and Geoelectrical resistivity techniques-a case study of Dhanbad district, Jharkhand, India. *J Ind Geophys Union* [Internet]. 16(2):55–63. http://www.j-igu.in/Archives/16-2/paper3_srivastava.pdf
- Stavi I, Siad SM, Kyriazopoulos AP, Halbac-Cotoara-Zamfir R. 2020. Water runoff harvesting systems for restoration of degraded rangelands: A review of challenges and opportunities. *J Environ Manage* [Internet]. 255(July 2019):109823. <https://doi.org/10.1016/j.jenvman.2019.109823>
- Strahler AN. 1957. Quantitative analysis of watershed geomorphology. *Trans Am Geophys Union*. 38:913–920.
- Strahler AN. 1964. Quantitative geomorphology of drainage basins and channel networks. In: Chow VT, editor. *Handb Appl Hydrol*. New York: McGraw Hill; p. 39–76.
- Subrahmanya KR, Grangadhara Bhat H. 1995. Revised geological map of Dakshina Kannada-utilising IRS data and aerial Photographs. In: *Remote Sens GIS Environ Planin*. New Delhi: Tata Me Graw-Hill Publishing Company Ltd.; p. 160–165.
- Subrahmanya KR, Jayappa KS. 1987. Origin of Netravati-Gurupur Estuarine System. In: *Natn Sem Estuar Manag*. Trivandrum; p. 70–72.
- Subramanya KR. 1987. Evolution of the Western ghats, India - a simple model. *Jour Geol Soc India*. 29:85–89.
- Sukhija BS, Nagabhushanam P, Reddy D V. 1996. Groundwater recharge in semi-arid regions of india: An overview of results obtained using tracers. *Hydrogeol J*. 4(3):50–71.
- Suphunvorrnop T. 1985. *A Guide to SCS Runoff Procedures*. Florida.
- Suresh Babu P, Mishra SK. 2011. Improved SCS-CN–Inspired Model. *J Hydrol Eng*. 17(11):1164–1172.
- Suresh Babu P, Mishra SK. 2012. Improved SCS-CN–Inspired Model. *J Hydrol Eng* [Internet]. 17(11):1164–1172. <https://ascelibrary.org/doi/abs/10.1061/%28ASCE%29HE.1943-5584.0000435>
- Thapa R, Gupta S, Guin S, Kaur H. 2017. Assessment of groundwater potential zones using multi-influencing factor (MIF) and GIS: a case study from Birbhum district, West Bengal. *Appl Water Sci* [Internet]. 7:4117–4131.

<https://link.springer.com/article/10.1007/s13201-017-0571-z>

Thapa R, Gupta S, Guin S, Kaur H. 2018. Sensitivity analysis and mapping the potential groundwater vulnerability zones in Birbhum district, India: A comparative approach between vulnerability models. *Water Sci* [Internet]. 32(1):44–66. <https://doi.org/10.1016/j.wsj.2018.02.003>

Thornthwaite CW. 1948. *An Approach toward a Rational Classification of Climate*. [place unknown].

Tiwari G, Shukla JP. 2015. A review on Remote Sensing and GIS techniques in water resource development and management with special reference to groundwater. *Int J Remote Sens Geosci* [Internet]. 4(1):10–16. www.ijrsg.com

Todd DK, Mays LW. 2005. *Groundwater Hydrology* [Internet]. 3rd ed. New Jersey: John Wiley & Sons. http://sutlib2.sut.ac.th/sut_contents/H108410.pdf

Typical resistivity values for different rocks (geosci.xyz). https://em.geosci.xyz/content/physical_properties/electrical_conductivity/electrical_conductivity_values.html#resistivity-table1

Uddin MG, Nash S, Olbert AI. 2021. A review of water quality index models and their use for assessing surface water quality. *Ecol Indic*. 122:107218.

UN. 1967. Hydrogeologic map of Lebanon. *Carte hydrogeologique ´ du Liban au 1/100000me*. Beyrouth, Liban.

USDA. 1986. *Urban Hydrology for Small Watersheds* [Internet]. Second Ed. Washington, DC. <https://tamug-ir.tdl.org/bitstream/handle/1969.3/24438/6545-UrbanHydrologyforSmallWatersheds.pdf?sequence=1&isAllowed=y>

USDA, NRCS. 2010. *Groundwater Recharge*. In: *Natl Eng Handb* [Internet]. VI. Washington, D.C; p. 33.1-33.9. <https://directives.sc.gov.usda.gov/OpenNonWebContent.aspx?content=26986.wba>

Utom AU, Odoh BI, Okoro AU. 2012. Estimation of Aquifer Transmissivity Using Dar Zarrouk Parameters Derived from Surface Resistivity Measurements: A Case History from Parts of Enugu Town (Nigeria). *J Water Resour Prot* [Internet]. 4:993–1000. <http://dx.doi.org/10.4236/jwarp.2012.412115PublishedOnlineDecember2012>

Vengosh A, Keren R. 1996. Chemical modifications of groundwater contaminated by recharge of treated sewage effluent. *J Contam Hydrol*. 23(4):347–360.

Venkateswara Rao B, Briz-Kishore BH. 1991. A methodology for locating potential aquifers in a typical semi-arid region in India using resistivity and hydrogeologic parameters. *Geoexploration*. 27(1–2):55–64.

Victor Mockus. 1972. Hydrographs, Mockus Victor Design. In: Mckeever V, Owen W, Rallison R, editors. Natl Eng Handb [Internet]. SECTION 4. Washington, DC: USDA; p. 127. http://www.irrigationtoolbox.com/NEH/Part630_Hydrology/neh630-ch21.pdf

Virupaksha HS, Lokesh KN. 2019. Electrical resistivity, remote sensing and geographic information system approach for mapping groundwater potential zones in coastal aquifers of Gurpur watershed. *Geocarto Int* [Internet]. 0(0):1–15. <https://www.tandfonline.com/action/journalInformation?journalCode=tgei20>

Waikar ML, Nilawar AP. 2014. Identification of Groundwater Potential Zone using Remote Sensing and GIS Technique. 3(5):12163–12174.

Warsi T, Kumar VS, Kumar D, Nandan MJ, Biswas G, Kumar Sahadevan D, Manikyamba C, Rao TV, Rangarajan R, Ahmed S, Chandrasekhar V. 2020. Integration of geophysics and petrography for identifying the aquifer and the rock type: A case study from Giddalur, Andhra Pradesh, India. *J Earth Syst Sci*. 129(1):1–13.

Wenner, Schlumberger and di-pole di-pole arrays of electrical resistivity method. [http://www.ukm.edu.my/rahim/Resistivity lecture.htm](http://www.ukm.edu.my/rahim/Resistivity%20lecture.htm)

Winsauer WO, Shearin HM. 1952. Resistivity of Brine-Saturated Sands in Relation to Pore Geometry. *Am Assoc Pet Geol Bull* [Internet]. 36. <http://search.datapages.com/data/doi/10.1306/3D9343F4-16B1-11D7-8645000102C1865D>

Xiong W, Li Y, Pfister S, Zhang W, Wang C, Wang P. 2020. Improving water ecosystem sustainability of urban water system by management strategies optimization. *J Environ Manage*. 254(April 2019).

Yousef AH, Priju CPP, Prasad NBBN. 2015. Delineation of Groundwater Potential Zones in Deep Midland Aquifers along Bharathapuzha River Basin , Kerala using Geophysical Methods. *Aquat Procedia* [Internet]. 4(Icwrcoe):1039–1046. <https://www.sciencedirect.com/science/article/pii/S2214241X15001327>

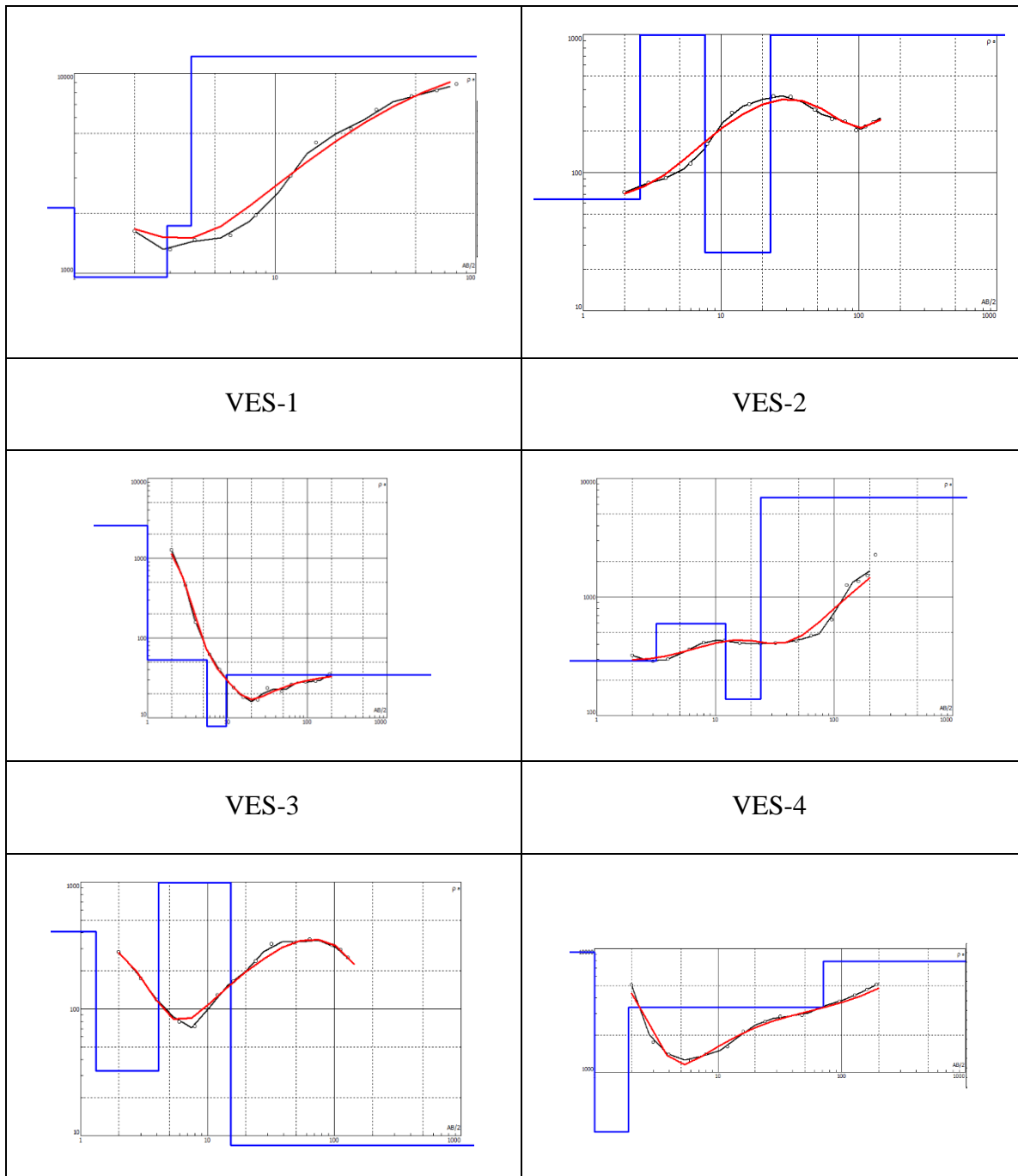
Zhan X, Huang ML. 2004. ArcCN-Runoff: An ArcGIS tool for generating curve number and runoff maps. *Environ Model Softw*. 19(10):875–879.

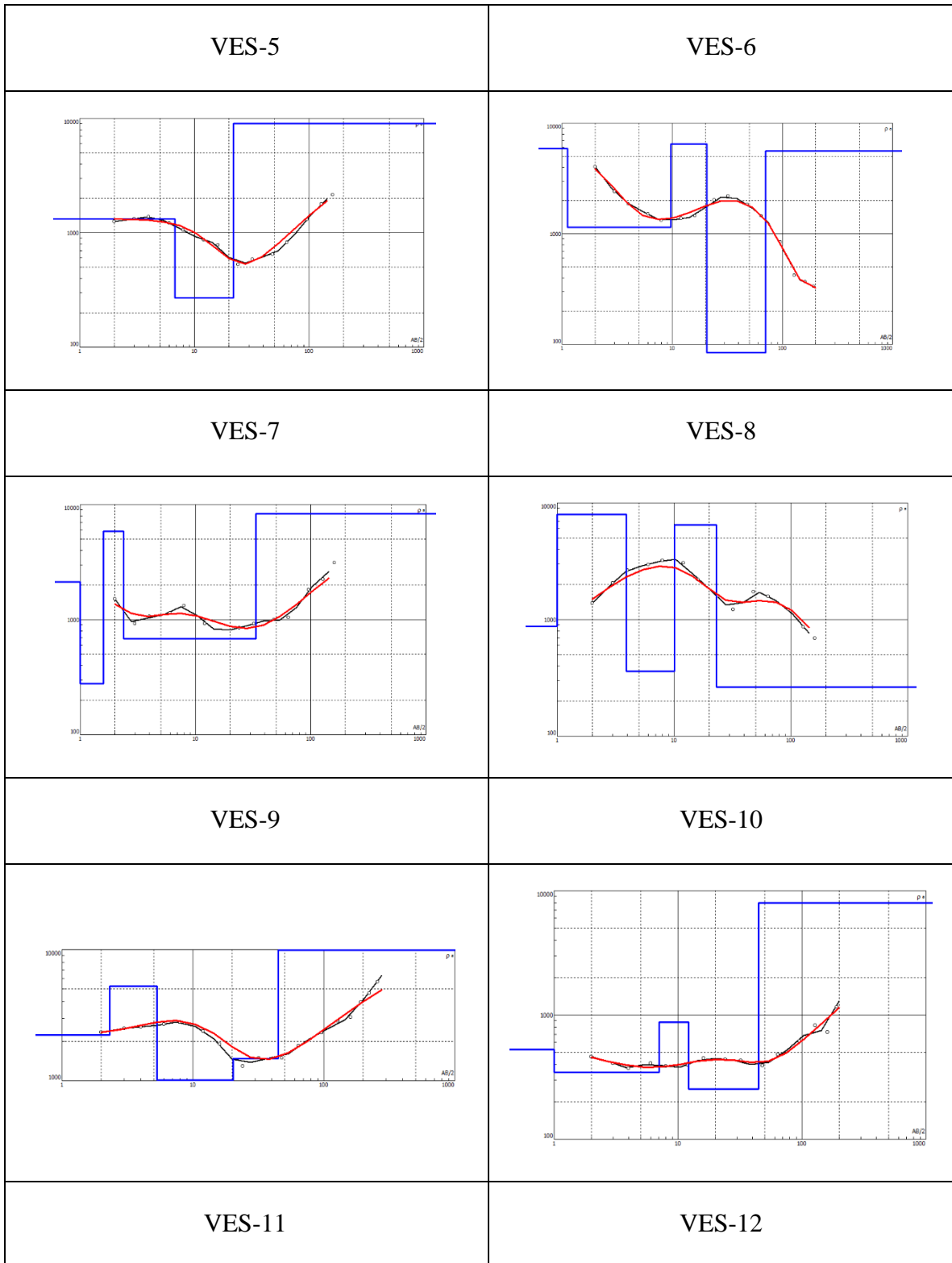
Zhang D, Gersberg RM, Wilhelm C, Voigt M. 2009. Decentralized water management: rainwater harvesting and greywater reuse in an urban area of Beijing, China. *Urban Water J* [Internet]. 6(5):375–385. <http://www.tandfonline.com/doi/abs/10.1080/15730620902934827>

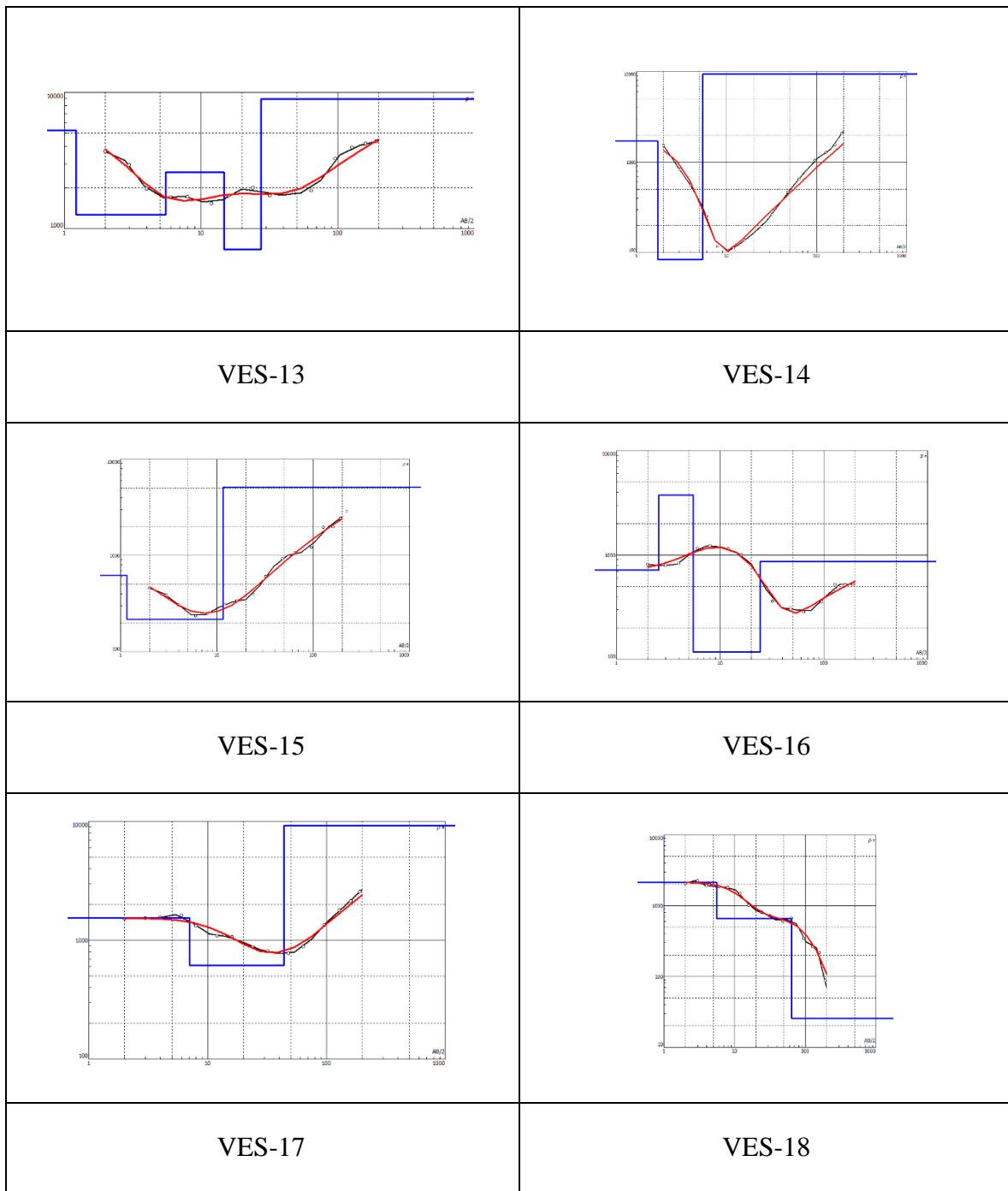
Zohdy AAR. 1969. The use of Schlumberger and Equatorial soundings in groundwater investigations near El Paso, Texas. *Geophysics* [Internet]. 34(5):713–728. <http://library.seg.org/doi/10.1190/1.1440042>

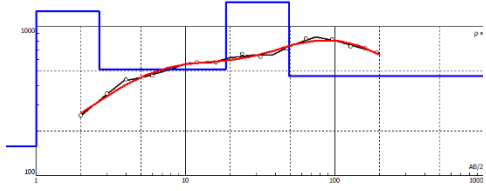
APPENDIX-A

Electrical resistivity plots generated using Curve matching interpretation technique for 35 VES locations

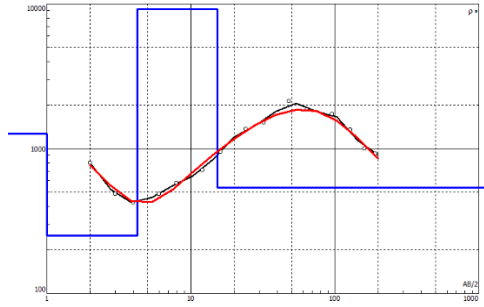




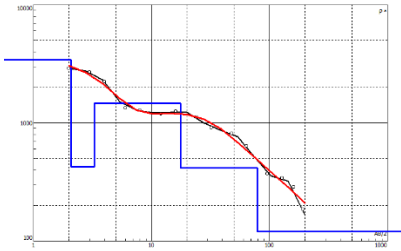




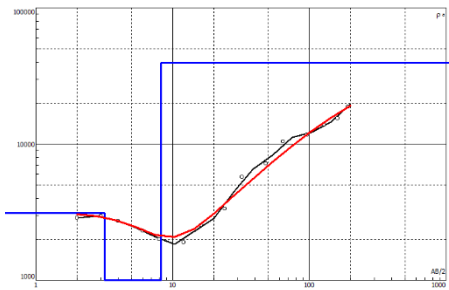
VES-19



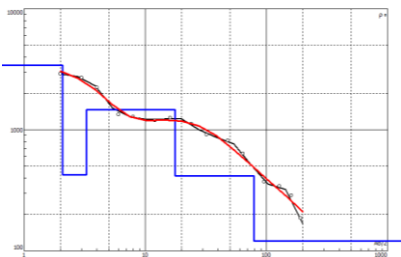
VES-20



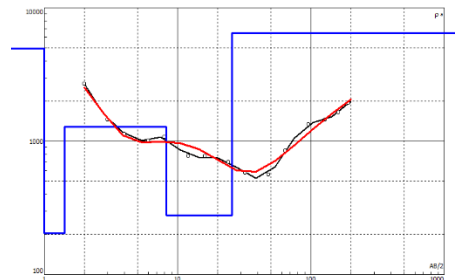
VES-21



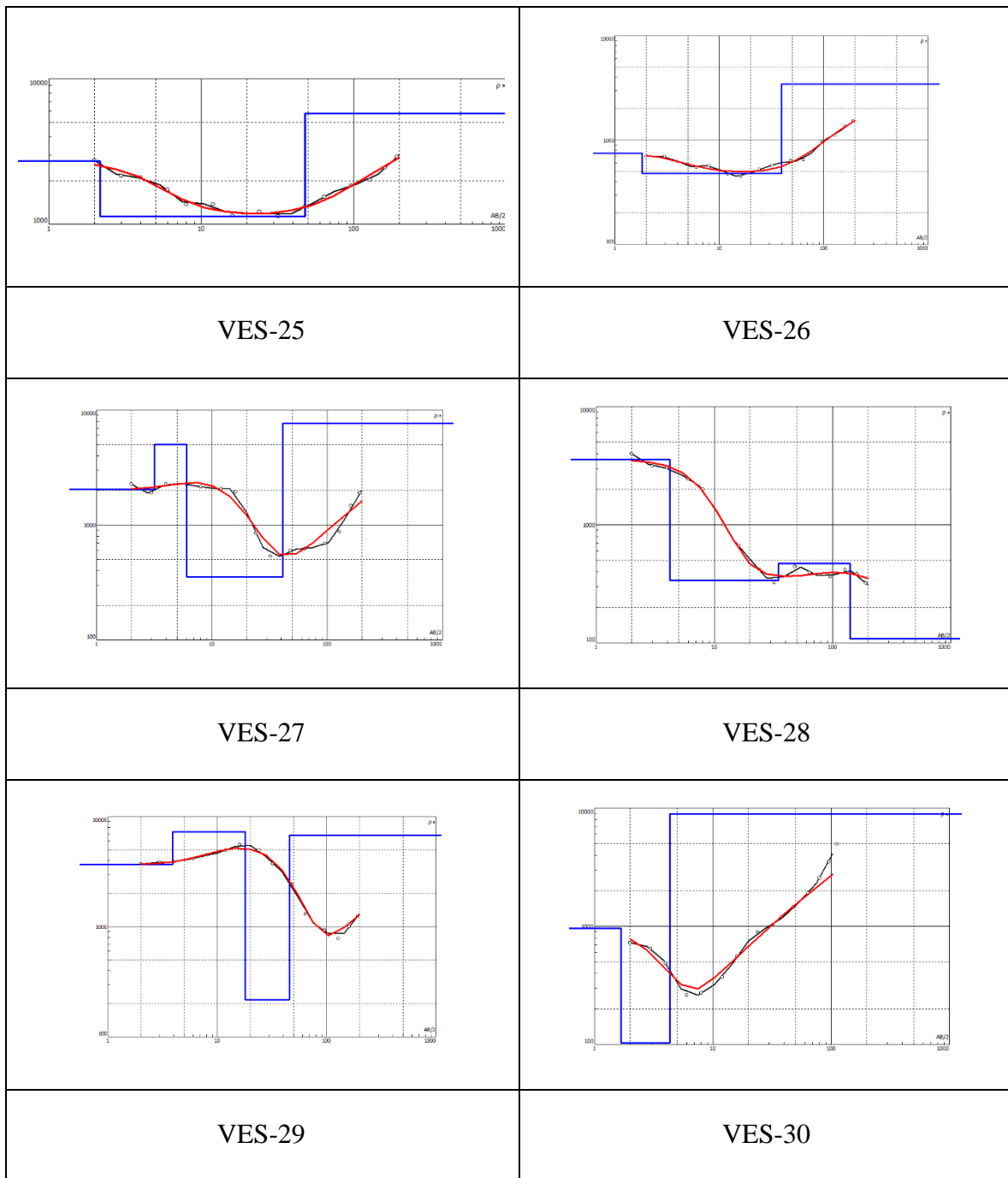
VES-22



VES-23

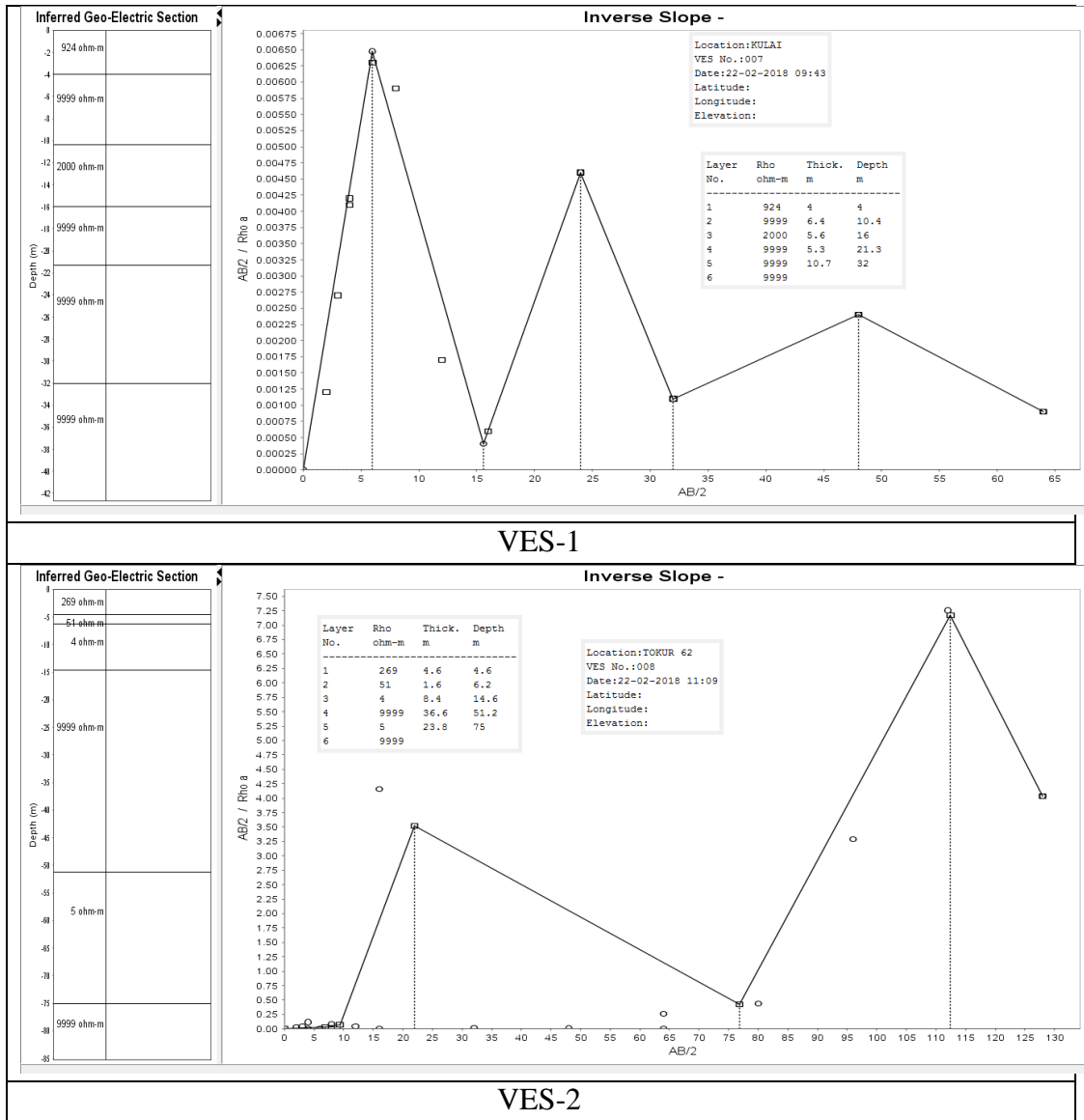


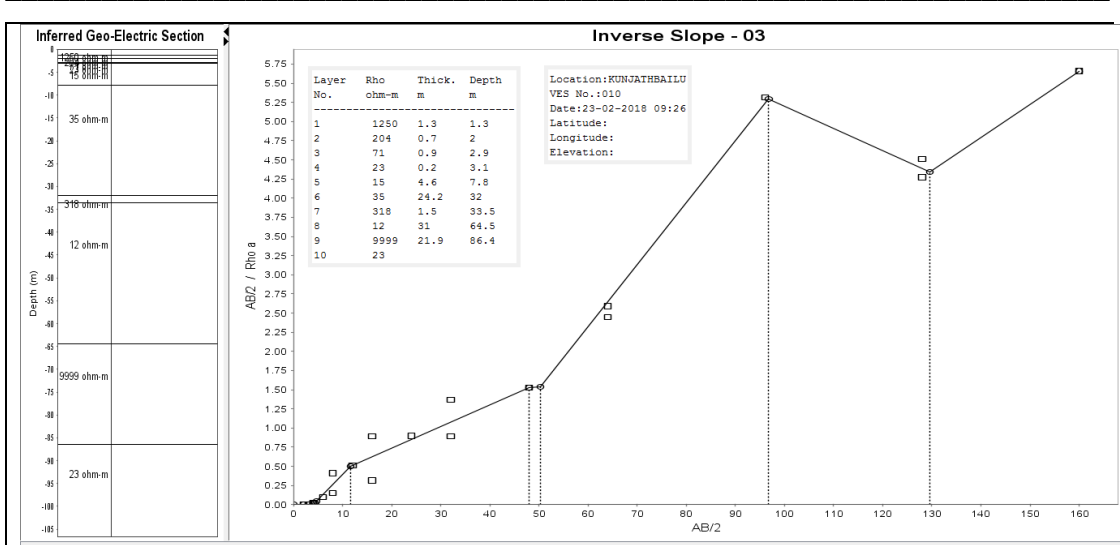
VES-24



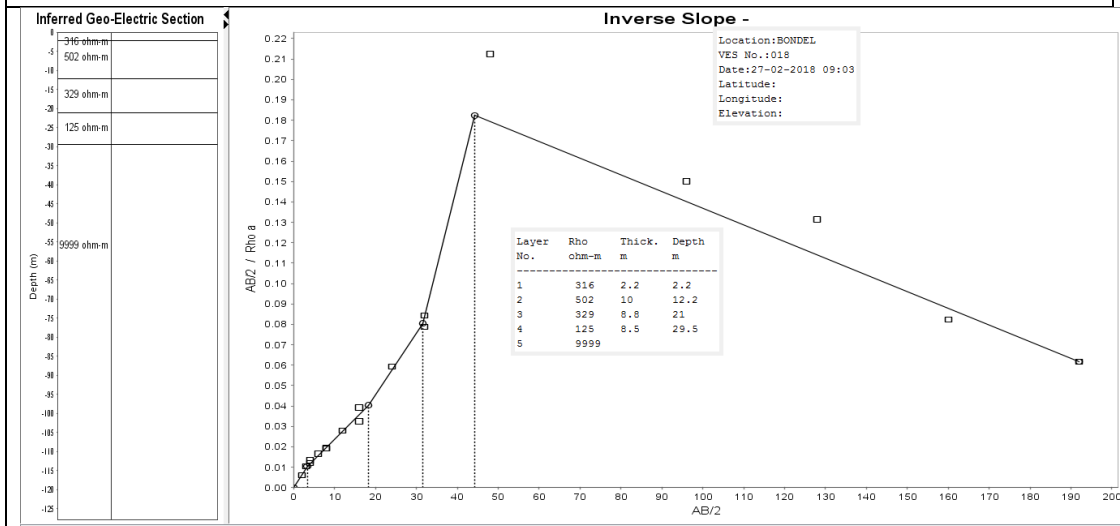
<p>VES-31</p>	<p>VES-32</p>
<p>VES-33</p>	<p>VES-34</p>
<p>VES-35</p>	

Electrical resistivity plots generated using inverse slope interpretation technique for 35 VES locations

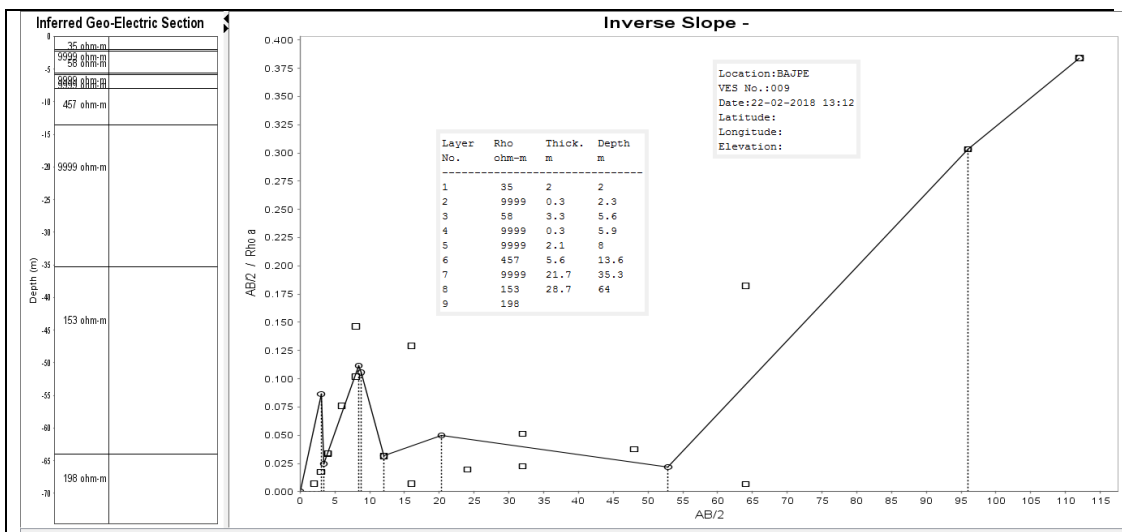




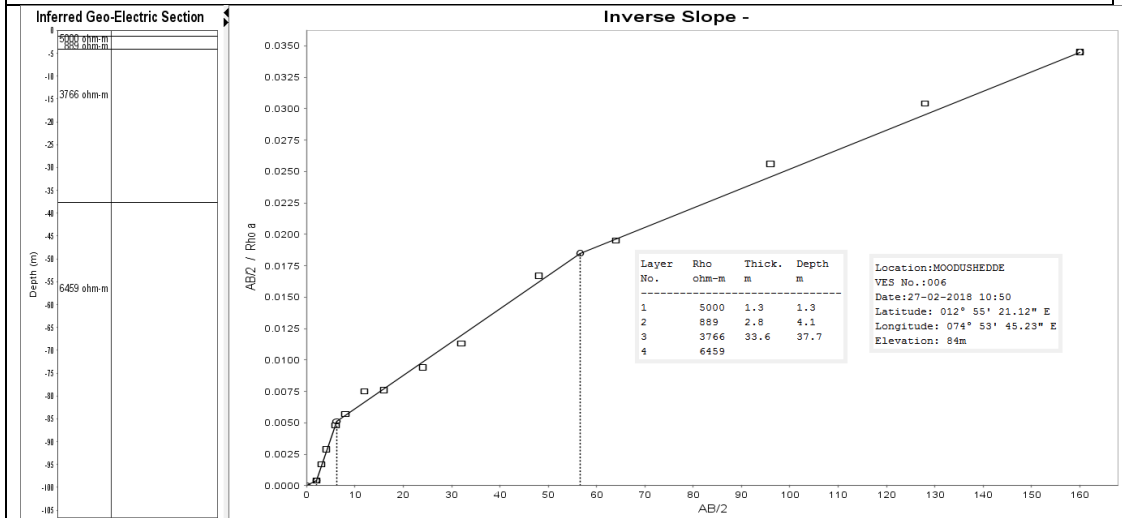
VES-3



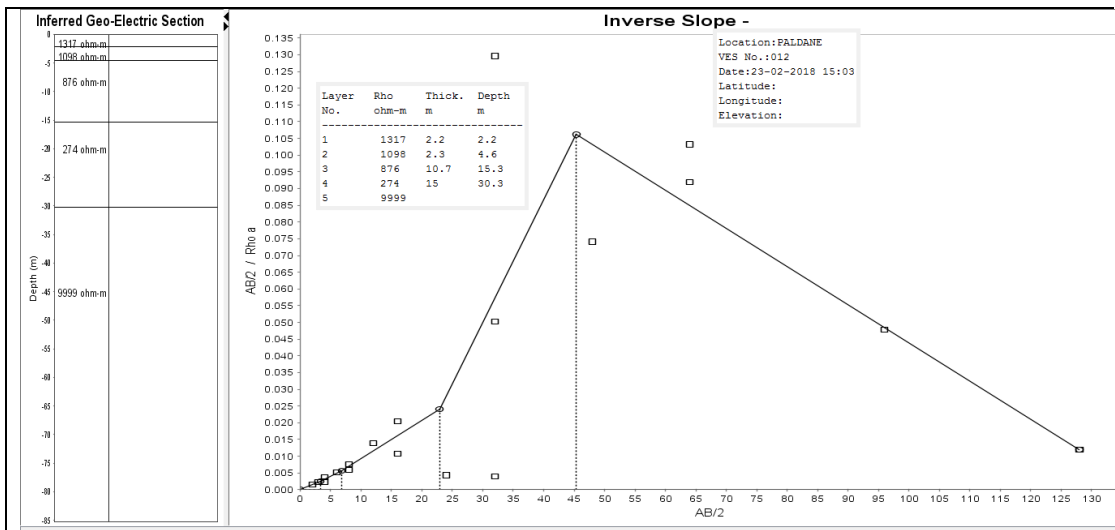
VES-4



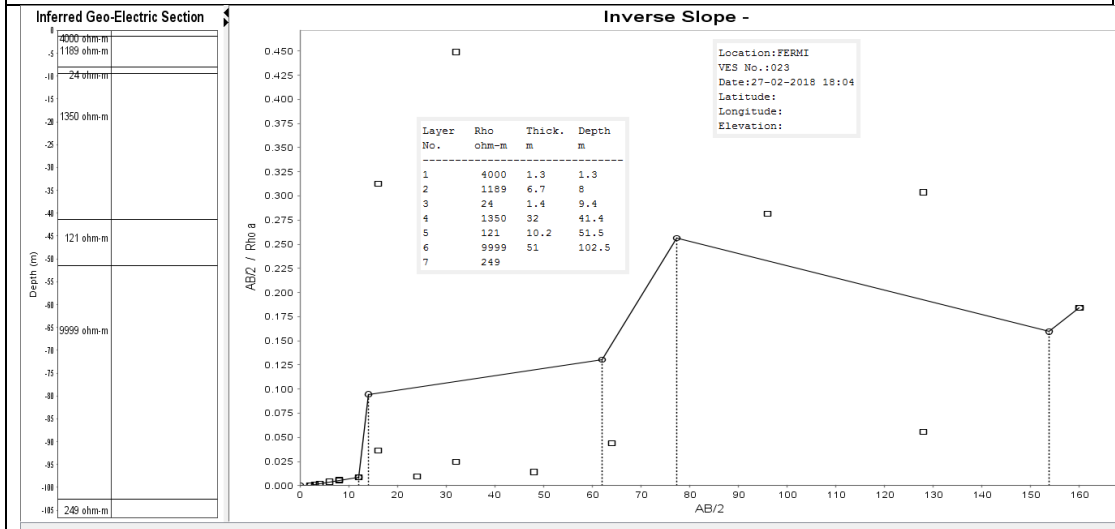
VES-5



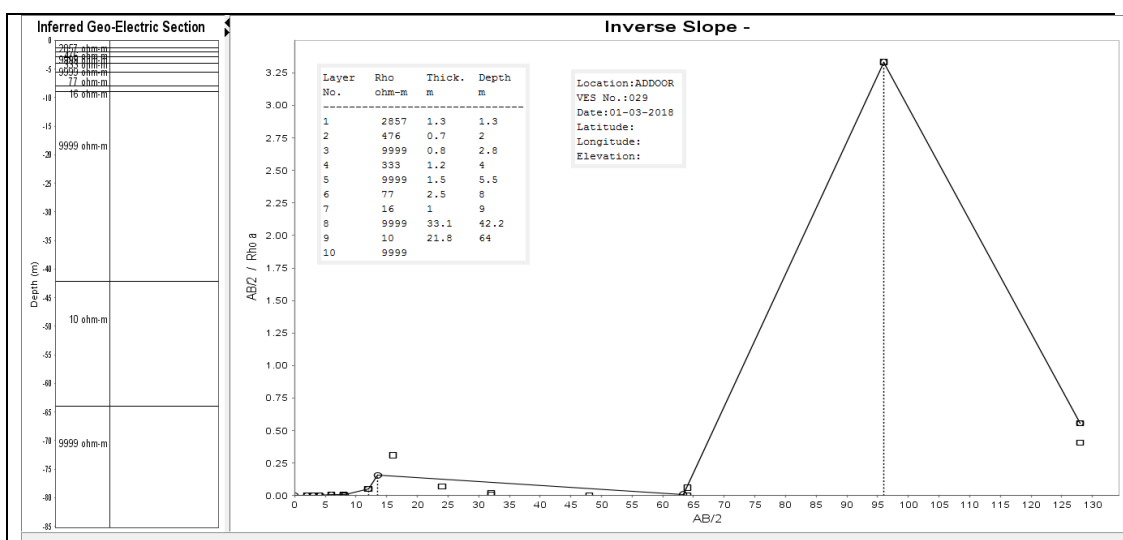
VES-6



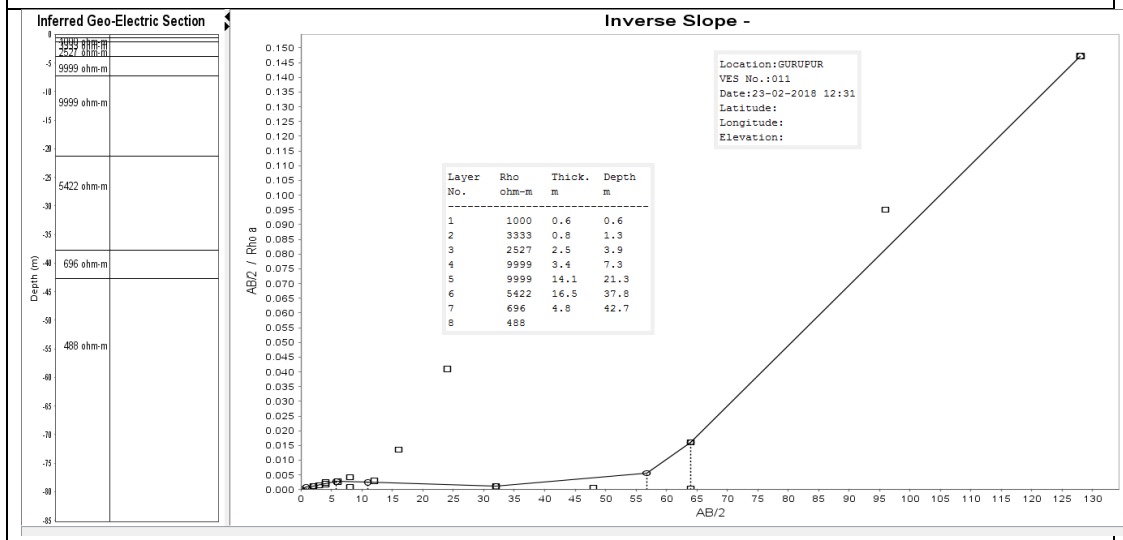
VES-7



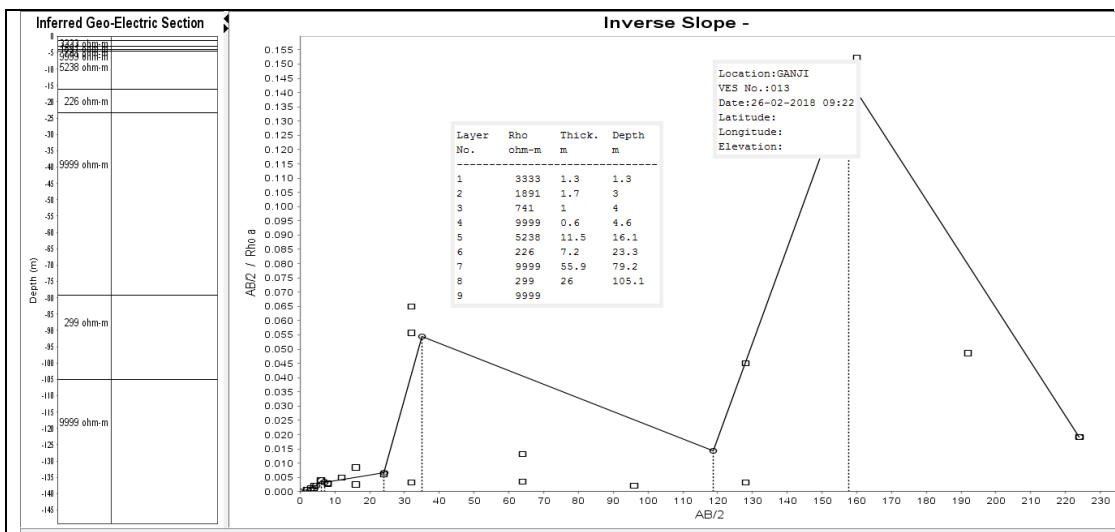
VES-8



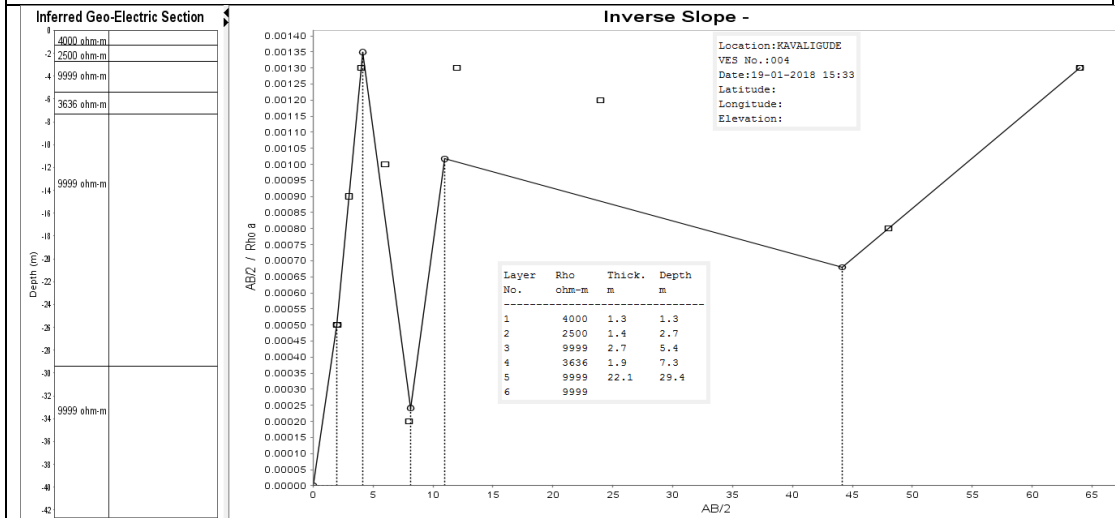
VES-9



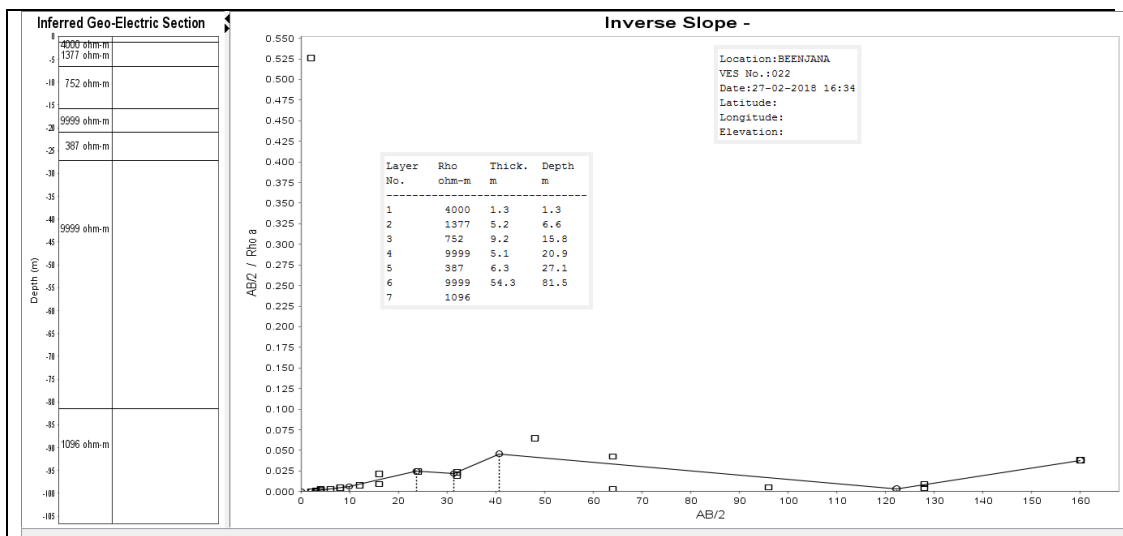
VES-10



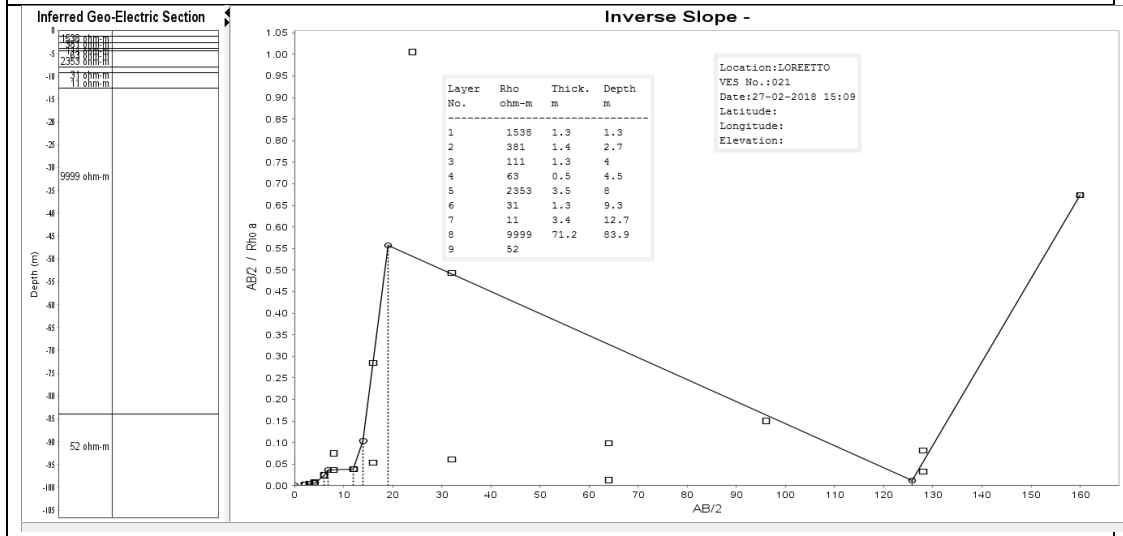
VES-11



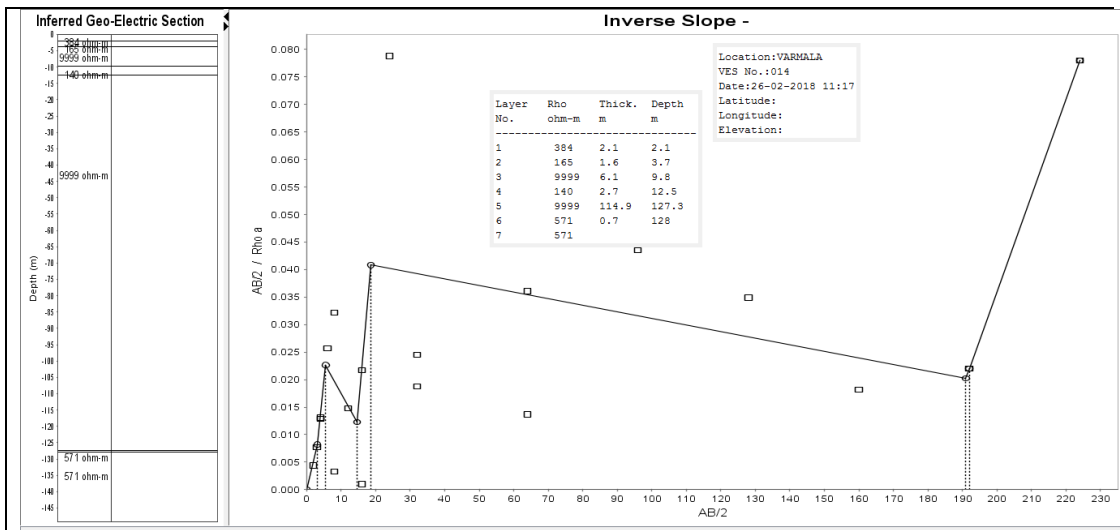
VES-12



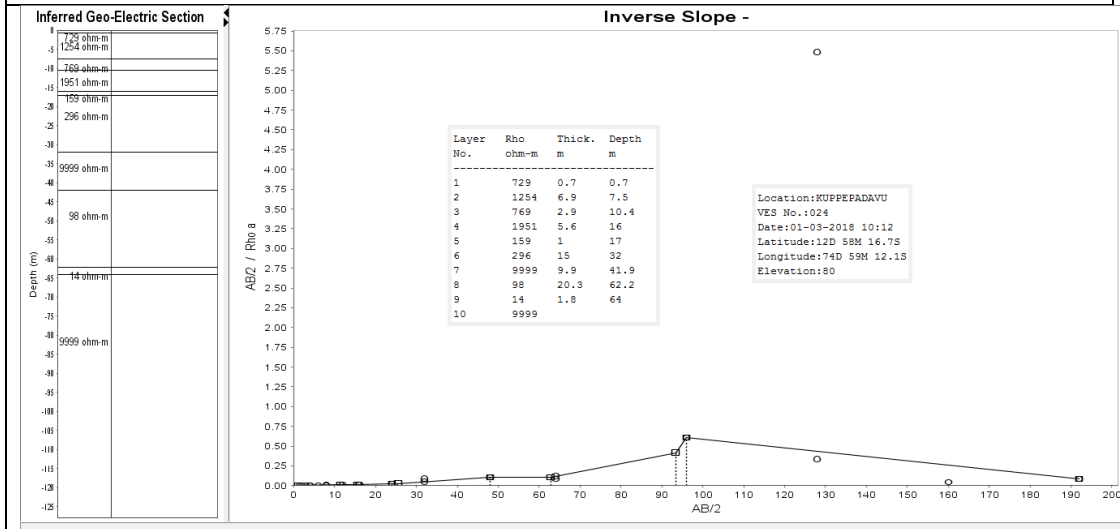
VES-13



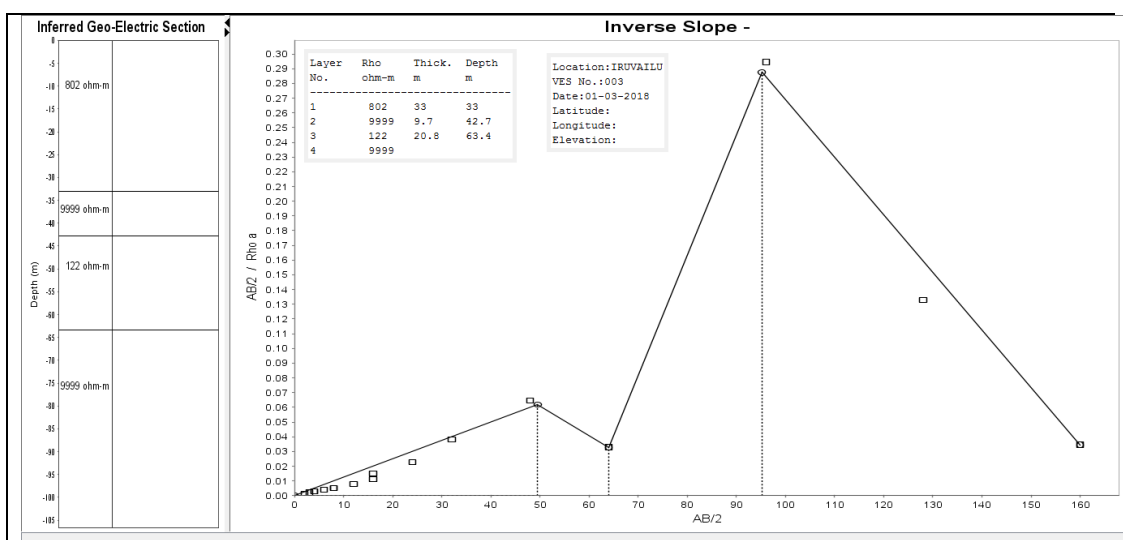
VES-14



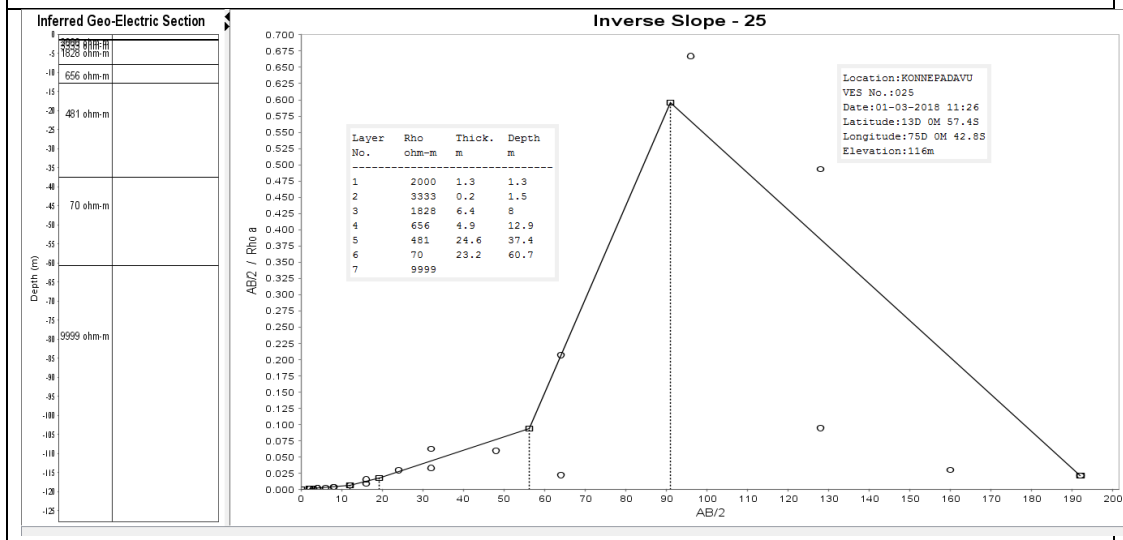
VES-15



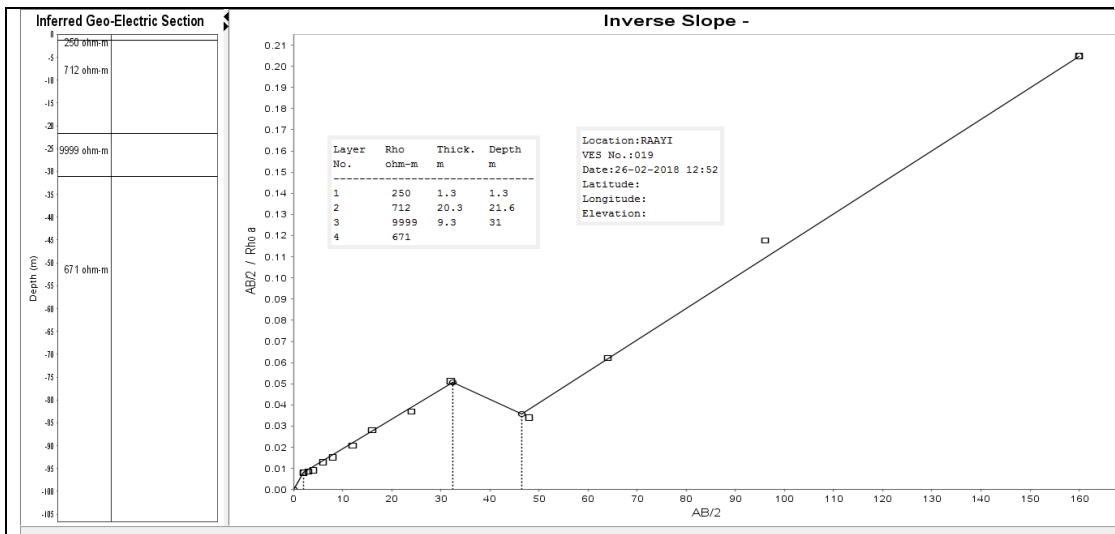
VES-16



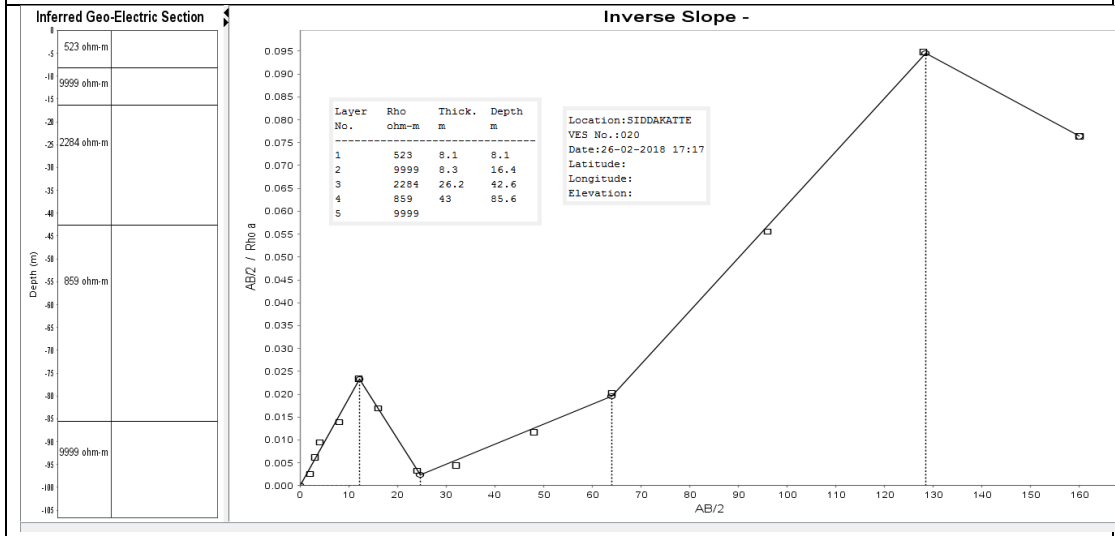
VES-17



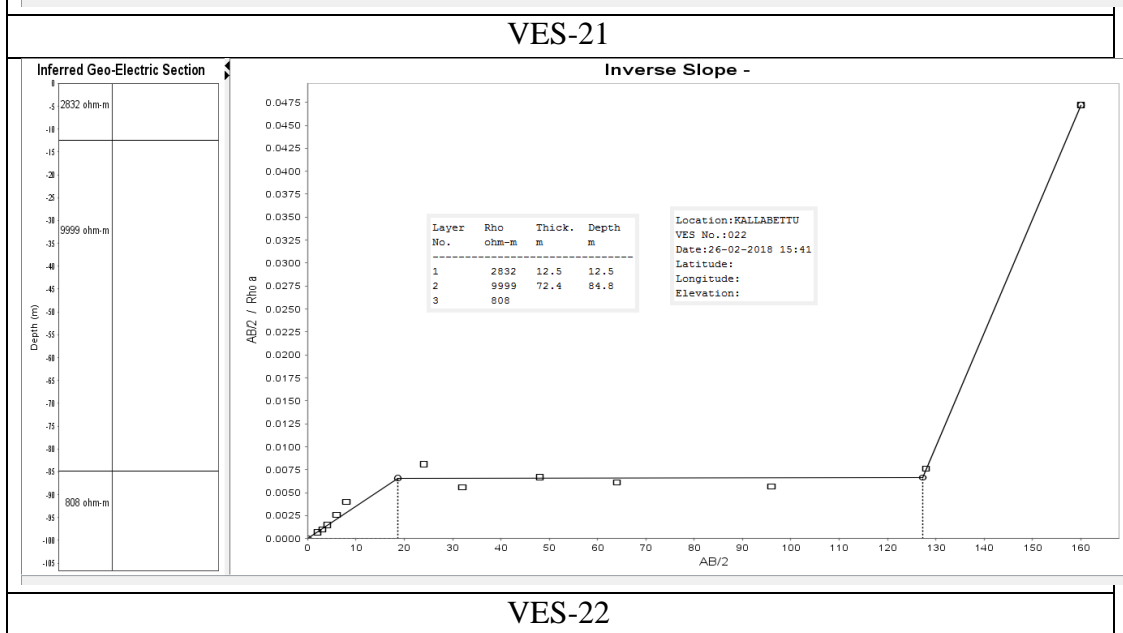
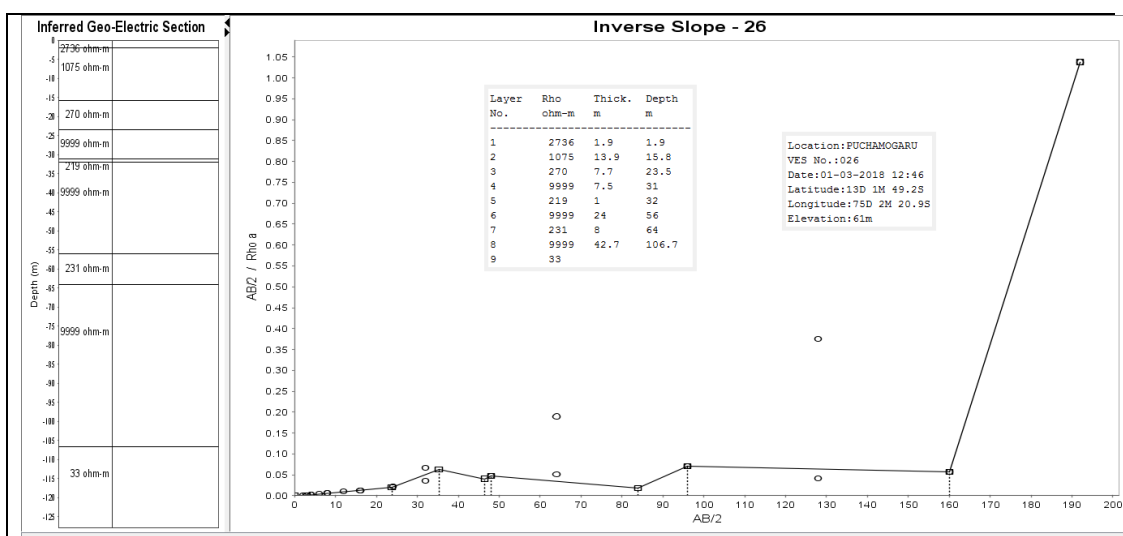
VES-18



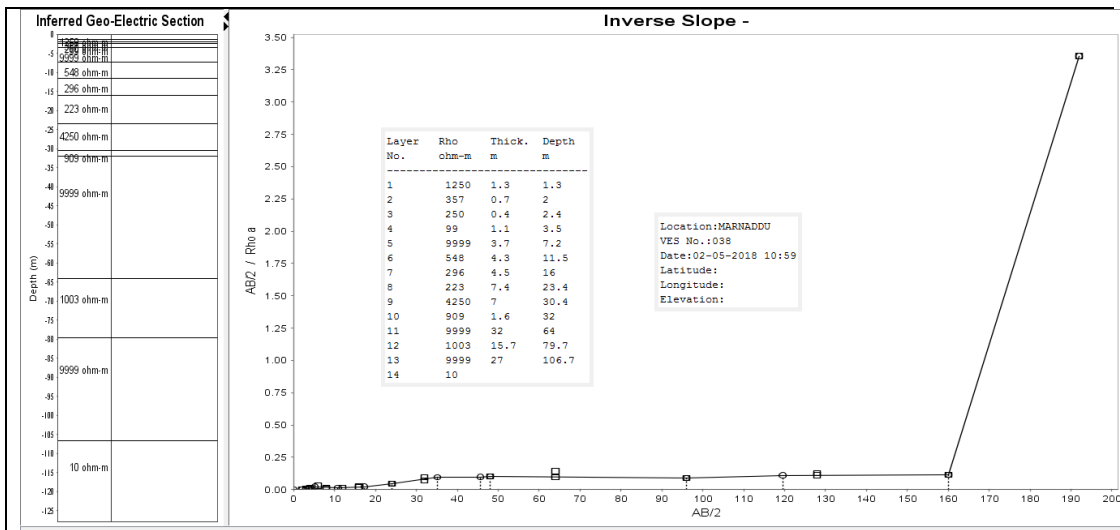
VES-19



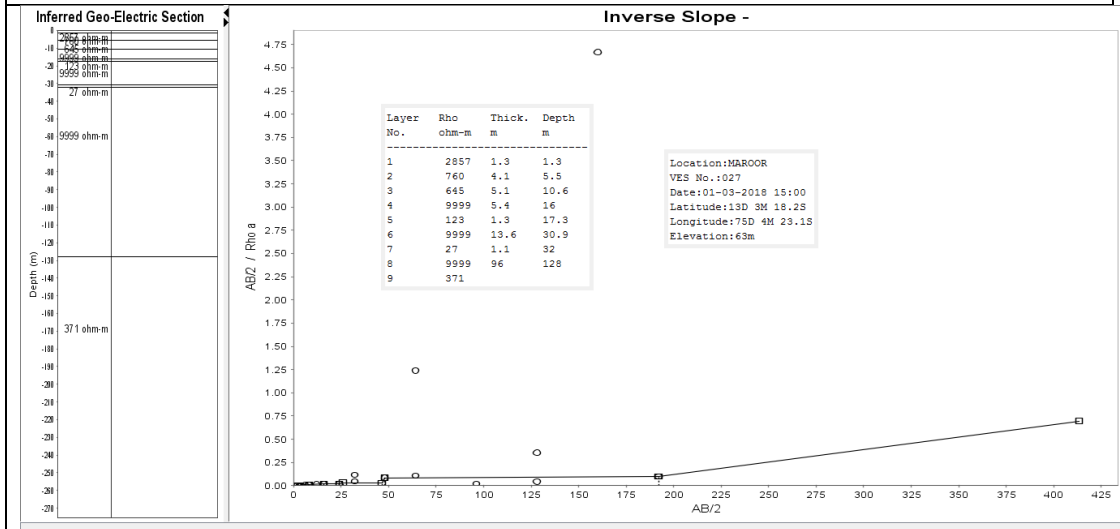
VES-20



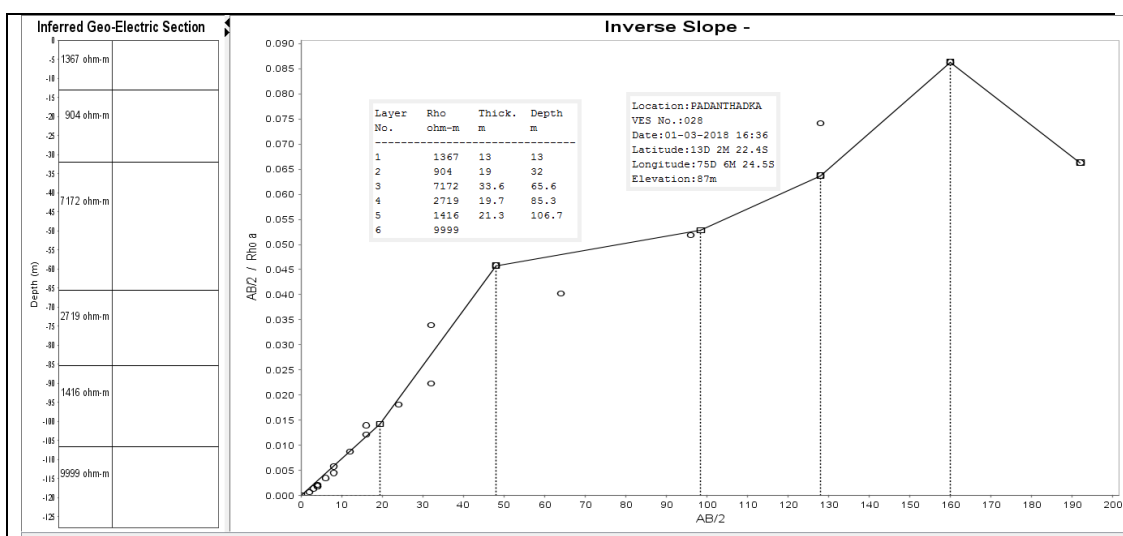
VES-22



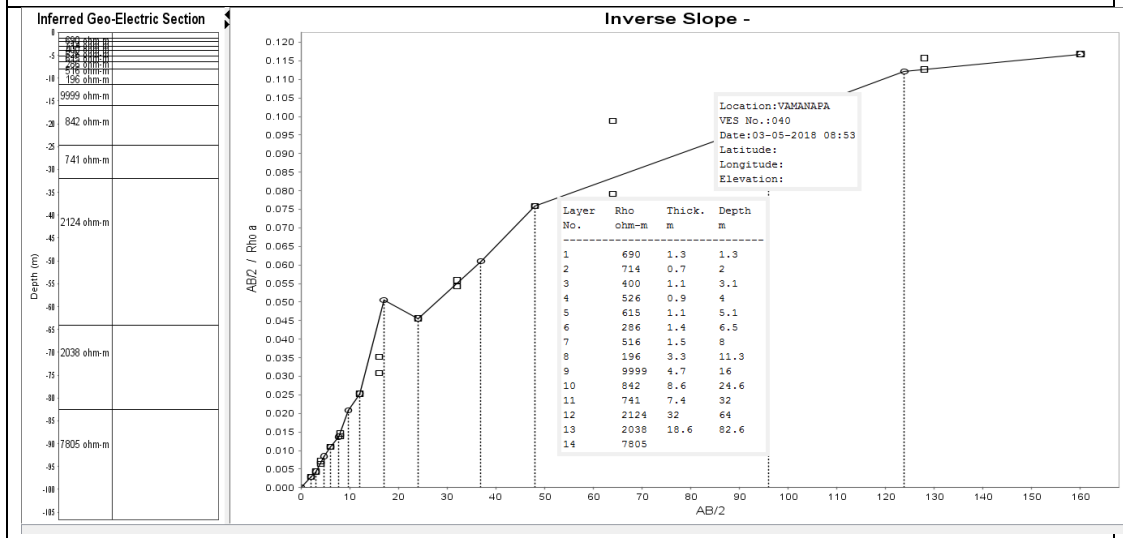
VES-23



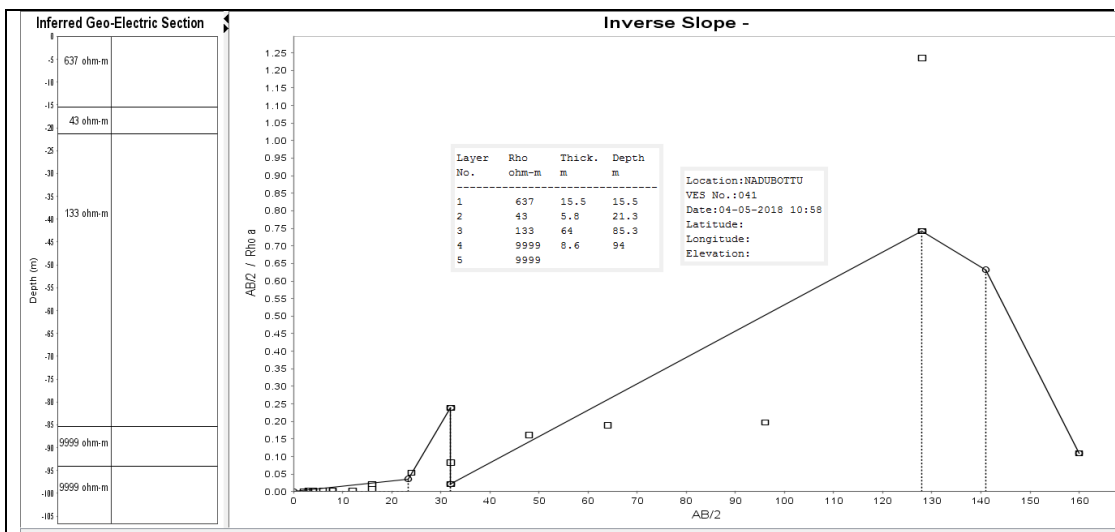
VES-24



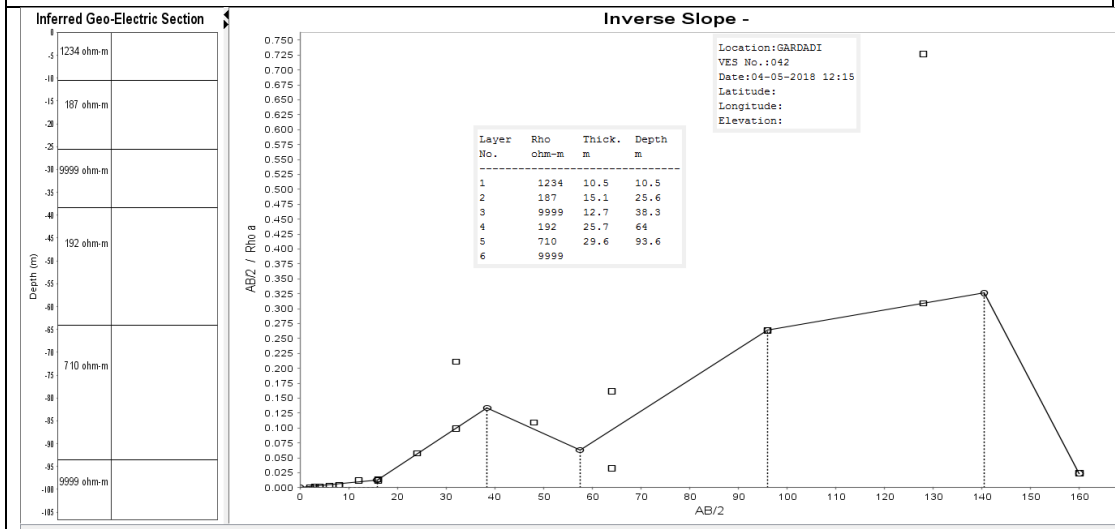
VES-25



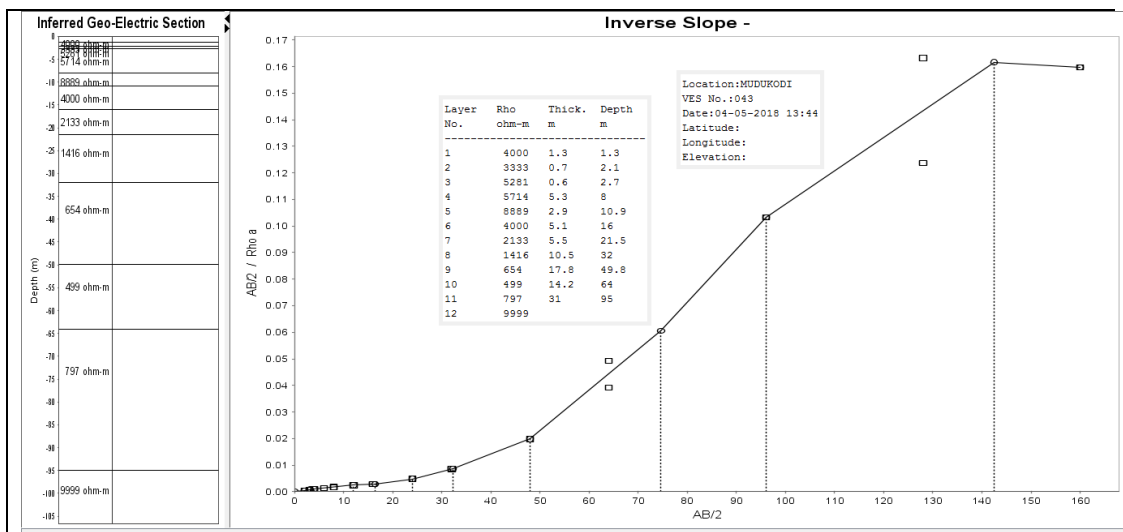
VES-26



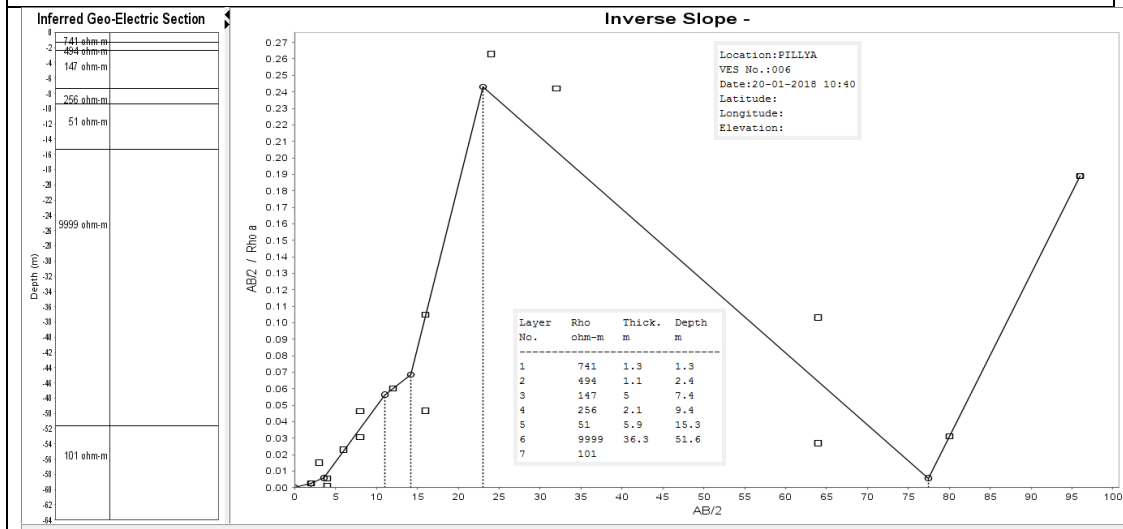
VES-27



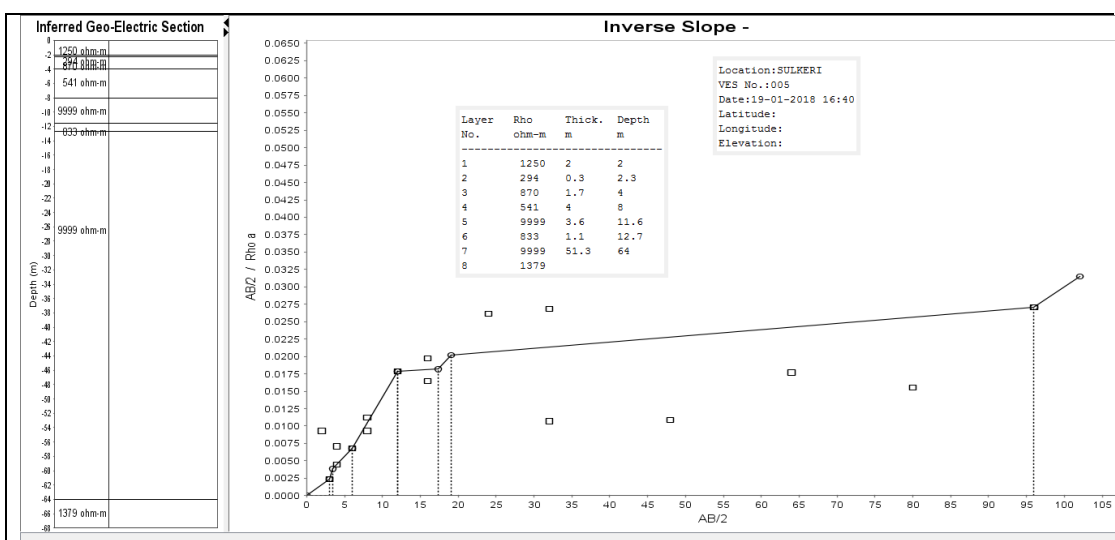
VES-28



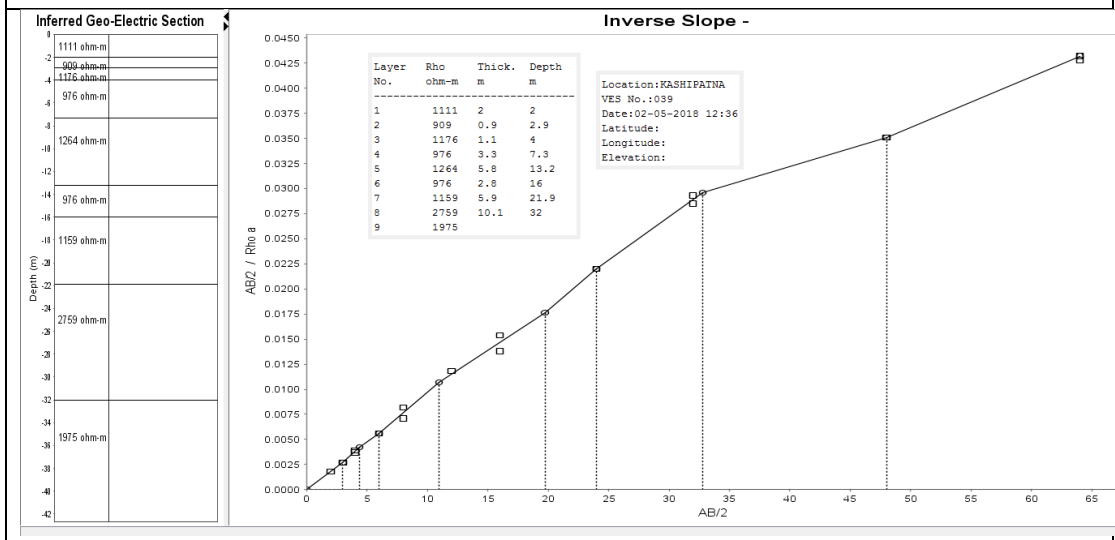
VES-29



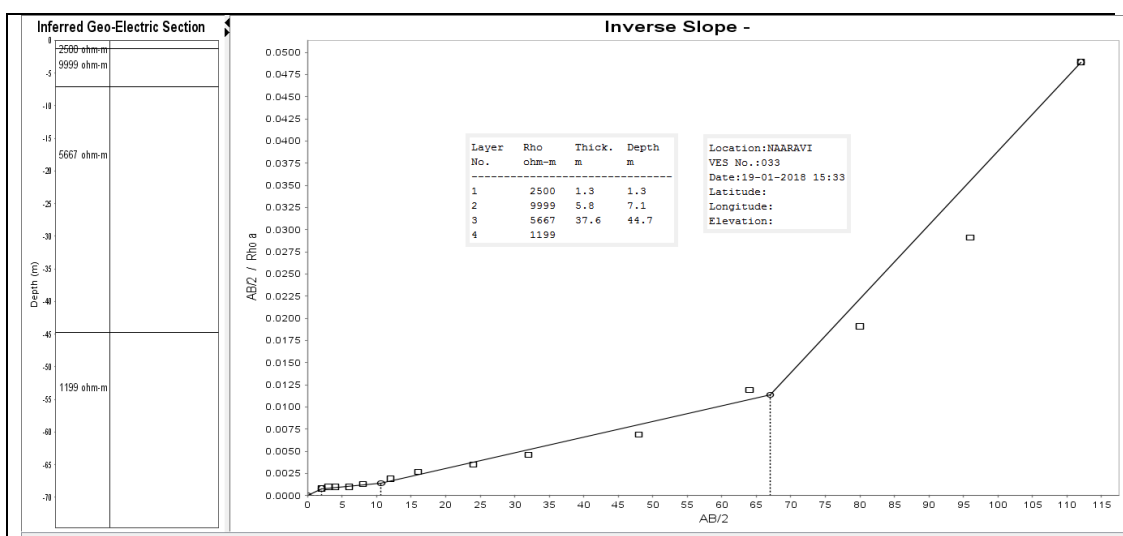
VES-30



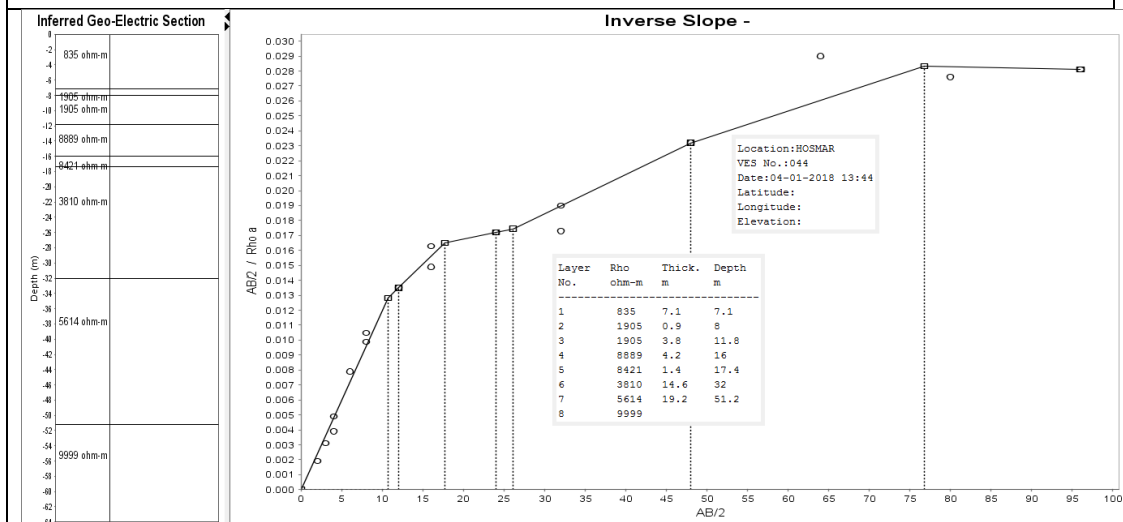
VES-31



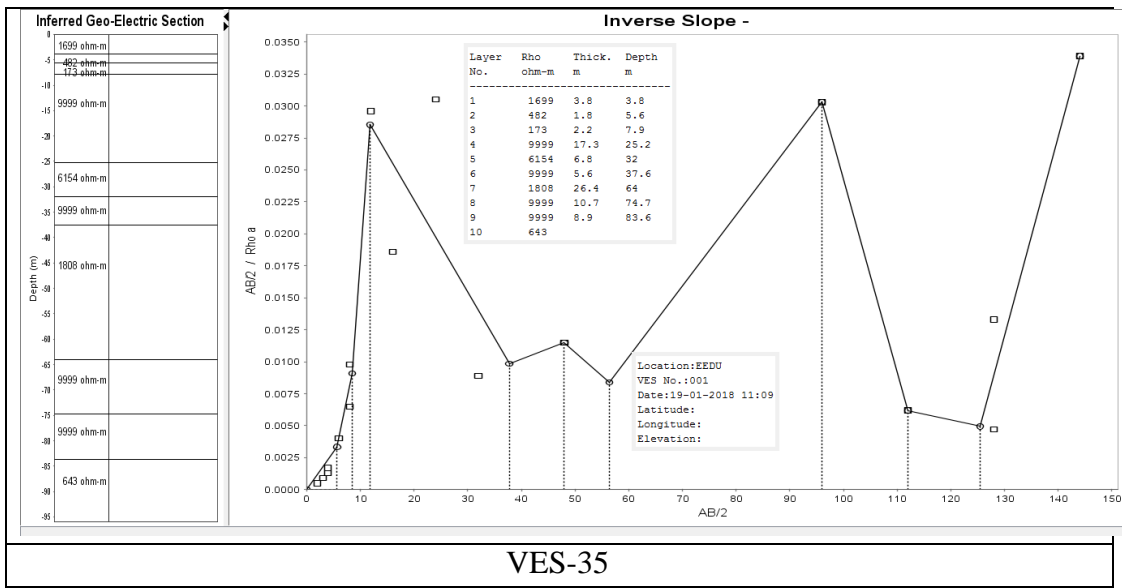
VES-32



VES-33



VES-34



APPENDIX-B

Groundwater quality data

Appendix - B 1 Groundwater Quality analysis and anion – cation balance for Phase-I (Monsoon)

Sl. No.	Smpl. No.	Ca ²⁺	Mg ²⁺	Na ⁺	K ⁺	Fe ⁺	Cations [C]	(C-A) < (±0.2)	Anions [A]	F ⁻	Cl ⁻	TA	NO ₃ ⁻	SO ₄ ²⁻
		mg/l	mg/l	mg/l	mg/l	mg/l	meq/l	meq/l	meq/l	mg/l	mg/l	mg/l	ppm	ppm
1	G1	1.44	0.51	9.30	2.38	0.03	0.58	0.02	0.56	0.05	17.16	2.98	0.17	0.68
2	G2	6.81	1.60	7.42	1.75	0.00	0.84	-0.01	0.84	0.16	14.41	0.57	0.37	20.16
3	G3	17.40	0.68	10.11	2.63	0.24	1.43	0.03	1.40	0.06	17.93	0.39	9.40	35.40
4	G4	19.68	0.76	10.07	2.35	0.01	1.54	0.06	1.48	0.10	18.04	0.57	8.36	39.70
5	G5	7.59	0.90	3.22	0.29	0.00	0.60	0.02	0.58	0.14	5.71	20.65	0.00	0.09
6	G6	11.32	1.49	4.56	0.59	0.26	0.90	0.02	0.88	0.00	8.31	29.22	0.64	2.48
7	G7	19.67	0.49	7.24	1.75	0.00	1.38	0.02	1.36	0.00	13.74	34.52	2.02	12.03
8	G8	7.32	4.04	2.93	0.47	0.00	0.83	0.01	0.83	0.15	6.18	0.09	7.33	25.55
9	G9	2.46	0.86	3.40	0.32	0.00	0.35	-0.01	0.36	0.06	6.68	2.07	1.52	4.86
10	G10	6.74	0.89	6.68	1.70	0.00	0.74	0.04	0.71	0.06	12.06	10.88	1.61	5.90
11	G11	9.55	0.61	6.31	1.42	0.06	0.84	0.03	0.80	0.13	11.52	20.65	0.23	2.88
12	G12	0.43	2.99	5.15	0.81	0.00	0.51	0.08	0.43	0.07	8.89	3.83	0.92	4.39
13	G13	11.01	4.72	3.25	0.58	0.00	1.09	0.07	1.02	0.06	5.99	4.83	7.09	30.87
14	G14	3.96	8.13	4.09	0.70	0.00	1.06	0.00	1.06	0.11	8.23	2.80	7.66	31.32
15	G15	3.65	0.39	3.51	0.78	0.00	0.39	0.05	0.34	0.09	6.78	3.83	0.24	3.06
16	G16	11.33	0.88	7.85	1.68	0.00	1.02	0.01	1.01	0.00	14.70	26.38	0.37	2.99
17	G17	10.02	1.37	3.59	0.94	0.00	0.79	0.06	0.73	0.02	6.63	26.38	0.07	0.91
18	G18	3.43	0.51	3.41	0.61	0.00	0.38	0.09	0.29	0.15	5.92	2.98	0.50	2.56
19	G19	12.73	0.56	3.99	0.60	0.00	0.87	0.06	0.81	0.03	6.93	2.80	4.50	23.35
20	G20	12.23	2.65	4.25	0.45	0.00	1.02	0.04	0.99	0.05	7.41	0.89	7.20	30.96
21	G21	10.52	1.14	11.93	2.69	0.07	1.20	0.05	1.15	0.00	21.92	2.26	4.01	20.34

22	G22	2.01	6.25	3.38	0.65	0.00	0.78	0.02	0.76	0.00	6.41	26.38	0.45	1.92
23	G23	1.44	4.46	3.34	0.43	0.08	0.59	0.05	0.55	0.12	6.32	17.92	0.05	0.41
24	G24	1.85	0.50	2.91	0.49	0.00	0.27	0.07	0.20	0.13	5.23	2.26	0.14	0.48
25	G25	3.91	0.25	3.81	0.53	0.00	0.39	0.06	0.33	0.09	6.37	1.63	1.42	4.78
26	G26	0.64	0.04	6.96	1.58	0.08	0.38	0.01	0.37	0.09	12.30	0.39	0.11	0.46
27	G27	5.89	4.31	3.78	0.94	0.00	0.83	0.01	0.82	0.00	8.02	0.39	1.95	26.89
28	G28	0.73	5.08	4.57	1.17	0.00	0.68	0.00	0.69	0.00	9.43	0.39	3.25	17.29
29	G29	2.13	0.46	6.58	1.63	0.00	0.47	0.03	0.44	0.13	11.96	0.89	0.91	3.40
30	G30	8.71	0.88	4.61	0.79	0.02	0.73	0.03	0.70	0.00	8.52	15.35	0.89	6.47
31	G31	3.66	4.39	5.19	1.09	0.01	0.80	0.06	0.74	0.08	9.03	15.35	0.84	7.77
32	G32	6.53	2.90	4.69	0.69	0.00	0.78	0.04	0.75	0.16	9.21	2.80	0.61	20.34
33	G33	4.04	0.48	5.35	0.78	0.01	0.49	0.08	0.42	0.10	9.66	6.01	0.21	1.02
34	G34	20.87	1.17	5.47	0.90	0.00	1.39	0.03	1.37	0.16	10.32	7.40	2.50	42.78
35	G35	33.30	2.35	4.94	0.90	0.00	2.09	0.04	2.04	0.19	8.92	20.65	15.54	54.22
36	G36	20.90	1.31	6.45	1.47	0.00	1.47	0.03	1.43	0.08	12.08	0.89	9.17	44.62
37	G37	31.29	2.36	4.99	0.77	0.07	1.99	-0.02	2.01	0.03	9.78	42.46	7.52	36.58
38	G38	22.63	1.52	11.14	2.77	0.00	1.81	0.05	1.75	0.02	21.02	43.83	3.19	11.15
39	G39	20.47	2.58	8.78	1.97	0.00	1.66	0.01	1.65	0.00	16.46	38.99	3.07	17.15
40	G40	19.40	3.67	13.31	2.89	0.00	1.92	0.02	1.90	0.06	24.27	31.96	3.20	25.08
41	G41	7.42	5.17	4.15	0.96	0.00	1.00	-0.01	1.01	0.15	8.59	9.02	7.06	22.71
42	G42	10.95	2.87	5.96	1.05	0.00	1.07	0.05	1.02	0.16	10.39	15.35	0.12	19.96
43	G43	0.84	9.12	5.01	1.07	0.00	1.03	0.04	1.00	0.00	9.35	17.92	3.59	15.29
44	G44	3.41	0.58	3.51	0.75	0.00	0.39	0.03	0.36	0.03	7.07	1.63	1.51	4.85
45	G45	7.27	1.58	4.73	1.23	0.01	0.73	0.07	0.66	0.00	8.71	13.00	1.04	6.59
46	G46	14.75	7.75	4.92	1.23	0.05	1.61	0.02	1.59	0.05	9.68	2.98	13.75	49.96
47	G47	4.13	0.36	12.05	2.84	0.12	0.83	0.05	0.78	0.21	21.96	3.83	0.18	3.82
48	G48	4.25	0.35	3.84	0.83	0.00	0.43	0.03	0.40	0.11	6.80	6.01	0.92	3.58
49	G49	14.87	2.10	4.24	0.46	0.00	1.11	0.04	1.07	0.03	7.57	40.85	0.12	1.66
50	G50	6.55	1.42	6.72	1.65	0.00	0.78	0.01	0.77	0.17	13.11	3.83	0.46	15.12
51	G51	5.27	0.14	10.73	2.80	0.00	0.81	0.03	0.78	0.11	19.50	2.98	1.63	7.05

Appendix - B 2Groundwater Quality analysis and anion – cation balance for Phase-II (Post-monsoon)

Sl. No.	Smpl. No.	Ca ²⁺	Mg ²⁺	Fe	Na ⁺	K ⁺	Cations [C]	(C-A) < (±0.2)	Anions [A]	F ⁻	Cl ⁻	HCO ₃	NO ₃ ⁻	SO ₄ ²⁻
		mg/l	mg/l	ppm	mg/l	mg/l	meq/l	meq/l	meq/l	mg/l	mg/l	mg/l	ppm	ppm
1	G1	3.74	1.99	0.11	11.32	4.16	0.95	0.10	0.85	0.18	17.92	9.5	0.42	7.24
2	G2	3.33	2.1	0	12.28	4.31	0.98	0.09	0.90	0.16	20.81	8.15	0.42	6.71
3	G3	7.38	0.72	0.3	7.93	3.59	0.86	0.07	0.80	0.13	13.29	11.43	0.39	8.97
4	G4	1.25	3.06	0.06	9.03	2.87	0.78	0.07	0.71	0.16	14.45	7.36	0.35	7.01
5	G5	9.06	1.31	0	18.13	5.71	1.49	0.08	1.41	0.18	30.63	20.23	0.37	6.73
6	G6	27.16	2.81	0.27	8.27	3.6	2.03	0.08	1.96	0.69	13.29	67.13	0.36	11.22
7	G7	66.48	1.07	0	10.44	3.47	3.94	0.10	3.84	0.74	16.76	148.31	0.36	18.95
8	G8	1.28	2.98	0	22.89	8.13	1.51	0.08	1.43	0.19	39.88	5.06	0.40	9.4
9	G9	4.22	0.96	0	20.44	5.56	1.32	0.06	1.26	0.19	34.68	4.94	0.36	8.65
10	G10	56.27	0.5	0	14.17	5.66	3.60	0.09	3.51	0.15	24.28	123.8	0.66	16.53
11	G11	38.61	0.31	0.1	9.57	3.78	2.46	0.08	2.38	0.21	15.61	88.68	0.55	7.68
12	G12	17.77	1.13	0	13.22	5.95	1.70	0.14	1.57	0.1	21.96	39.93	0.48	6.81
13	G13	11.86	3.13	0	19.41	5.08	1.82	0.05	1.77	0.1	33.52	31.24	0.95	9.03
14	G14	17.05	0.97	0	37.83	11.01	2.85	0.08	2.77	0.12	65.89	34.5	5.87	6.23
15	G15	14	0.96	0	18.17	4.1	1.67	0.06	1.61	0.16	30.63	30.05	0.95	6.37
16	G16	55.44	2.78	0.35	22.12	7.1	4.13	0.09	4.04	0.34	37.57	136.31	0.40	12.04
17	G17	36.08	0.72	1.11	6.81	3.55	2.24	0.09	2.15	0.28	10.98	76.94	0.39	14.08
18	G18	16.29	3.53	0	30.81	9.2	2.67	0.08	2.59	0.17	53.18	40.71	2.68	11.24
19	G19	3.23	1.55	0	32.11	8.81	1.91	0.08	1.83	0.14	55.49	5.41	0.59	6.96
20	G20	5.96	0.5	0	28.16	8.92	1.79	0.08	1.71	0.15	49.71	5.65	0.34	9.09
21	G21	3.19	1	0.08	8.47	3.56	0.70	0.06	0.64	0.15	14.45	2.59	0.40	8.35
22	G22	54.99	0.17	0.97	9.77	1.92	3.22	0.03	3.19	0.37	16.18	116.57	0.36	19.27
23	G23	32.53	0.95	0.1	9.95	2.86	2.20	0.05	2.15	0.24	16.18	69.76	0.41	13.97
24	G24	36.59	2.9	0	13.58	4.98	2.78	0.09	2.69	0.15	22.54	92.81	0.85	8.81
25	G25	14.45	0.91	0	11.53	3.74	1.39	0.07	1.32	0.16	19.07	28.14	0.35	10.43
26	G26	5.54	0.9	0.09	14.71	4.77	1.11	0.09	1.03	0.17	24.85	8.36	0.40	7.25

Appendix-B

27	G27	3.47	1.76	0	21.46	5.51	1.39	0.06	1.34	0.36	36.99	5.22	0.41	8.75
28	G28	28.53	2.48	0	61.15	19.06	4.77	0.11	4.66	0.15	108.66	73.13	0.00	6.48
29	G29	34.99	1.85	0	42.6	11.46	4.04	0.05	3.98	0.18	75.14	83.37	0.59	9.08
30	G30	28.88	3.44	0.05	8.53	4.38	2.20	0.09	2.11	0.41	14.45	79.23	0.36	5.54
31	G31	4.73	3.35	0.07	13.85	3.91	1.21	0.08	1.13	0.2	22.54	22.03	0.41	2.44
32	G32	5.52	0.21	0	26.31	6.85	1.61	0.05	1.56	0.19	45.08	10.25	1.11	2.98
33	G33	6.08	2.13	0.08	8.92	2.94	0.94	0.06	0.88	0.17	15.03	18.37	0.39	3.9
34	G34	4.35	1.8	0	7.93	3.9	0.81	0.11	0.70	0.18	12.14	14.91	0.30	2.44
35	G35	9.52	0.29	0	9.85	3.96	1.03	0.08	0.94	0.2	16.18	21.88	0.38	2.15
36	G36	4.35	2.32	0	31.27	9.31	2.00	0.10	1.90	0.2	53.75	14.79	1.70	2.97
37	G37	39.34	3.22	0.11	11.22	4.06	2.81	0.07	2.75	0.22	19.07	96.82	0.58	12.69
38	G38	97.99	1.19	0	22.35	6.21	6.10	0.05	6.05	0.22	38.73	222.5	3.18	21.92
39	G39	30.83	3.6	0.42	12.96	4.05	2.50	0.05	2.44	0.35	22.54	83.53	0.38	6.31
40	G40	35.58	3.28	0	11.56	2.28	2.60	0.06	2.54	0.25	18.5	91.76	0.49	8.52
41	G41	41.57	0.28	0	15.76	4.22	2.88	0.07	2.81	0.3	26.59	88.3	0.45	14.01
42	G42	14.14	3.16	0	11.66	5.43	1.61	0.08	1.52	0.27	20.23	41.21	0.67	5.68
43	G43	38.31	0.97	0	10.79	2.28	2.51	0.03	2.49	0.31	17.92	89.18	0.38	9.2
44	G44	4.95	1.74	0	11.41	3.15	0.97	0.07	0.90	0.27	19.07	11.33	0.67	5.95
45	G45	32.98	1.44	0.09	26.69	6.42	3.08	0.03	3.06	0.37	46.24	77.52	2.01	8.2
46	G46	3.84	1.32	0.06	9.81	3.19	0.81	0.06	0.75	0.21	16.18	9.05	0.35	5
47	G47	3.61	3.6	0.15	10.14	4.8	1.04	0.08	0.96	0.25	17.34	17.68	0.44	5.14
48	G48	23.66	2.93	0	13.19	4	2.09	0.06	2.03	0.26	22.54	50.25	0.44	18.34
49	G49	106.17	2.89	0	19.28	6.5	6.52	0.09	6.44	0.24	32.95	246.25	3.71	25.17
50	G50	8.05	3.39	0	10.05	2.18	1.17	0.03	1.14	0.26	16.76	27.15	0.42	5.78
51	G51	15.95	1.04	0	17.21	5.42	1.77	0.08	1.69	0.26	29.48	34.27	2.25	6.62

Appendix - B 3 Groundwater Quality analysis and anion – cation balance for Phase-III (Pre-monsoon)

Sl. No.	Smpl No.	Ca ²⁺	Mg ²⁺	Fe	Na ⁺	K ⁺	Cations [C]	(C-A) < (±0.2)	Anions [A]	F ⁻	Cl ⁻	TA	NO ₃ ⁻	SO ₄ ²⁻
		mg/l	mg/l	ppm	mg/l	mg/l	meq/l	meq/l	meq/l	mg/l	mg/l	mg/l	ppm	ppm
1	G1	2.86	0.12	0.17	18.61	4.77	1.09	-0.06	1.15	0.26	32.95	5.71	1.97	3.0074
2	G2	2.38	1.34	0.09	14.84	3.50	0.96	-0.07	1.03	0.23	26.01	8.87	2.84	3.1589
3	G3	0.95	1.28	0.07	20.22	5.26	1.17	-0.06	1.23	0.17	35.84	4.29	1.91	4.5773
4	G4	0.95	2.21	0.08	20.15	4.71	1.23	-0.07	1.29	0.22	35.26	10.22	1.53	2.8697
5	G5	2.38	1.81	0.05	9.12	1.18	0.69	-0.08	0.77	0.27	15.03	11.85	1.93	3.214
6	G6	11.90	7.65	0.02	14.48	3.49	1.94	-0.11	2.05	0.37	25.43	60.58	1.90	3.5032
7	G7	26.19	12.92	0.19	6.81	0.63	2.68	-0.14	2.82	1.01	10.98	112.15	2.46	8.1855
8	G8	0.95	1.28	0.04	13.37	3.41	0.82	-0.10	0.92	0.32	23.70	5.97	1.96	4.0678
9	G9	0.48	1.11	0.02	12.62	2.85	0.74	-0.11	0.85	0.28	21.96	6.85	2.45	1.9057
10	G10	17.14	7.72	0.02	10.31	1.61	1.98	-0.11	2.09	0.33	17.34	63.34	2.19	13.433
11	G11	20.48	8.02	0.14	6.50	1.16	1.99	-0.09	2.08	1.02	10.98	79.97	2.18	4.0127
12	G12	24.76	7.13	0.02	8.19	1.39	2.21	1.11	1.10	0.42	13.87	31.21	0.67	2.305
13	G13	7.14	4.50	0.05	7.01	1.57	1.07	-0.10	1.17	0.42	12.14	32.55	2.48	5.6515
14	G14	1.43	3.32	0.00	15.70	3.36	1.11	-0.11	1.23	0.32	27.17	17.83	2.22	2.429
15	G15	12.38	8.75	0.03	7.18	1.87	1.69	-0.11	1.80	0.60	12.72	62.88	2.18	5.6378
16	G16	18.57	16.61	0.14	6.83	1.23	2.62	-0.10	2.72	0.88	11.56	109.20	2.62	5.8581
17	G17	9.05	13.56	0.25	7.97	1.21	1.94	-0.10	2.04	0.74	13.29	72.91	2.28	6.3539
18	G18	3.81	3.73	0.04	8.50	0.90	0.89	-0.09	0.97	0.33	13.87	20.83	2.51	5.2522
19	G19	1.43	0.53	0.13	23.87	5.38	1.29	-0.05	1.34	0.28	41.62	0.25	2.16	5.445
20	G20	1.43	10.29	0.05	6.59	1.66	1.24	-0.06	1.31	0.27	11.56	42.68	2.76	3.3379
21	G21	6.67	17.33	0.05	6.76	1.30	2.08	-0.06	2.14	0.28	11.56	85.27	2.43	2.8008
22	G22	8.57	11.53	0.14	5.82	0.98	1.65	-0.14	1.79	1.15	9.83	52.32	1.86	17.95
23	G23	10.00	17.17	0.12	7.63	1.06	2.27	-0.09	2.36	0.61	12.72	84.70	2.09	11.504
24	G24	6.19	4.61	0.09	13.93	3.17	1.37	-0.10	1.48	0.36	24.28	30.28	2.87	5.8581
25	G25	3.81	6.52	0.04	7.57	1.87	1.10	-0.11	1.21	0.43	13.29	33.38	3.72	3.9301
26	G26	2.86	2.45	0.03	7.44	0.81	0.69	-0.11	0.80	0.37	12.14	15.05	1.24	5.445

27	G27	0.95	1.75	0.04	5.70	1.25	0.47	-0.11	0.58	0.31	9.83	6.20	3.04	5.3792
28	G28	2.38	1.34	0.04	13.15	3.25	0.88	-0.12	1.00	0.40	23.12	10.52	3.20	3.3188
29	G29	0.95	0.82	0.02	9.23	1.58	0.56	-0.05	0.61	0.30	15.61	1.83	2.72	3.4036
30	G30	11.43	11.19	0.28	10.39	2.17	2.00	-0.10	2.10	1.46	17.92	70.37	2.43	3.4619
31	G31	4.29	2.98	0.00	9.38	1.37	0.90	-0.14	1.04	0.50	15.61	17.42	4.66	7.0425
32	G32	1.43	1.46	0.01	10.95	1.81	0.71	-0.11	0.82	0.45	18.50	6.54	3.64	4.0678
33	G33	3.33	3.09	0.03	9.88	1.80	0.89	-0.12	1.02	0.48	16.76	17.97	3.42	5.1558
34	G34	1.90	1.17	0.00	12.91	2.95	0.83	-0.09	0.92	0.46	22.54	6.84	2.49	4.1091
35	G35	3.81	3.26	0.04	9.98	1.55	0.93	-0.12	1.05	0.57	16.76	21.91	2.48	3.4205
36	G36	1.90	2.56	0.01	22.28	5.53	1.42	-0.11	1.53	0.46	39.30	14.50	2.70	2.9661
37	G37	28.10	14.55	0.00	17.56	3.94	3.45	-0.08	3.53	0.72	30.63	112.33	2.40	16.71
38	G38	51.43	34.78	0.03	26.63	5.79	6.72	-0.13	6.85	0.62	46.24	236.65	2.82	35.233
39	G39	19.52	6.74	0.02	8.30	1.92	1.93	-0.10	2.04	0.71	14.45	67.66	2.92	9.301
40	G40	12.86	10.32	0.04	11.93	2.11	2.06	-0.10	2.15	1.04	20.23	64.51	3.21	9.0118
41	G41	13.33	16.07	0.03	13.04	2.75	2.62	-0.12	2.74	1.08	22.54	79.16	3.77	19.437
42	G42	9.52	14.67	0.05	10.02	2.14	2.17	-0.12	2.29	1.44	17.34	60.01	2.67	22.962
43	G43	24.76	9.14	0.01	7.02	1.50	2.32	-0.12	2.45	0.78	12.14	91.00	2.89	9.5076
44	G44	2.38	1.81	0.03	9.46	2.47	0.74	-0.09	0.83	0.48	16.76	2.33	2.57	11.615
45	G45	10.48	13.16	0.01	24.10	5.67	2.79	-0.13	2.92	0.88	42.19	69.79	6.24	9.2184
46	G46	2.86	1.52	0.01	7.69	1.66	0.64	-0.12	0.76	0.68	13.29	10.19	2.75	5.1144
47	G47	2.86	3.38	0.02	8.49	0.92	0.81	-0.08	0.89	0.57	13.87	13.31	4.26	6.6706
48	G48	10.95	5.44	0.01	13.44	3.30	1.66	-0.08	1.74	0.52	23.70	33.32	3.51	15.636
49	G49	58.57	23.01	0.02	21.46	5.60	5.88	-0.16	6.04	0.75	38.15	216.52	4.22	25.069
50	G50	4.76	3.15	0.02	9.06	1.17	0.92	-0.09	1.01	0.79	15.03	19.26	2.88	5.4863
51	G51	4.29	6.23	0.01	20.50	4.11	1.72	-0.08	1.80	0.54	35.26	30.07	1.84	7.0149

APPENDIX-C

Plates of field and laboratory studies

	
<p>VES – Resistivity data acquiring</p>	<p>VES – Resistivity data acquiring</p>
	
<p>Surface water sampling</p>	<p>Existing recharge structure</p>
	
<p>Handpump groundwater sampling</p>	<p>GW Sampling in an Arecanut plantation</p>



Groundwater sampling in settlement



UV Spectrophotometer



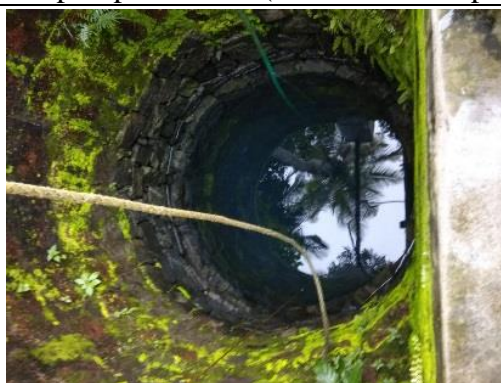
Borewell groundwater sampling



Handpump for water (less than 3m depth)



GW Sampling near rubber plantation



GW Sampling in an agricultural field.

 A photograph showing a group of people in a forested area. In the foreground, a man wearing a blue cap and a red and blue striped shirt is looking towards the camera. In the background, other people are visible on a dirt path, some with equipment.	 A photograph of a laboratory setting. A man in a white shirt and glasses is in the foreground, looking at the camera. Behind him, another man in a brown t-shirt is visible. The lab contains various pieces of equipment and white containers.
<p>VES in the forest area</p>	<p>Laboratory analysis of samples</p>
 A photograph of a man in a black t-shirt standing behind a laboratory bench. On the bench, there are several bottles of reagents and indicators, some in brown and some in white.	 A photograph of a circular, shallow well or pond. The water is dark and still, surrounded by a concrete or stone rim. The area is overgrown with moss and vegetation, suggesting a dry or shaded environment.
<p>Preparation of reagents and indicators</p>	<p>Surface level water (during summer)</p>
 A photograph of a man in a red and blue striped shirt working in a laboratory. He is pouring liquid from a beaker into a larger container on a scale. A digital scale is visible on the bench.	 A photograph of an open field. Several people are gathered around a piece of equipment on the ground. One person is kneeling and operating the equipment, while others stand nearby. The ground is dry and brown.
<p>Preparation of EDTA</p>	<p>VES in Open ground</p>

APPENDIX-D**Author Biography (brief)**

- **Author name:** Virupaksha H. S.
- **Author full name:** Virupaksha Shivakumar Hebbalu
- **Designation:** Research Scholar as of 2020/11/30
- **Department:** Civil Engineering
- **Affiliation:** National Institute of Technology Karnataka, Surathkal – 575025, Mangaluru, Karnataka, India.
- **Gmail id:** virupaksha.773@gmail.com
- **Institution mail id:** cv15f13@nitk.edu.in
- **Field of expertise:** Hydrogeology, Remote Sensing, GIS, Hydrology, Geophysics
- **Research interest(s):** Groundwater exploration, Groundwater recharge, and water quality studies.
- **ORCID :** 0000-0002-2807-4453
- **Google Scholar ID:**
<https://scholar.google.co.in/citations?hl=en&user=keELBjIAAAAJ>
- **Web of Science Researcher ID:** [U-8813-2019](#)
- **SCOPUS author ID(s):** 57209575928; 57213152299
- **Review activity:** Geocarto International ([1752-0762](#)) with identifier ID: TedXW3VO
- **Journal membership:** Geological Society of India: Bangalore, Karnataka, IN. 2017-02 to 2020-01 | member Service.

Research Publication(s)**Journal articles (published):**

- Electrical resistivity, remote sensing and geographic information system approach for mapping groundwater potential zones in coastal aquifers of Gurpur watershed. Geocarto International. 2019 | journal-article. DOI: 10.1080/10106049.2019.1624986. EID: 2-s2.0-85068145781. Part of ISBN: 10106049.
- Multivariate statistics and water quality index (WQI) approach for geochemical assessment of groundwater quality—a case study of KanaviHalla Sub-Basin, Belagavi, India. Environmental Geochemistry and Health. 2020 | journal-article. DOI: 10.1007/s10653-019-00500-6. EID: 2-s2.0-85077596700. Part of ISBN: 15732983 02694042.

Journal articles (communicated):

- The assessment of groundwater quality and its suitability for drinking purposes using Water Quality Index method - a case study of Gurpur watershed, west coast of India.
- Electrical Resistivity and Geographic Information System approach for mapping Groundwater Potential Zones in Gurpur watershed of Coastal Karnataka, India.
- The assessment of effective groundwater recharge using geographic information system, remote sensing and electrical resistivity method in Gurpur watershed, west coast of India.

Conference proceeding:

- Assessment of Hydraulic and Geoelectric parameters of the Aquifers and their relationship using Vertical Electrical Sounding in Gurpur watershed, West-coast of India (To be published in Springer proceedings).

Abstract publication:

- Assessment of Hydraulic and Geoelectric parameters of the Aquifers and their relationship using Vertical Electrical Sounding in Gurpur watershed, West-coast of India